AFRL-HE-BR-TR-2007-0001

NONSURGICAL BRAIN ACTIVITY RECOVERY FROM A CAP CONTAINING MULTIPLE ELECTROENCEPHALOGRAM RECORDING SITES

David Cohoon

L3-Communications Services Group

September 2006
Final Report for February 2006 to September 2006

Air Force Research Laboratory
Human Effectiveness Directorate
Information Operations and Special Programs Division
Brooks-City-Base TX 78235

NOTICE

Using Government drawings, specifications, or other data included in this document for any purpose other than Government procurement does not in any way obligate the U.S. Government. The fact that the Government formulated or supplied the drawings, specifications, or other data does not license the holder or any other person or corporation; or convey any rights or permission to manufacture, use, or sell any patented invention that may relate to them.

This report was cleared for public release by the 311 HSW/PA, Brooks City-Base TX and is releasable to the National Technical Information Service (NTIS). It will be available to the general public, including foreign nationals.

THIS TECHNICAL REPORT IS APPROVED FOR PUBLICATION.

//Signed//
ANTHONY S. CARVER, CAPT, USAF
Project Manager

//Signed//
JAMES W. RICKMAN, MAJ, USAF
Chief, Special Projects Branch

This report is published in the interest of scientific and technical information exchange and its publication does not constitute the Government's approval or disapproval of its ideas or findings.

REPORT DOCUMENTATION PAGE

Form Approved
OMB No. 0704-0188

1. REPORT DATE *(DD-MM-YYYY)*	**2. REPORT TYPE**	**3. DATES COVERED** *(From - To)*
22-09-2006	Final	February 2006 - September 2006

4. TITLE AND SUBTITLE
Nonsurgical Brain Activity Recovery From a Cap Containing Multiple Electroencephalogram Recording Sites

5a. CONTRACT NUMBER
F41624-03-D-6002-0008

5b. GRANT NUMBER

5c. PROGRAM ELEMENT NUMBER

6. AUTHOR(S)
David Cohoon

5d. PROJECT NUMBER
7184

5e. TASK NUMBER
X1

5f. WORK UNIT NUMBER
3B

7. PERFORMING ORGANIZATION NAME(S) AND ADDRESS(ES)
L3-Communications Services Group, 6100
Bandera Rd., San Antonio, TX 78238

8. PERFORMING ORGANIZATION REPORT NUMBER

9. SPONSORING / MONITORING AGENCY NAME(S) AND ADDRESS(ES)
Air Force Materiel Command
Air Force Research Laboratory Human Effectiveness Directorate Information Operations & Special Programs Division (AFRL/HEX)
2486 Gillingham Dr
Brooks City-Base, TX 78235

10. SPONSOR/MONITOR'S ACRONYM(S)
AFRL/HEX

11. SPONSOR/MONITOR'S REPORT NUMBER(S)
AFRL-HE-BR-TR-2007-0001

12. DISTRIBUTION / AVAILABILITY STATEMENT
Approved for public release: distribution unlimited.

13. SUPPLEMENTARY NOTES
Cleared for public release PA 07-014: 05 Jan 07
Final report delivered by the contractor (L3-Communications) to the government (AFRL/HEX).

14. ABSTRACT
The goal of this project is to invert electroencephalogram data to brain activity using a novel and accurate algorithm. This algorithm can be used for research and development of brain-machine interfaces, potentially to include prosthetic control, surveillance and lie detection. This report details the mathematical and physical theory behind the algorithm developed during this effort. The algorithm is novel in that it does not use the quasistatic approximation throughout the space, instead using it only at the boundaries between material media. The output of the algorithm consists of three-dimensional currents at dipoles located at pre-specified locations. The number of such dipoles is limited to one third of the number of electroencephalogram electrodes, so they are best regarded as neuronal aggregates instead of individual neurons. The algorithm has been executed on up to five seconds of 128-electrode electroencephalogram data sampled at 2048 Hertz. Numerical results are provided in graphical format.

15. SUBJECT TERMS
NEURAL INVERSION; NON-INVASIVE NEURAL CONTROL; INVERSE; PROSTHETIC; NON-INVASIVE; BRAIN-MACHINE INTERFACE; ELECTROENCEPHALOGRAM; SPHERICAL-HARMONIC; SCALP POTENTIAL.

16. SECURITY CLASSIFICATION OF:			**17. LIMITATION OF ABSTRACT**	**18. NUMBER OF PAGES**	**19a. NAME OF RESPONSIBLE PERSON**
a. REPORT	**b. ABSTRACT**	**c. THIS PAGE**			Dr. Grant Erdmann
U	U	U	SAR	217	**19b. TELEPHONE NUMBER** *(include area code)*

Standard Form 298 (Rev. 8-98)
Prescribed by ANSI Std. Z39.18

THIS PAGE INTENTIONALLY LEFT BLANK

Contents

NONSURGICAL BRAIN ACTIVITY RECOVERY FROM
A CAP CONTAINING MULTIPLE ELECTROENCEPHALOGRAM RECORDING SITES

AFRL / HEX TEAM

1 Four Parts of the Brain Activity Recovery Programs

A major purpose of our work to give amputees a natural control of an artificial limb with their thoughts without any surgical penetration of brain tissue; we are using an inverse source solution to aid in this effort. Dr. Todd Kuiken (Brown [22], September 14, 2006) has accomplished this with Jesse Sullivan and Claudia Mitchell by connecting nerves in the chest to an artificial limb. We have developed an algorithm to recover the brain neuronal signals at sites within the brain tissue from 128 or more electroencephalogram recordings in a cap which fits over the handicapped persons head. Each EEG recorder had its own operational amplifier. There are four classes of computer processing efforts.

First, the raw EEG recordings were detrended so that operational amplifier drift was removed and so that the net average voltage at each recording site was zero. Selected plots of the raw EEG data are supplied in this report.

Next we created a dynamic head surface voltage representation over the entire surface of the head from the full time profiles of activity at 128 or more EEG recording sites and the relationship between the voltage values at these sites at each recording time. There are two approaches to dynamic head surface voltage function representation. One approach is computationally slow, involving large matrices which we would pre-factor ahead of time for the handicapped person, but which has the potential for recovery of brain activity at many sites throughout the brain.

The first dynamic head surface voltage representation method, which we programmed uses the full time profile of activity at each of $N = 128$ or more recording sites and, for each recording time, the relationships between voltage values at all sites at this time; this is potentially a great deal of information that may be used for brain activity recovery. These head surface voltage representation matrices are quite large but the matrix entries are completely independent of brain activity and consequently their singular value decomposition could be carried out ahead of time for the handicapped person enabling him or her to respond rapidly to stimulus as the matrix multiplication of the decomposition factors by the EEG stimulus vectors could be carried out with parallel processors and even with one processor the computational complexity of the process would depend only on the square of the matrix column dimension. This approach has the potential for recovery of a great deal of brain activity.

A computationally simpler approach first would match the full time profile of activity at each EEG recording site with a Fourier series and then find the head surface representation from the Fourier components. With this approach, if the number of EEG recording sites were N, the number of potential neuronal activity locations at which brain activity could be recovered would be N/3. I plan to program this as a check on the first program which is

the one we are using. This method would also have the potential to provide real help to the handicapped person if we could expand the number of EEG recording sites.

The third suite of programs is brain activity recovery using our dynamic voltage inverse source solution by the creation of multiple equations relating the dynamic head surface voltage distributions to internal brain activity for each frequency component. The first part of this effort is to create brain-activity independent interrogating scalar functions of the spatial variables and frequency which satisfy the tissue interface boundary conditions that they are continuous across tissue interfaces and that tissue permittivity, which is a function of frequency, times the normal component of the gradient of the interrogating scalar function is continuous across tissue interfaces. These are the same boundary conditions satisfied by the dynamic voltage which starts out as a function proportional to the divergence of the vector potential of brain activity.

What this means is that vector calculus may be used to obtain equations directly relating scalp surface interrogation to internal brain activity. The mathematical theory is provided in this report. The voltage itself is continuous across tissue interfaces as the electic field vector stimulated by brain activity at all sites is finite. Since there are no net charges due to brain activity at tissue interfaces, the tissue permittivity times the normal component of the voltage gradient is continuous across tissue interfaces. This suite of calculations based on singular value decomposition of the matrices defining the relationships between head surface measurments and internal brain activity give us a Fourier series representation of the three components of the neuronal current vectors at each potential site of brain activity. As there is a separate singular value decomposition for each frequency component the computational complexity of the recovery here is smaller than that of the voltage head surface representation.

The final program gives the time profile of activity on individual neuronal sites from the recovered Fourier coefficients giving us a 3Q+1 column data set where the row indexed by the time t contains

$$t \rightarrow$$

$$(t, J_{(1,x)}, J_{(1,y)}, J_{(1,z)}, \cdots, J_{(q,x)}, J_{(q,y)}, J_{(q,z)}, \cdots, J_{(Q,x)}, J_{(Q,y)}, J_{(Q,z)})$$

where there are Q possible sites of neuronal activity.

2 Steps In Using the Algorithm

This is the outline of the steps in using our algorithm

1. Define the head geometry and electromagnetic properties of each tissue region.
2. Format the EEG recordings into data files $\boldsymbol{x}_j$, t_k, and $V_j(t_k)$ where j runs from 1 through J and k runs from 1 through K.
3. Select a lattice of dipoles $\boldsymbol{x}_{(dipole,n)}$.
4. Choose the frequencies ω_{p_1} of interest.
5. For each frequency ω_{p_1} choose the interrogating functions $\psi_{(q,p_1)}(\boldsymbol{x})$.

6. The code will then solve for the currents, transform the currents to the time domain and output the results to a data file.

3 Data Showing the Recovery of Brain Activity from Discrete Recordings of Time Profiles of EEG Voltages at 128 Recording Sites

We create a dynamic head surface voltage distribution from the 128 EEG recordings using the relationships at each time value of voltages at all of these sites. We then interrogate this voltage distribution so that with each interrogation we obtain a relationship between the EEG recordings and internal brain activity at a lattice of possible sites of brain activity. A singular value decomposition is used for each frequency component to recover the transmembrane current vector components at each site for each frequency component. Another program processes this data and gives us the time profile of brain activity at the internal sites displayed in the following plots.

3.1 Graphical Data Showing the Recovery of Brain Activity from EEG Recordings

We provide the reader with two data sets. The first consists of using the full 5 seconds of data at 128 EEG recording sites to recover low frequency brain activity at 16 internal sites with 30 evenly spaced frequencies from .2 to 6 Hertz. The second consists of using 1 second of EEG data to recover low frequency components of brain activity at 17 internal sites for 30 frequency components from 1 to 30 Hertz.

3.1.1 Recovery of 30 Evenly Spaced Frequency Components from 1 to 6 Hertz at 16 Potential Sites of Brain Activity with Using 5 Seconds of Data

We find a dynamic representation of brain activity, we interrogate it with brain activity independent scalar interrogating functions that satisfy the same boundary conditions that are satisifed by the dynamic voltage wave. We go from the scalp surface through the skull bone without surgery to the brain activity. We process this recovery by recording the time profile of each component of neuronal activity on each site of potential brain activity. There are now three computer programs DYNHSV.FOR which produces the dynamic head surface voltage representation, EEBARIS.FOR which is the brain activity recovery inverse source solution which uses the output from DYNHSV.FOR, and produces output for the plotting program EEGPLOT.FOR which plots the recovered currents as a function of time. These are carried out for 30 frequency components from .2 to 5 Hertz

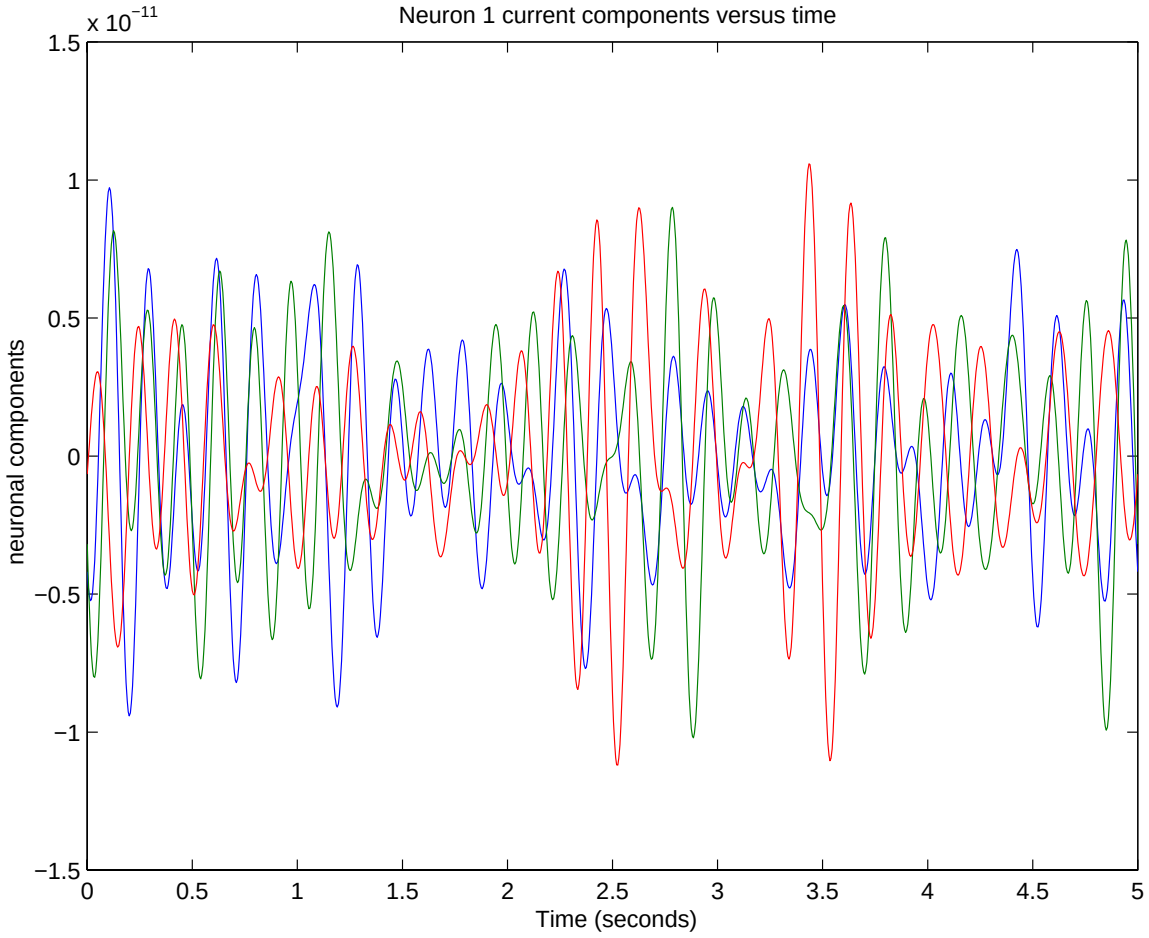

Figure 1: Recovered Neuron 1 Current Components Versus Time

For $q = 1$ the neuronal location, in spherical coordinates is,

$$(r_q, \theta_q, \phi_q) = (0800, 1., 0.) \tag{3.1.1.1}$$

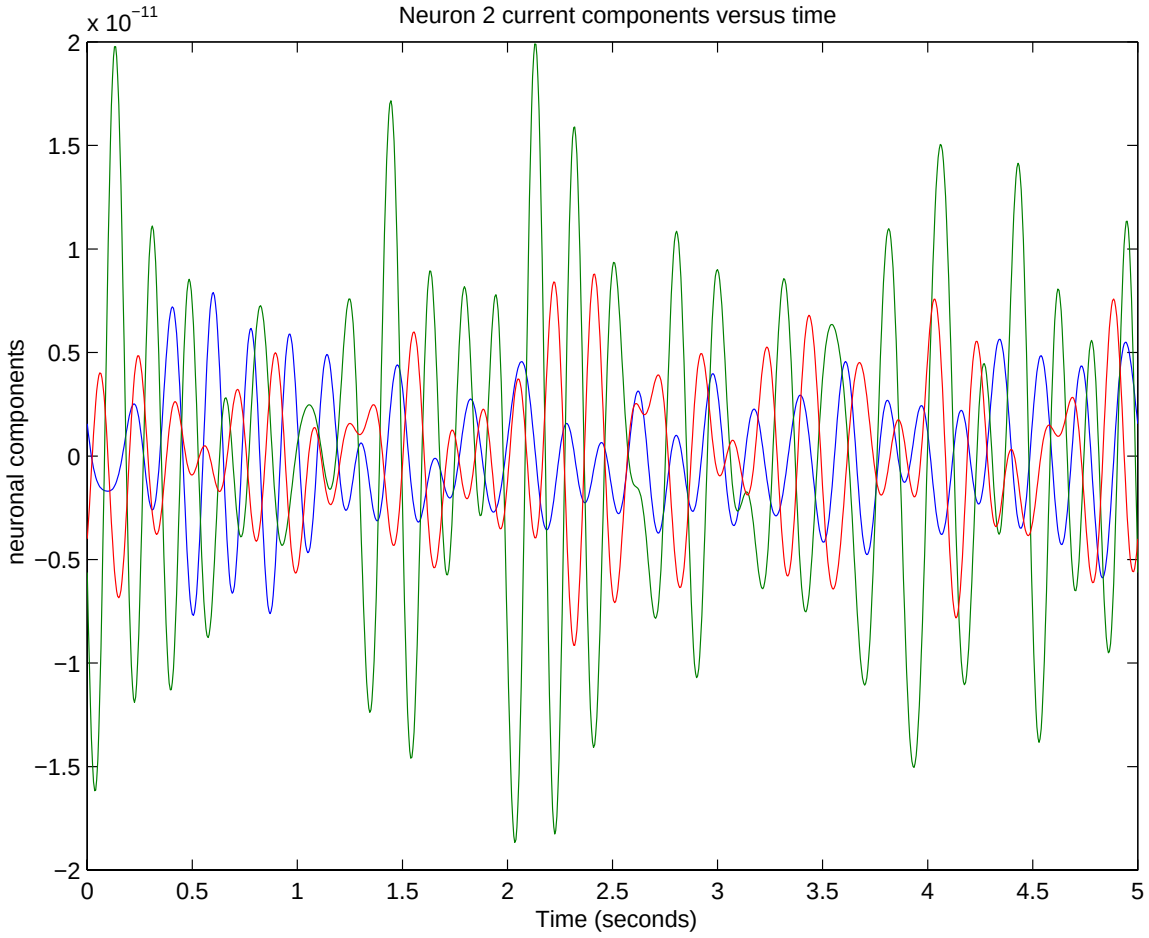

Figure 2: Recovered Neuron 2 Current Components Versus Time

For $q = 2$ the neuronal location, in spherical coordinates is,

$$(r_q, \theta_q, \phi_q) = (.0800, 46., 0.) \tag{3.1.1.2}$$

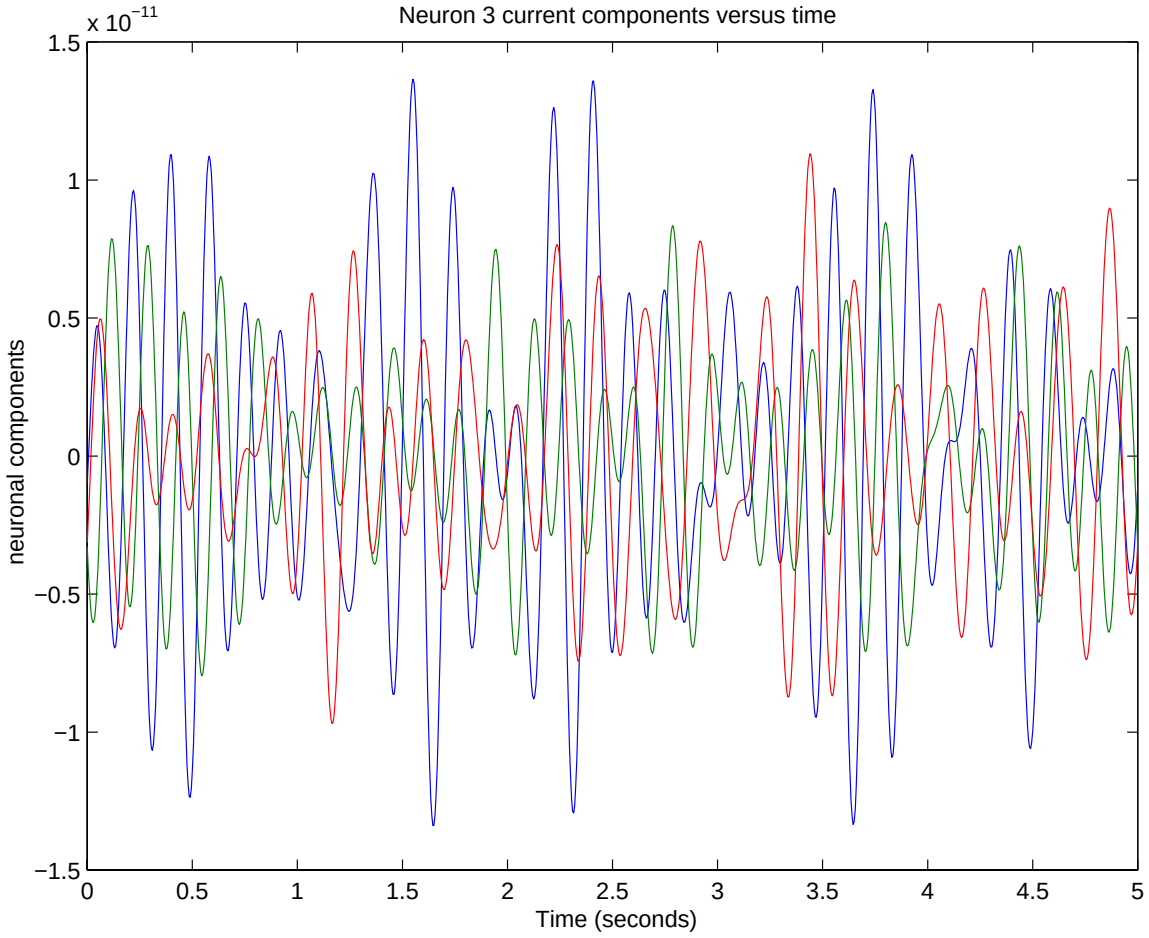

Figure 3: Recovered Neuron 3 Current Components Versus Time

For $q = 3$ the neuronal location, in spherical coordinates is,

$$(r_q, \theta_q, \phi_q) = (.0800, 46., 90.) \tag{3.1.1.3}$$

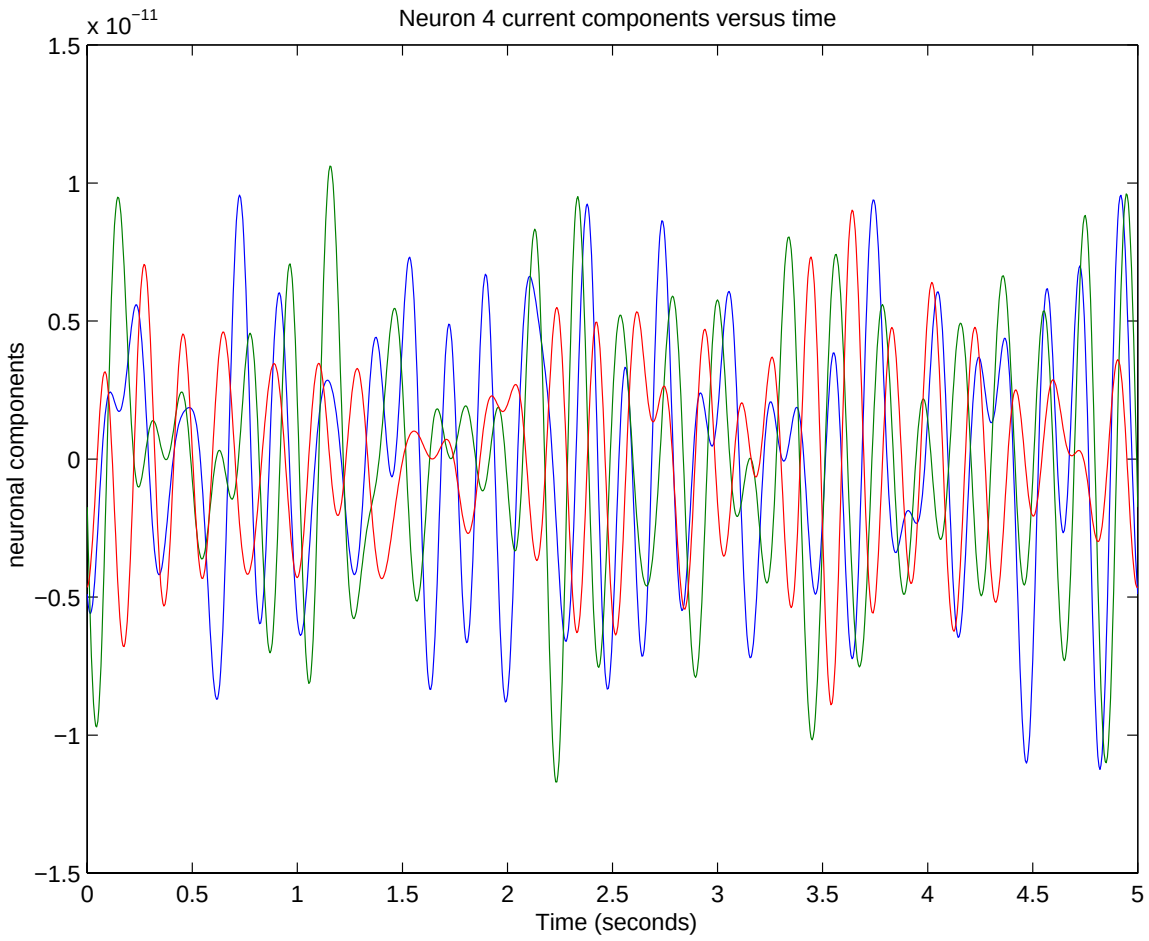

Figure 4: Recovered Neuron 4 Current Components Versus Time

For $q = 4$ the neuronal location, in spherical coordinates is,

$$(r_q, \theta_q, \phi_q) = (.0800, 46., 270.) \tag{3.1.1.4}$$

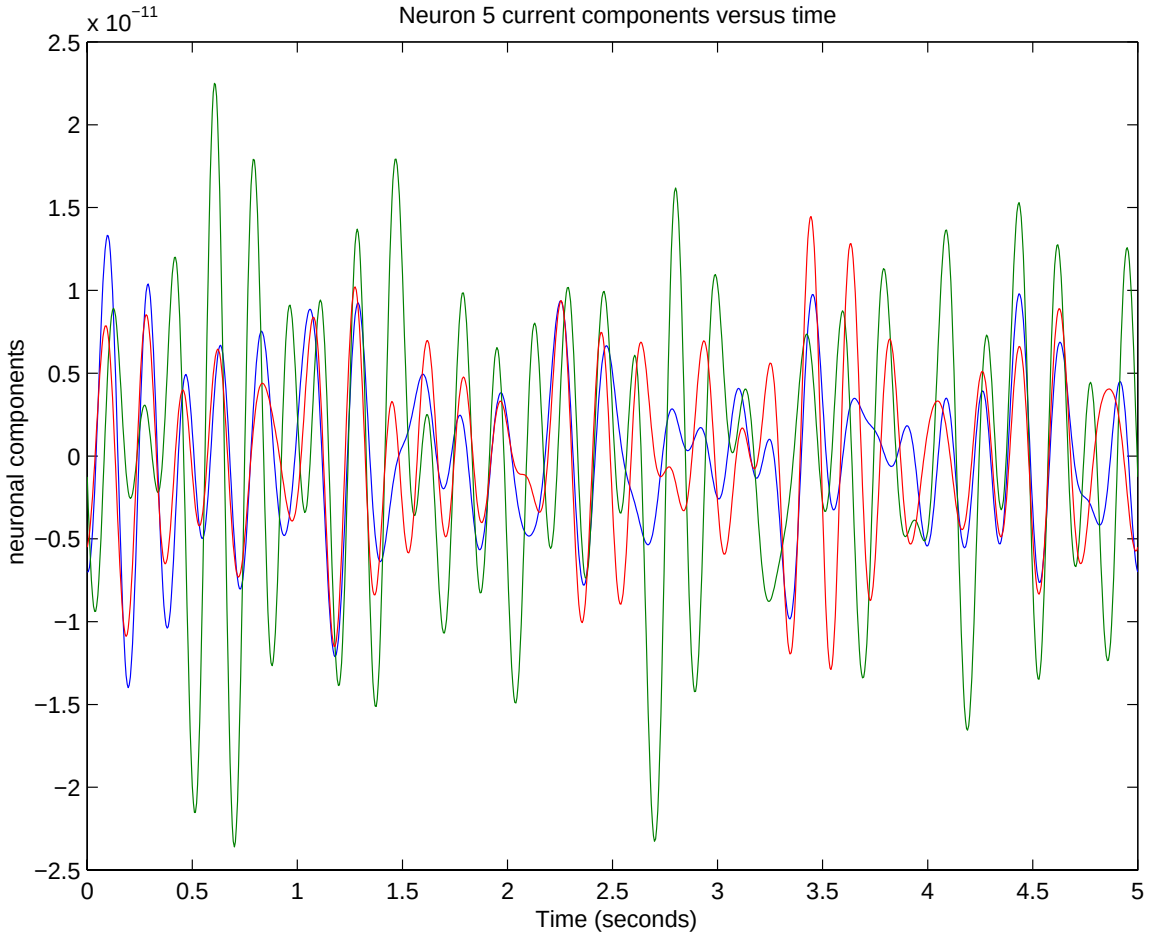

Figure 5: Recovered Neuron 5 Current Components Versus Time

For $q = 5$ the neuronal location, in spherical coordinates is,

$$(r_q, \theta_q, \phi_q) = (.0800, 46., 180.) \tag{3.1.1.5}$$

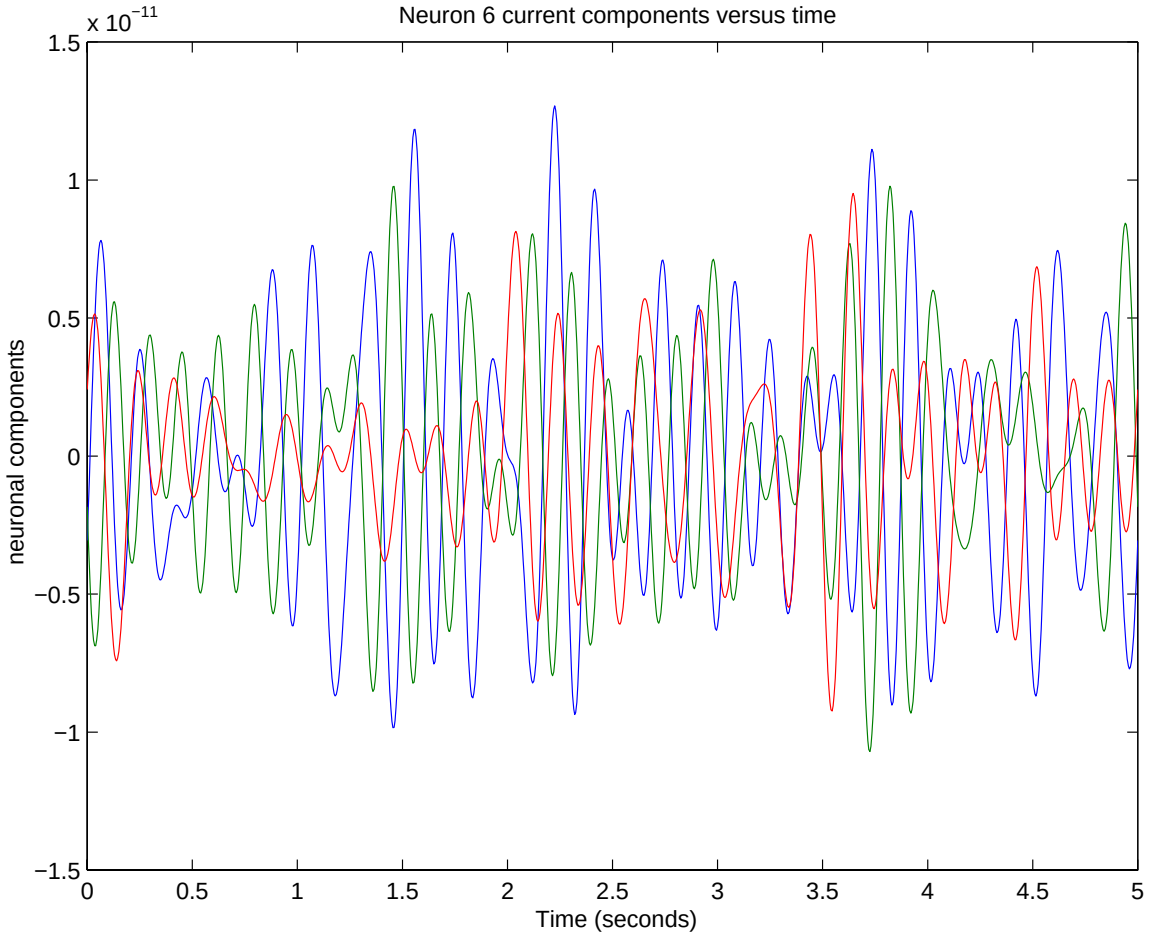

Figure 6: Recovered Neuron 6 Current Components Versus Time

For $q = 6$ the neuronal location, in spherical coordinates is,

$$(r_q, \theta_q, \phi_q) = (.0800, 60., 39.) \tag{3.1.1.6}$$

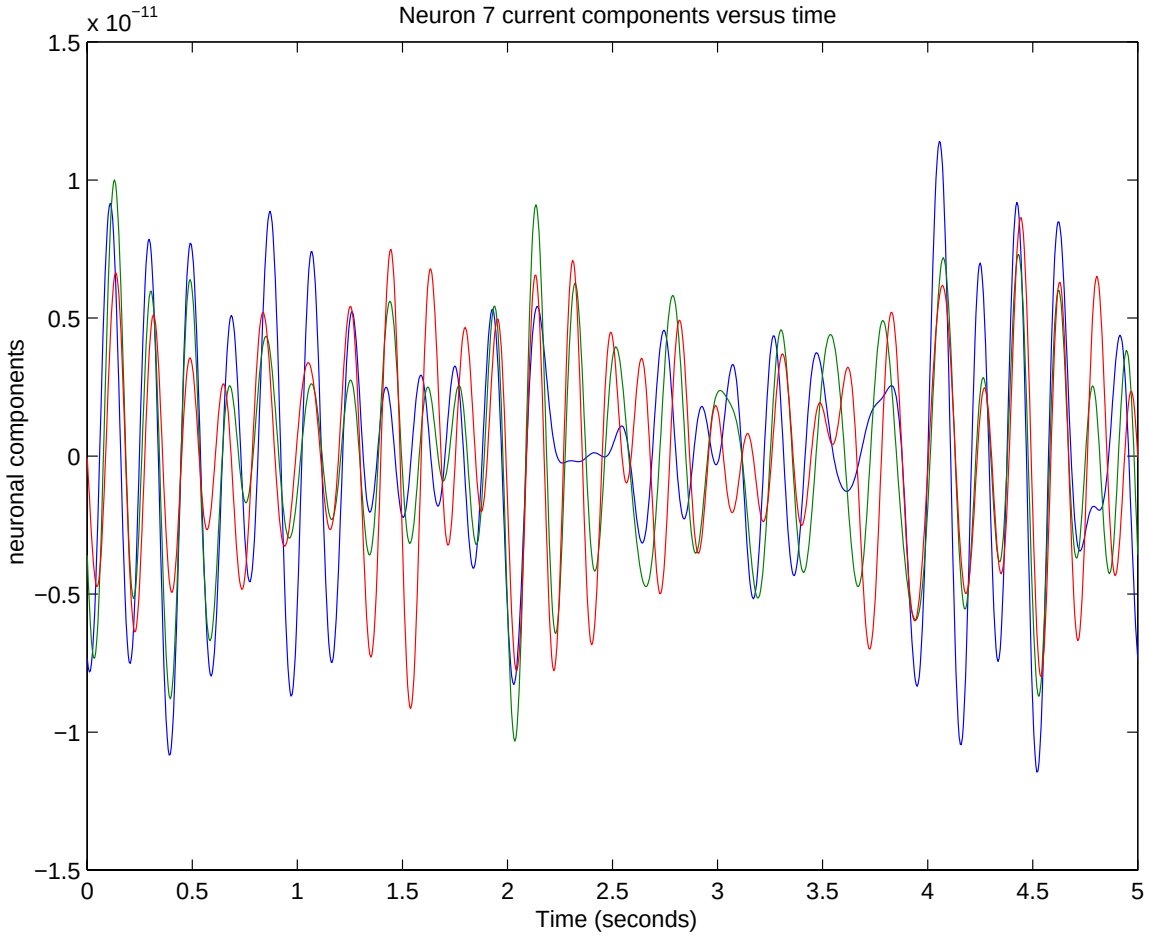

Figure 7: Recovered Neuron 7 Current Components Versus Time

For $q = 7$ the neuronal location, in spherical coordinates is,

$$(r_q, \theta_q, \phi_q) = (.0800, 60., 321.) \tag{3.1.1.7}$$

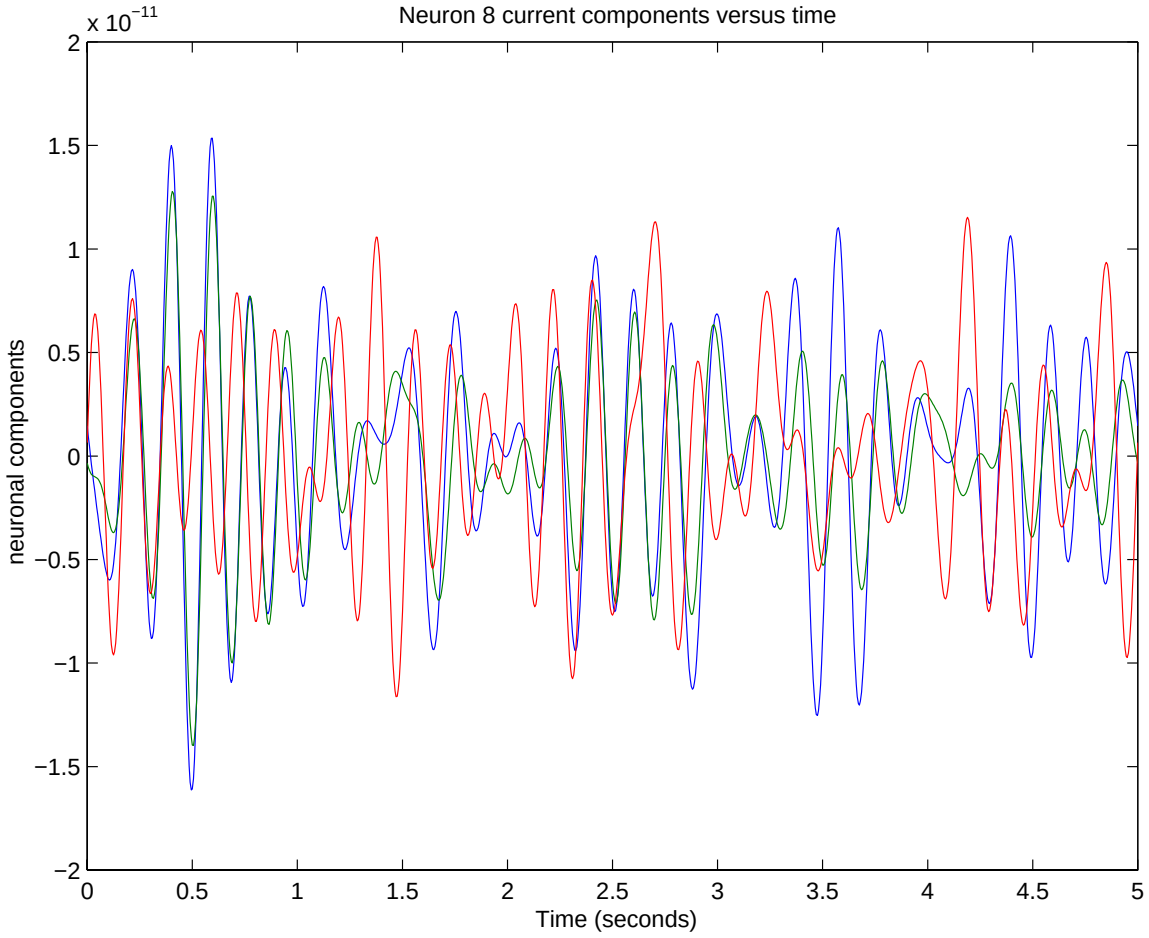

Figure 8: Recovered Neuron 8 Current Components Versus Time

For $q = 8$ the neuronal location, in spherical coordinates is,

$$(r_q, \theta_q, \phi_q) = (.0800, 60., 141.) \tag{3.1.1.8}$$

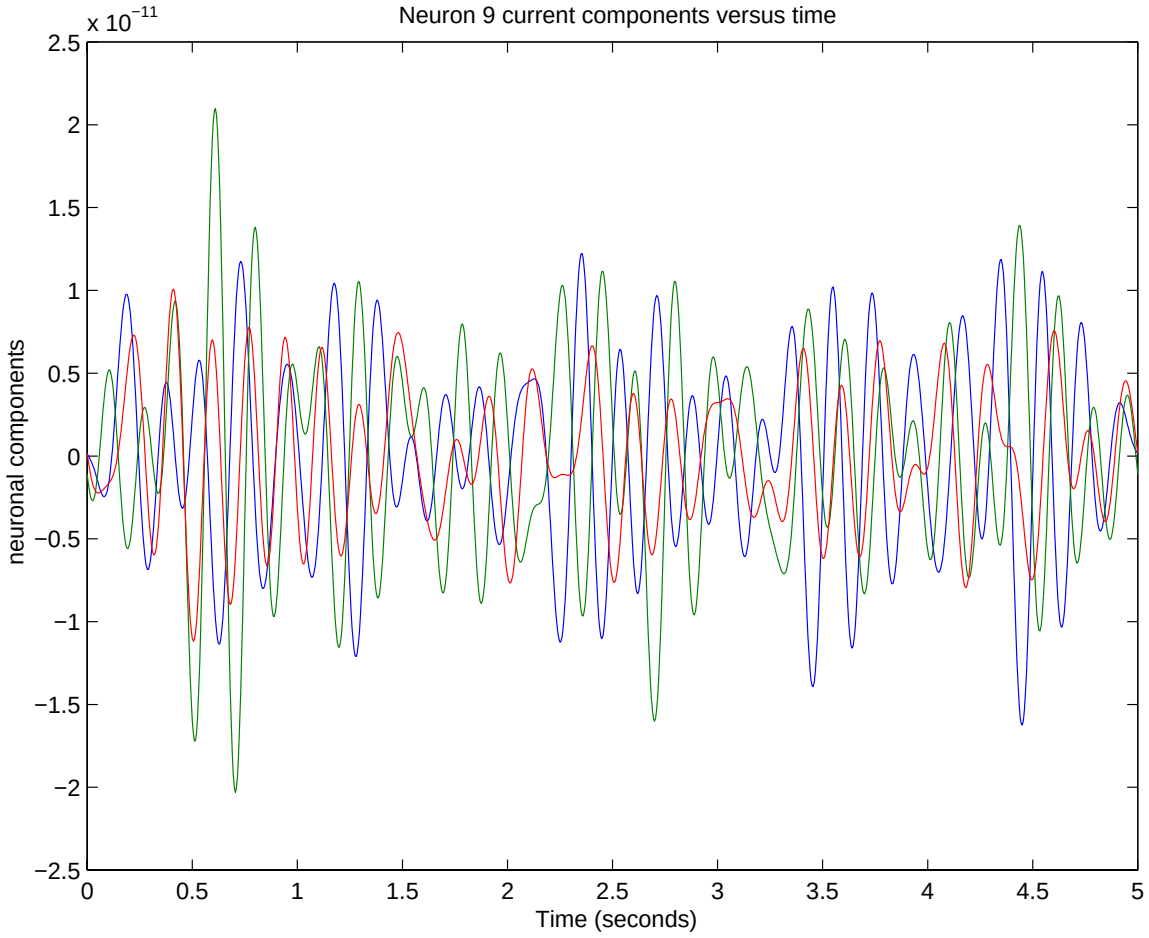

Figure 9: Recovered Neuron 9 Current Components Versus Time

For $q = 9$ the neuronal location, in spherical coordinates is,

$$(r_q, \theta_q, \phi_q) = (.0800, 60., 229.) \tag{3.1.1.9}$$

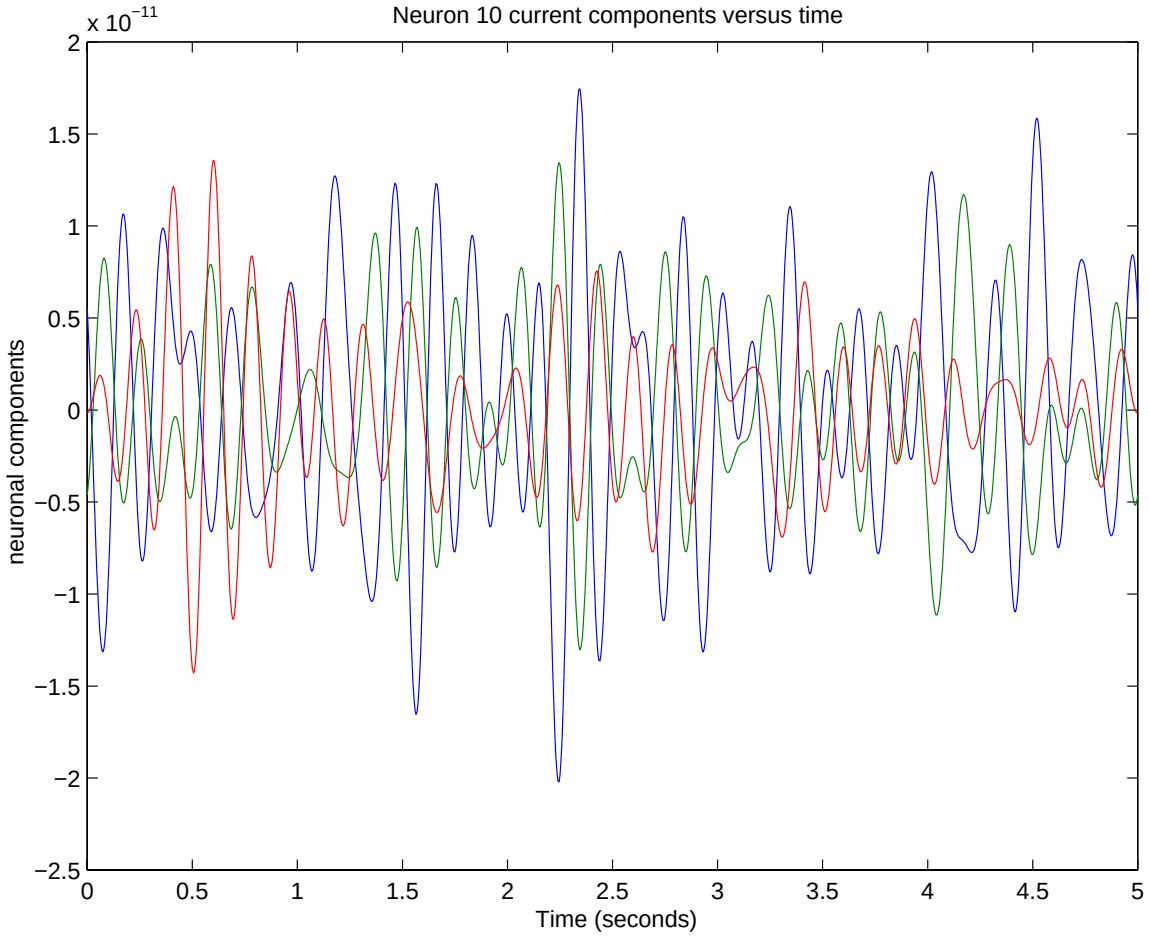

Figure 10: Recovered Neuron 10 Current Components Versus Time

For $q = 10$ the neuronal location, in spherical coordinates is,

$$(r_q, \theta_q, \phi_q) = (.0800, 92., 242.) \tag{3.1.1.10}$$

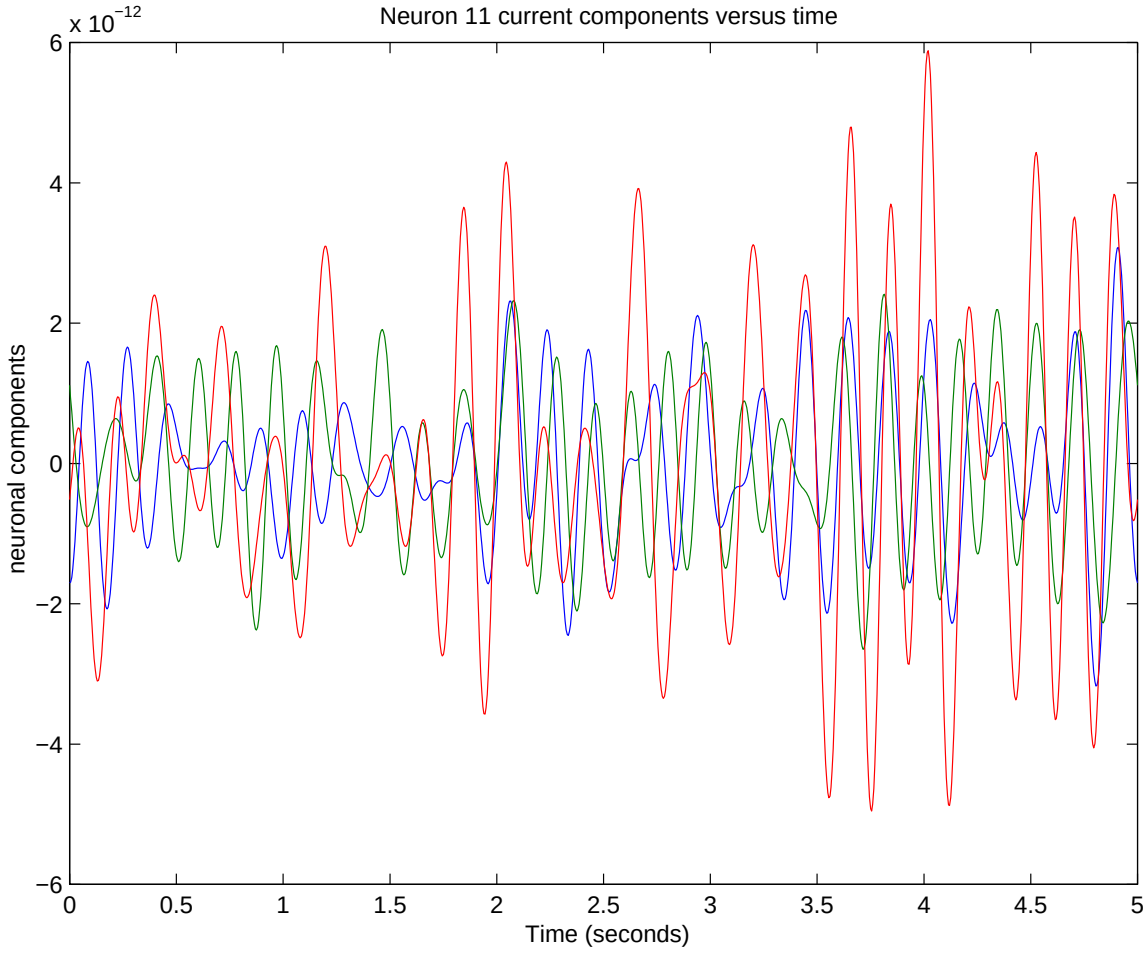

Figure 11: Recovered Neuron 11 Current Components Versus Time

For $q = 11$ the neuronal location, in spherical coordinates is,

$$(r_q, \theta_q, \phi_q) = (.0800, 92., 18.) \tag{3.1.1.11}$$

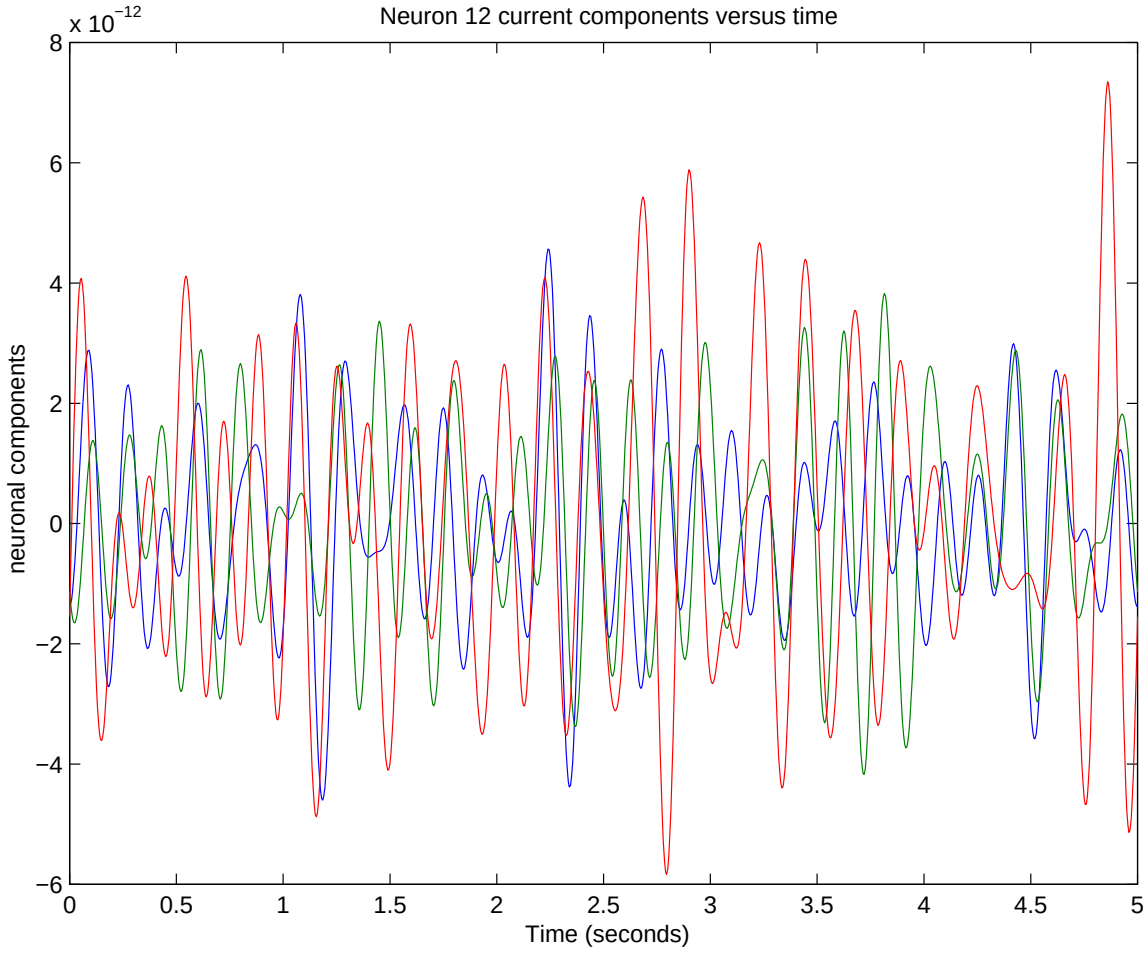

Figure 12: Recovered Neuron 12 Current Components Versus Time

For $q = 12$ the neuronal location, in spherical coordinates is,

$$(r_q, \theta_q, \phi_q) = (.0800, 92., 90.) \tag{3.1.1.12}$$

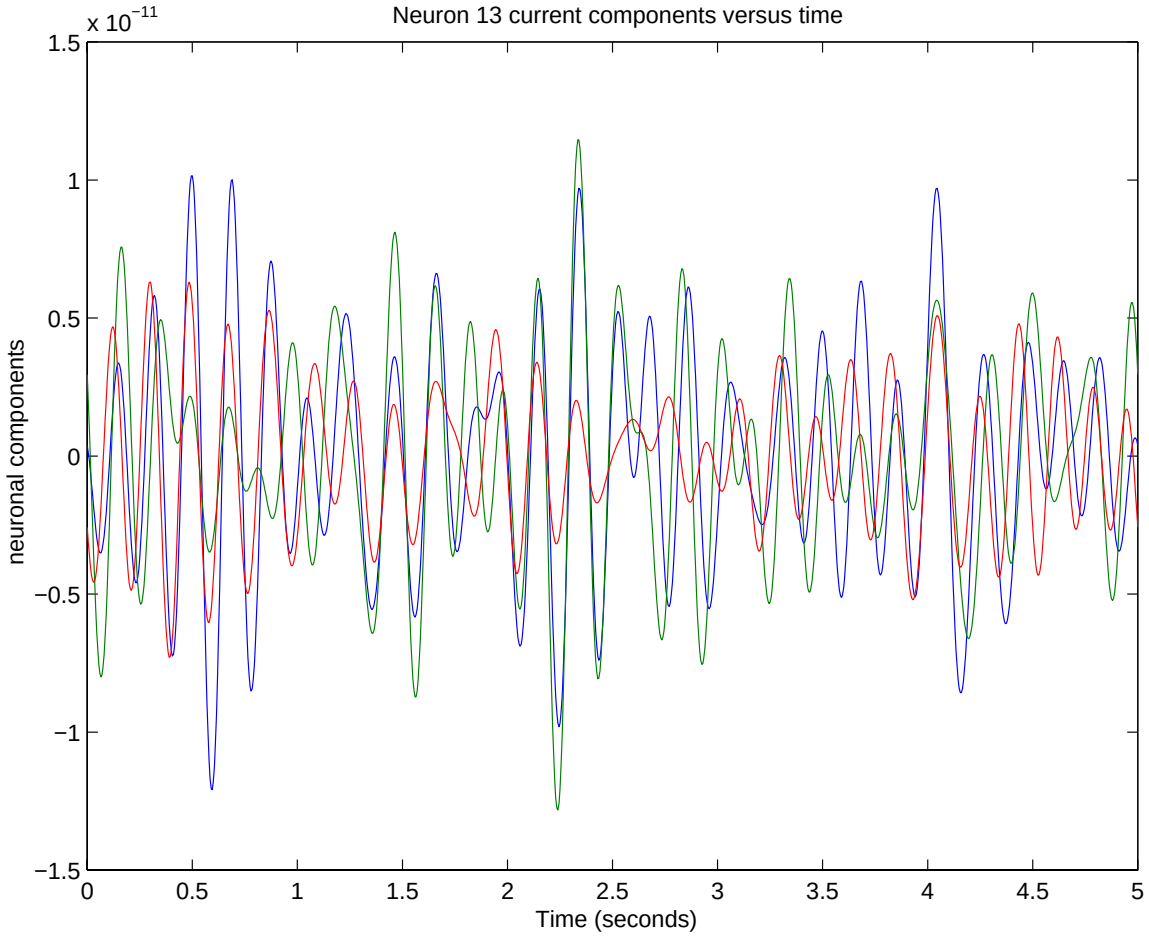

Figure 13: Recovered Neuron 13 Current Components Versus Time

For $q = 13$ the neuronal location, in spherical coordinates is,

$$(r_q, \theta_q, \phi_q) = (.0800, 92., 270.) \tag{3.1.1.13}$$

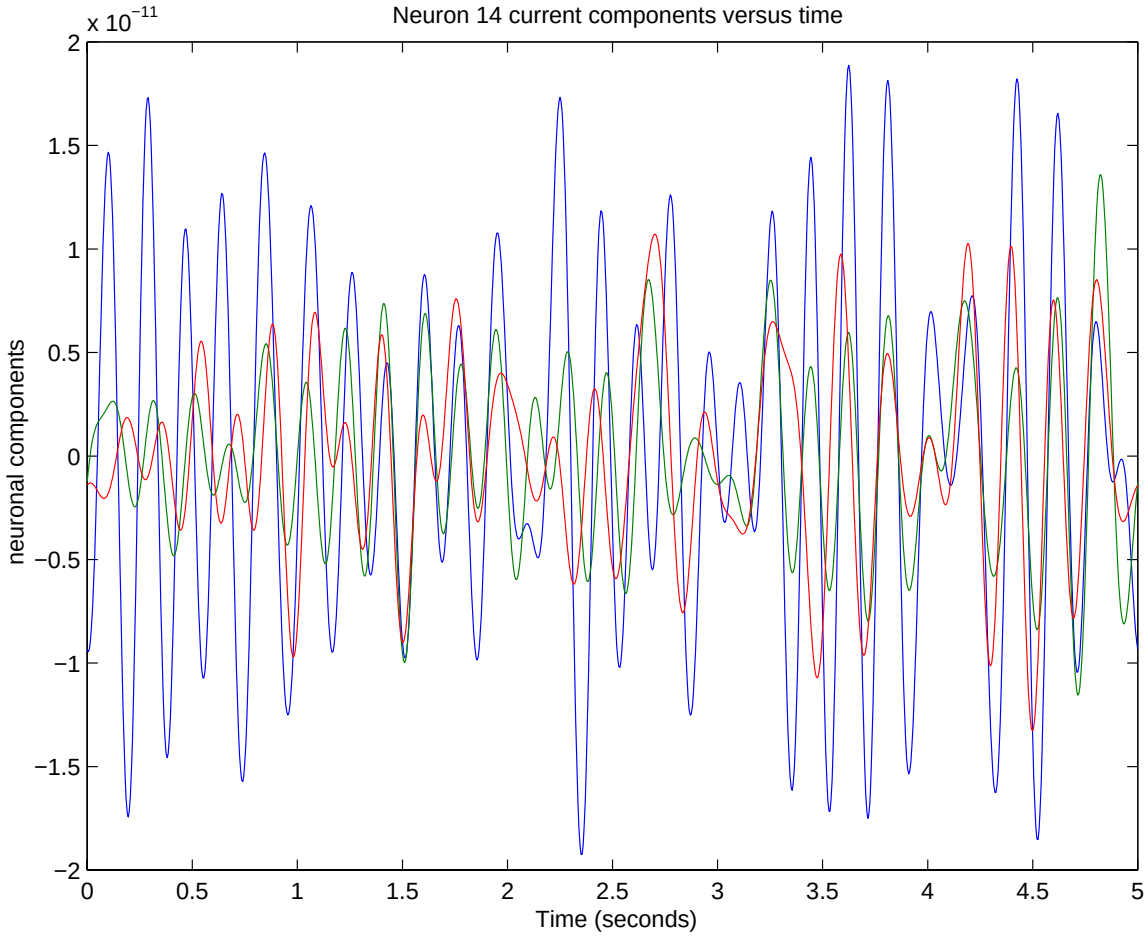

Figure 14: Recovered Neuron 14 Current Components Versus Time

For $q = 14$ the neuronal location, in spherical coordinates is,

$$(r_q, \theta_q, \phi_q) = (.0800, 92., 162.) \tag{3.1.1.14}$$

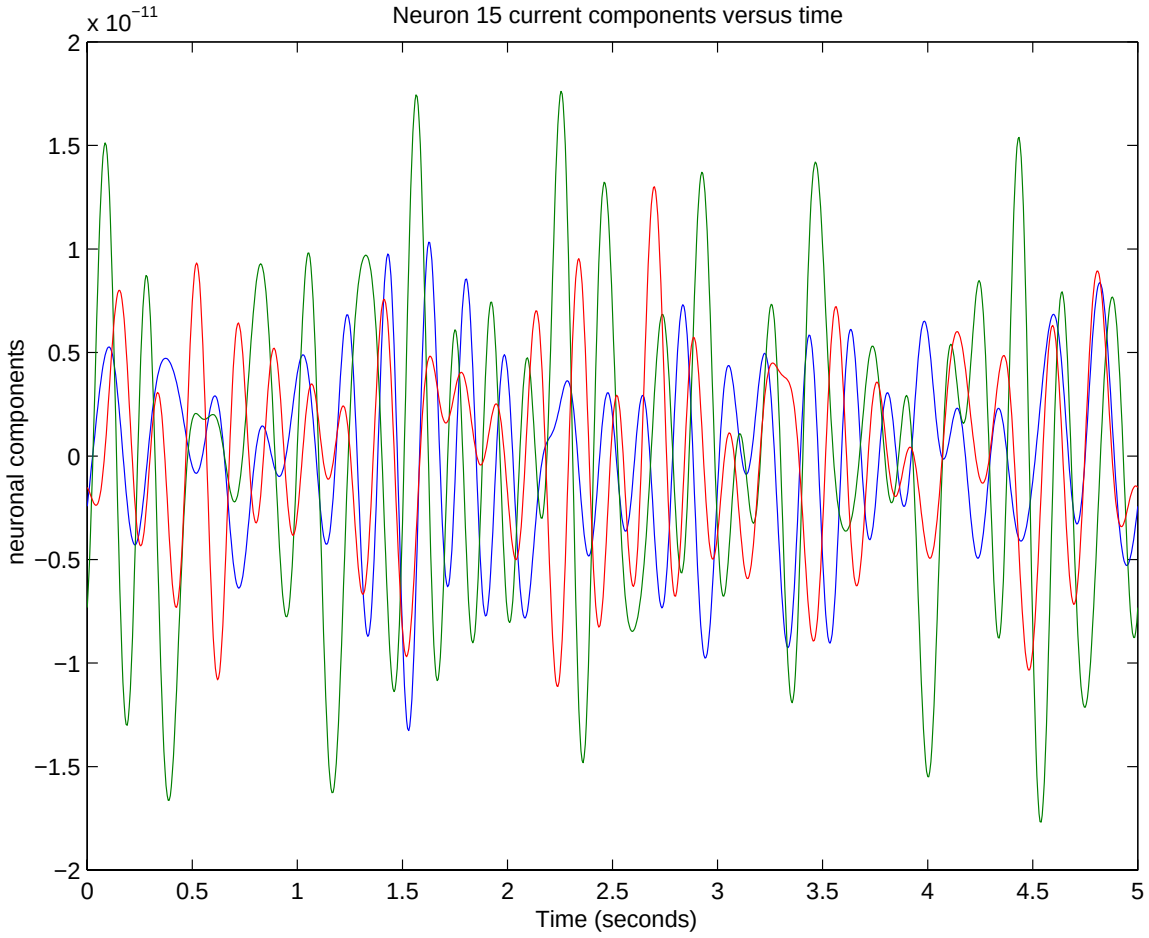

Figure 15: Recovered Neuron 15 Current Components Versus Time

For $q = 15$ the neuronal location, in spherical coordinates is,

$$(r_q, \theta_q, \phi_q) = (.0800, 92., 198.) \tag{3.1.1.15}$$

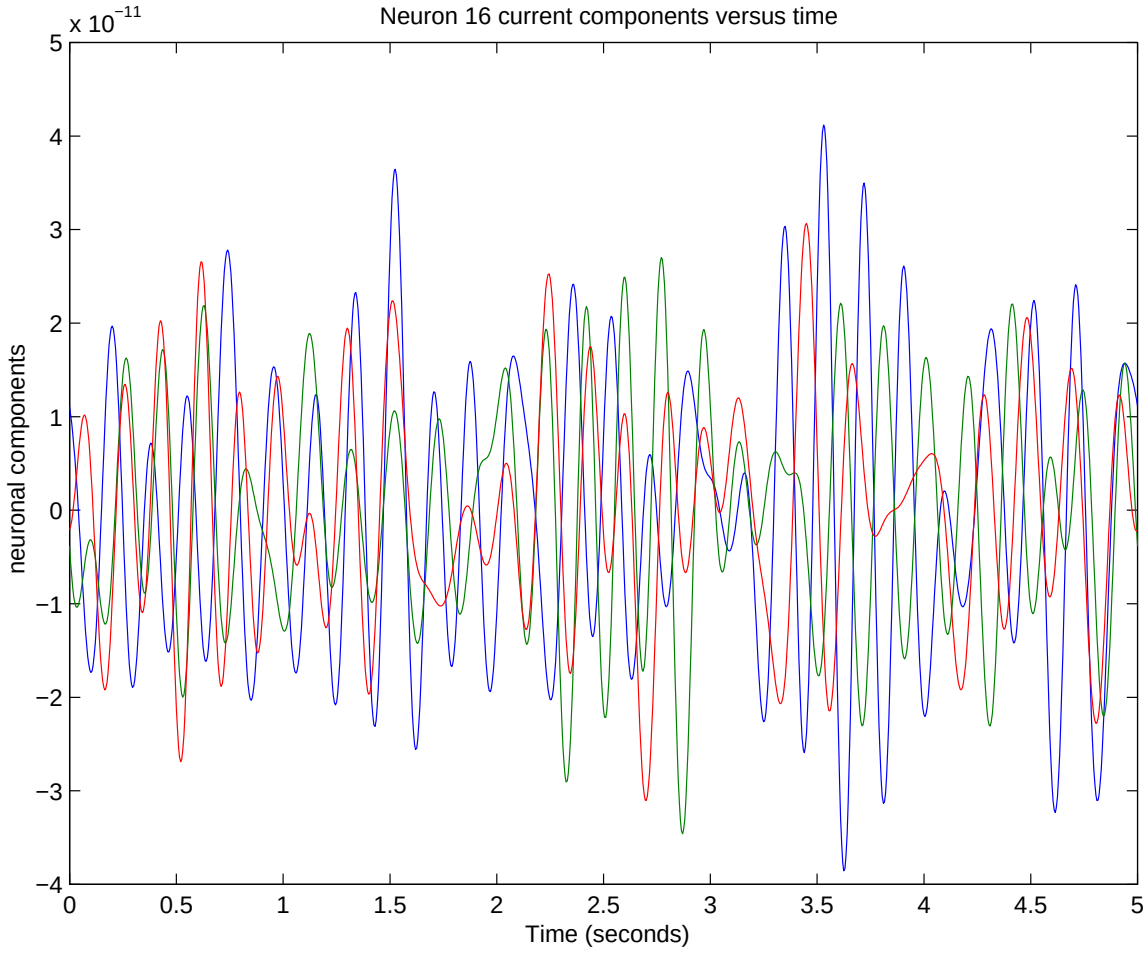

Figure 16: Recovered Neuron 15 Current Components Versus Time

For $q = 16$ the neuronal location, in spherical coordinates is,

$$(r_q, \theta_q, \phi_q) = (.0800, 92., 180.) \tag{3.1.1.16}$$

3.1.2 Frequency Components and Neuronal Source and Neural Source Locations for the 5 Seconds of Data

For $q = 1$ the neuronal location, in spherical coordinates is,

$$(r_q, \theta_q, \phi_q) = (.0800, 1., 0.) \tag{3.1.2.1}$$

For $q = 2$ the neuronal location, in spherical coordinates is,

$$(r_q, \theta_q, \phi_q) = (.0800, 46., 0.) \tag{3.1.2.2}$$

For $q = 3$ the neuronal location, in spherical coordinates is,

$$(r_q, \theta_q, \phi_q) = (.0800, 46., 90.) \tag{3.1.2.3}$$

For $q = 4$ the neuronal location, in spherical coordinates is,

$$(r_q, \theta_q, \phi_q) = (.0800, 46., 270.) \tag{3.1.2.4}$$

For $q = 5$ the neuronal location, in spherical coordinates is,

$$(r_q, \theta_q, \phi_q) = (.0800, 46., 180.) \tag{3.1.2.5}$$

For $q = 6$ the neuronal location, in spherical coordinates is,

$$(r_q, \theta_q, \phi_q) = (.0800, 60., 39.) \tag{3.1.2.6}$$

For $q = 7$ the neuronal location, in spherical coordinates is,

$$(r_q, \theta_q, \phi_q) = (.0800, 60., 321.) \tag{3.1.2.7}$$

For $q = 8$ the neuronal location, in spherical coordinates is,

$$(r_q, \theta_q, \phi_q) = (.0800, 60., 141.) \tag{3.1.2.8}$$

For $q = 9$ the neuronal location, in spherical coordinates is,

$$(r_q, \theta_q, \phi_q) = (.0800, 60., 229.) \tag{3.1.2.9}$$

For $q = 10$ the neuronal location, in spherical coordinates is,

$$(r_q, \theta_q, \phi_q) = (.0800, 92., 242.) \tag{3.1.2.10}$$

For $q = 11$ the neuronal location, in spherical coordinates is,

$$(r_q, \theta_q, \phi_q) = (.0800, 92., 18.) \tag{3.1.2.11}$$

For $q = 12$ the neuronal location, in spherical coordinates is,

$$(r_q, \theta_q, \phi_q) = (.0800, 92., 90.) \tag{3.1.2.12}$$

For $q = 13$ the neuronal location, in spherical coordinates is,

$$(r_q, \theta_q, \phi_q) = (.0800, 92., 270.) \tag{3.1.2.13}$$

For $q = 14$ the neuronal location, in spherical coordinates is,

$$(r_q, \theta_q, \phi_q) = (.0800, 92., 162.) \tag{3.1.2.14}$$

For $q = 15$ the neuronal location, in spherical coordinates is,

$$(r_q, \theta_q, \phi_q) = (.0800, 92., 198.) \tag{3.1.2.15}$$

For $q = 16$ the neuronal location, in spherical coordinates is,

$$(r_q, \theta_q, \phi_q) = (.0800, 92., 180.) \tag{3.1.2.16}$$

The set of 30 frequencies, in Hertz, for frequency components recovered are

$$\mathcal{F} = \{.2, .4, .6, .8, 1.0, 1.2, 1.4, 1.6, 1.8, 2.0, \cdots, 5.0, 5.2, 5.4, 5.6, 5.8, 6.0\} \tag{3.1.2.17}$$

3.1.3 Recovery of 30 Evenly Spaced Frequency Components from 1 to 30 Hertz at 17 Potential Sites of Brain Activity for 1 Second of EEG Data

We find a dynamic representation of brain activity, we interrogate it with brain activity independent scalar interrogating functions that satisfy the same boundary conditions that are satisifed by the dynamic voltage wave. We go from the scalp surface through the skull bone without surgery to the brain activity. We process this recovery by recording the time profile of each component of neuronal activity on each site of potential brain activity. There are now three computer programs DYNHSV.FOR which produces the dynamic head surface voltage representation, EEBARIS.FOR which is the brain activity recovery inverse source solution which uses the output from DYNHSV.FOR, and produces output for the plotting program EEGPLOT.FOR which plots the recovered currents as a function of time. These are carried out for 30 evenly spaced frequency components from 1 to 30 Hertz

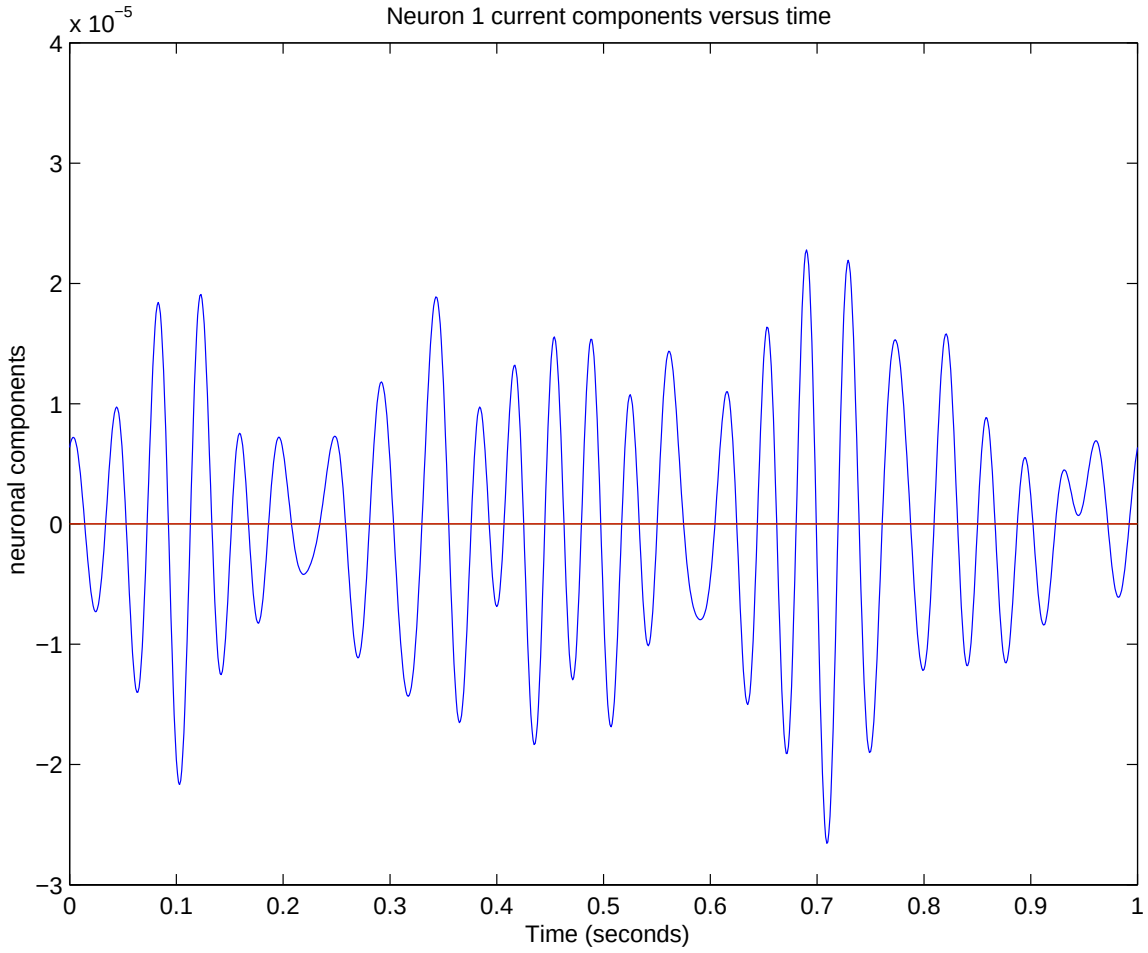

Figure 17: Recovered Neuron 1 Current Components Versus Time

For $q = 1$ the neuronal location, in spherical coordinates is,

$$(r_q, \theta_q, \phi_q) = (.0100, 1., 0.) \tag{3.1.3.1}$$

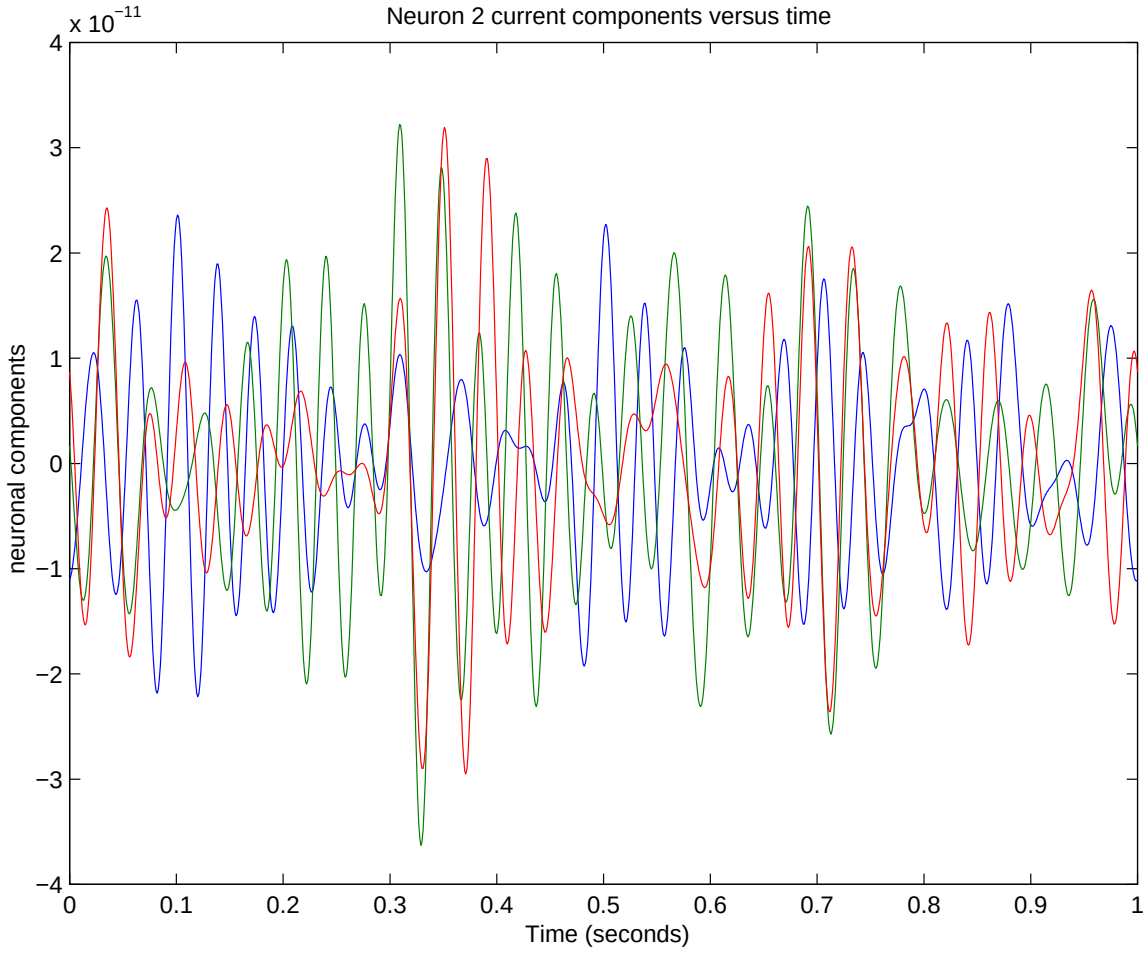

Figure 18: Recovered Neuron 2 Current Components Versus Time

For $q = 2$ the neuronal location, in spherical coordinates is,

$$(r_q, \theta_q, \phi_q) = (.0800, 1., 0.) \tag{3.1.3.2}$$

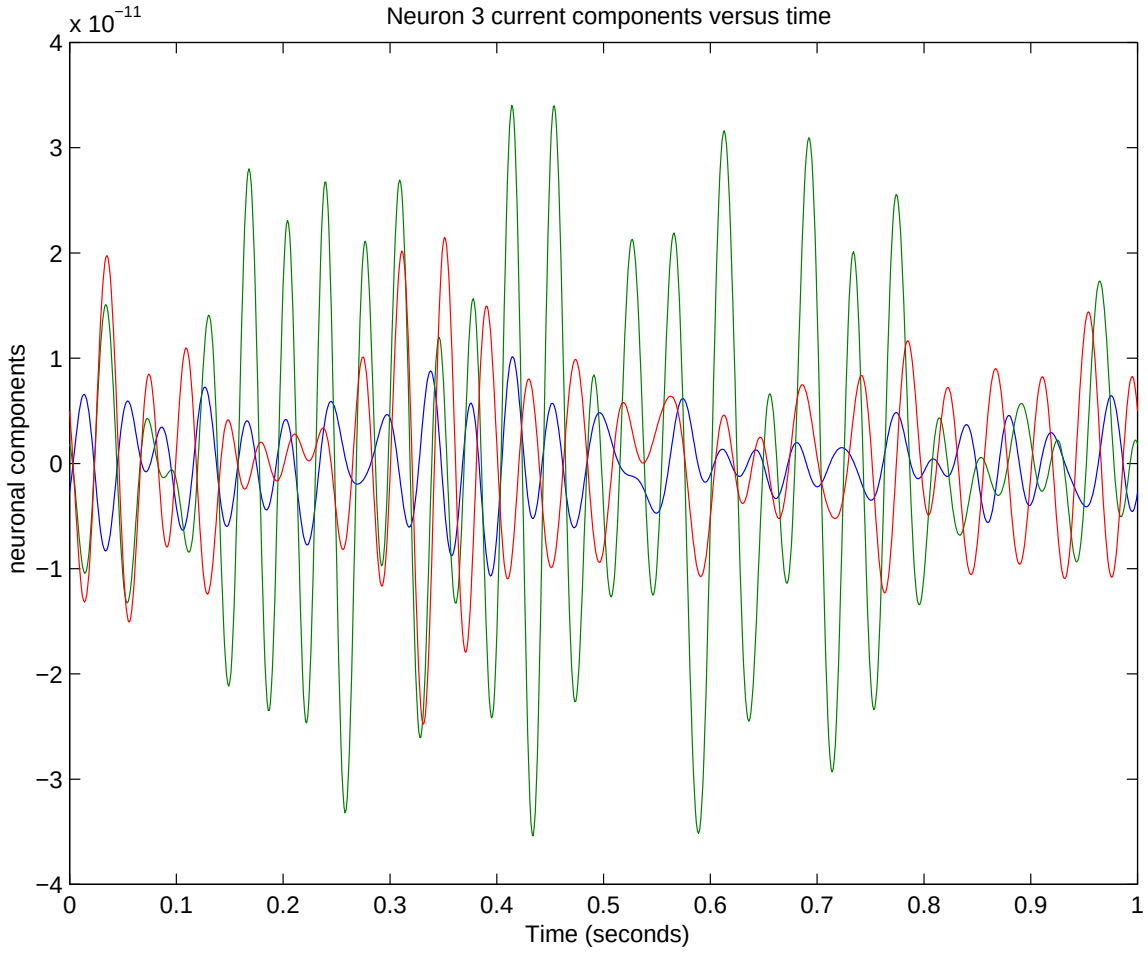

Figure 19: Recovered Neuron 3 Current Components Versus Time

For $q = 3$ the neuronal location, in spherical coordinates is,

$$(r_q, \theta_q, \phi_q) = (.0800, 46., 0.) \tag{3.1.3.3}$$

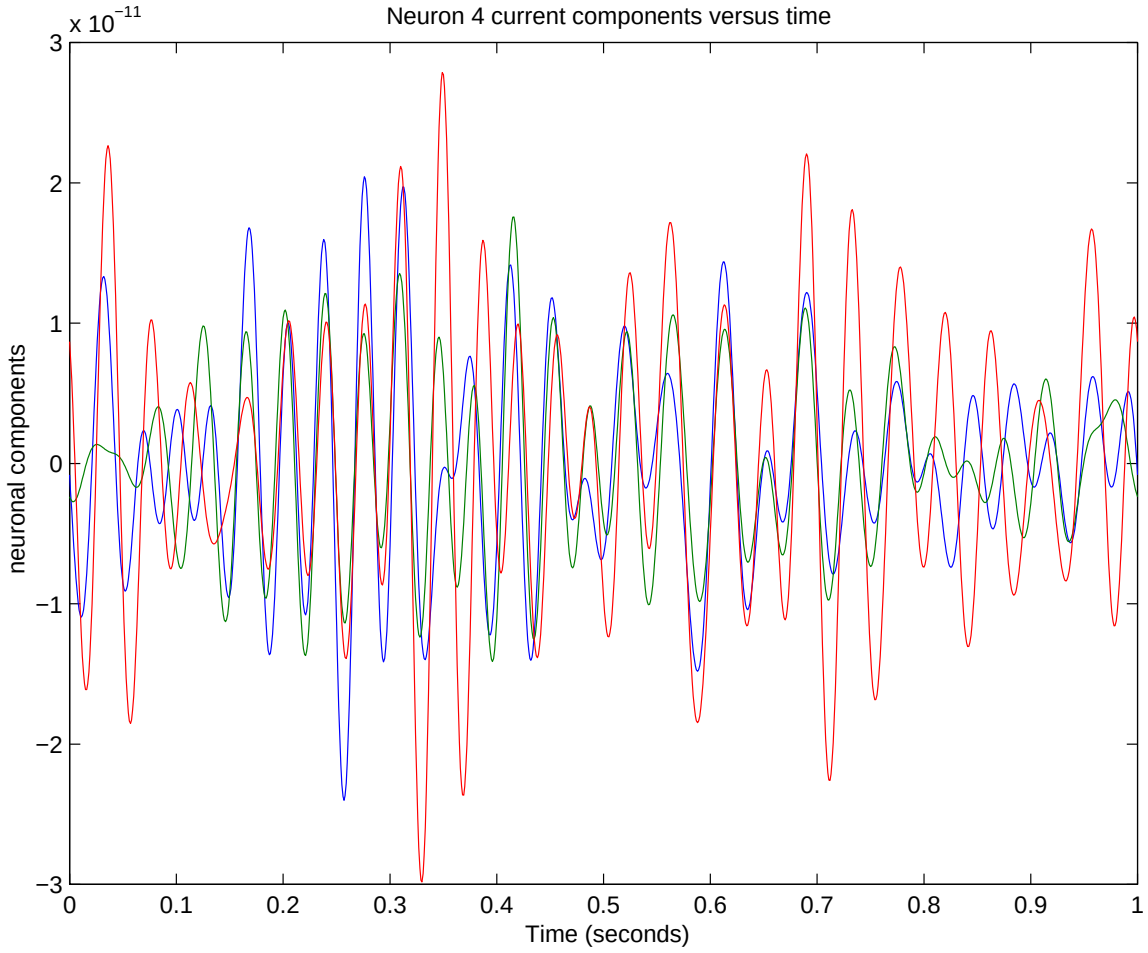

Figure 20: Recovered Neuron 4 Current Components Versus Time

For $q = 4$ the neuronal location, in spherical coordinates is,

$$(r_q, \theta_q, \phi_q) = (.0800, 46., 90.) \tag{3.1.3.4}$$

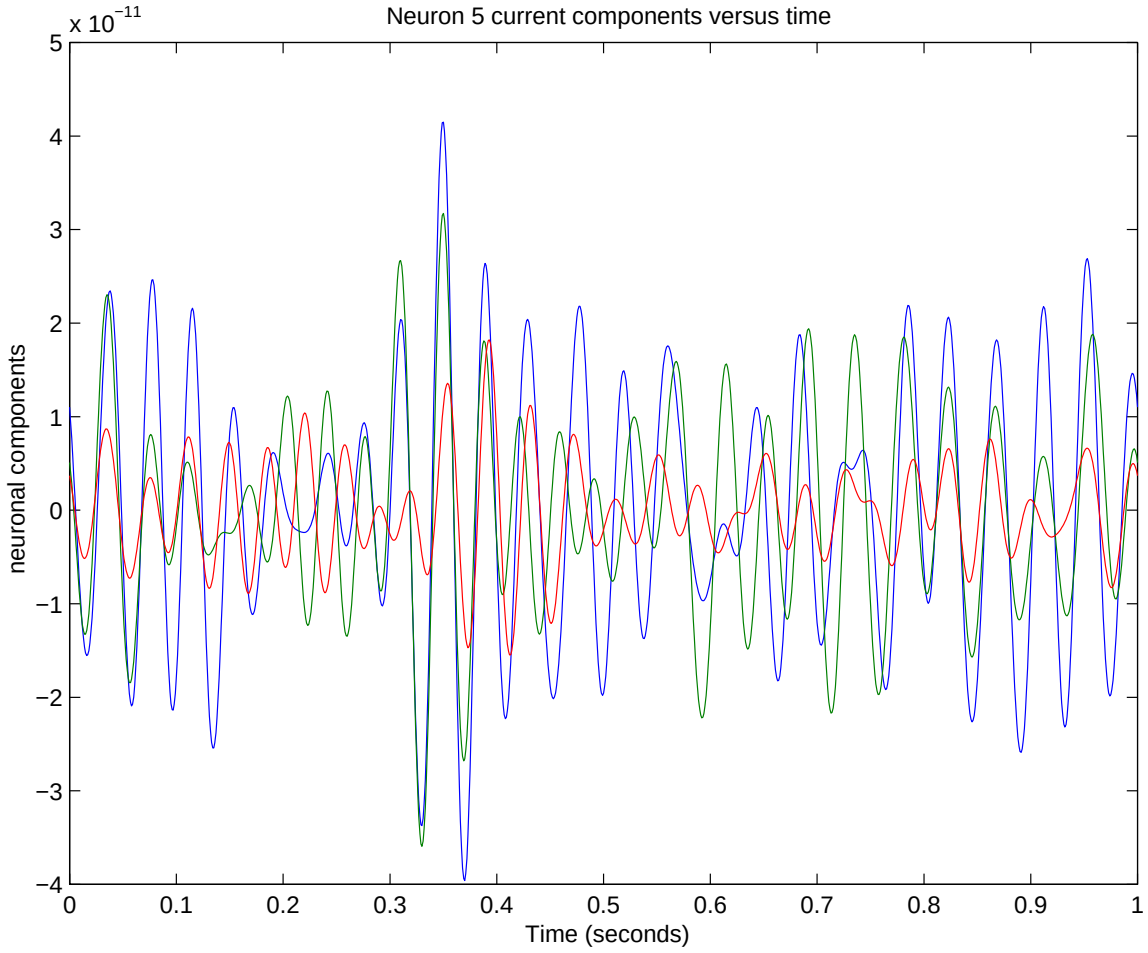

Figure 21: Recovered Neuron 5 Current Components Versus Time

For $q = 5$ the neuronal location, in spherical coordinates is,

$$(r_q, \theta_q, \phi_q) = (.0800, 46., 270.) \tag{3.1.3.5}$$

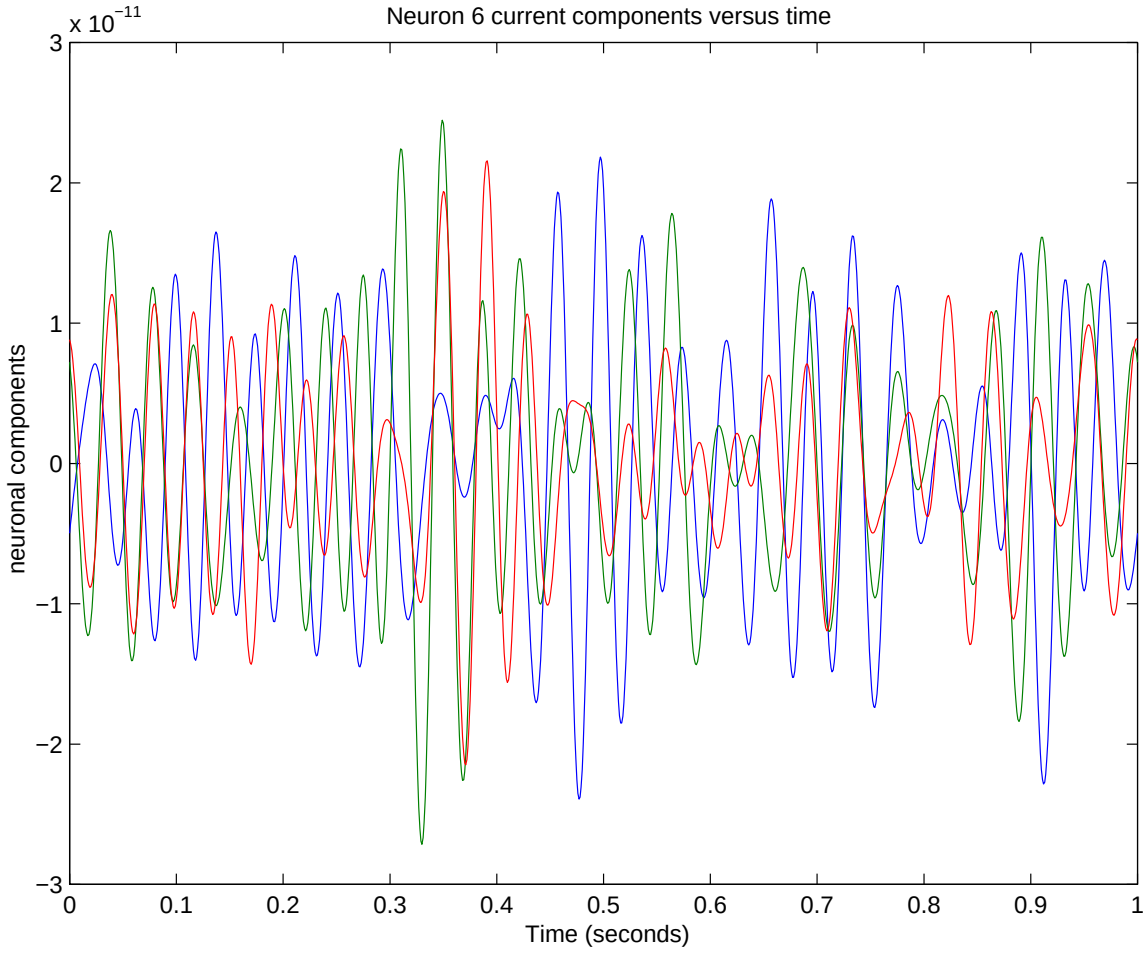

Figure 22: Recovered Neuron 6 Current Components Versus Time

For $q = 6$ the neuronal location, in spherical coordinates is,

$$(r_q, \theta_q, \phi_q) = (.0800, 46., 180.) \tag{3.1.3.6}$$

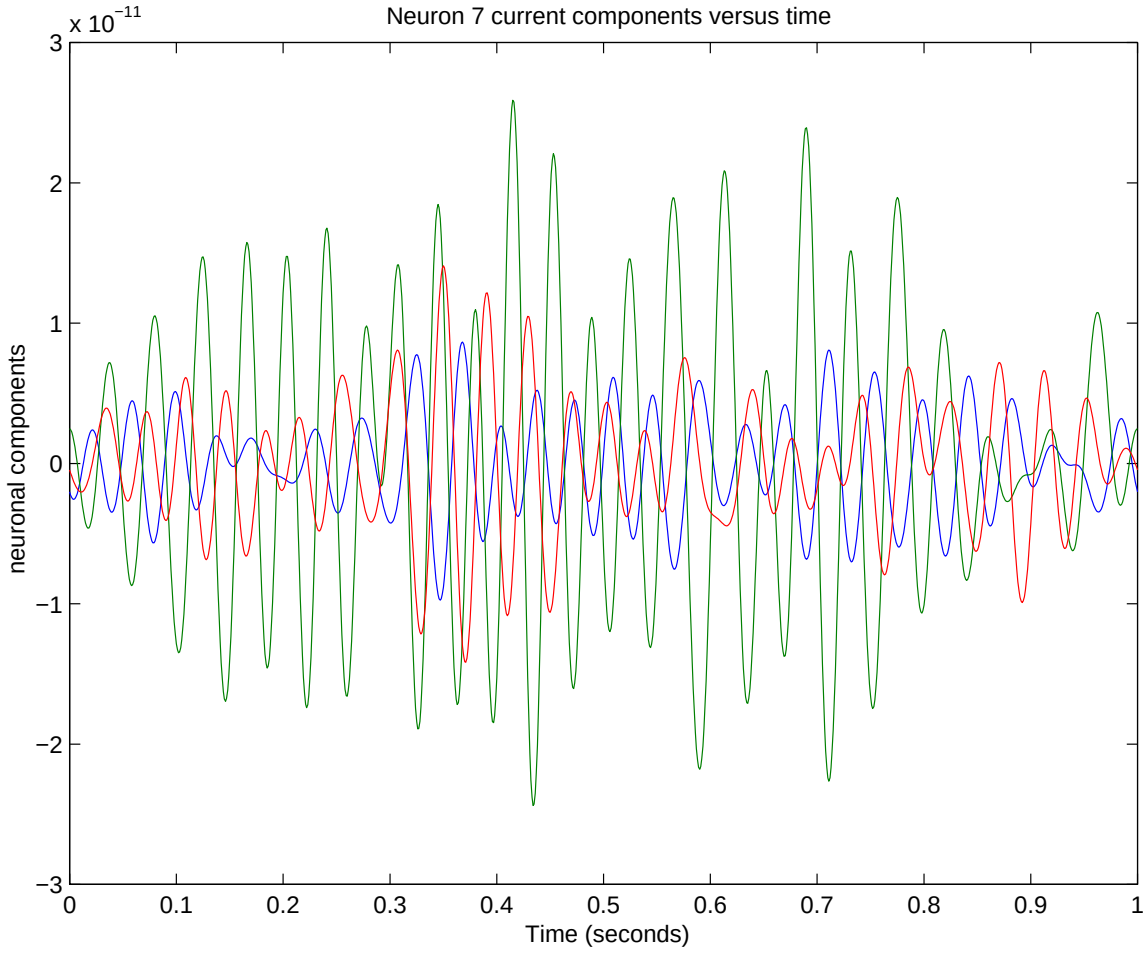

Figure 23: Recovered Neuron 7 Current Components Versus Time

For $q = 7$ the neuronal location, in spherical coordinates is,

$$(r_q, \theta_q, \phi_q) = (.0800, 60., 39.) \tag{3.1.3.7}$$

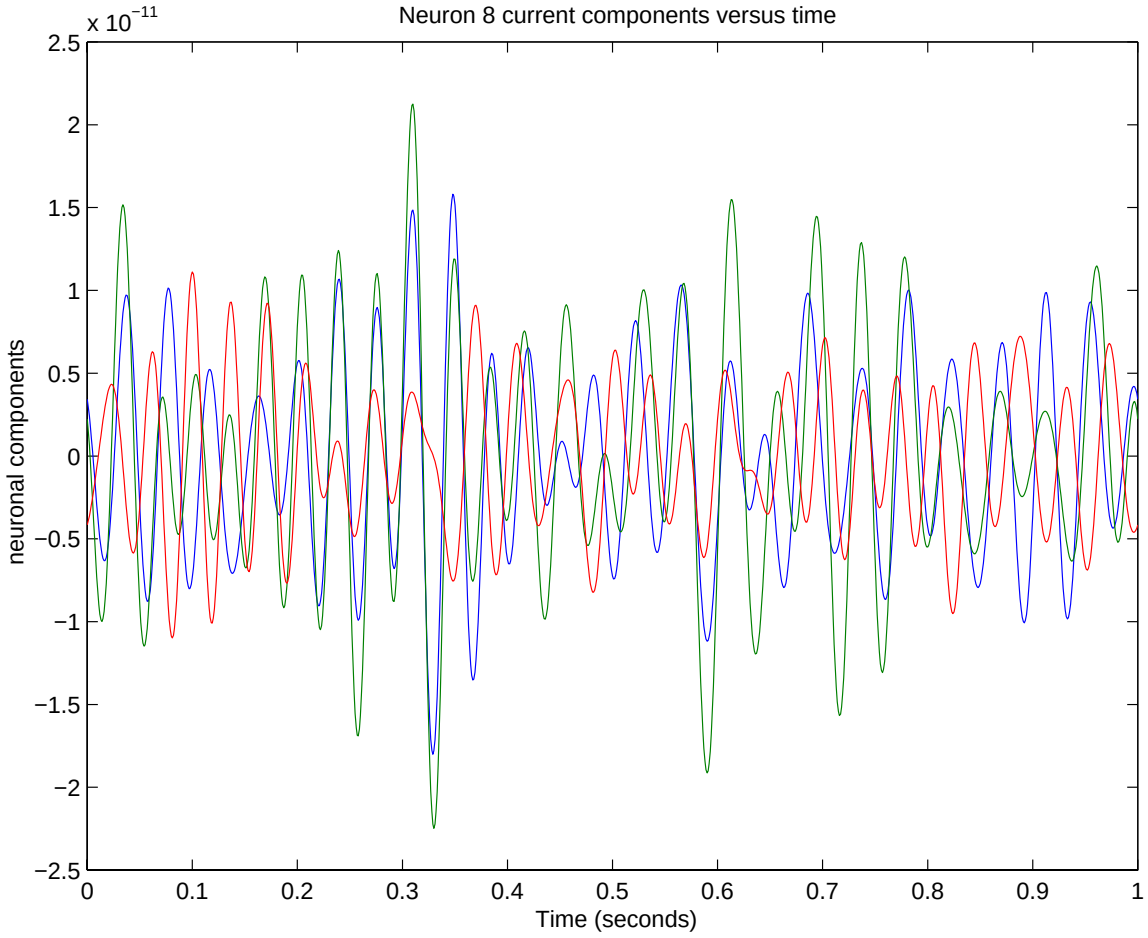

Figure 24: Recovered Neuron 8 Current Components Versus Time

For $q = 8$ the neuronal location, in spherical coordinates is,

$$(r_q, \theta_q, \phi_q) = (.0800, 60., 321.) \tag{3.1.3.8}$$

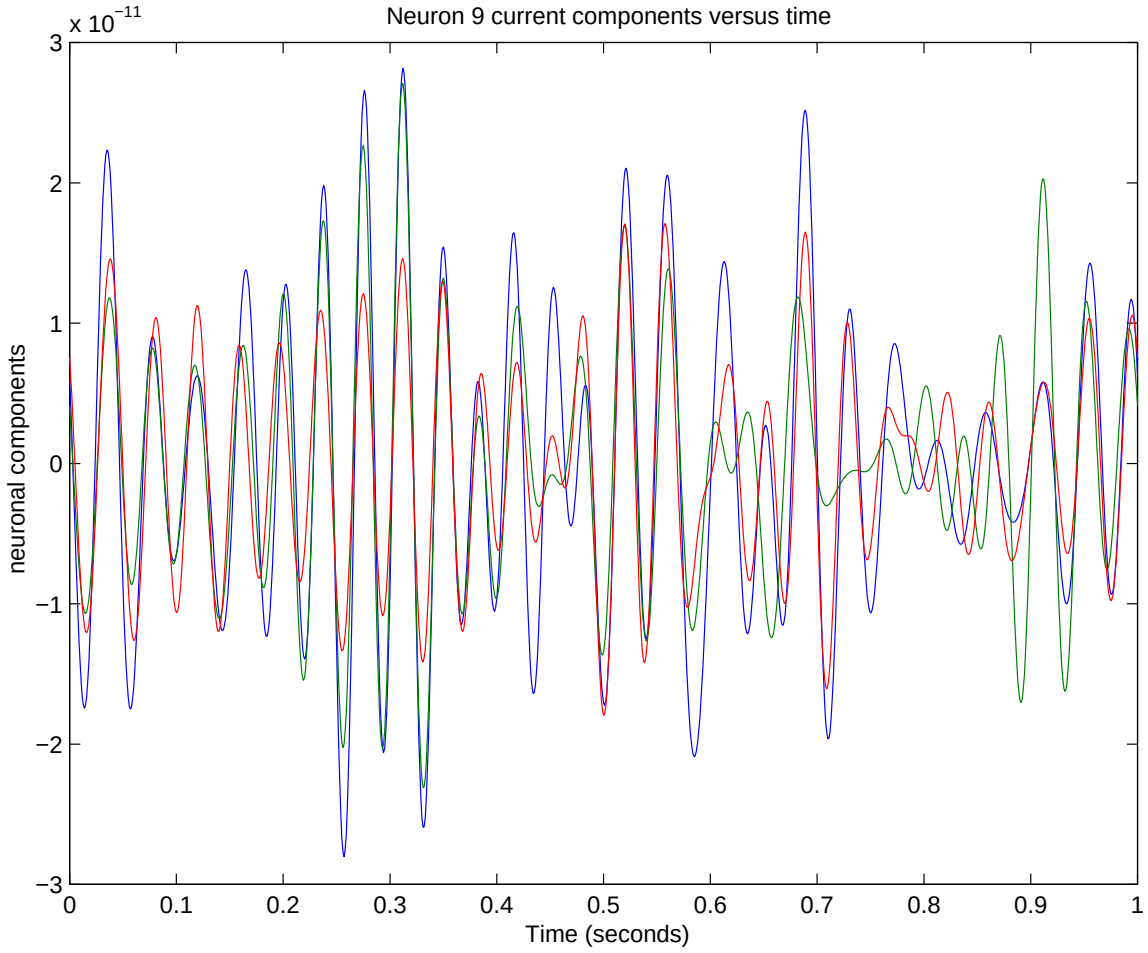

Figure 25: Recovered Neuron 9 Current Components Versus Time

For $q = 9$ the neuronal location, in spherical coordinates is,

$$(r_q, \theta_q, \phi_q) = (.0800, 60., 141.) \tag{3.1.3.9}$$

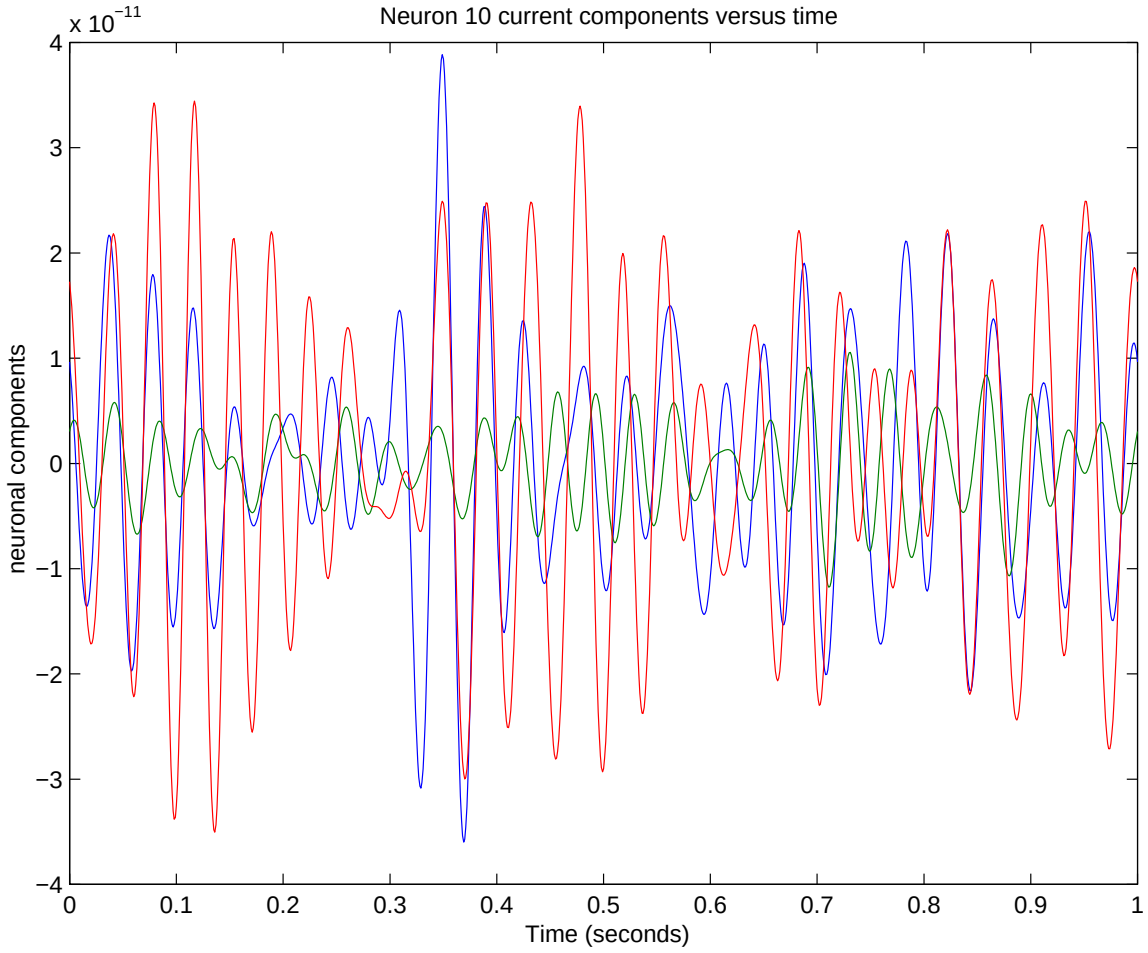

Figure 26: Recovered Neuron 10 Current Components Versus Time

For $q = 10$ the neuronal location, in spherical coordinates is,

$$(r_q, \theta_q, \phi_q) = (.0800, 60., 229.) \tag{3.1.3.10}$$

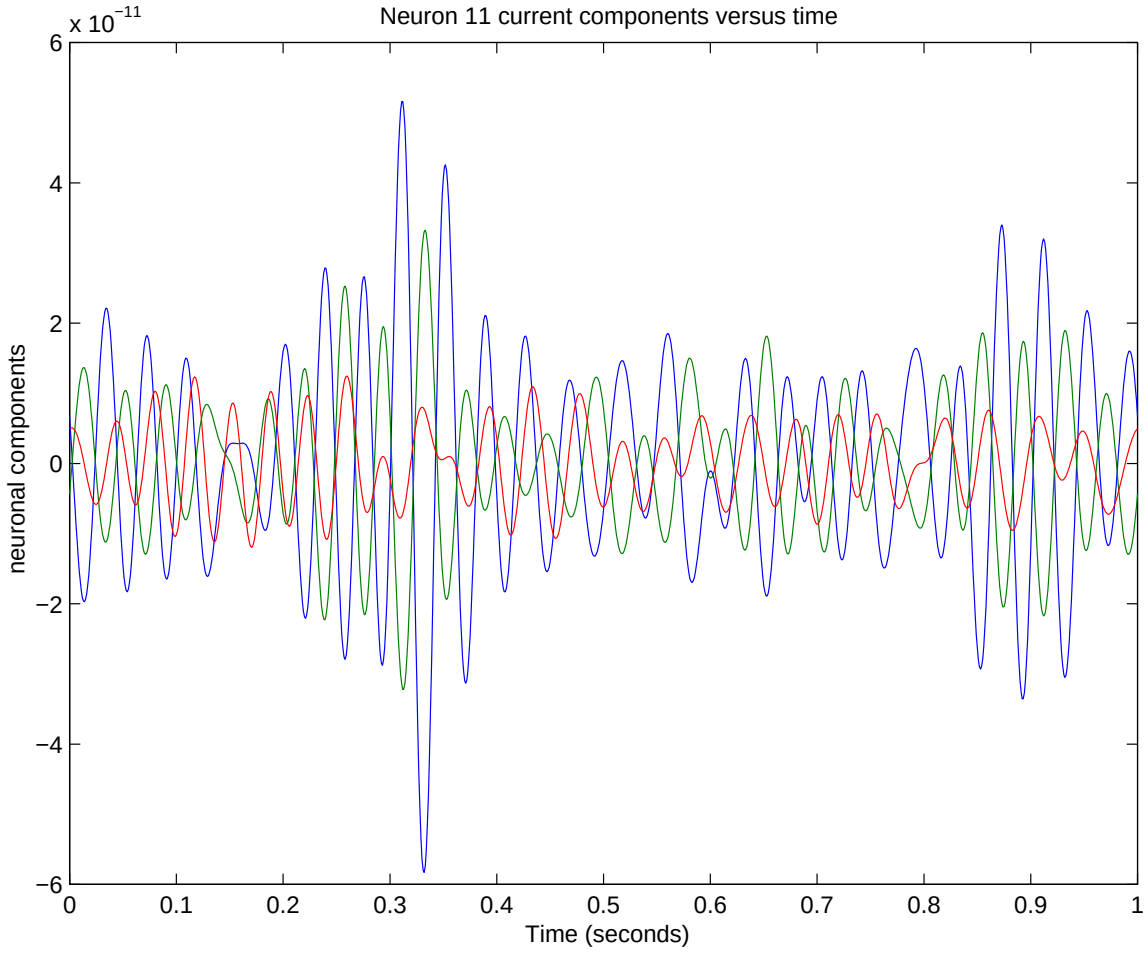

Figure 27: Recovered Neuron 11 Current Components Versus Time

For $q = 11$ the neuronal location, in spherical coordinates is,

$$(r_q, \theta_q, \phi_q) = (.0800, 92., 242.) \tag{3.1.3.11}$$

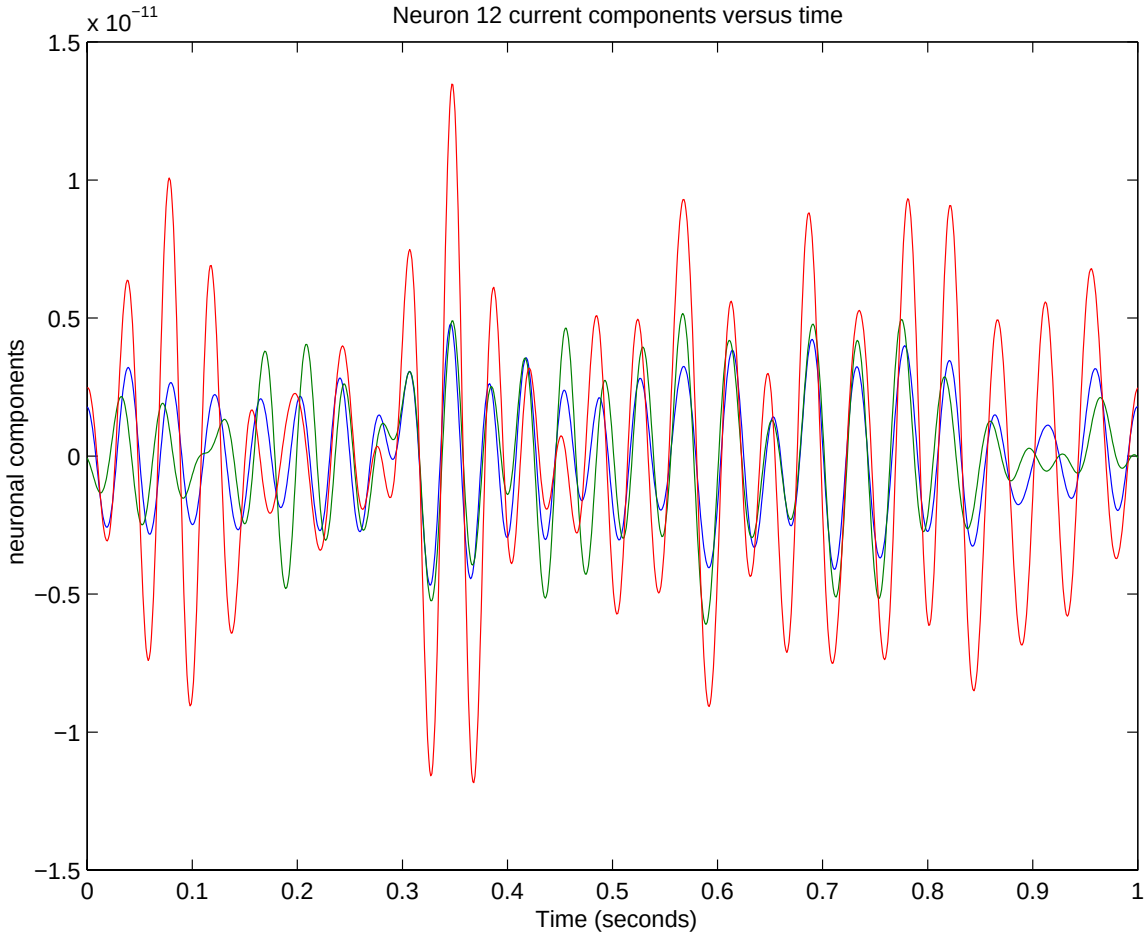

Figure 28: Recovered Neuron 12 Current Components Versus Time

For $q = 12$ the neuronal location, in spherical coordinates is,

$$(r_q, \theta_q, \phi_q) = (.0800, 92., 18.) \tag{3.1.3.12}$$

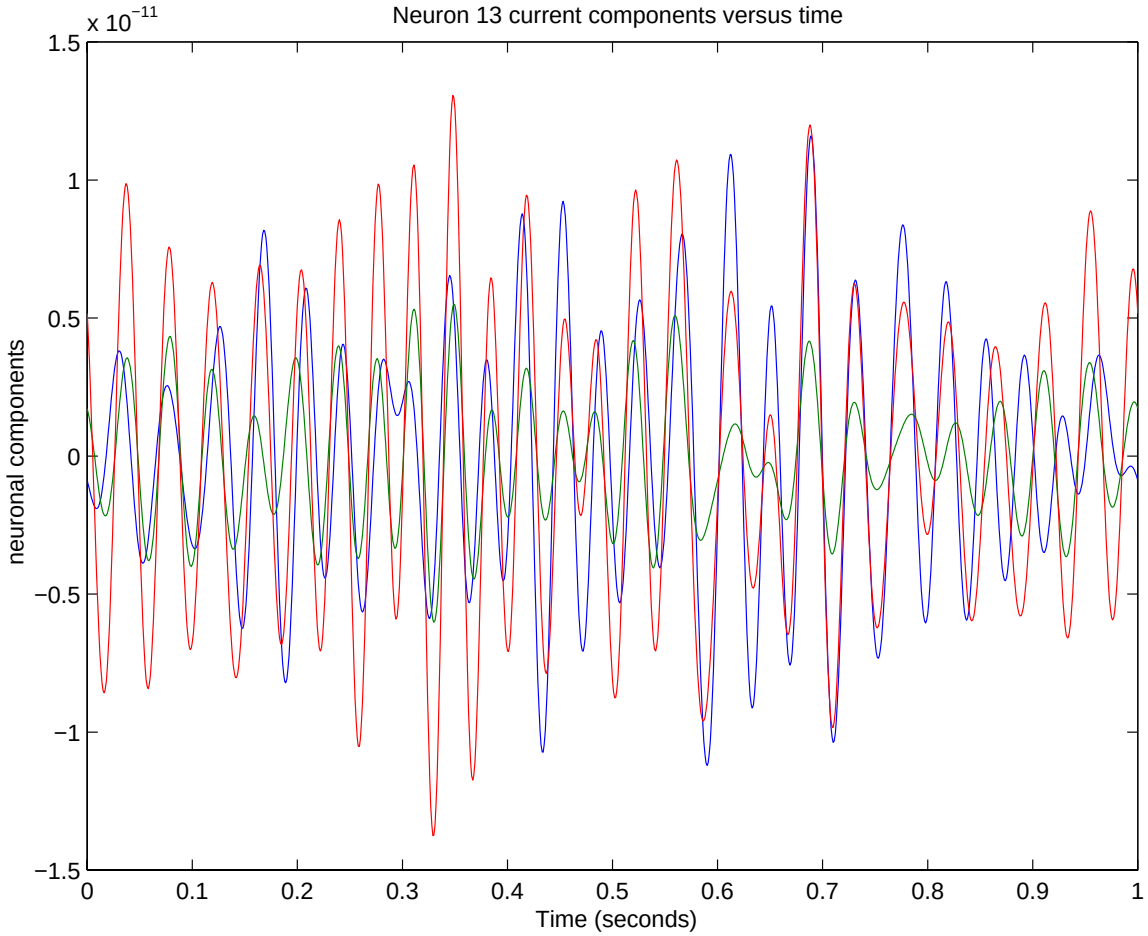

Figure 29: Recovered Neuron 13 Current Components Versus Time

For $q = 13$ the neuronal location, in spherical coordinates is,

$$(r_q, \theta_q, \phi_q) = (.0800, 92., 90.) \tag{3.1.3.13}$$

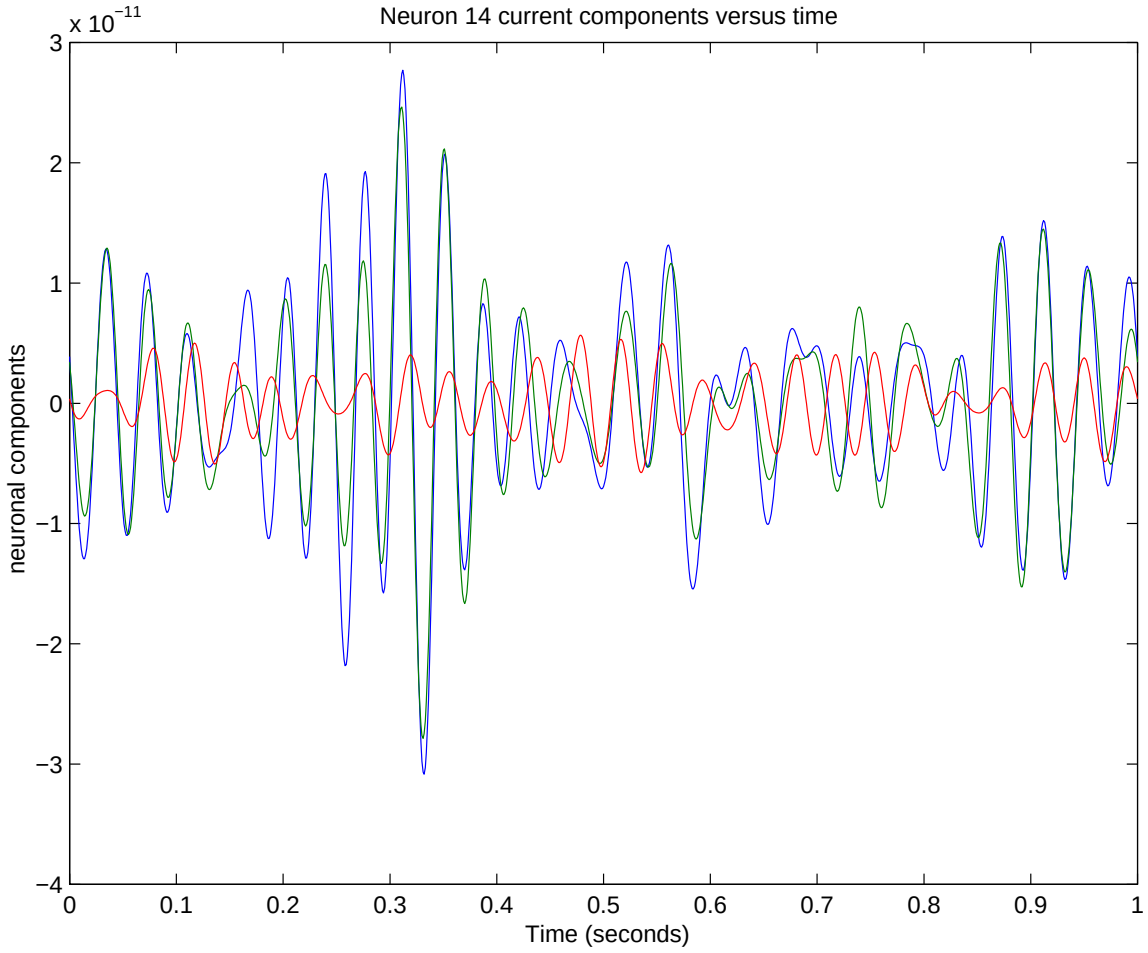

Figure 30: Recovered Neuron 14 Current Components Versus Time

For $q = 14$ the neuronal location, in spherical coordinates is,

$$(r_q, \theta_q, \phi_q) = (.0800, 92., 270.) \tag{3.1.3.14}$$

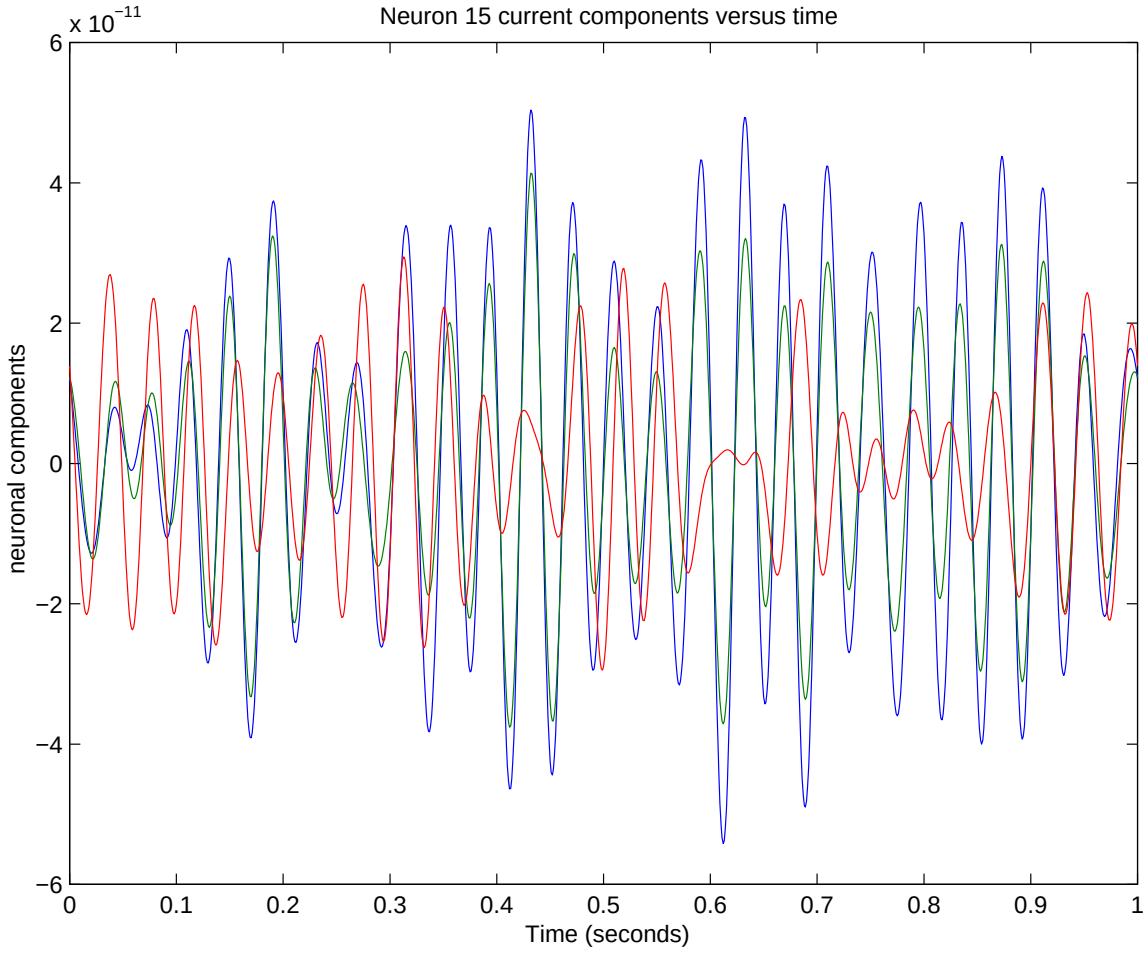

Figure 31: Recovered Neuron 15 Current Components Versus Time

For $q = 15$ the neuronal location, in spherical coordinates is,

$$(r_q, \theta_q, \phi_q) = (.0800, 92., 162.) \tag{3.1.3.15}$$

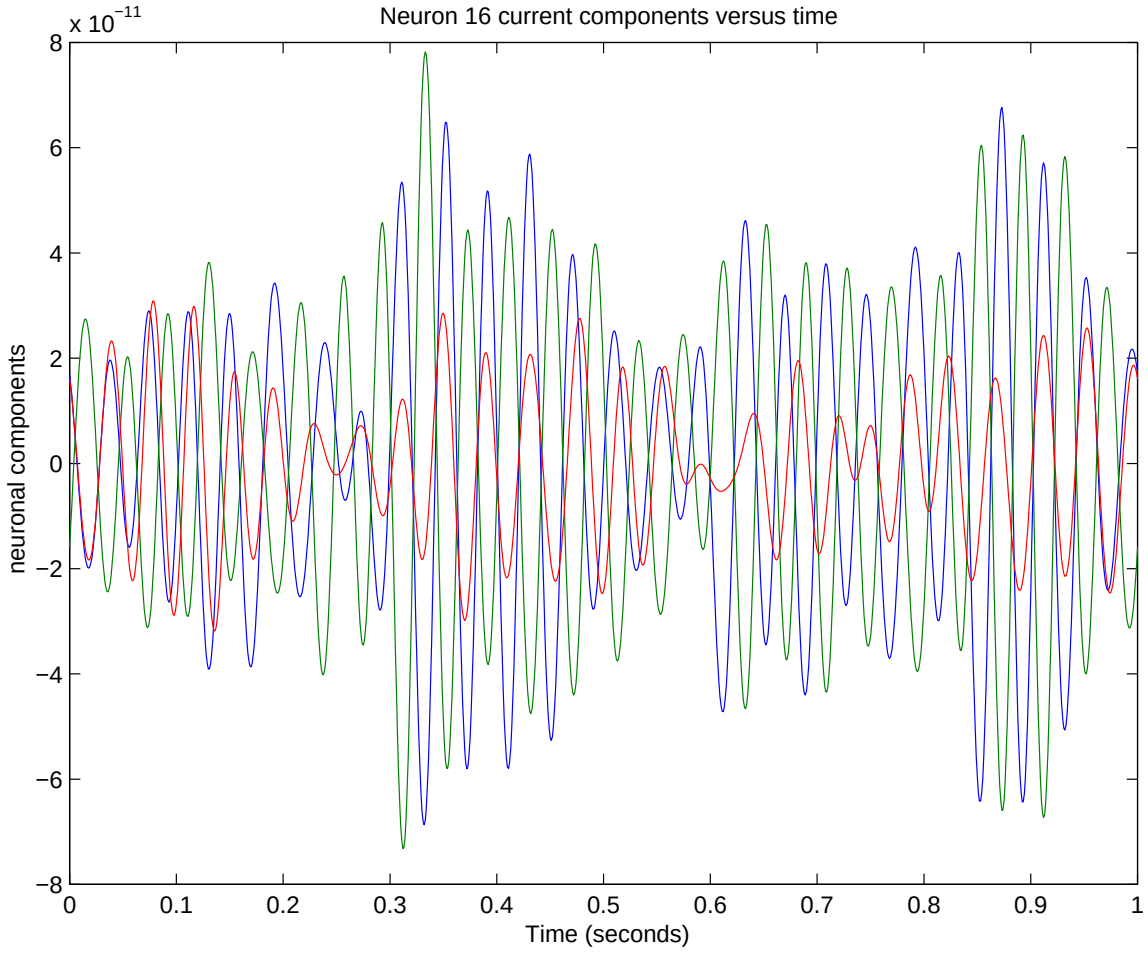

Figure 32: Recovered Neuron 16 Current Components Versus Time

For $q = 16$ the neuronal location, in spherical coordinates is,

$$(r_q, \theta_q, \phi_q) = (.0800, 92., 198.) \tag{3.1.3.16}$$

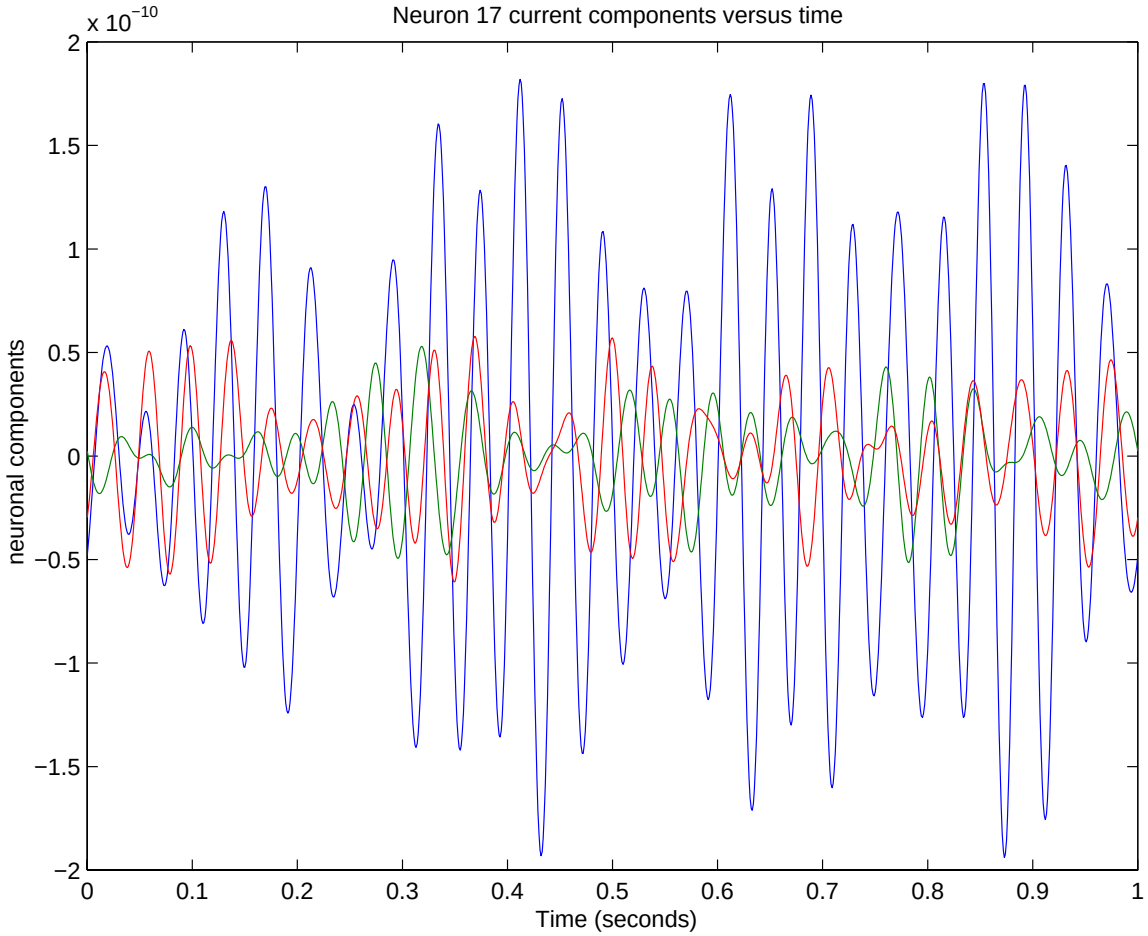

Figure 33: Recovered Neuron 17 Current Components Versus Time

For $q = 17$ the neuronal location, in spherical coordinates is,

$$(r_q, \theta_q, \phi_q) = (.0800, 92., 180.) \tag{3.1.3.17}$$

3.1.4 Frequency Components and Neuronal Source Locations Recovered Using 1 Second of EEG Data at 128 EEG Recording Sites

For $q = 1$ the neuronal location, in spherical coordinates is,

$$(r_q, \theta_q, \phi_q) = (.0100, 1., 0.) \tag{3.1.4.1}$$

For $q = 2$ the neuronal location, in spherical coordinates is,

$$(r_q, \theta_q, \phi_q) = (.0800, 1., 0.) \tag{3.1.4.2}$$

For $q = 3$ the neuronal location, in spherical coordinates is,

$$(r_q, \theta_q, \phi_q) = (.0800, 46., 0.) \tag{3.1.4.3}$$

For $q = 4$ the neuronal location, in spherical coordinates is,

$$(r_q, \theta_q, \phi_q) = (.0800, 46., 90.) \tag{3.1.4.4}$$

For $q = 5$ the neuronal location, in spherical coordinates is,

$$(r_q, \theta_q, \phi_q) = (.0800, 46., 270.) \tag{3.1.4.5}$$

For $q = 6$ the neuronal location, in spherical coordinates is,

$$(r_q, \theta_q, \phi_q) = (.0800, 46., 180.) \tag{3.1.4.6}$$

For $q = 7$ the neuronal location, in spherical coordinates is,

$$(r_q, \theta_q, \phi_q) = (.0800, 60., 39.) \tag{3.1.4.7}$$

For $q = 8$ the neuronal location, in spherical coordinates is,

$$(r_q, \theta_q, \phi_q) = (.0800, 60., 321.) \tag{3.1.4.8}$$

For $q = 9$ the neuronal location, in spherical coordinates is,

$$(r_q, \theta_q, \phi_q) = (.0800, 60., 141.) \tag{3.1.4.9}$$

For $q = 10$ the neuronal location, in spherical coordinates is,

$$(r_q, \theta_q, \phi_q) = (.0800, 60., 229.) \tag{3.1.4.10}$$

For $q = 11$ the neuronal location, in spherical coordinates is,

$$(r_q, \theta_q, \phi_q) = (.0800, 92., 242.) \tag{3.1.4.11}$$

For $q = 12$ the neuronal location, in spherical coordinates is,

$$(r_q, \theta_q, \phi_q) = (.0800, 92., 18.) \tag{3.1.4.12}$$

For $q = 13$ the neuronal location, in spherical coordinates is,

$$(r_q, \theta_q, \phi_q) = (.0800, 92., 90.) \tag{3.1.4.13}$$

For $q = 14$ the neuronal location, in spherical coordinates is,

$$(r_q, \theta_q, \phi_q) = (.0800, 92., 270.) \tag{3.1.4.14}$$

For $q = 15$ the neuronal location, in spherical coordinates is,

$$(r_q, \theta_q, \phi_q) = (.0800, 92., 162.) \tag{3.1.4.15}$$

For $q = 16$ the neuronal location, in spherical coordinates is,

$$(r_q, \theta_q, \phi_q) = (.0800, 92., 198.) \tag{3.1.4.16}$$

For $q = 17$ the neuronal location, in spherical coordinates is,

$$(r_q, \theta_q, \phi_q) = (.0800, 92., 180.) \tag{3.1.4.17}$$

The set of 30 frequencies, in Hertz, for frequency components recovered are

$$\mathcal{F} =$$

$$\{1, 3, 3, 4, 5, 6, 7, 8, 9, 10, 11, 12, 13, 14, 15, 16, 17, 18, 19, 20, 21, 22, 23, 24, 25, 26, 27, 28, 29, 30\} \tag{3.1.4.18}$$

4 The Divergence and the Curl in Orthogonal Coordinate Systems

We use vector calculus relationships to solve the inverse source problem of non-surgical recovery of brain activity.

4.1 General Orthogonal Coordinate Systems

The surface of the head may be considered to be a locally Euclidean structure. The Gauss divergence theorem is used to relate head surface EEG recordings to internal brain activity.

4.1.1 The form of the Curl, Divergence, and Laplacian in a General Orthogonal Coordinate System

Let us suppose that we have a mapping from a Cartesian product of intervals in u, v, and w space into x, y, and z space given by

$$(u, v, w) \to (x(u, v, w), y(u, v, w), z(u, v, w)) \tag{4.1.1.1}$$

so that the coordinate surfaces

$$u(x, y, z) = u_0 \tag{4.1.1.2}$$

$$v(x,y,z) = v_0 \tag{4.1.1.3}$$

$$w(x,y,z) = w_0 \tag{4.1.1.4}$$

are orthogonal in the sense that the coordinate surfaces (4.1.1.2), (4.1.1.3), (4.1.1.4) are defined by setting the three functions of Cartesian coordinates x, y, and z given by

$$(x,y,z) \rightarrow (u(x,y,z), v(x,y,z), w(x,y,z)) \tag{4.1.1.5}$$

equal to a constant and letting $\boldsymbol{e}_u$, $\boldsymbol{e}_v$, and $\boldsymbol{e}_w$ respectively be the unit length normal vectors to these surfaces we can define the curl and divergence operators. If we consider the traditional unit vectors $\boldsymbol{i}$, $\boldsymbol{j}$, and $\boldsymbol{k}$ of three dimensional Euclidean space and recognize that if we consider a point

$$(u,v,w) \rightarrow (x(u,v,w), y(u,v,w), z(u,v,w)) \tag{4.1.1.6}$$

and allow just one of u, v, or w to vary at a time we generate three curves whose tangent vectors are

$$h_u \boldsymbol{e}_u = \frac{\partial x}{\partial u}\boldsymbol{i} + \frac{\partial y}{\partial u}\boldsymbol{j} + \frac{\partial z}{\partial u}\boldsymbol{k} \tag{4.1.1.7}$$

$$h_v \boldsymbol{e}_v = \frac{\partial x}{\partial v}\boldsymbol{i} + \frac{\partial y}{\partial v}\boldsymbol{j} + \frac{\partial z}{\partial v}\boldsymbol{k} \tag{4.1.1.8}$$

and

$$h_w \boldsymbol{e}_w = \frac{\partial x}{\partial w}\boldsymbol{i} + \frac{\partial y}{\partial w}\boldsymbol{j} + \frac{\partial z}{\partial w}\boldsymbol{k} \tag{4.1.1.9}$$

For an orthogonal coordinate system it is assumed that these three tangent vectors where it is assumed that the vectors $\boldsymbol{e}_u$, $\boldsymbol{e}_v$, and $\boldsymbol{e}_w$ all have length one, which means, for example, that h_u, h_v, and h_w are the lengths of these tangent vectors and

$$|| \boldsymbol{e}_u ||^2 = \boldsymbol{e}_u \cdot \boldsymbol{e}_u = 1 \tag{4.1.1.10}$$

or more compactly that

$$(\boldsymbol{e}_u \cdot \boldsymbol{e}_u, \boldsymbol{e}_v \cdot \boldsymbol{e}_v, \boldsymbol{e}_w \cdot \boldsymbol{e}_w) = (1,1,1) \tag{4.1.1.11}$$

so that the functions h_u, h_v, and h_w appearing in equation (4.1.1.7), (4.1.1.8), and (4.1.1.9) are given by

$$(h_u \boldsymbol{e}_u) \cdot (h_u \boldsymbol{e}_u) = h_u^2 = \left(\frac{\partial x}{\partial u}\right)^2 + \left(\frac{\partial y}{\partial u}\right)^2 + \left(\frac{\partial z}{\partial u}\right)^2 \tag{4.1.1.12}$$

where

$$(h_v \boldsymbol{e}_v) \cdot (h_v \boldsymbol{e}_v) = h_v^2 = \left(\frac{\partial x}{\partial v}\right)^2 + \left(\frac{\partial y}{\partial v}\right)^2 + \left(\frac{\partial z}{\partial v}\right)^2 \tag{4.1.1.13}$$

and

$$(h_w \boldsymbol{e}_w) \cdot (h_w \boldsymbol{e}_w) = h_w^2 = \left(\frac{\partial x}{\partial w}\right)^2 + \left(\frac{\partial y}{\partial w}\right)^2 + \left(\frac{\partial z}{\partial w}\right)^2 \tag{4.1.1.14}$$

In addition we assume that at every point the normal vectors $\boldsymbol{e}_u$, $\boldsymbol{e}_v$, and $\boldsymbol{e}_w$ to the intersecting coordinate surfaces defined by setting u, v, and w equal to the value at a prescribed point (x,y,z) are pairwise orthogonal in the sense that

$$\boldsymbol{e}_u \cdot \boldsymbol{e}_v = \boldsymbol{e}_u \cdot \boldsymbol{e}_w = \boldsymbol{e}_v \cdot \boldsymbol{e}_w = 0 \tag{4.1.1.15}$$

Using this orthogonality relationship (4.1.1.15) and the unit length relationship (4.1.1.11) we have by the chain rule for partial differentiation that

$$\frac{\partial u}{\partial u} = \frac{\partial u}{\partial x}\partial x \partial u + \frac{\partial u}{\partial y}\partial y \partial u + \frac{\partial u}{\partial z}\partial z \partial u =$$

$$\left(\frac{\partial u}{\partial x}\boldsymbol{i} + \frac{\partial u}{\partial y}\boldsymbol{j} + \frac{\partial u}{\partial y}\boldsymbol{k}\right) \cdot \left(\frac{\partial x}{\partial u}\boldsymbol{i} + \frac{\partial y}{\partial u}\boldsymbol{j} + \frac{\partial z}{\partial u}\boldsymbol{k}\right) = \tag{4.1.1.16}$$

so that

$$\frac{\partial u}{\partial u} = \nabla(u) \cdot h_u \boldsymbol{e}_u = 1 \tag{4.1.1.17}$$

$$\frac{\partial u}{\partial v} = \nabla(u) \cdot h_v \boldsymbol{e}_v = 0 \tag{4.1.1.18}$$

$$\frac{\partial u}{\partial w} = \nabla(u) \cdot h_w \boldsymbol{e}_w = 0 \tag{4.1.1.19}$$

Now since $\boldsymbol{e}_u$, $\boldsymbol{e}_v$, and $\boldsymbol{e}_w$ are independent, we may write at each point,

$$\nabla(u) = A\boldsymbol{e}_u + B\boldsymbol{e}_v + C\boldsymbol{e}_w \tag{4.1.1.20}$$

for some constants A, B, and C which depend on the point (x, y, z) at which the gradient of u is computed. Combining equations (4.1.1.15) and (4.1.1.17) we determine that

$$\frac{1}{h_u} = \nabla(u) \cdot \boldsymbol{e}_u = A\boldsymbol{e}_u \cdot \boldsymbol{e}_u = A \tag{4.1.1.21}$$

$$0 = \nabla(u) \cdot \boldsymbol{e}_v = B\boldsymbol{e}_u \cdot \boldsymbol{e}_v = B \tag{4.1.1.22}$$

This shows that

$$\nabla(u) = \frac{1}{h_u}\boldsymbol{e}_u \tag{4.1.1.23}$$

A similar argument shows that

$$\nabla(v) = \frac{1}{h_v}\boldsymbol{e}_v \tag{4.1.1.24}$$

and

$$\nabla(w) = \frac{1}{h_w}\boldsymbol{e}_w \tag{4.1.1.25}$$

Equations (4.1.1.23), (4.1.1.24), and (4.1.1.25) are what we would expect, namely, that the gradients of the functions defining the constant coordinate surfaces should be perpendicular to these surfaces. We note that equations (4.1.1.23) and (4.1.1.7) are consistent in the sense that

$$\nabla(u) \cdot \left(\frac{\partial x}{\partial u}\boldsymbol{i} + \frac{\partial y}{\partial u}\boldsymbol{j} + \frac{\partial z}{\partial u}\boldsymbol{k}\right) = \frac{1}{h_u}\boldsymbol{e}_u \cdot (h_u \boldsymbol{e}_u) = 1 \tag{4.1.1.26}$$

The equations that we use, explicitly, in determination of the gradient in a general orthogonal system, are however, derived from equations (4.1.1.7), (4.1.1.13), and (4.1.1.14) and are

$$\boldsymbol{e}_u = \frac{1}{h_u}\left(\frac{\partial x}{\partial u}\boldsymbol{i} + \frac{\partial y}{\partial u}\boldsymbol{j} + \frac{\partial z}{\partial u}\boldsymbol{k}\right) \tag{4.1.1.27}$$

$$\boldsymbol{e}_v = \frac{1}{h_v}\left(\frac{\partial x}{\partial v}\boldsymbol{i} + \frac{\partial y}{\partial v}\boldsymbol{j} + \frac{\partial z}{\partial v}\boldsymbol{k}\right) \tag{4.1.1.28}$$

and

$$\boldsymbol{e}_w = \frac{1}{h_w}\left(\frac{\partial x}{\partial w}\boldsymbol{i} + \frac{\partial y}{\partial w}\boldsymbol{j} + \frac{\partial z}{\partial w}\boldsymbol{k}\right) \tag{4.1.1.29}$$

Thus, for an orthogonal coordinate transformation the tangent vectors defined by equations (4.1.1.7), (4.1.1.8), and (4.1.1.9) are parallel, respectively, to the gradients of the coordinate surfaces defined by equations (4.1.1.2), (4.1.1.3), and (4.1.1.4). Let $f(x, y, z)$ be a continuously differentiable function of x, y, and z and suppose that D, E, and F are complex numbers such that

$$\frac{\partial f}{\partial x}\boldsymbol{i} + \frac{\partial f}{\partial y}\boldsymbol{j} + \frac{\partial f}{\partial z}\boldsymbol{k} = D\boldsymbol{e}_u + E\boldsymbol{e}_v + F\boldsymbol{e}_w \tag{4.1.1.30}$$

Then, equation (4.1.1.7) or equation (4.1.1.27) says that

$$\left(\frac{\partial f}{\partial x}\boldsymbol{i} + \frac{\partial f}{\partial y}\boldsymbol{j} + \frac{\partial f}{\partial z}\boldsymbol{k}\right) \cdot \boldsymbol{e}_u =$$

$$\left(\frac{\partial f}{\partial x}\boldsymbol{i} + \frac{\partial f}{\partial y}\boldsymbol{j} + \frac{\partial f}{\partial z}\boldsymbol{k}\right) \cdot \left(\frac{\partial x}{\partial u}\boldsymbol{i} + \frac{\partial y}{\partial u}\boldsymbol{j} + \frac{\partial z}{\partial u}\boldsymbol{k}\right)\frac{1}{h_u}$$

$$= D\boldsymbol{e}_u \cdot \boldsymbol{e}_u = D = \frac{1}{h_u}\left[\frac{\partial f}{\partial x}\frac{\partial x}{\partial u} + \frac{\partial f}{\partial y}\frac{\partial y}{\partial u} + \frac{\partial f}{\partial z}\frac{\partial z}{\partial u}\right] = \frac{1}{h_u}\frac{\partial f}{\partial u} \tag{4.1.1.31}$$

Similarly equation (4.1.1.8) tells us that

$$E = E\boldsymbol{e}_v \cdot \boldsymbol{e}_v = \frac{1}{h_v}\left[\frac{\partial f}{\partial x}\frac{\partial x}{\partial v} + \frac{\partial f}{\partial y}\frac{\partial y}{\partial v} + \frac{\partial f}{\partial z}\frac{\partial z}{\partial v}\right] = \frac{1}{h_v}\frac{\partial f}{\partial v} \tag{4.1.1.32}$$

From equation (4.1.1.9) and (4.1.1.30) we see that

$$F = F\boldsymbol{e}_w \cdot \boldsymbol{e}_w = \frac{1}{h_w}\left[\frac{\partial f}{\partial x}\frac{\partial x}{\partial w} + \frac{\partial f}{\partial y}\frac{\partial y}{\partial w} + \frac{\partial f}{\partial z}\frac{\partial z}{\partial w}\right] = \frac{1}{h_w}\frac{\partial f}{\partial w} \tag{4.1.1.33}$$

From equations (4.1.1.31), (4.1.1.32), and (4.1.1.33) we see that

$$\nabla(f) = \frac{1}{h_u}\left(\frac{\partial f}{\partial u}\right)\boldsymbol{e}_u + \frac{1}{h_v}\left(\frac{\partial f}{\partial v}\right)\boldsymbol{e}_v + \frac{1}{h_w}\left(\frac{\partial f}{\partial w}\right)\boldsymbol{e}_w \tag{4.1.1.34}$$

Next, we express the curl operation in any coordinate system. We know that since in general if Ψ is a continuously differentiable function and $\boldsymbol{A}$ is a continuously differentiable vector field that

$$\nabla \times (\Psi\boldsymbol{A}) = \Psi\nabla \times (\boldsymbol{A}) + \nabla(\Psi) \times \boldsymbol{A} \tag{4.1.1.35}$$

the fact that the curl of a gradient is the zero vector tells us that with

$$\boldsymbol{A} = \nabla(\Phi) \tag{4.1.1.36}$$

we have

$$\nabla \times (\Psi\,\nabla(\Phi)) = \nabla(\Psi) \times \nabla(\Phi) \tag{4.1.1.37}$$

With this notation it can be proven that the curl is given by

$$\nabla \times (\boldsymbol{F}) = \nabla \times (F_u \boldsymbol{e}_u + F_v \boldsymbol{e}_v) + F_w \boldsymbol{e}_w) =$$
$$\left\{ \frac{1}{h_u h_v h_w} \right\} \left(\left[\frac{\partial}{\partial v}(F_w h_w) - \frac{\partial}{\partial w}(F_v h_v) \right] h_u \boldsymbol{e}_u + \right.$$
$$\left[\frac{\partial}{\partial w}(F_u h_u) - \frac{\partial}{\partial u}(F_w h_w) \right] h_v \boldsymbol{e}_v +$$
$$\left. \left[\frac{\partial}{\partial u}(F_v h_v) - \frac{\partial}{\partial v}(F_u h_u) \right] h_w \boldsymbol{e}_w \right) \tag{4.1.1.38}$$

which gives us a curl in any orthogonal coordinate system.

Finally, we express the divergence in any orthogonal coordinate system. The key to this development is the use of the identity

$$\nabla \cdot (\Phi \boldsymbol{A}) = \nabla(\Phi) \cdot \boldsymbol{A} + \Phi \, \nabla \cdot (\boldsymbol{A}) \tag{4.1.1.39}$$

so that

$$\nabla \cdot (F_u \boldsymbol{e}_u + F_v \boldsymbol{e}_v + F_w \boldsymbol{e}_w) =$$
$$\nabla(F_u) \cdot \boldsymbol{e}_u + \nabla(F_v) \cdot \boldsymbol{e}_v + \nabla(F_w) \cdot \boldsymbol{e}_w +$$
$$F_u \, \nabla \cdot (\boldsymbol{e}_u) + F_v \, \nabla \cdot (\boldsymbol{e}_v) + F_w \, \nabla \cdot (\boldsymbol{e}_w) \tag{4.1.1.40}$$

We have the following theorem.

Theorem 4.1 *For all vector fields* $\boldsymbol{F}$ *we have*

$$\nabla \cdot (F_u \boldsymbol{e}_u + F_v \boldsymbol{e}_v + F_w \boldsymbol{e}_w) =$$
$$\nabla(F_u) \cdot \boldsymbol{e}_u + \nabla(F_v) \cdot \boldsymbol{e}_v + \nabla(F_w) \cdot \boldsymbol{e}_w +$$
$$\left(\frac{F_u}{h_u h_v h_w} \right) \frac{\partial}{\partial u}(h_v h_w) + \left(\frac{F_v}{h_u h_v h_w} \right) \frac{\partial}{\partial v}(h_u h_w) + \left(\frac{F_w}{h_u h_v h_w} \right) \frac{\partial}{\partial w}(h_u h_v) \tag{4.1.1.41}$$

or said differently

$$\nabla \cdot (F_u \boldsymbol{e}_u + F_v \boldsymbol{e}_v + F_w \boldsymbol{e}_w) =$$
$$\frac{1}{h_u h_v h_w} \left(\frac{\partial}{\partial u}(F_u h_v h_w) + \frac{\partial}{\partial v}(F_v h_w h_u) + \frac{\partial}{\partial w}(F_w h_w h_v) \right) \tag{4.1.1.42}$$

Proof of Theorem. Equations (4.1.1.7), (4.1.1.8), and (4.1.1.9) will enable us to express $\boldsymbol{i}$, $\boldsymbol{j}$, and $\boldsymbol{k}$ in terms of $\boldsymbol{e}_u$, $\boldsymbol{e}_v$, and $\boldsymbol{e}_w$ as follows. Since we know that $\boldsymbol{e}_u$, $\boldsymbol{e}_v$, and $\boldsymbol{e}_w$ as follows. If

$$\boldsymbol{i} = A_1 \boldsymbol{e}_u + B_1 \boldsymbol{e}_v + C_1 \boldsymbol{e}_w \tag{4.1.1.43}$$

so that from (4.1.1.7), (4.1.1.8), and (4.1.1.9) we have

$$(\boldsymbol{i} \cdot \boldsymbol{e}_u, \boldsymbol{i} \cdot \boldsymbol{e}_v, \boldsymbol{i} \cdot \boldsymbol{e}_w) = (A_1, B_1, C_1)$$
$$= \left(\frac{1}{h_u} \frac{\partial x}{\partial u}, \frac{1}{h_v} \frac{\partial x}{\partial v}, \frac{1}{h_w} \frac{\partial x}{\partial w} \right) \tag{4.1.1.44}$$

Similarly, with the use of (4.1.1.7), (4.1.1.8), and (4.1.1.9) we have

$$(\boldsymbol{j}\cdot\boldsymbol{e}_u, \boldsymbol{j}\cdot\boldsymbol{e}_v, \boldsymbol{j}\cdot\boldsymbol{e}_w)$$
$$= \left(\frac{1}{h_u}\frac{\partial y}{\partial u}, \frac{1}{h_v}\frac{\partial y}{\partial v}, \frac{1}{h_w}\frac{\partial y}{\partial w}\right) \tag{4.1.1.45}$$

and

$$(\boldsymbol{k}\cdot\boldsymbol{e}_u, \boldsymbol{k}\cdot\boldsymbol{e}_v, \boldsymbol{k}\cdot\boldsymbol{e}_w)$$
$$= \left(\frac{1}{h_u}\frac{\partial z}{\partial u}, \frac{1}{h_v}\frac{\partial z}{\partial v}, \frac{1}{h_w}\frac{\partial z}{\partial w}\right) \tag{4.1.1.46}$$

Making use of the fact that for all continuously differentiable f and all continuously differentiable vector fields $\boldsymbol{A}$ we have

$$\nabla\cdot(f\boldsymbol{A}) = \nabla(f)\cdot\boldsymbol{A} + f\,\nabla\cdot(\boldsymbol{A}) \tag{4.1.1.47}$$

so that with

$$\boldsymbol{F} = F_u\boldsymbol{e}_u + F_v\boldsymbol{e}_v + F_w\boldsymbol{e}_w \tag{4.1.1.48}$$

and equation (4.1.1.47) we have

$$\nabla\cdot(\boldsymbol{F}) = \nabla\cdot(F_u\boldsymbol{e}_u) + \nabla\cdot(F_v\boldsymbol{e}_v) + \nabla\cdot(F_w\boldsymbol{e}_w) =$$
$$\nabla(F_u)\cdot\boldsymbol{e}_u + \nabla(F_v)\cdot\boldsymbol{e}_v + \nabla(F_w)\cdot\boldsymbol{e}_w +$$
$$F_u\,\nabla\cdot(\boldsymbol{e}_u) + F_v\,\nabla\cdot(\boldsymbol{e}_v) + F_w\,\nabla\cdot(\boldsymbol{e}_w) \tag{4.1.1.49}$$

To compute the first divergence term on the right side of (4.1.1.49) we must get $\boldsymbol{e}_u$ in terms of $\boldsymbol{i}$, $\boldsymbol{j}$, and $\boldsymbol{k}$. Observe that equations (4.1.1.44), (4.1.1.45), and (4.1.1.46) imply that

$$\boldsymbol{e}_u = \frac{1}{h_u}\frac{\partial x}{\partial u}\boldsymbol{i} + \frac{1}{h_u}\frac{\partial y}{\partial u}\boldsymbol{j} + \frac{1}{h_u}\frac{\partial z}{\partial u}\boldsymbol{k} \tag{4.1.1.50}$$

so that

$$\nabla\cdot(\boldsymbol{e}_u) =$$
$$\frac{\partial}{\partial x}\left(\frac{1}{h_u}\frac{\partial x}{\partial u}\right) + \frac{\partial}{\partial y}\left(\frac{1}{h_u}\frac{\partial y}{\partial u}\right) + \frac{\partial}{\partial z}\left(\frac{1}{h_u}\frac{\partial z}{\partial u}\right) =$$
$$\frac{\partial}{\partial u}\left(\frac{1}{h_u}\frac{\partial x}{\partial u}\right)\frac{\partial u}{\partial x} + \frac{\partial}{\partial v}\left(\frac{1}{h_u}\frac{\partial x}{\partial u}\right)\frac{\partial v}{\partial x} + \frac{\partial}{\partial w}\left(\frac{1}{h_u}\frac{\partial x}{\partial u}\right)\frac{\partial w}{\partial x} +$$
$$\frac{\partial}{\partial u}\left(\frac{1}{h_u}\frac{\partial y}{\partial u}\right)\frac{\partial u}{\partial y} + \frac{\partial}{\partial v}\left(\frac{1}{h_u}\frac{\partial y}{\partial u}\right)\frac{\partial v}{\partial y} + \frac{\partial}{\partial w}\left(\frac{1}{h_u}\frac{\partial y}{\partial u}\right)\frac{\partial w}{\partial y} +$$
$$\frac{\partial}{\partial u}\left(\frac{1}{h_u}\frac{\partial z}{\partial u}\right)\frac{\partial u}{\partial z} + \frac{\partial}{\partial v}\left(\frac{1}{h_u}\frac{\partial z}{\partial u}\right)\frac{\partial v}{\partial z} + \frac{\partial}{\partial w}\left(\frac{1}{h_u}\frac{\partial z}{\partial u}\right)\frac{\partial w}{\partial z} =$$
$$\left(\frac{\partial}{\partial u}\boldsymbol{e}_u\right)\cdot\nabla(u) + \left(\frac{\partial}{\partial v}\boldsymbol{e}_u\right)\cdot\nabla(v) + \left(\frac{\partial}{\partial w}\boldsymbol{e}_u\right)\cdot\nabla(w) \tag{4.1.1.51}$$

From the fact that

$$(\nabla(u), \nabla(v), \nabla(w)) = \left(\frac{\boldsymbol{e}_u}{h_u}, \frac{\boldsymbol{e}_v}{h_v}, \frac{e_w}{h_w}\right) \tag{4.1.1.52}$$

which means, since

$$\boldsymbol{e}_u \cdot \boldsymbol{e}_u = 1 \tag{4.1.1.53}$$

that

$$\left(\frac{\partial}{\partial u}\boldsymbol{e}_u\right) \cdot \boldsymbol{e}_u + \boldsymbol{e}_u \cdot \left(\frac{\partial}{\partial u}\boldsymbol{e}_u\right) = 0 \tag{4.1.1.54}$$

so that

$$\nabla\cdot(\boldsymbol{e}_u) = \left(\frac{\partial}{\partial v}\boldsymbol{e}_u\right) \cdot \frac{\boldsymbol{e}_v}{h_v} + \left(\frac{\partial}{\partial w}\boldsymbol{e}_u\right) \cdot \frac{\boldsymbol{e}_w}{h_w} \tag{4.1.1.55}$$

Now observe that the first term on the right side of equation (4.1.1.55) is

$$\left(\frac{\partial}{\partial v}\boldsymbol{e}_u\right) \cdot \frac{\boldsymbol{e}_v}{h_v} =$$

$$\frac{\partial}{\partial v}\left\{\left[\left(\frac{\partial x}{\partial u}\right)^2 + \left(\frac{\partial y}{\partial u}\right)^2 + \left(\frac{\partial z}{\partial u}\right)^2\right]^{-1/2}\left(\frac{\partial x}{\partial u}\boldsymbol{i} + \frac{\partial y}{\partial u}\boldsymbol{j} + \frac{\partial z}{\partial u}\boldsymbol{k}\right)\right\}\cdot\left(\frac{1}{h_v^2}\right)\left\{\frac{\partial x}{\partial v}\boldsymbol{i} + \frac{\partial y}{\partial v}\boldsymbol{j} + \frac{\partial z}{\partial v}\boldsymbol{k}\right\}$$

$$(-1/2)\left[\left(\frac{\partial x}{\partial u}\right)^2 + \left(\frac{\partial y}{\partial u}\right)^2 + \left(\frac{\partial z}{\partial u}\right)^2\right]^{-3/2}\left[2\left(\frac{\partial x}{\partial u}\frac{\partial^2 x}{\partial v \partial u} + \frac{\partial y}{\partial u}\frac{\partial^2 y}{\partial v \partial u} + \frac{\partial z}{\partial u}\frac{\partial^2 z}{\partial v \partial u}\right)\right] h_u \boldsymbol{e}_u \cdot \frac{\boldsymbol{e}_v}{h_v}$$

$$+\frac{1}{h_u h_v^2}\left[\frac{\partial^2 x}{\partial v \partial u}\frac{\partial x}{\partial v} + \frac{\partial^2 y}{\partial v \partial u}\frac{\partial y}{\partial v} + \frac{\partial^2 z}{\partial v \partial u}\frac{\partial z}{\partial v}\right]$$

$$= \frac{1}{h_u h_v^2}\left[\frac{\partial^2 x}{\partial v \partial u}\frac{\partial x}{\partial v} + \frac{\partial^2 y}{\partial v \partial u}\frac{\partial y}{\partial v} + \frac{\partial^2 z}{\partial v \partial u}\frac{\partial z}{\partial v}\right] = \frac{1}{h_u h_v}\frac{\partial h_v}{\partial u} \tag{4.1.1.56}$$

The right side of equation (4.1.1.56) is given, since,

$$h_v = \sqrt{h_v^2} = \sqrt{\left(\frac{\partial x}{\partial v}\right)^2 + \left(\frac{\partial y}{\partial v}\right)^2 + \left(\frac{\partial z}{\partial v}\right)^2 +} \tag{4.1.1.57}$$

implies that

$$\frac{\partial}{\partial u}\sqrt{h_v^2} = \frac{1}{2}\left(\frac{1}{\sqrt{h_v^2}}\right)\left(\frac{\partial h_v^2}{\partial u}\right) \tag{4.1.1.58}$$

that

$$\frac{1}{h_u h_v}\frac{\partial h_v}{\partial u} = \frac{1}{h_u h_v^2}\frac{\partial h_v^2}{\partial u} =$$

$$\frac{1}{h_u h_v^2}\frac{1}{2}\left[2\left(\frac{\partial^2 x}{\partial u \partial v}\frac{\partial x}{\partial v} + \frac{\partial^2 y}{\partial u}\partial v\frac{\partial y}{\partial v} + \frac{\partial^2 z}{\partial u}\partial v\frac{\partial z}{\partial v}\right)\right] \tag{4.1.1.59}$$

which means that

$$\frac{\partial \boldsymbol{e}_u}{\partial v} \cdot \frac{e_v}{h_v} = \frac{1}{h_u h_v}\frac{\partial h_v}{\partial u} \tag{4.1.1.60}$$

The second term is obtained by by replacing the v in the right side of equation (4.1.1.56) or (4.1.1.60) by w so that

$$\frac{\partial \boldsymbol{e}_u}{\partial w} \cdot \frac{e_w}{h_w} = \frac{1}{h_u h_w} \frac{\partial h_w}{\partial u} \tag{4.1.1.61}$$

By combining equations (4.1.1.60) and (4.1.1.61) it is clear that

$$F_u \, \nabla \cdot (\boldsymbol{e}_u) = F_u \left\{ \left(\frac{\partial \boldsymbol{e}_u}{\partial v} \right) \cdot \frac{\boldsymbol{e}_v}{h_v} + \left(\frac{\partial \boldsymbol{e}_u}{\partial w} \right) \cdot \frac{\boldsymbol{e}_w}{h_w} \right\}$$

$$= \left\{ \frac{F_u}{h_u h_v} \frac{\partial h_v}{\partial u} + \frac{F_u}{h_u h_w} \frac{\partial h_w}{\partial u} = \frac{F_u}{h_u h_v h_w} \frac{\partial}{\partial u} (h_v h_w) \right\} \tag{4.1.1.62}$$

Continuing with this analysis we see that

$$\frac{F_u}{h_u h_v h_w} \frac{\partial}{\partial u} (h_v h_w) = F_u \, \nabla \cdot (\boldsymbol{e}_u) \tag{4.1.1.63}$$

$$\frac{F_v}{h_u h_v h_w} \frac{\partial}{\partial v} (h_u h_w) = F_v \, \nabla \cdot (\boldsymbol{e}_v) \tag{4.1.1.64}$$

and

$$\frac{F_w}{h_u h_v h_w} \frac{\partial}{\partial w} (h_u h_v) = F_w \, \nabla \cdot (\boldsymbol{e}_w) \tag{4.1.1.65}$$

It follows from this that

$$\nabla \cdot (F_u \boldsymbol{e}_u + F_v \boldsymbol{e}_v + F_w \boldsymbol{e}_w) =$$

$$\frac{1}{h_u} \frac{\partial F_u}{\partial u} + \frac{1}{h_v} \frac{\partial F_v}{\partial v} + \frac{1}{h_w} \frac{\partial F_w}{\partial w} +$$

$$\frac{F_u}{h_u h_v h_w} \frac{\partial}{\partial u} h_v h_w + \frac{F_v}{h_u h_v h_w} \frac{\partial}{\partial v} h_u h_w + \frac{F_u}{h_u h_v h_w} \frac{\partial}{\partial w} h_u h_v$$

$$= \frac{1}{h_u h_v h_w} \left[\frac{\partial}{\partial u} (h_v h_w F_u) + \frac{\partial}{\partial v} (h_u h_w F_v) + \frac{\partial}{\partial w} (h_u h_v F_w) \right] \tag{4.1.1.66}$$

which completes the proof of the theorem.

With these results we have the following representation of the Laplace operator Δ in a general orthogonal coordinate system.

Theorem 4.2 *In a general orthogonal coordinate system the Laplacian or the divergence of the gradient and, in view of equations (4.1.1.66) and (4.1.1.34) is given by*

$$\nabla \cdot (\nabla (f)) =$$

$$\frac{1}{h_u h_v h_w} \left[\frac{\partial}{\partial u} \left(\frac{h_v h_w}{h_u} \frac{\partial f}{\partial u} \right) + \frac{\partial}{\partial v} \left(\frac{h_u h_w}{h_v} \frac{\partial f}{\partial v} \right) + \frac{\partial}{\partial w} \left(\frac{h_u h_v}{h_w} \frac{\partial f}{\partial w} \right) \right] \tag{4.1.1.67}$$

In the spherical coordinate system we have

$$(h_r, h_\theta, h_\phi) = (1, r, r\sin(\theta)) \tag{4.1.1.68}$$

so that in spherical coordinates

$$\nabla(f) = \frac{\partial f}{\partial r}\boldsymbol{e}_r + \frac{1}{r}\frac{\partial f}{\partial \theta}\boldsymbol{e}_\theta + \frac{1}{r\sin(\theta)}\frac{\partial f}{\partial \phi}\boldsymbol{e}_\phi \tag{4.1.1.69}$$

and

$$\nabla\cdot(F_r\boldsymbol{e}_r + F_\theta\boldsymbol{e}_\theta + F_\phi\boldsymbol{e}_\phi) =$$
$$\frac{1}{r^2\sin(\theta)}\left[\left(\frac{\partial}{\partial r}\right)(r^2\sin(\theta)F_r) + \left(\frac{\partial}{\partial \theta}\right)(r\sin(\theta)F_\theta) + \left(\frac{\partial}{\partial \phi}\right)(rF_\phi)\right] \tag{4.1.1.70}$$

and the Laplacian is given by

$$\Delta f = \frac{1}{r^2\sin(\theta)}\left[\frac{\partial}{\partial r}\left(r^2\sin(\theta)\frac{\partial f}{\partial r}\right) + \frac{\partial}{\partial \theta}\left(\sin(\theta)\frac{\partial f}{\partial \theta}\right) + \frac{\partial}{\partial \phi}\left(\frac{1}{\sin(\theta)}\frac{\partial f}{\partial \phi}\right)\right] \tag{4.1.1.71}$$

Finally, in spherical coordinates the curl operation is from (4.1.1.38) given by

$$\nabla \times (F_r\boldsymbol{e}_r + F_\theta\boldsymbol{e}_\theta + F_\phi\boldsymbol{e}_\phi) =$$
$$\left[\frac{1}{r^2\sin(\theta)}\left\{\frac{\partial}{\partial \theta}(F_\phi r\sin(\theta))\right\} - \frac{1}{r^2\sin(\theta)}\left\{\frac{\partial}{\partial \phi}(F_\theta r)\right\}\right]\boldsymbol{e}_r$$
$$+\left[\frac{1}{r\sin(\theta)}\left\{\frac{\partial}{\partial \phi}(F_r)\right\} - \frac{1}{r\sin(\theta)}\left\{\frac{\partial}{\partial r}(F_\phi r\sin(\theta))\right\}\right]\boldsymbol{e}_\theta$$
$$+\left[\frac{1}{r}\left\{\frac{\partial}{\partial r}(F_\theta r)\right\} - \frac{1}{r}\left\{\frac{\partial}{\partial \theta}(F_r)\right\}\right]\boldsymbol{e}_\theta \tag{4.1.1.72}$$

5 The Inverse Source Solution

We describe the inverse source solution which goes from a dynamic voltage distribution on the head surface to internal brain activity. We start off with the construction of the brain-activity independent interrogating scalar functions.

5.1 Construction of the Scalar Functions for Interrogation of the Dynamic Head Surface Voltage Distribution and the Brain Activity Recovery Relationships

Since the dynamic voltage wave generated by brain activity satisfies the condition that the voltage and the permittivity times the normal component of the the gradient of the dynamic voltage is continuous across tissue interfaces. The interrogating scalar functions in tissue region with index p that are multiples of the associated Legendre function $P_n^m(\cos(\theta))$ that are denoted by

$$(p, n, m) \rightarrow \psi_{(p,n,m)}(r, \theta, \phi) \tag{5.1.0.1}$$

need to satisfy the same boundary conditions in order we can relate head surface measurements to internal brain activity.

5.1.1 Voltage Boundary Value Conditions

We want to recover brain activity to help handicapped people operate and artificial limb from nonsurgical measurements of voltage distributions outside the head. Zhou ([140], page 9, equation (1.1.49)) gives the interface boundary conditions as (i) the voltage is continuous across surfaces separating different tissue regions and (ii) the tissue permittivity times the normal component of the voltage gradient is continuous across surfaces separating different tissue regions. If (i) did not hold, since there is a finite resistence per unit thickness in tissue layers, there would be an infinite current across the tissue interface. If (ii) did not hold there would be a net charge on the separating surface.

5.1.2 The Representation of the Interrogating Scalar Functions for Relating Head Surface EEG Recordings and Internal Brain Activity

We define the product

$$(p, \ell, j) \to \mathcal{E}(p, \ell, j) \tag{5.1.2.1}$$

as

$$\mathcal{E}(p, \ell, j) = \epsilon(p, (-1)^{\ell} j\omega) k(p, (-1)^{\ell} j\omega) \tag{5.1.2.2}$$

of permittivity and the propagation constant

We define

$$\tilde{z}_p = k(p+1, (-1)^{\ell} j\omega) R_p \tag{5.1.2.3}$$

where $r = R_p$ is the outer boundary of the brain tissue interface, region when $p = 1$ and for $p = 1$

$$z_1 = z_p = k(p, (-1)^{\ell} j\omega) R_p \tag{5.1.2.4}$$

We define the interrogating scalar functions in tissue region p as

$$\psi^{(\ell,j)}_{(p,n,m)}(r, \theta, \phi) = j_n(k(p, (-1)^{\ell} j\omega) r) P^m_n(\cos(\theta)) \exp(im\phi) h^{(\ell)}_n(z_1) C^{(\ell,j)}_{(p,n,1)}$$

$$+ h^{(\ell)}_n(k(p, (-1)^{\ell} j\omega) r) P^m_n(\cos(\theta)) \exp(im\phi) j_n(z_1) C^{(\ell,j)}_{(p,n,2)} \tag{5.1.2.5}$$

These interrogating functions are all solutions of the scalar Helmholtz equation ([110])

$$\Delta \psi^{(\ell,j)}_{(p,n,m)} + k(p, (-1)^{\ell} j\omega)^2 \psi^{(\ell,j)}_{(p,n,m)} = 0 \tag{5.1.2.6}$$

where Δ is the Laplacian defined in Cartesian coordinates by

$$\Delta = \frac{\partial^2}{\partial x^2} + \frac{\partial^2}{\partial y^2} + \frac{\partial^2}{\partial z^2} \tag{5.1.2.7}$$

Since ([118]) for every smooth vector field $\boldsymbol{G}$ there is a smooth vector field $\boldsymbol{F}$ such that

$$\Delta \boldsymbol{F} = \boldsymbol{G} \tag{5.1.2.8}$$

then by the vector field identity

$$\boldsymbol{G} = \Delta \boldsymbol{F} = \nabla(\nabla \cdot (\boldsymbol{F}) + \nabla \times (\nabla \times (-\boldsymbol{F}) \tag{5.1.2.9}$$

we have the proof that every smooth vector field $\boldsymbol{G}$ is a gradient plus a curl. In the brain tissue region when $p = 1$ the function $\psi^{(\ell,j)}_{(p,n,m)}$ defined by (5.1.2.5) must be bounded which means that when $p = 1$

$$C^{(\ell,j)}_{(p,n,2)} = 0 \tag{5.1.2.10}$$

defined by

5.1.3 The Transition Matrix Relationship Ensuring Continuity of the Interrogating Scalar Function and Permittivity Times its Normal Derivative across Tissue Interfaces while Reducing Overflow and Underflow

We have

$$\lim_{z\to z_p}\begin{bmatrix} j_n(z)h^{(\ell)}_n(z_1) & h^{(\ell)}_n(z)j_n(z_1) \\ \mathcal{E}(p,(-1)^\ell j\omega)\left\{(d/dz)j_n(z)\right\}h^{(\ell)}_n(z_1) & \mathcal{E}(p,(-1)^\ell j\omega)\left\{(d/dz)h^{(\ell)}_n(z)\right\}j_n(z_1)\end{bmatrix}$$

$$\cdot\begin{bmatrix} C^{(\ell,j)}_{(p,n,1)} \\ C^{(\ell,j)}_{(p,n,2)}\end{bmatrix} =$$

$$\lim_{z\to \tilde{z}_p}\begin{bmatrix} j_n(z)h^{(\ell)}_n(z_1) & h^{(\ell)}_n(z)j_n(z_1) \\ \mathcal{E}(p+1,(-1)^\ell j\omega)\left\{(d/dz)j_n(z)\right\}h^{(\ell)}_n(z_1) & \mathcal{E}(p+1,(-1)^\ell j\omega)\left\{(d/dz)h^{(\ell)}_n(z)\right\}j_n(z_1)\end{bmatrix}$$

$$\cdot\begin{bmatrix} C^{(\ell,j)}_{(p+1,n,1)} \\ C^{(\ell,j)}_{(p+1,n,2)}\end{bmatrix} \tag{5.1.3.1}$$

In matrix language equation (5.1.3.1) may be reexpressed as

$$T^{(\ell,j)}_{(p,n)}\begin{bmatrix} C^{(\ell,j)}_{(p,n,1)} \\ C^{(\ell,j)}_{(p,n,2)}\end{bmatrix} = S^{(\ell,j)}_{(p,n)}\begin{bmatrix} C^{(\ell,j)}_{(p+1,n,1)} \\ C^{(\ell,j)}_{(p+1,n,2)}\end{bmatrix} \tag{5.1.3.2}$$

The multiplying matrices appearing in equation (5.1.3.2) are actually defined by equation (5.1.3.1) so that

$$S^{(\ell,j)}_{(p,n)} =$$

$$\lim_{z\to \tilde{z}_p}\begin{bmatrix} j_n(z)h^{(\ell)}_n(z_1) & h^{(\ell)}_n(z)j_n(z_1) \\ \mathcal{E}(p+1,(-1)^\ell j\omega)\left\{(d/dz)j_n(z)\right\}h^{(\ell)}_n(z_1) & \mathcal{E}(p+1,(-1)^\ell j\omega)\left\{(d/dz)h^{(\ell)}_n(z)\right\}j_n(z_1)\end{bmatrix} \tag{5.1.3.3}$$

where $\tilde{z}_p$ is given by equation (5.1.2.3). The matrix $T^{(\ell,j)}_{(p,n)}$ is defined by

$$T^{(\ell,j)}_{(p,n)} =$$

$$\lim_{z\to z_p}\begin{bmatrix} j_n(z)h^{(\ell)}_n(z_1) & h^{(\ell)}_n(z)j_n(z_1) \\ \mathcal{E}(p,(-1)^\ell j\omega)\left\{(d/dz)j_n(z)\right\}h^{(\ell)}_n(z_1) & \mathcal{E}(p,(-1)^\ell j\omega)\left\{(d/dz)h^{(\ell)}_n(z)\right\}j_n(z_1)\end{bmatrix} \tag{5.1.3.4}$$

where z_p is given by (5.1.2.4), j_n is a spherical Bessel function, and $h^{(\ell)}_n$ is a spherical Hankel function.

5.1.4 The $S^{(\ell,j)}_{(p+1,n)}$ Transition Matrices for Going through the Skull Bone to the Head Surface

For consistency we multiply the spherical Hankel function columns of the transition matrices by the same $j_n(z_1)$ where z_p is given by (5.1.2.4) and the spherical Bessel function columns of We define

$$\tilde{z}_{p+1} = k(p+2, (-1)^\ell j\omega) R_{p+1} \tag{5.1.4.1}$$

where p is the index of brain tissue. We have

$$S^{(\ell,j)}_{(p+1,n)} =$$

$$\lim_{z \to \tilde{z}_{p+1}} \begin{bmatrix} j_n(z) h_n^{(\ell)}(z_1) & h_n^{(\ell)}(z) j_n(z_1) \\ \mathcal{E}(p+1, (-1)^\ell j\omega) \left\{ (d/dz) j_n(z) \right\} h_n^{(\ell)}(z_1) & \mathcal{E}(p+1, (-1)^\ell j\omega) \left\{ (d/dz) h_n^{(\ell)}(z) \right\} j_n(z_1) \end{bmatrix} \tag{5.1.4.2}$$

where z_1 is the same argument of the spherical Bessel or Hankel function matrix column vector multiplier defined by (5.1.2.4).

5.1.5 Definition of the $T^{(\ell,j)}_{(p+1,n)}$ Transition Matrices for Going through the Skull Bone to the Head Surface

Here we define

$$z_{p+1} = k(p+1, (-1)^\ell j\omega) R_{p+1} \tag{5.1.5.1}$$

and for consistency z_p is the same argument of the spherical Bessel or Hankel function matrix column vector multiplier defined by (5.1.2.4). The matrix $T^{(\ell,j)}_{(p+1,n)}$ is given by

$$T^{(\ell,j)}_{(p+1,n)} =$$

$$\lim_{z \to z_{p+1}} \begin{bmatrix} j_n(z) h_n^{(\ell)}(z_1) & h_n^{(\ell)}(z) j_n(z_1) \\ \mathcal{E}(p, (-1)^\ell j\omega) \left\{ (d/dz) j_n(z) \right\} h_n^{(\ell)}(z_1) & \mathcal{E}(p, (-1)^\ell j\omega) \left\{ (d/dz) h_n^{(\ell)}(z) \right\} j_n(z_1) \end{bmatrix} \tag{5.1.5.2}$$

5.1.6 Exact Formula Determinant of the Transition Matrices (5.1.3.3) in Equation (5.1.3.2) Using Wronskian Relations

The basic Wronskian Relationship involving spherical Bessel functions $j_n(z)$ and Neumann functions $y_n(z)$ ([1]) is is

$$j_n(z) \left\{ \left(\frac{d}{dz} \right) y_n(z) \right\} - \left\{ \left(\frac{d}{dz} \right) j_n(z) \right\} y_n(z) = \frac{1}{z^2} \tag{5.1.6.1}$$

The derived Wronskian relationship is

$$j_n(z) \left\{ \left(\frac{d}{dz} \right) h_n^{(\ell)}(z) \right\} - \left\{ \left(\frac{d}{dz} \right) j_n(z) \right\} h_n^{(\ell)}(z) = \frac{-i(-1)^\ell}{z^2} \tag{5.1.6.2}$$

From equations (5.1.6.2) and (5.1.3.2) we deduce that

$$\det(S^{(\ell,j)}_{(p,n)}) = \Delta^{(\ell,j)}_{(S,p,n)}$$

$$= \mathcal{E}(p+1,(-1)^{\ell}j\omega)\left(\frac{-i(-1)^{\ell}}{[k(p+1,(-1)^{\ell}j\omega)R_p]^2}\right)\left\{j_n(z_p)h^{(\ell)}_n(z_1)\right\} \tag{5.1.6.3}$$

where z_1 is given by (5.1.2.4), where $\tilde{z}_p$ is given by (5.1.2.3) and $\mathcal{E}(p+1,(-1)^{\ell}j\omega)$ is given by (5.1.2.2). In a following section we will show numerical results comparing the exact formula (5.1.6.3) with the numerical formula

$$\det(S^{(\ell,j)}_{(p,n)}) = \Delta^{(\ell,j)}_{(S,p,n)}$$

$$= \left\{S^{(\ell,j)}_{(p,n)}(1,1)S^{(\ell,j)}_{(p,n)}(2,2) - S^{(\ell,j)}_{(p,n)}(1,2)S^{(\ell,j)}_{(p,n)}(2,1)\right\} \tag{5.1.6.4}$$

where $S^{(\ell,j)}_{(p,n)}$ is given by (5.1.3.3).

5.1.7 Accurate Determination of the Representation of the Interrogating Scalar Functions Outside the Skull Bone

The first step is to have a numerically accurate inverse of the transition matrix $S^{(\ell,j)}_{(n,p)}$ defined by (5.1.3.3) and (5.1.2.3) whose exact formula determinant $\Delta^{(\ell,j)}_{(S,p,n)}$ is given by (5.1.6.3) where $\tilde{z}_p$ is given by (5.1.2.3) and $\mathcal{E}(p+1,(-1)^{\ell}j\omega)$ is given by (5.1.2.2). We have for the inverse of the matrix given by (5.1.3.3)

$$\left(S^{(\ell,j)}_{(n,p)}\right)^{-1} =$$

$$\frac{1}{\Delta^{(\ell,j)}_{(S,p,n)}}\begin{bmatrix} S^{(\ell,j)}_{(n,p)}(2,2) & -S^{(\ell,j)}_{(n,p)}(1,2) \\ -S^{(\ell,j)}_{(n,p)}(2,1) & S^{(\ell,j)}_{(n,p)}(1,1) \end{bmatrix} \tag{5.1.7.1}$$

where the determinant is given by (5.1.6.3). The expansion coefficients are then determined by

$$\begin{bmatrix} C^{(\ell,j)}_{(p+1,n,1)} \\ C^{(\ell,j)}_{(p+1,n,2)} \end{bmatrix} = \left(S^{(\ell,j)}_{(n,p)}\right)^{-1} T^{(\ell,j)}_{(n,p)} \begin{bmatrix} C^{(\ell,j)}_{(p,n,1)} \\ C^{(\ell,j)}_{(p,n,2)} \end{bmatrix} \tag{5.1.7.2}$$

where $T^{(\ell,j)}_{(p,n)}$ is defined by (5.1.3.4) and $(S^{(\ell,j)}_{(p,n)})^{-1}$ is defined by (5.1.7.1), and where in brain tissue $p = 1$. Because the interrogating function must be differentiable in all tissue regions we have for the brain tissue region

$$\begin{bmatrix} C^{(\ell,j)}_{(p,n,1)} \\ C^{(\ell,j)}_{(p,n,2)} \end{bmatrix}_{p=1} = \begin{bmatrix} 1 \\ 0 \end{bmatrix} \tag{5.1.7.3}$$

5.2 The Use of Interrogating Scalar Functions to Recover Brain Activity from a Dynamic Head Surface Voltage Distribution

We rigorously define the dynamic voltage frequency components, its connection to the divergence of the vector potential. and the boundary condtions and partial differential equations that they satisfy; we then show that for all interrogating scalar functions ψ that satisfy the same partial differential equations and boundary conditions that there is a relationship between measurements outside the brain and

5.2.1 Rigorous Determination of Brain Activity from EEG Measurements

The rigorous EEG inversion method uses electrodynamics concepts found in Kovetz ([74], page 160 and Jackson ([66], page 219). From the electrodynamics concepts in Kovetz ([74], page 160) and Jackson ([66]) we develop a boundary value problem which enables us to predict, using the Lorenz guage identity, the vector potential, the electric field $\boldsymbol{E}$, and the magnetic field $\boldsymbol{H}$ outside the head that are stimulated by brain activity.

The electrdynamics relationships ([74], page 160) give us relationships between electric fields $\boldsymbol{E}$ and magnetic fields $\boldsymbol{H}$ that are stimulated by brain activity. We know that tangential components of $\boldsymbol{E}$ and $\boldsymbol{H}$ are continuous across tissue interfaces. Coupling this with the two electrodynamics relationships and the Lorenz gauge relationship gives us boundary conditions satisfied by the vector potential and gives us a way of predicting it in intermediate tissue layers and outside the head.

These vector fields give us predictions of the EEG voltage and the gradient of the EEG voltage outside the head. We square the difference between predictions and measurements and compute partial derivatives with respect to the coefficients representing internal brain activity. This gives us a system of linear equations in the coefficients

$$\mathrm{q} \rightarrow c(n, m, \overline{\ell}, (-1)^{\ell} j\omega, p, \mathrm{q})(U_{\mathrm{q}}, V_{\mathrm{q}}, W_{\mathrm{q}}) \tag{5.2.1.1}$$

where q is an index for a potential site of a priori unknown brain activity in the total internal vector potential equation (9.5.4.1) representing internal brain activity to external EEG measurements where

$$c(n, m, \overline{\ell}, (-1)^{\ell} j\omega, p, \mathrm{q}) =$$
$$\left(\frac{(n- \mid m \mid)!}{(n+ \mid m \mid)!}\right) Z_n^{(\overline{\ell})}(k(p, (-1)^{\ell} j\omega) r_q) P_n^{|m|}(\cos(\theta_q)) \exp(-im\phi_q) \tag{5.2.1.2}$$

where if $\overline{\ell}$ is zero $Z_n^{(\overline{\ell})}(z)$ is the spherical Bessel function $j_n(z)$.

The elements of this matrix relating brain activity to EEG measurements are independent of any brain activity.

To rigorously define voltage when the electric vector is nonconservative we, following the notation in Kovetz ([74], page160) write

$$\boldsymbol{E} = -\frac{\partial \boldsymbol{A}}{\partial t} - \nabla(V) \tag{5.2.1.3}$$

and

$$\boldsymbol{H} = \left(\frac{1}{\mu}\right) \nabla \times (\boldsymbol{A}) \tag{5.2.1.4}$$

If ρ represents the total charge density and $\boldsymbol{J}$ represents the total current density so that for time harmonic radiation with a time dependence of

$$t \to \exp(i(-1)^{\ell}\omega t), \tag{5.2.1.5}$$

which is a postive frequency for $\ell = 2$ and a negative frequency for $\ell = 1$, we have

$$\nabla\cdot(\boldsymbol{D}) = \rho \tag{5.2.1.6}$$

and

$$\nabla \times (\boldsymbol{H}) = \frac{\partial \boldsymbol{D}}{\partial t} + \boldsymbol{J} \tag{5.2.1.7}$$

where $\boldsymbol{D}$ is the displacement vector and $\boldsymbol{J}$ is the current density. From (5.2.1.3) we have, in spherical coordinates, where

$$\nabla(V) = \boldsymbol{e}_r \frac{\partial V}{\partial r} + \frac{1}{r}\boldsymbol{e}_\theta \frac{\partial V}{\partial \theta} + \left(\frac{1}{r\sin(\theta)}\right)\frac{\partial V}{\partial \phi} \tag{5.2.1.8}$$

Thus, separating equation (5.2.1.3) into its three components we have

$$E_r = -\frac{\partial A_r}{\partial t} - \frac{\partial V}{\partial r} \tag{5.2.1.9}$$

$$E_\theta = -\frac{\partial A_\theta}{\partial t} - \frac{1}{r}\frac{\partial V}{\partial \theta} \tag{5.2.1.10}$$

and

$$E_\phi = -\frac{\partial A_\theta}{\partial t} - \left(\frac{1}{r\sin(\theta)}\right)\frac{\partial V}{\partial \phi} \tag{5.2.1.11}$$

We decompose the brain wave signals into components whose time dependencies are of the form We shall prove that outside the head, the charge density ρ is zero so that

$$\Delta V + k(p+2, (-1)^{\ell}\omega)^2 V = \frac{\rho}{\epsilon_0} = 0 \tag{5.2.1.12}$$

where

$$(\ell, \omega) \to k(p+2, (-1)^{\ell}\omega) \tag{5.2.1.13}$$

is the propagation constant in the tissue region outside the head and the vector potential $\boldsymbol{A}$ and the voltage are related by the Lorenz gauge condition ([74], equation 44.4, page 160) which waves with a time dependence of the form (5.2.1.5) are related by

$$i(-1)^{\ell}\omega\,\nabla\cdot(\boldsymbol{A}) - k(p+2, (-1)^{\ell}\omega)^2 V = 0 \tag{5.2.1.14}$$

or solving for V in equation (5.2.1.14) that

$$V = \left(\frac{i(-1)^{\ell}\omega}{k(p+2, (-1)^{\ell}\omega)^2}\right)\nabla\cdot(\boldsymbol{A}) \tag{5.2.1.15}$$

and

$$\Delta \boldsymbol{A} = k(p+2, (-1)^{\ell}\omega)^2 \boldsymbol{A} = -\mu_0 \boldsymbol{J} = 0 \tag{5.2.1.16}$$

We have found linear equations which relate the Hirvonen vector potential (9.5.3.2) representing the brain activity to rigorously to EEG measurements outside the head. We could start with the known expansion in brain tissue and hypothesize a reflected vector potential in brain tissue, a transmitted and reflected vector potential in the skull bone region and a transmitted vector potential outside the skull the we use to obtain the EEG prediction. We then use the vector potential discovered by measurement to predict the EEG measurement. Jackson ([66], page 219) gives the same equations in Gaussian units. The vector potential (9.5.3.2) uses the three vector fields (9.4.1.12), (9.4.1.13), and (9.4.1.15). However, only the first one has a nonzero divergence since the others are multiples of curls of the others. Thus, each Lorenz guage relationship using the true EEG voltage at an EEG measurement point gives us an equation involving the expansion coefficients multiplying the vector fields (9.4.1.12) for each EEG frequency component. We, thus, write out the Fourier series for the predicted voltage in terms of the expansion coefficients multiplying the zero curl vector fields given by (9.4.1.12). We square the difference between the predicted voltage time profile defined by (5.2.1.15) and the measured EEG voltage and integrate over an entire time interval. We take the partial derivatives with respect to the (9.4.1.12) vector field expansion coefficients giving a linear system of equations in all the, a priori, unknown expansion coefficients for each EEG measurement point. This, gives us the coefficients multiplying the nonzero curl vector fields (9.4.1.12) that appear in the representation of the vector potential. By solving the boundary value problem described above we find the vector potential representation inside the head which causes the coefficients of the vector fields (9.4.1.12) to match the EEG measurements. The internal brain wave current density equations are then determined by applying the Helmholtz operator to the brain-tissue vector potential.

5.2.2 Gauge EEG Voltages for Each Frequency Component

We suppose that the scattering body is partitioned into regions of constant permittivity. The magnetic field is derived from the vector potential by

$$\boldsymbol{H} = \frac{1}{\mu}\nabla \times (\boldsymbol{A}) \tag{5.2.2.1}$$

The electric vector is related to this vector potential, $\boldsymbol{A}$, which has the form defined by (9.5.3.2) uses the three vector fields (9.4.1.12), (9.4.1.13), and (9.4.1.15). and the true EEG voltage V by

$$\boldsymbol{E} = \frac{\partial \boldsymbol{A}}{\partial t} - \nabla(V) \tag{5.2.2.2}$$

If the time dependence of a frequency component of the electric vector and magnetic vectors stimulated by brain activity is

$$t \to \exp(i(-1)^{\ell}\omega t) \tag{5.2.2.3}$$

then for this frequency component equation (5.2.2.2) has the form

$$\boldsymbol{E}_{(\ell,\omega)} = -i(-1)^{\ell}\omega \boldsymbol{A} - \nabla(V) \tag{5.2.2.4}$$

If $\boldsymbol{D}$ is the displacement vector and ρ is the charge density, then

$$\nabla\cdot(\boldsymbol{D}) = \rho \tag{5.2.2.5}$$

and in a region of constant permittivity $\epsilon((-1)^{\ell}\omega)$

$$\nabla\cdot(\boldsymbol{E}) = \frac{\rho}{\epsilon((-1)^{\ell}\omega)} \tag{5.2.2.6}$$

and for the frequency component described by (5.2.2.3) equation (5.2.2.2) has the form

$$\boldsymbol{E} = -i(-1)^{\ell}\omega\,\nabla\cdot(\boldsymbol{A}) - \nabla(V) \tag{5.2.2.7}$$

Applying the divergence operation (4.1.1.42) to each side of (5.2.2.7) and using the Laplacian, Δ, definition (4.1.1.67) that the Laplacian, Δ, of the EEG voltage V is

$$\Delta V = \nabla\cdot(\nabla(V)) \tag{5.2.2.8}$$

we have

$$\nabla\cdot(\boldsymbol{E}) = -i(-1)^{\ell}\omega\,\nabla\cdot(\boldsymbol{A}) - \Delta V = \frac{\rho}{\epsilon((-1)^{\ell}\omega)} \tag{5.2.2.9}$$

Rearranging terms in (5.2.2.9) and adding and subtracting

$$(\ell,\omega) \rightarrow k^2 = \omega^2\epsilon((-1)^{\ell}\omega)\mu \tag{5.2.2.10}$$

judiciously in (5.2.2.9) we have

$$\Delta V + k^2V + \left\{i(-1)^{\ell}\omega\,\nabla\cdot(\boldsymbol{A}) - k^2V\right\} = -\frac{\rho}{\epsilon} \tag{5.2.2.11}$$

Factoring in (5.2.2.11) making use of

$$-k^2 = i(-1)^{\ell}\omega\left\{i(-1)^{\ell}\omega\mu\epsilon\right\} \tag{5.2.2.12}$$

Equations (5.2.2.11) and (5.2.2.12) give

$$\Delta V + k((-1)^{\ell}\omega)^2V + i(-1)^{\ell}\omega\left\{\nabla\cdot(\boldsymbol{A}) + i(-1)^{\ell}\omega\mu\epsilon V\right\} = -\frac{\rho}{\epsilon} \tag{5.2.2.13}$$

which is exactly the frequency component form of the first part of equation (44.3) in Kovetz([74], page 160). For the frequency component with time dependence (5.2.2.3) the curl (9.4.1.7) of the electric vector $\boldsymbol{E}$ stimulated by brain activity has the form

$$\nabla\times(\boldsymbol{H}) = i(-1)^{\ell}\omega\epsilon\boldsymbol{E} + \boldsymbol{J} \tag{5.2.2.14}$$

Thus, applying the curl operation (9.4.1.7) to each side of (5.2.2.1) gives us after using the general identity

$$\nabla\times(\nabla\times(\boldsymbol{A})) = \nabla(\nabla\cdot(\boldsymbol{A}) - \Delta\boldsymbol{A} \tag{5.2.2.15}$$

where Δ is defined by (4.1.1.67) the relationship

$$\nabla\times(\boldsymbol{H}) = \frac{1}{\mu}\nabla\times(\nabla\times(\boldsymbol{A})) =$$

$$\frac{1}{\mu}\left[\nabla(\nabla\cdot(\boldsymbol{A}) - \Delta\boldsymbol{A}\right]$$

$$= i(-1)^{\ell}\omega\epsilon\left[-i(-1)^{\ell}\omega\boldsymbol{A} - \nabla(V)\right] + \boldsymbol{J} \tag{5.2.2.16}$$

Rearranging terms in (5.2.2.16) after multiplying all terms by the magnetic permeability μ gives with Δ defined by (4.1.1.67)

$$\Delta\boldsymbol{A} + i(-1)^{\ell}\omega\epsilon\left\{-i(-1)^{\ell}\right\}\boldsymbol{A}$$

$$-\nabla(\nabla\cdot(\boldsymbol{A}) - i(-1)^{\ell}\omega\mu\epsilon\,\nabla(V) = -\mu\boldsymbol{J} \tag{5.2.2.17}$$

Using (5.2.2.10) and (5.2.2.12) in (5.2.2.17) gives us

$$\Delta\boldsymbol{A} + k^2\boldsymbol{A} - \nabla\left[\nabla\cdot(\boldsymbol{A}) + i(-1)^{\ell}\omega\mu\epsilon V\right] = -\mu\boldsymbol{J} \tag{5.2.2.18}$$

If we set

$$\left[\nabla\cdot(\boldsymbol{A}) + i(-1)^{\ell}\omega\mu\epsilon V\right] = 0 \tag{5.2.2.19}$$

and substitute (5.2.2.19) into (5.2.2.13) we have the rigorous EEG voltage equation

$$\Delta V + k^2 V = \frac{\rho}{\epsilon} \tag{5.2.2.20}$$

which is exactly the first part of equation (44.5) of Kovetz ([74], page 161) for the frequency component whose time dependence is given by (5.2.2.3). If we substitute (5.2.2.19) into (5.2.2.18) we have

$$\Delta\boldsymbol{A} + k^2\boldsymbol{A} = -\mu\boldsymbol{J} \tag{5.2.2.21}$$

which is exactly the second part of equation (44.5) of Kovetz ([74], page 161) for the frequency component whose time dependence is (5.2.2.3). For each frequency component with time dependence (5.2.2.3) the EEG voltage is

$$V = \left[\frac{1}{i(-1)^{\ell}\omega\mu}\right]\nabla\cdot(\boldsymbol{A}) \tag{5.2.2.22}$$

which is exactly the Lorentz guage condition, equation 44.4, of Kovetz (citeKovetz, page 160). Thus, the magnetic vector $\boldsymbol{H}$ stimulated by brain activity is defined in terms of the vector potential $\boldsymbol{A}$ by (5.2.2.3) and the electric vector $\boldsymbol{E}$ stimulated by brain activity is defined in terms of the brain activity vector potential $\boldsymbol{A}$ defined in brain tissue by (9.5.3.2) as

$$\boldsymbol{E} = -i(-1)^{\ell}\omega\boldsymbol{A} - \left\{\frac{1}{i(-1)^{\ell}\omega\mu\epsilon}\right\}\nabla(\nabla\cdot(\boldsymbol{A}) \tag{5.2.2.23}$$

We can carry the non-conservative vector field EEG voltage from brain-tissue underneath the skull bone, through the skull bone, to the region outside the head by requiring that V and the function

$$(\ell, \omega, r, \theta, \phi) \rightarrow \epsilon((-1)^{\ell}\omega)\,\nabla(V)\cdot\boldsymbol{n} \tag{5.2.2.24}$$

where $\boldsymbol{n}$ is the normal vector to the tissue interface separating two different tissue regions, be continuous across the interfaces.

5.2.3 A Proof that the Divergence of the Vector Fields $\boldsymbol{L}_{(n,p)}^{(m,\tilde{\ell},(-1)^{\ell}\omega)}$ Associated with Brain Activity are all Solutions of the EEG Voltage Equation

The purpose of this section is to carefully proof that the zero curl vector field defined by (9.4.1.12) used in (9.5.4.1) to represent the vector potential from all sources of brain activity has a divergence which satisfies

$$\Delta\left\{\nabla\cdot(\boldsymbol{L}_{(n,p)}^{(m,\tilde{\ell},(-1)^{\ell}j\omega)})\right\}+k^2\left\{\nabla\cdot(\boldsymbol{L}_{(n,p)}^{(m,\tilde{\ell},(-1)^{\ell}j\omega)})\right\}=0 \tag{5.2.3.1}$$

which is the same equation (5.2.2.20) that is satisfied by the EEG voltage when the charge density ρ is set to zero.

For the frequency component whose time dependence is given by (5.2.2.3), the zero curl component of the vector potential is

$$\boldsymbol{L}_{(n,p)}^{(m,\tilde{\ell},(-1)^{\ell}\omega)}=$$

$$\left(\frac{d}{dz}\right)Z_n^{(\tilde{\ell})}(z)\mid_{z=k(p,(-1)^{\ell}\omega)r}P_n^m((\cos(\theta))\exp(im\phi)\boldsymbol{e}_r$$

$$+\left(\frac{Z_n^{(\tilde{\ell})}(k(p,(-1)^{\ell}j\omega)r)}{k(p,(-1)^{\ell}\omega)r}\right)\left[\frac{d}{d\theta}P_n^m(\cos(\theta))\boldsymbol{e}_\theta+im\left(\frac{P_n^m(\cos(\theta))}{\sin(\theta)}\right)\boldsymbol{e}_\phi\right]\exp(im\phi) \tag{5.2.3.2}$$

The divergence in spherical coordinates is, using (4.1.1.42), given by

$$\nabla\cdot(F_r\boldsymbol{e}_r+F_\theta\boldsymbol{e}_\theta+F_\phi\boldsymbol{e}_\phi)=$$

$$\frac{1}{r^2\sin(\theta)}\left[\left(\frac{\partial}{\partial r}\right)(r^2\sin(\theta)F_r)+\left(\frac{\partial}{\partial\theta}\right)(r\sin(\theta)F_\theta)+\left(\frac{\partial}{\partial\phi}\right)(rF_\phi)\right] \tag{5.2.3.3}$$

As a simple check on (5.2.3.3) note that according to (4.1.1.42)

$$\nabla\cdot(r\boldsymbol{e}_r)=\nabla\cdot(x\boldsymbol{e}_x+y\boldsymbol{e}_y+z\boldsymbol{e}_z)=3 \tag{5.2.3.4}$$

and using (5.2.3.3)

$$\nabla\cdot(r\boldsymbol{e}_r)=\frac{1}{r^2\sin(\theta)}\left(\frac{\partial}{\partial r}\right)[(r^2\sin(\theta))r]=\frac{1}{r^2}\frac{\partial}{\partial r}r^3=\frac{3r^2}{r^2}=3 \tag{5.2.3.5}$$

We need Bessel's equation (9.4.1.1) for spherical Bessel functions in the form

$$\left(\frac{1}{z^2}\right)\frac{d}{dz}\left(z^2\frac{dZ_n^{(\tilde{\ell})}(z)}{dz}\right)=[\frac{n(n+1)}{z^2}-1]Z_n^{(\tilde{\ell})}(z) \tag{5.2.3.6}$$

where the general spherical Bessel function is defined by (9.4.1.10). We also need the ordinary differential equation for the associated Legendre function differential equation (9.4.1.2) in the form

$$\frac{1}{\sin(\theta)}\frac{d}{d\theta}\left[\sin(\theta)\left(\frac{d}{d\theta}\right)P_n^m(\cos(\theta))\right]=\left(\frac{m^2}{\sin^2(\theta))}\right)P_n^m(\cos(\theta))-n(n+1)P_n^m(\cos(\theta)) \tag{5.2.3.7}$$

The first term of the divergence of the vector field (5.2.3.2) is with F_r being the $\boldsymbol{e}_r$ component of (5.2.3.2) is, using (5.2.3.6), given by

$$\frac{1}{r^2\sin(\theta)}\left[\left(\frac{\partial}{\partial r}\right)(r^2\sin(\theta)F_r)\right]$$

$$= \frac{1}{r^2}\left[\left(\frac{\partial}{\partial r}\right)(r^2\sin(\theta)F_r)\right]$$

$$= \frac{1}{r^2}\left(\frac{\partial}{\partial r}\right)\left[r^2\frac{d}{dz}Z_n^{(\tilde{\ell})}(z)\mid_{z=k(p,(-1)^\ell\omega)r} P_n^m((\cos(\theta))\exp(im\phi)\right]$$

$$= k\left\{\frac{1}{k^2r^2}\left(\frac{\partial}{\partial kr}\right)\left[k^2r^2\frac{d}{dz}Z_n^{(\tilde{\ell})}(z)\mid_{z=k(p,(-1)^\ell\omega)r} P_n^m((\cos(\theta))\exp(im\phi)\right]\right\}$$

$$= k\left\{\frac{1}{z^2}\frac{d}{dz}\left[z^2\frac{d}{dz}Z_n^{(\tilde{\ell})}(z)\right]\mid_{z=k(p,(-1)^\ell\omega)r}\right\} P_n^m((\cos(\theta))\exp(im\phi)$$

$$= k\left[\frac{n(n+1)}{k^2r^2}-1\right]P_n^m((\cos(\theta))\exp(im\phi) \tag{5.2.3.8}$$

The second term of the divergence (5.2.3.3) from (5.2.3.2) with

$$F_\theta = \left(\frac{Z_n^{(\tilde{\ell})}(k(p,(-1)^\ell\omega)r)}{k(p,(-1)^\ell\omega)r}\right)\left[\frac{d}{d\theta}P_n^m(\cos(\theta))\right]\exp(im\phi) \tag{5.2.3.9}$$

and considering the associated Legendre function differential equation in the easy-to-use form (5.2.3.7) is given by

$$\frac{1}{r^2\sin(\theta)}\left(\frac{\partial}{\partial\theta}\right)(r\sin(\theta)F_\theta) =$$

$$= \frac{1}{r^2}\left(\frac{Z_n^{(\tilde{\ell})}(k(p,(-1)^\ell\omega)r)}{k(p,(-1)^\ell\omega)r}\right)\left[\frac{1}{\sin(\theta)}\frac{d}{d\theta}\left(r\sin(\theta)\frac{dP_n^m(\cos(\theta))}{d\theta}\right)\right]\exp(im\phi)$$

$$= k\left(\left[\frac{Z_n^{(\tilde{\ell})}(z)}{z^2}\right]\mid_{z=k(p,(-1)^\ell\omega)r}\right)\left[+m^2\frac{P_n^m(\cos(\theta))}{\sin^2(\theta)}-n(n+1)P_n^m(\cos(\theta))\right]\exp(im\phi) \tag{5.2.3.10}$$

The third and final term in the computation of the divergence of the zero curl vector field appearing in the equation (9.5.4.1) for the vector potential of brain activity from all sources is using (5.2.3.2) with

$$F_\phi = \left(\frac{Z_n^{(\tilde{\ell})}(k(p,(-1)^\ell\omega)r)}{k(p,(-1)^\ell\omega)r}\right)\left[im\left(\frac{P_n^m(\cos(\theta))}{\sin(\theta)}\right)\right]\exp(im\phi) \tag{5.2.3.11}$$

and the divergence formula (5.2.3.3) given by

$$\frac{1}{r^2\sin(\theta)}\left(\frac{\partial}{\partial\phi}\right)(rF_\phi) = k\left\{\frac{1}{kr\sin(\theta)}\left(\frac{Z_n^{(\tilde{\ell})}(k(p,(-1)^\ell\omega)r)}{k(p,(-1)^\ell\omega)r}\right)\left[im\left(\frac{P_n^m(\cos(\theta))}{\sin(\theta)}\right)\right]\left(\frac{\partial}{\partial\phi}\right)\exp(im\phi)\right\}$$

$$= k \left(\left[\frac{Z_n^{(\tilde{\ell})}(z)}{z^2} \right] |_{z=k(p,(-1)^{\ell}\omega)r} \right) \left[-m^2 \frac{P_n^m(\cos(\theta))}{\sin^2(\theta)} \right] \exp(im\phi) \tag{5.2.3.12}$$

where in (5.2.3.12) we used the fact that

$$im \frac{\partial}{\partial \phi} \exp(im\phi) = -m^2 \exp(im\phi) \tag{5.2.3.13}$$

Adding up the contributions (5.2.3.8), (5.2.3.10), and (5.2.3.12) of the three terms of the divergence of the zero curl vector field $\boldsymbol{L}_{(n,p)}^{(m,\tilde{\ell},(-1)^{\ell}\omega)}$ we obtain

$$\nabla \cdot (\boldsymbol{L}_{(n,p)}^{(m,\tilde{\ell},(-1)^{\ell}\omega)}) = -k \left\{ [Z_n^{(\tilde{\ell})}(z)] |_{z=k(p,(-1)^{\ell}\omega)r} \right\} P_n^m(\cos(\theta)) \exp(im\phi) \tag{5.2.3.14}$$

which is a known solution of the EEG voltage scalar Helmholtz equation

$$\Delta V + k^2 V = 0 \tag{5.2.3.15}$$

so that the sum of the divergences of the $\boldsymbol{L}_{(n,p)}^{(m,\tilde{\ell},(-1)^{\ell}\omega)}$ terms of the vector potential represents the EEG voltage.

5.2.4 Notation for Unit Vectors Orthogonal to Coordinate Planes

If $\boldsymbol{e}_x$, $\boldsymbol{e}_y$ and $\boldsymbol{e}_z$ are the length 1 coordinate vectors perpendicular, respectively, to the coordinate planes defined, respectively, by setting x, y, and z equal to a constant, then, the three unit vectors perpendicular to coordinate surfaces for spherical coordinates may be expressed in terms of the vector $\boldsymbol{r}$ from the origin to the brain wave signal observation point given by

$$\boldsymbol{r} = r\sin(\theta)\cos(\phi)\boldsymbol{e}_x + r\sin(\theta)\sin(\phi)\boldsymbol{e}_y + r\cos(\theta)\boldsymbol{e}_z \tag{5.2.4.1}$$

These three spherical coordinate unit vectors are

$$\boldsymbol{e}_r = \frac{1}{r}\boldsymbol{r} = \sin(\theta)\cos(\phi)\boldsymbol{e}_x + \sin(\theta)\sin(\phi)\boldsymbol{e}_y + \cos(\theta)\boldsymbol{e}_z \tag{5.2.4.2}$$

$$\boldsymbol{e}_\theta = \frac{1}{r}\left(\frac{d}{d\theta}\right)\boldsymbol{r} = \cos(\theta)\cos(\phi)\boldsymbol{e}_x + \cos(\theta)\sin(\phi)\boldsymbol{e}_y - \sin(\theta)\boldsymbol{e}_z \tag{5.2.4.3}$$

and

$$\boldsymbol{e}_\phi = \frac{1}{r\sin(\theta)}\left(\frac{d}{d\phi}\right)\boldsymbol{r} = -\sin(\phi)\boldsymbol{e}_x + \cos(\phi)\boldsymbol{e}_y \tag{5.2.4.4}$$

5.2.5 Notation for the Unit Vector e_q Defining the Neuronal Orientations and the Vector Potentials and Derived Source Magnetic and Electric Fields Associated with Brain Activity

We are attempting to recover the brain wave signal history file on each neuron in a lattice that represents solutions of the nonlinear systems of differential equations describing brain activity and that may be used to calculate the trans-membrane current at Gaussian quadrature points

in order to accurately determine Fourier coefficients in a Fourier series representation of the brain wave signal. The brain wave signal, as a Fourier series, is such that the transmembrane current at the qth location inside the brain has the form of the infinite sum

$$I_q(t) = C(d/dt)V_q(t) = \text{trans-membrane current} = \sum_{j=1}^{\infty} \left\{ \tilde{\alpha}_{(q,j)} \exp(ij\omega t) + \tilde{\beta}_{(q,j)} \exp(-ij\omega t) \right\} =$$

$$\sum_{j=1}^{\infty} \left\{ \left(\frac{(\mathrm{a}_{(q,j)} - ib_{(q,j)})}{2} \right) \exp(ij\omega t) + \left(\frac{(\mathrm{a}_{(q,j)} + ib_{(q,j)})}{2} \right) \exp(-ij\omega t) \right\} \tag{5.2.5.1}$$

where the complex Fourier coefficients of the real signal are

$$\left(\tilde{\alpha}_{(q,j)}, \tilde{\beta}_{(q,j)} \right) = \left(\frac{(\mathrm{a}_{(q,j)} - ib_{(q,j)})}{2}, \frac{(\mathrm{a}_{(q,j)} + ib_{(q,j)})}{2} \right) \tag{5.2.5.2}$$

Thus, the H field source for example then has the form

$$\boldsymbol{H}_{source}(t) = (1/\mu)\nabla \times (\boldsymbol{A}_p(t)) \tag{5.2.5.3}$$

where $\boldsymbol{A}_p$ is the vector potential in region p of assocated with the total contribution from individual trans-membrane currents $I_q(t)$ at locations $\boldsymbol{r}_q$ inside the head given by

$$\boldsymbol{A}_p = \sum_{q=1}^{M} \sum_{j=1}^{\infty} \left[\sum_{\ell=1}^{2} \left(\frac{(\mathrm{a}_{(q,j)} - (-1)^{\ell} ib_{(q,j)})}{2} \right) \boldsymbol{A}_{(p,q)}(\ell, (-1)^{\ell} j\omega, t) \right] \tag{5.2.5.4}$$

where $\boldsymbol{r}_q$ is the qth source of brain wave activity and p is the layer index with p=1 for a brain tissue source and

$$\boldsymbol{A}_{(p,q)}(\tilde{\ell}, (-1)^{\ell} j\omega, t) = \mu/(4\pi) \exp(i(-1)^{\ell} j\omega t) \frac{\exp(-i(-1)^{\tilde{\ell}} k(p, (-1)^{\ell} j\omega) \mid \boldsymbol{r} - \boldsymbol{r}_q \mid)}{\mid \boldsymbol{r} - \boldsymbol{r}_q \mid} \boldsymbol{e}_q \tag{5.2.5.5}$$

where $\boldsymbol{r}$ is the observation point and $\boldsymbol{r}_q$ is the brain wave source location. and μ is the magnetic permeability of brain tissue and

$$\begin{aligned} \boldsymbol{e}_q &= U_q \boldsymbol{e}_x + V_q \boldsymbol{e}_y + W_q \boldsymbol{e}_z \\ &= W_q \left(\cos(\theta) \boldsymbol{e}_r - \sin(\theta) \boldsymbol{e}_\theta \right) + \\ &\left(\frac{U_q - iV_q}{2} \right) \exp(i\phi) \left[\sin(\theta) \boldsymbol{e}_r + \cos(\theta) \boldsymbol{e}_\theta + i \boldsymbol{e}_\phi \right] \\ &+ \left(\frac{U_q + iV_q}{2} \right) \exp(i\phi) \left[\sin(\theta) \boldsymbol{e}_r + \cos(\theta) \boldsymbol{e}_\theta - i \boldsymbol{e}_\phi \right] \end{aligned} \tag{5.2.5.6}$$

In practice our inverse source solution recovers directly the Fourier coefficients and uses these to represent the brain activity on individual neurons.

We can derive the magnetic fields stimulated directly by the brain wave activity as

$$\boldsymbol{H}_{source}(t) = (1/\mu)\nabla \times (\boldsymbol{A}_p) =$$

$$\sum_{q=1}^{M}\left\{\sum_{j=1}^{\infty}\left[\sum_{\ell=1}^{2}\left(\frac{(\mathrm{a}_{(q,j)}-(-1)^{\ell}ib_{(q,j)})}{2}\right)(1/\mu)\nabla\times(\boldsymbol{A}_{(p,q)}(\ell,(-1)^{\ell}j\omega,t))\right]\right\} \qquad (5.2.5.7)$$

However, because brain tissue is dispersive, and the brain tissue permittivity $\epsilon(p,(-1)^{\ell}j\omega)$ depends on the time dependencies $\exp(i(-1)^{\ell}j\omega t)$ of the components of the brain wave signal you have to write

$$\boldsymbol{E}_{source} = (1/\mu)\sum_{q=1}^{M}\sum_{j=1}^{\infty}\left\{\sum_{\ell=1}^{2}\left\{\right.\right.$$
$$\left.\left.\left[\left(\frac{[\mathrm{a}_{(q,j)} - (-1)^{\ell} i b_{(q,j)}]}{2}\right)\left(\frac{1}{(i(-1)^{\ell}\omega\epsilon(p,(-1)^{\ell}j\omega)}\right)\nabla\times(\nabla\times(\boldsymbol{A}_{(p,q)}(\ell,(-1)^{\ell}j\omega,t)))\right]\right\}\right\} \tag{5.2.5.8}$$

Note that for each Fourier series index, j, you have to use the brain tissue permittivity

$$(p,\ell,j\omega) \rightarrow \epsilon(p,(-1)^{\ell}j\omega) \tag{5.2.5.9}$$

5.2.6 Relationship for the Recovery of Brain Activity and the Dynamic Voltage Relationship Between Voltage and Trans-Membrane Current and the Relationship Between Head Surface Measurements and Brain Activity

From Kovetz ([74]) and the use of the fundamental solution of the Helmholtz operator we have the dynamic voltage relationship

$$\Delta V + k((-1)^{\ell}j\omega)^2 V = \left(\frac{i(-1)^{\ell}j\omega)}{k(p,(-1)^{\ell}j\omega)^2}\right)\nabla\cdot(\boldsymbol{J}) \tag{5.2.6.1}$$

between the total dynamic voltage in the brain tissue region and the trans-membrane neuronal current distribution $\boldsymbol{J}$ for the projection of the voltage on the component with the time dependence

$$t \rightarrow \exp(i(-1)^{\ell}j\omega t) \tag{5.2.6.2}$$

The relationship for going from the outside of the head into brain tissue is with $\boldsymbol{n}$ denoting the normal vector to the head surface is, with ψ denoting any brain-activity independent function differentiable in each tissue region and which is continuous along with permittivity times the tissue permittivity times the normal component of its derivative across tissue interfaces, the suface and volume integral relationship relating external measurements to internal brain activity is given by

$$\int_{\partial\Omega}\epsilon(p+2,(-1)^{\ell}j\omega)\left\{\psi\,\nabla(V) - \nabla(\psi)V\right\}\cdot\boldsymbol{n}d\text{area}$$
$$= \epsilon(p,(-1)^{\ell}j\omega)\left(\frac{i(-1)^{\ell}j\omega}{k(p,(-1)^{\ell}j\omega)^2}\right)\int_{\Omega}\psi\,\nabla\cdot(\boldsymbol{J})((-1)^{\ell}j\omega)d\text{volume}$$
$$= -\left(\frac{\epsilon(p,(-1)^{\ell}j\omega)\left\{(-1)^{\ell}j\omega\right\}}{k(p,(-1)^{\ell}j\omega)^2}\right)\int_{\Omega}\left\{\frac{\partial\psi}{\partial x}J_x(\ell,j) + \frac{\partial\psi}{\partial y}J_y(\ell,j) + \frac{\partial\psi}{\partial z}J_z(\ell,j)\right\}d\text{volume}$$
$$= -\left(\frac{\epsilon(p,(-1)^{\ell}j\omega)\left\{(-1)^{\ell}j\omega\right\}}{k(p,(-1)^{\ell}j\omega)^2}\right)\sum_{q=1}^{Q}\left[\frac{\partial\psi}{\partial x}J_x(q,\ell,j) + \frac{\partial\psi}{\partial y}J_y(q,\ell,j) + \frac{\partial\psi}{\partial z}J_z(q,\ell,j)\right]_{(r,\theta,\phi)=(r_q,\theta_q,\phi_q)} \tag{5.2.6.3}$$

The whole idea is to solve a system of equations derived from (5.2.6.3) for many different interrogating functions ψ obtaining the complex quantities $J_x(q,\ell,j)$, $J_y(q,\ell,j)$, and $J_z(q,\ell,j)$ which represent the complex trans-membrane currents with frequency component

$$t \to \exp(i(-1)^{\ell} j\omega t) \tag{5.2.6.4}$$

To create the matrix elements using (5.2.6.3) we need the fact that

$$\frac{\partial\psi}{\partial x} = \sin(\theta)\cos(\phi)\frac{\partial\psi}{\partial r} + \left(\frac{\cos(\theta)\cos(\phi)}{r}\right)\frac{\partial\psi}{\partial\theta} + \left(\frac{-\sin(\phi)}{r\sin(\theta)}\right)\frac{\partial\psi}{\partial\phi} \tag{5.2.6.5}$$

$$\frac{\partial\psi}{\partial y} = \sin(\theta)\sin(\phi)\frac{\partial\psi}{\partial r} + \left(\frac{\cos(\theta)\sin(\phi)}{r}\right)\frac{\partial\psi}{\partial\theta} + \left(\frac{\cos(\phi)}{r\sin(\theta)}\right)\frac{\partial\psi}{\partial\phi} \tag{5.2.6.6}$$

and

$$\frac{\partial\psi}{\partial z} = \cos(\theta)\frac{\partial\psi}{\partial r} + \left(\frac{-\sin(\theta)}{r}\right)\frac{\partial\psi}{\partial\theta} \tag{5.2.6.7}$$

These relationships are derived immediately from representing the gradient in spherical and Cartesian coordinates and using the fact that its value is independent of the coordinate system used to represent it and the representation

$$\nabla(\psi) = \frac{\partial\psi}{\partial r}\boldsymbol{e}_r + \frac{1}{r}\frac{\partial\psi}{\partial\theta}\boldsymbol{e}_\theta + \frac{1}{r\sin(\theta)}\frac{\partial\psi}{\partial\phi}\boldsymbol{e}_\phi \tag{5.2.6.8}$$

Equation (5.2.6.3) gives us the means of recovering brain activity from a dynamic head surface voltage distribution.

5.2.7 The Use of Orthogonality Relationships for Rapid Interrogation of the Dynamic Head Surface Voltage Distribution

We use the follwing lemma concerning the orthogonality of associated Legendre or Ferrer functions ([133], page 323) which states that

Lemma 5.1

$$\int_0^{\pi} P_n^m(\cos(\theta)) \cdot P_r^m(\cos(\theta))\sin(\theta)d\theta = \delta_{(n,r)}\frac{2}{2n+1}\cdot\frac{(n+m)!}{(n-m)!} \tag{5.2.7.1}$$

where

$$\delta_{(n,r)} = \begin{cases} 0 & n \neq r \\ 1 & n = r \end{cases} \tag{5.2.7.2}$$

and the fact that

$$\int_0^{2\pi} \exp(-im\phi)\exp(i\tilde{m}\phi)d\phi = \delta_{(m,\tilde{m})}2\pi \tag{5.2.7.3}$$

We use (5.2.7.1) and (5.2.7.3) to interrogate the $V_{(\ell,j)}$ components of the head surface dynamic voltage.

The derived dynamic head surface dynamic voltage distribution is given by

$$V = V(r,\theta,\phi,t) = \sum_{j=1}^{J}\sum_{\ell=1}^{2}\left(V_{(\ell,j)}(r,\theta,\phi)\exp(i(-1)^{\ell}\mathrm{j}\omega t)\right) = \sum_{j=1}^{J}\sum_{\ell=1}^{2}\sum_{\tilde{n}=0}^{\tilde{n}=N}\sum_{\tilde{m}=-\tilde{n}}^{\tilde{m}=+\tilde{n}}\Bigg\{$$

$$c(\tilde{n},\tilde{m},\mathrm{j},\ell)h_{\tilde{n}}^{(\ell)}(k((-1)^{\ell}j\omega)r)P_{\tilde{n}}^{|\tilde{m}|}(\cos(\theta))\exp(i\tilde{m}\phi)\exp(i(-1)^{\ell}\mathrm{j}\omega t)\quad\Bigg\} \tag{5.2.7.4}$$

In equation (5.2.7.4) the calculated dynamic head surface voltage components are

$$V_{(\ell,j)}(r,\theta,\phi) =$$

$$\sum_{\tilde{n}=0}^{\tilde{n}=N}\sum_{\tilde{m}=-\tilde{n}}^{\tilde{m}=+\tilde{n}} V_{(p+2,\tilde{n},\tilde{m})}^{(\ell,j)}h_{\tilde{n}}^{(\ell)}(k(p+2,(-1)^{\ell}j\omega)r)P_{\tilde{n}}^{\tilde{m}}(\cos(\theta))\exp(i\tilde{m}\phi) \tag{5.2.7.5}$$

where we have used the notation

$$V_{(p+2,n,m)}^{(\ell,j)} = c(\tilde{n},\tilde{m},\mathrm{j},\ell) \tag{5.2.7.6}$$

We interrogate the $V_{(\ell,j)}$ with the complex conjugate

We interrogate the $V_{(\ell,j)}$ in region $p+2$ outside the skull by the complex conjugates if the interrogating functions

$$\psi_{(p+2,n,-m)}^{(\ell,j)}(r,\theta,\phi) = j_n(k(p+2,(-1)^{\ell}j\omega)r)P_n^{|m|}(\cos(\theta))\exp(i-m\phi)h_n^{(\ell)}(z_1)C_{(p+2,n,1)}^{(\ell,j)}$$

$$+h_n^{(\ell)}(k(p+2,(-1)^{\ell}j\omega)r)P_n^{m}(\cos(\theta))\exp(im\phi)j_n(z_1)C_{(p+2,n,2)}^{(\ell,j)} \tag{5.2.7.7}$$

Using the orthogonality relationships (5.2.7.1) and (5.2.7.3) we have upon interrogating $V_{(\ell,j)}$ with the interrogating function defined by (5.2.7.7) the exact evaluations

$$\int_{\phi=0}^{\phi=2\pi}\int_{\theta=0}^{\theta=\pi}\left\{\left(\frac{\partial}{\partial r}\right)\psi_{(p+2,n,-m)}^{(\ell,j)}\right\}V_{(\ell,j)}\sin(\theta)d\theta d\phi =$$

$$k(p+2,(-1)^{\ell}j\omega)\left(\frac{2}{2n+1}\left[\frac{(n+\mid m\mid)!}{(n-\mid m\mid)!}\right]\right)\Bigg\{\quad\left(\lim_{z\to\tilde{z}_{p+1}}\left[\left(\frac{d}{dz}\right)j_n(z)\right]h_n^{(\ell)}(z_1)C_{(p+2,n,1)}^{(\ell,j)}V_{(p+2,n,m)}^{(\ell,j)}\right.$$

$$+\quad\left.\lim_{z\to\tilde{z}_{p+1}}\left[\left(\frac{d}{dz}\right)h_n^{(\ell)}(z)\right]j_n(z_1)C_{(p+2,n,2)}^{(\ell,j)}V_{(p+2,n,m)}^{(\ell,j)}\right\}h_{\tilde{n}}^{(\ell)}(k(p+2,(-1)^{\ell}j\omega)R_{p+1}) \tag{5.2.7.8}$$

where z_1 is given by (5.1.2.4).

The other orthogonality relationship that we use is

$$\int_{\phi=0}^{\phi=2\pi}\int_{\theta=0}^{\theta=\pi}\left\{\psi_{(p+2,n,-m)}^{(\ell,j)}\right\}\left\{\left(\frac{\partial}{\partial r}\right)V_{(\ell,j)}\right\}\sin(\theta)d\theta d\phi =$$

$$k(p+2,(-1)^{\ell}j\omega)\left(\frac{2}{2n+1}\left[\frac{(n+\mid m\mid)!}{(n-\mid m\mid)!}\right]\right)\Bigg\{\quad\left(\lim_{z\to\tilde{z}_{p+1}}\left[j_n(z)\right]h_n^{(\ell)}(z_1)C_{(p+2,n,1)}^{(\ell,j)}V_{(p+2,n,m)}^{(\ell,j)}\right.$$

$$+\quad\left.\lim_{z\to\tilde{z}_{p+1}}\left[h_n^{(\ell)}(z)\right]j_n(z_1)C_{(p+2,n,2)}^{(\ell,j)}V_{(p+2,n,m)}^{(\ell,j)}\right\}\left[\lim_{z\to k(p+2,(-1)^{\ell}j\omega)R_{p+1}}\left(\frac{d}{dz}\right)h_{\tilde{n}}^{(\ell)}(z)\right] \tag{5.2.7.9}$$

where z_1 is given by (5.1.2.4) and

$$\tilde{z}_{p+1} = k(p+2,(-1)^{\ell}j\omega)R_{p+1} \tag{5.2.7.10}$$

In the next section we show the accuracy of the determination of the interrogating scalar functions.

The surface integral and the right side of the derived linear system is

$$\epsilon(p+2,(-1)^{\ell}j\omega)\int_{\phi=0}^{\phi=2\pi}\int_{\theta=0}^{\theta=\pi}\left[\ \psi^{(\ell,j)}_{(p+2,n,-m)}\left(\frac{\partial}{\partial r}V_{(\ell,j)}\right)-\left(\frac{\partial}{\partial r}\psi^{(\ell,j)}_{(p+2,n,-m)}\right)V_{(\ell,j)}\right]\sin(\theta)d\theta d\phi$$

$$=\epsilon(p+2,(-1)^{\ell}j\omega)k(p+2,(-1)^{\ell}j\omega)\left(\frac{2}{2n+1}\right)\frac{(n+\mid m\mid)!}{(n-\mid m\mid)!}\left[V^{(\ell,j)}_{(p+2,n,m)}\right]\Bigg[$$

$$\lim_{z\to\tilde{z}_{p+1}}\left(\left\{C^{(\ell,j)}_{(p+2,n,1)}j_n(z)h^{(\ell)}_n(z_1)+C^{(\ell,j)}_{(p+2,n,2)}h^{(\ell)}_n(z)j_n(z_1)\right\}\frac{d}{dz}h^{(\ell)}_n(z)j_n(z_1)\right)\quad-$$

$$\lim_{z\to\tilde{z}_{p+1}}\left(\left\{C^{(\ell,j)}_{(p+2,n,1)}\left(\frac{d}{dz}j_n(z)\right)h^{(\ell)}_n(z_1)+C^{(\ell,j)}_{(p+2,n,2)}\left(\frac{d}{dz}h^{(\ell)}_n(z)\right)j_n(z_1)h^{(\ell)}_n(z)\right\}h^{(\ell)}_n(z)j_n(\tilde{z}_{p+1})\right)\Bigg] \tag{5.2.7.11}$$

Equation (5.2.7.11) represents an exact formula evaluation of the surface integral in (5.2.6.3).

5.3 Input and Output for the Inverse Source Computer Program

We describe the input and output variables for the four computer programs. A key input is the set of dynamic head surface representation expansion coefficients defined in (5.2.7.4) whose cardinality is limited by the maximum spherical Hankel function index n and the number of frequency components used, the set of frequencies being recovered, the head geometry, and the coordinates describing the locations of potential brain activity.

5.3.1 Program for Recovery of Neuronal Current Density Components

The input data for this program includes the locations within the head at which brain activity is recovered. The qth site has the location

$$q \to (r_q, \theta_q, \phi_q)$$

in spherical coordinates which may be converted to Cartesian coordinates by

$$(x_q, y_q, z_q) = (r_q\sin(\theta_q)\cos(\phi_q), r_q\sin(\theta_q)\sin(\phi_q), r_q\cos(\theta_q))$$

We need from the head surface representation program the expansion coefficients

$$(n,m,\ell,j) \to c(n,m,\ell,j) \tag{5.3.1.1}$$

appearing in equation (5.2.7.4) that are used in the represenation of the head surface voltage in equation (5.2.7.4).

5.4 Trans-membrane Current Orientations, Vector Potentials, Helmholtz Operators, Interrogating Scalar Functions, and Matrix Relationships for Brain Activity Recovery

We suppose that we have a dynamic head surface voltage distribution. We use vector calculus to find a relationship between this head surface voltage distribution and brain activity without surgery.

5.4.1 A Direct Derivation of the Dynamic Voltage Inversion Relationship

The inversion will reveal the activity on multiple neuronal sources from noninvasive voltage distribution measurements outside the skull bone. We communicate the essence of the derivation by considering a single neuronal source with orientation

$$\boldsymbol{e}_{\mathrm{q}} = \sin(\alpha_{\mathrm{q}})\cos(\beta_{\mathrm{q}})\boldsymbol{e}_{\mathrm{x}} + \sin(\alpha_{\mathrm{q}})\sin(\beta_{\mathrm{q}})\boldsymbol{e}_{\mathrm{y}} + \cos(\alpha_{\mathrm{q}})\boldsymbol{e}_{\mathrm{z}} \tag{5.4.1.1}$$

at location

$$\boldsymbol{r}_{\mathrm{q}} = (x_{\mathrm{q}}, y_{\mathrm{q}}, z_{\mathrm{q}}) = (r_{\mathrm{q}}\sin(\theta_{\mathrm{q}})\cos(\phi_{\mathrm{q}}), r_{\mathrm{q}}\sin(\theta_{\mathrm{q}})\sin(\phi_{\mathrm{q}}), r_{\mathrm{q}}\cos(\theta_{\mathrm{q}})) \tag{5.4.1.2}$$

and having strength $P((-1)^{\ell}\omega)$ for the time dependence

$$t \to \exp(i(-1)^{\ell}\omega t) \tag{5.4.1.3}$$

so that at the observation point

$$\boldsymbol{r} = (x, y, z) = (r\sin(\theta)\cos(\phi), r\sin(\theta)\sin(\phi), r\cos(\theta)) \tag{5.4.1.4}$$

the vector potential defining the stimulated electromagnetic activity is

$$\boldsymbol{A}_q = \left(\frac{\exp(-i(-1)^{\ell}k(p,(-1)^{\ell}\omega)d_q)}{4\pi d_q}\right)\boldsymbol{e}_{\mathrm{q}}P^{(q)}((-1)^{\ell}\omega)\exp(i(-1)^{\ell}\omega t) \tag{5.4.1.5}$$

where

$$d_q = \sqrt{(x-x_{\mathrm{q}})^2 + (y-y_{\mathrm{q}})^2 + (z-z_{\mathrm{q}})^2} \tag{5.4.1.6}$$

From Sneddon and Read ([103] 2005) and Morse and Feshbach ([86]) we have from the derivation of the fundamental solution of the Helmholtz operator that the action of the Helmholtz operator on the vector potential (5.4.1.5) is

$$\Delta\boldsymbol{A}_q + k(p,(-1)^{\ell}\omega)^2\boldsymbol{A}_{\boldsymbol{q}} = -\boldsymbol{P}_q((-1)^{\ell}\omega)\exp(i(-1)^{\ell}\omega t)\delta(\boldsymbol{r}-\boldsymbol{r}_{\mathrm{q}}) \tag{5.4.1.7}$$

where

$$\boldsymbol{P}_q((-1)^{\ell}\omega) = \boldsymbol{e}_{\mathrm{q}}P^{(q)}((-1)^{\ell}\omega) \tag{5.4.1.8}$$

so that if for all positive real numbers ξ

$$\phi_{\xi}\in C_c^{\infty}(\mathbb{R}^3) \tag{5.4.1.9}$$

is such that if for all

$$f \in C^{\infty}(\mathbb{R}^3) \tag{5.4.1.10}$$

we have

$$f(\boldsymbol{r}_{\mathrm{q}}) = \langle \delta(\boldsymbol{r} - \boldsymbol{r}_{\mathrm{q}}), f(\boldsymbol{r}) \rangle = \lim_{\xi \to 0} \int_{\mathbb{R}^3} \phi_{\xi}(\boldsymbol{r} - \boldsymbol{r}_{\mathrm{q}}) f(\boldsymbol{r}) d\mathrm{volume} \tag{5.4.1.11}$$

then in the weak topology sense

$$\lim_{\xi \to 0} \phi_{\xi}(\boldsymbol{r} - \boldsymbol{r}_{\mathrm{q}}) = \delta(\boldsymbol{r} - \boldsymbol{r}_{\mathrm{q}}) \tag{5.4.1.12}$$

This says that the Dirac delta function is a limit of a sequence ϕ_{ξ} of infinitely differentiable functions with compact support.

The total vector potential associated with brain activity from Q internal sites is

$$\boldsymbol{A} = \sum_{q=1}^{Q} \boldsymbol{A}_q \tag{5.4.1.13}$$

5.4.2 Key Identity for Recovery of Brain Activity Using Dynamic Voltages

The key identity for recovery of brain activity, in its pure and simple form, is then simply to say that for any smooth interrogating function ψ that if Ω is an open subset of brain tissue containing the brain activity then integration by parts tells us that

$$\int_{\Omega} \psi \left\{ \Delta \, \nabla \cdot (\boldsymbol{A}) + k(p, (-1)^{\ell}\omega)^2 \, \nabla \cdot (\boldsymbol{A}) \right\} d\mathrm{volume}$$

$$= \int_{\Omega} \{ -\nabla(\psi) \} \cdot \left\{ \Delta \boldsymbol{A} + k(p, (-1)^{\ell}\omega)^2 \boldsymbol{A} \right\} d\mathrm{volume}$$

$$= \int_{\Omega} \{ -\nabla(\psi) \} \cdot \left\{ \Delta \boldsymbol{A} + k(p, (-1)^{\ell}\omega)^2 \boldsymbol{A} \right\} d\mathrm{volume}$$

$$= \lim_{\xi \to 0} \int_{\Omega} \{ -\nabla(\psi) \} \cdot \left\{ (-1) \sum_{\mathrm{q}=1}^{\mathrm{q}=Q} \phi_{\xi}(\boldsymbol{r} - \boldsymbol{r}_q) \boldsymbol{P}^{(q)}((-1)^{\ell}\omega, t) \right\} d\mathrm{volume}$$

$$= \sum_{q=1}^{Q} \left(\lim_{(x,y,z) \to (x_{\mathrm{q}}, y_{\mathrm{q}}, z_{\mathrm{q}})} \right) \cdot \left\{ \right.$$

$$\left[\left\{ \frac{\partial \psi}{\partial x} P_{\mathrm{x}}^{(q)}((-1)^{\ell}\omega, t) + \frac{\partial \psi}{\partial y} P_{\mathrm{y}}^{(q)}((-1)^{\ell}\omega, t) + \frac{\partial \psi}{\partial z} P_{\mathrm{z}}^{(q)}((-1)^{\ell}\omega, t) \right\} \right] \Bigg\} \tag{5.4.2.1}$$

where

$$\begin{bmatrix} P_{\mathrm{x}}^{(q)}((-1)^{\ell}\omega, t) \\ P_{\mathrm{y}}^{(q)}((-1)^{\ell}\omega, t) \\ P_{\mathrm{z}}^{(q)}((-1)^{\ell}\omega, t)) \end{bmatrix}$$

$$= \begin{bmatrix} P^{(q)}((-1)^{\ell}\omega)\exp(i(-1)^{\ell}\omega t)\sin(\alpha_{\mathrm{q}})\cos(\beta_{\mathrm{q}}) \\ P^{(q)}((-1)^{\ell}\omega)\exp(i(-1)^{\ell}\omega t)\sin(\alpha_{\mathrm{q}})\sin(\beta_{\mathrm{q}}) \\ P^{(q)}((-1)^{\ell}\omega)\exp(i(-1)^{\ell}\omega t)\cos(\alpha_{\mathrm{q}}) \end{bmatrix} \tag{5.4.2.2}$$

We define for $d = d_q$

$$\Psi(d) = \left[\frac{-i(-1)^{\ell}k(p_q,(-1)^{\ell}\omega)d - 1}{4\pi d^3}\right]\exp(-i(-1)^{\ell}k(p,(-1)^{\ell}\omega)d) \tag{5.4.2.3}$$

The partial derivative of $\Psi(d)$ with respect to d is

$$\frac{\partial \Psi}{\partial d} = \frac{\partial \Psi(p,d,(-1)^{\ell}\omega)}{\partial d} = \Bigg[\quad (-i)(-1)^{\ell}k(p,(-1)^{\ell}\omega)\Psi(p,d,(-1)^{\ell}\omega)$$

$$+\left(\frac{(-i)(-1)^{\ell}k(p,(-1)^{\ell}\omega)d}{4\pi d^4}\right)\exp(-i(-1)^{\ell}k(p,(-1)^{\ell}\omega)d)$$

$$\left(+(-3)\frac{-i(-1)^{\ell}k(p,(-1)^{\ell}\omega)d-1}{4\pi d^4}\right)\exp(-i(-1)^{\ell}k(p,(-1)^{\ell}\omega)d)\Bigg] \tag{5.4.2.4}$$

An alternative form of equation (5.4.2.4) is

$$\frac{\partial \Psi}{\partial d} =$$

$$\left\{\frac{(-3)\left[-i(-1)^{\ell}k(p,(-1)^{\ell}\omega)d-1\right]-[k(p,(-1)^{\ell}\omega)d]^2}{4\pi d^4}\right\}\exp(-i(-1)^{\ell}k(p,(-1)^{\ell}\omega)d) \tag{5.4.2.5}$$

The divergence of the vector potential is proportional to the voltage. If $\boldsymbol{V}_q$ is the vector from the qth site of brain activity to the observation point, then

$$\boldsymbol{V}_q = (x-x_{\mathrm{q}})\boldsymbol{e}_{\mathrm{x}} + (y-y_{\mathrm{q}})\boldsymbol{e}_{\mathrm{y}} + (z-z_{\mathrm{q}})\boldsymbol{e}_{\mathrm{z}} \tag{5.4.2.6}$$

and

$$\nabla\cdot(\boldsymbol{A_q}) = \Psi(d_q)(\boldsymbol{V}_q\cdot\boldsymbol{e}_{\mathrm{q}})P^{(q)}((-1)^{\ell}\omega)\exp(-i(-1)^{\ell}\omega t) \tag{5.4.2.7}$$

where $\boldsymbol{V}_q$ is given by (5.4.2.6), Ψ is given by (5.4.2.3) and the source strength and orientation is given by (5.4.2.2).

We have for the components of the gradient, the relationships

$$\left(\frac{\partial}{\partial \mathrm{x}}\right)\nabla\cdot(\boldsymbol{A}_q) = \lim_{d\to d_q}\left[\left\{\frac{\partial\Psi(d)}{\partial d}\left(\frac{x-x_{\mathrm{q}}}{d}\right)\right\}(\boldsymbol{V}\cdot\boldsymbol{e}_{\mathrm{q}}) \quad +\Psi(d)\sin(\alpha_{\mathrm{q}})\cos(\beta_{\mathrm{q}})\right] \tag{5.4.2.8}$$

$$\left(\frac{\partial}{\partial \mathrm{y}}\right)\nabla\cdot(\boldsymbol{A}_q) = \lim_{d\to d_q}\left[\left\{\frac{\partial\Psi(d)}{\partial d}\left(\frac{y-y_{\mathrm{q}}}{d}\right)\right\}(\boldsymbol{V}\cdot\boldsymbol{e}_{\mathrm{q}}) \quad +\Psi(d)\sin(\alpha_{\mathrm{q}})\sin(\beta_{\mathrm{q}})\right] \tag{5.4.2.9}$$

and

$$\left(\frac{\partial}{\partial \mathrm{z}}\right)\nabla\cdot(\boldsymbol{A}_q) = \lim_{d\to d_q}\left[\left\{\frac{\partial\Psi(d)}{\partial d}\left(\frac{z-z_{\mathrm{q}}}{d}\right)\right\}(\boldsymbol{V}\cdot\boldsymbol{e}_{\mathrm{q}}) + \Psi(d)\cos(\alpha_{\mathrm{q}})\right] \tag{5.4.2.10}$$

For spherical coordinates and the total vector potential of brain activity we have

$$\left(\frac{\partial}{\partial r}\right)\nabla\cdot(\boldsymbol{A}) = \left[\sin(\theta)\cos(\phi)\frac{\partial}{\partial x} + \sin(\theta)\sin(\phi)\frac{\partial}{\partial y} + \cos(\theta)\frac{\partial}{\partial z}\right]\nabla\cdot(\boldsymbol{A}) \tag{5.4.2.11}$$

5.4.3 Relationship for Using Scalp Measurements to Recover Brain Activity from Dynamic Voltages

If we correctly define an interrogating scalar function ψ and the total vector potential $\boldsymbol{A}$ in each tissue region and outside the skull, the inversion relationship is with $\partial\Omega$ denoting the boundary of tissue regions Ω comprising the head.

$$\int_{\partial\Omega} \epsilon(p+2,(-1)^{\ell}j\omega)\left\{\psi\,\nabla(\nabla\cdot(\boldsymbol{A})-\nabla\cdot(\boldsymbol{A})\,\nabla(\psi)\right\}\cdot\boldsymbol{n}d\text{area}$$

$$=\int_{\Omega}\epsilon(p,(-1)^{\ell}j\omega)\,\nabla\cdot\left\{\psi\,\nabla(\nabla\cdot(\boldsymbol{A})-\nabla\cdot(\boldsymbol{A})\,\nabla(\psi)\right\}d\text{volume}$$

$$=\int_{\Omega}\epsilon(p,(-1)^{\ell}j\omega)\left\{\right.$$
$$\nabla(\psi)\cdot\nabla(\nabla\cdot(\boldsymbol{A}))+\psi\,\nabla\cdot(\nabla(\nabla\cdot(\boldsymbol{A})))$$
$$-[\nabla(\nabla\cdot(\boldsymbol{A}))\cdot\nabla(\psi)$$
$$\left.+\nabla\cdot(\boldsymbol{A})\,\nabla\cdot(\nabla(\psi))]\right\}d\text{volume}$$

$$=\int_{\Omega}\epsilon(p,(-1)^{\ell}j\omega)\left\{\psi\Delta\,\nabla\cdot(\boldsymbol{A})-\nabla\cdot(\boldsymbol{A})\left[-k(p,(-1)^{\ell}\omega)^2\psi\right]\right\}d\text{volume}$$

$$=\int_{\Omega}\epsilon(p,(-1)^{\ell}j\omega)\psi\left\{\Delta\,\nabla\cdot(\boldsymbol{A})+\left[k(p,(-1)^{\ell}\omega)^2\right]\nabla\cdot(\boldsymbol{A})\right\}d\text{volume}$$

$$=-\int_{\Omega}\epsilon(p,(-1)^{\ell}j\omega)\left\{\psi\,\nabla\cdot(\boldsymbol{J}\right\}d\text{volume}=+\int\left\{\nabla(\psi)\cdot\boldsymbol{J}\right\}d\text{volume}$$

$$=+\epsilon(p,(-1)^{\ell}j\omega)\sum_{q=1}^{Q}\left\{\frac{\partial\psi}{\partial x}(r_{\mathrm{q}},\theta_{\mathrm{q}},\phi_{\mathrm{q}})P_{\mathrm{x}}^{(q)}((-1)^{\ell}\omega,t)\right.$$
$$\left.+\frac{\partial\psi}{\partial y}(r_{\mathrm{q}},\theta_{\mathrm{q}},\phi_{\mathrm{q}})P_{\mathrm{y}}^{(q)}((-1)^{\ell}\omega,t)+\frac{\partial\psi}{\partial z}(r_{\mathrm{q}},\theta_{\mathrm{q}},\phi_{\mathrm{q}})P_{\mathrm{z}}^{(q)}((-1)^{\ell}\omega,t)\right\}\tag{5.4.3.1}$$

The matrix equation is derived from the right side of (5.4.3.1). In equation (5.4.3.1) the partial derivatives of the interrogating scalar functions ψ are determined by by

$$\frac{\partial\psi}{\partial x}=\left\{\sin(\theta)\cos(\phi)\frac{\partial\psi}{\partial r}+\frac{\cos(\theta)\cos(\phi)}{r}\frac{\partial\psi}{\partial\theta}-\frac{\sin(\phi)}{r\sin(\theta)}\frac{\partial\psi}{\partial\phi}\right\}\tag{5.4.3.2}$$

$$\frac{\partial\psi}{\partial y}=\left\{\sin(\theta)\sin(\phi)\frac{\partial\psi}{\partial r}+\frac{\cos(\theta)\sin(\phi)}{r}\frac{\partial\psi}{\partial\theta}+\frac{\cos(\phi)}{r\sin(\theta)}\frac{\partial\psi}{\partial\phi}\right\}\tag{5.4.3.3}$$

and

$$\frac{\partial\psi}{\partial z}=\left\{\cos(\theta)\frac{\partial\psi}{\partial r}-\frac{\sin(\theta)}{r}\frac{\partial\psi}{\partial\theta}\right\}\tag{5.4.3.4}$$

In the brain tissue universe the function ψ can have the form

$$\psi=j_n(k(p,(-1)^{\ell}\omega)r)P_n^m(\cos(\theta))\exp(im\phi)\tag{5.4.3.5}$$

5.5 The Matrix Equation for Recovery of Brain Activity from EEG Recordings

The row index is for the matrix

$$(\mathrm{j},\ell) \to \overline{\overline{M}}^{(\mathrm{j},\ell)} \tag{5.5.0.1}$$

associated with the frequency component with time dependence

$$t \to \exp(-i(-1)^{\ell} j\omega t) \tag{5.5.0.2}$$

is

$$I_{\mathrm{row}}(n,m) = n^2 + (n+m+1) \tag{5.5.0.3}$$

and the column index which depends on the coordinate index I_{C} and the dipole index q is

$$J_{\mathrm{column}} = J_{\mathrm{column}}(\mathrm{q}, I_{\mathrm{C}}) = 3(q-1) + I_{\mathrm{C}} \tag{5.5.0.4}$$

The matrix entry is

$$\overline{\overline{M}}^{(\mathrm{j},\ell)}(I_{\mathrm{row}}(n,m), J_{\mathrm{column}})(\mathrm{q}, I_{\mathrm{C}}) =$$
$$\lim_{(x,y,z)\to(x_{\mathrm{q}},y_{\mathrm{q}},z_{\mathrm{q}})} \begin{cases} (\partial/\partial x)\psi^{(\ell,\mathrm{j})}_{(n,m)}(x,y,z) & \text{if} \quad I_{\mathrm{C}} = 1 \\ (\partial/\partial y)\psi^{(\ell,\mathrm{j})}_{(n,m)}(x,y,z) & \text{if} \quad I_{\mathrm{C}} = 2 \\ (\partial/\partial z)\psi^{(\ell,\mathrm{j})}_{(n,m)}(x,y,z) & \text{if} \quad I_{\mathrm{C}} = 3 \end{cases} \tag{5.5.0.5}$$

The matrix equation has the form

$$\overline{\overline{M}}^{(\mathrm{j},\ell)} \begin{bmatrix} P^{(1)}_{\mathrm{x}}((-1)^{\ell}\mathrm{j}\omega)) \\ P^{(1)}_{\mathrm{y}}((-1)^{\ell}\mathrm{j}\omega)) \\ P^{(1)}_{\mathrm{z}}((-1)^{\ell}\mathrm{j}\omega)) \\ \cdots \\ \cdots \\ \cdots \\ P^{(\mathrm{q})}_{\mathrm{x}}((-1)^{\ell}\mathrm{j}\omega)) \\ P^{(\mathrm{q})}_{\mathrm{y}}((-1)^{\ell}\mathrm{j}\omega)) \\ P^{(\mathrm{q})}_{\mathrm{z}}((-1)^{\ell}\mathrm{j}\omega)) \\ \cdots \\ \cdots \\ \cdots \\ P^{(\mathrm{Q})}_{\mathrm{x}}((-1)^{\ell}\mathrm{j}\omega)) \\ P^{(\mathrm{Q})}_{\mathrm{y}}((-1)^{\ell}\mathrm{j}\omega)) \\ P^{(\mathrm{Q})}_{\mathrm{z}}((-1)^{\ell}\mathrm{j}\omega)) \end{bmatrix} = \begin{bmatrix} \mathcal{S}(0,0) \\ \mathcal{S}(1,-1) \\ \mathcal{S}(1,0) \\ \mathcal{S}(1,+1) \\ \cdots \\ \cdots \\ \cdots \\ \mathcal{S}(n,-n) \\ \cdots \\ \cdots \\ \cdots \\ \mathcal{S}(n,+n) \\ \cdots \\ \cdots \\ \cdots \\ \mathcal{S}(N,-N) \\ \cdots \\ \cdots \\ \cdots \\ \mathcal{S}(N,0) \\ \cdots \\ \cdots \\ \cdots \\ \mathcal{S}(N,+N) \end{bmatrix} \tag{5.5.0.6}$$

5.6 Computer Comparison of Volume and Surface Integral Relationships for Brain Activity Recovery from EEG Recordings

The following is a comparison

n	m	integral value	integral type
2	-2	$3.368907528532080 \times 10^1 + i[1.009482236012442 \times 10^2]$	surface integral
2	-2	$3.368907528532062 \times 10^1 + i[1.009482236012455 \times 10^2]$	volume integral
2	-1	$-1.702135430384869 \times 10^1 + i[-2.299168366554281 \times 10^1]$	surface integral
2	-1	$-1.702135430384874 \times 10^1 + i[-2.299168366554279 \times 10^1]$	volume integral
2	0	$5.495104926656351 + i[1.099019699686706 \times 10^1]$	surface integral
2	0	$5.495104926656298 + i[1.099019699686709 \times 10^1]$	volume integral
2	1	$-8.180413502247294 + i[-2.741207074136922 \times 10^1]$	surface integral
2	1	$-8.180413502247248 + i[-2.741207074136920 \times 10^1]$	volume integral
2	2	$6.054493631657606 \times 10^1 + i[8.752005211996486 \times 10^1]$	surface integral
2	2	$6.054493631657589 \times 10^1 + i[8.752005211996534 \times 10^1]$	volume integral

6 Program for Detrending of Raw EEG Recordings

The raw data had net positive or net negative average voltages and also showed upward or downward drifting of the voltages.

6.1 Removal of Operational Amplifier Drift in EEG Recordings

A program was written to remove the operation amplifier drift in EEG recordings. The net recorded voltages were either all positive or all negative. The covariance of the voltage and time divided by the variance of the recorded times gave the slope of the best fitting line. The best-fit line was subtracted from the recorded voltage giving a signal whose average voltage was nearly zero. Computer output for all 128 recordings is shown in the computer data subsection.

6.1.1 The Mathematics of Removal of Drift from EEG Recordings

Suppose we have N EEG recording site time and voltage coordinates (T_1, V_1), (T_2, V_2), (T_3, V_3), $\cdots$, (T_N, V_N) representing the observed time and voltage coordinates. We wish

to find two numbers B_0 and B_1 such that the expression

$$S = S(B_0, B_1) = (V_1 - B_1 \cdot T_1 - B_0)^2 + (V_2 - B_1 \cdot T_2 - B_0)^2 + \cdots$$

$$+(V_i - B_1 \cdot T_i - B_0)^2 + \cdots + (V_{N-1} - B_1 \cdot T_{N-1} - B_0)^2 + (V_N - B_1 \cdot T_N - B_0)^2 \quad (6.1.1.1)$$

is as small as possible.

We collect terms in equation (6.1.1.1) by making use of the multiplication table:

MULTIPLY	V_i	$-B_1T_i$	$-B_0$
V_i	V_i^2	$-B_1T_iV_i$	$-B_0V_i$
$-B_1T_i$	$-B_1T_iV_i$	$B_1^2T_i^2$	$B_0B_1T_i$
$-B_0$	$-B_0V_i$	$B_0B_1T_i$	B_0^2

Regrouping so that $S(B_0, B_1)$ is more easily seen to be a polynomial in B_0 and B_1 we find that

$$S(B_0,B_1) = \left(\sum_{i=1}^{N} V_i^2\right) + \left(\sum_{i=1}^{N} T_i^2\right) B_1^2 + B_0^2 N$$
$$- \left(2\sum_{i=1}^{N} T_iV_i\right) B_1 - \left(2\sum_{i=1}^{N} V_i\right) B_0 + \left(2\sum_{i=1}^{N} T_i\right) B_0B_1 \qquad (6.1.1.2)$$

To analyze the terms we introduce the notation

$$N\overline{T} = \sum_{i=1}^{N} T_i \qquad (6.1.1.3)$$

and

$$N\overline{V} = \sum_{i=1}^{N} V_i \qquad (6.1.1.4)$$

where $\overline{T}$ and $\overline{V}$ denote the average values of the T_i and V_i. Collecting terms and substituting (6.1.1.3) and (6.1.1.4) into (6.1.1.2) we find that

$$S = N\left\{B_0^2 - 2B_0\left[\overline{V} - B_1\overline{T}\right]\right\} +$$
$$\left(\sum_{i=1}^{N} T_i^2\right) B_1^2 - 2\left(\sum_{i=1}^{N} T_iV_i\right) B_1 + \sum_{i=1}^{N} V_i^2 \qquad (6.1.1.5)$$

Adding the quantity,

$$N(\overline{V} - B_1\overline{T})^2 - N(\overline{V} - B_1\overline{T})^2 = 0 \qquad (6.1.1.6)$$

to the right side of equation (6.1.1.5) we obtain

$$S = N\left[\left\{B_0^2 - 2B_0\left[\overline{V} - B_1\overline{T}\right]\right\} + (\overline{V} - B_1\overline{T})^2\right] +$$
$$\left(\sum_{i=1}^{N} T_i^2\right) B_1^2 - 2\left(\sum_{i=1}^{N} T_iV_i\right) B_1 + \sum_{i=1}^{N} V_i^2 - N(\overline{V} - B_1\overline{T})^2 \qquad (6.1.1.7)$$

Simplifying equation (6.1.1.7) using the relation

$$(B_0 - (\overline{V} - B_1\overline{T}))^2 = B_0^2 - 2B_0(\overline{V} - B_1\overline{T}) + (\overline{V} - B_1\overline{T})^2 \qquad (6.1.1.8)$$

we see that (6.1.1.7) implies that

$$S = N(B_0 - (\overline{V} - B_1\overline{T}))^2 + B_1^2\left(\sum_{i=1}^{N} T_i^2 - N\overline{T}^2\right) -$$

$$2B_1\left(\left\{\sum_{i=1}^{N} T_iV_i\right\} - N\overline{TV}\right) + \sum_{i=1}^{N} V_i^2 - N\overline{V}^2 \tag{6.1.1.9}$$

Collecting terms and completing the square we find that

$$S = N(B_0 - (\overline{V} - B_1\overline{T}))^2 +$$

$$\left(\sum_{i=1}^{N} T_i^2 - N\overline{T}^2\right)\left[B_1 - \left(\frac{\sum_{i=1}^{N} T_iV_i - N\overline{TV}}{\sum_{i=1}^{N} T_i^2 - N\overline{T}^2}\right)\right]^2$$

$$+\left[\left(\sum_{i=1}^{N} V_i^2 - N\overline{V}^2\right)\left(\sum_{i=1}^{N} T_i^2 - N\overline{V}^2\right) - \left(\sum_{i=1}^{N} T_iV_i - N\overline{TV}\right)^2\right] / \left(\sum_{i=1}^{N} T_i^2 - N\overline{T}^2\right) \tag{6.1.1.10}$$

Thus, from (6.1.1.10) we conclude that the sum given by (6.1.1.7) is minimized if

$$B_1 = \left(\frac{\sum_{i=1}^{N} T_iV_i - N\overline{TV}}{\sum_{i=1}^{N} T_i^2 - N\overline{T}^2}\right) = \left(\frac{(\sum_{i=1}^{N} T_iV_i)/N - \overline{TV}}{(\sum_{i=1}^{N} T_i^2)/N - \overline{T}^2}\right) \tag{6.1.1.11}$$

which is the estimate of the covariance (Feller [42], p 330) of the T_i and V_i divided by the estimate of the variance (Feller [42], p 227) of the T_i, and B_0 is given by

$$B_0 = (\overline{V} - B_1\overline{T}) \tag{6.1.1.12}$$

Since $(\overline{T}, \overline{V})$ is on the line we note that

$$\overline{V} = B_1\overline{T} + B_0 \tag{6.1.1.13}$$

If

$$\alpha = \mid \boldsymbol{V} \mid \tag{6.1.1.14}$$

and

$$\beta = \mid \boldsymbol{T} \mid \tag{6.1.1.15}$$

and if $\boldsymbol{T}$ and $\boldsymbol{V}$ are linearly independent, then

$$\boldsymbol{Q} = \alpha\boldsymbol{X} - \beta\boldsymbol{V} \neq \boldsymbol{0} \tag{6.1.1.16}$$

which tells us that

$$\boldsymbol{Q} \cdot \boldsymbol{Q} > 0 \tag{6.1.1.17}$$

or equivalently

$$(\mid \boldsymbol{T} \mid)(\mid \boldsymbol{V} \mid) > \boldsymbol{T} \cdot \boldsymbol{V} \tag{6.1.1.18}$$

which is just a statement of the strict Cauchy-Schwarz inequality. If we let

$$\boldsymbol{V} = (1, 1, \cdots, 1) \tag{6.1.1.19}$$

then if

$$\boldsymbol{T} = (T_1, T_2, \cdots, T_i, \cdots, T_N) \tag{6.1.1.20}$$

$\boldsymbol{T}$ cannot possibly depend linearly on the $\boldsymbol{V}$ given by (6.1.1.19) and then (6.1.1.16) and consequently (6.1.1.18) is satisfied if there are as many as two different coordinates in $\boldsymbol{T}$, which is clearly the case when $\boldsymbol{T}$ represents the vector of observation times of the electroencephalogram. We see what this means by making the substitutions in the inequality (6.1.1.18) and squaring both sides, we obtain the result,

$$(T_1^2 + T_2^2 + \cdots + T_{n-1}^2 + T_n^2) \cdot N > (T_1 + T_2 + \cdots + T_{n-1} + T_n)^2 \tag{6.1.1.21}$$

which means that

$$\overline{T}^2 = \left(\frac{T_1 + T_2 + \cdots + T_n}{N}\right)^2 < \left(\frac{T_1^2 + T_2^2 + \cdots + T_n^2}{N}\right) \tag{6.1.1.22}$$

This last inequality (6.1.1.22) tells us that the denominator in (6.1.1.11) is nonzero and, therefore, that we can always get a best fitting straight line with a finite slope, which is our estimate of the drift of the recorded electroencephalogram voltage with respect to time, as long as the values T_i are not all identical. Furthermore, equation (6.1.1.13) implies that if we replace V_i by

$$\tilde{V}_i = V_i - B_1 \cdot T_i - B_0 \tag{6.1.1.23}$$

that the new detrended voltage variable $\tilde{V}_i$ has zero mean. Our purpose is the extraction of information content from the detrended electroencephalogram data.

6.1.2 Computer Data Showing the Results of Detrending the EEG Recordings

In this section the best fitting voltage versus time line at the EEG recording site with index e is

$$V_e = B_{(1,e)} T_e + B_{(0,e)} \tag{6.1.2.1}$$

A sample of the detrending from the first and 128th EEG recording site is

10240	=	NTIMES before READ(11
90.0087891	=	TARRAY(1)
95.0083008	=	TARRAY(NTIMES)
1 = IL	=	eeg lead index
2.49975586	=	average time value
8772.91659	=	original average voltage
0.00103979808	= B1 =	slope of best fitting line
7.60074828E-010	=	average of detrended voltage
128 = IL	=	eeg lead index
2042.29189	=	original average voltage
0.00407213127	= B1 =	slope of best fitting line
3.53542164E-010	=	average of detrended voltage

6.1.3 Voltage Versus Time Plots of EEG Data

In this section we have MATLAB plots of recordings of EEG voltage versus time data at individual lead points on the surface of the skull. I provide the plots and a copy of the FORTRAN program and matlab plotting files.

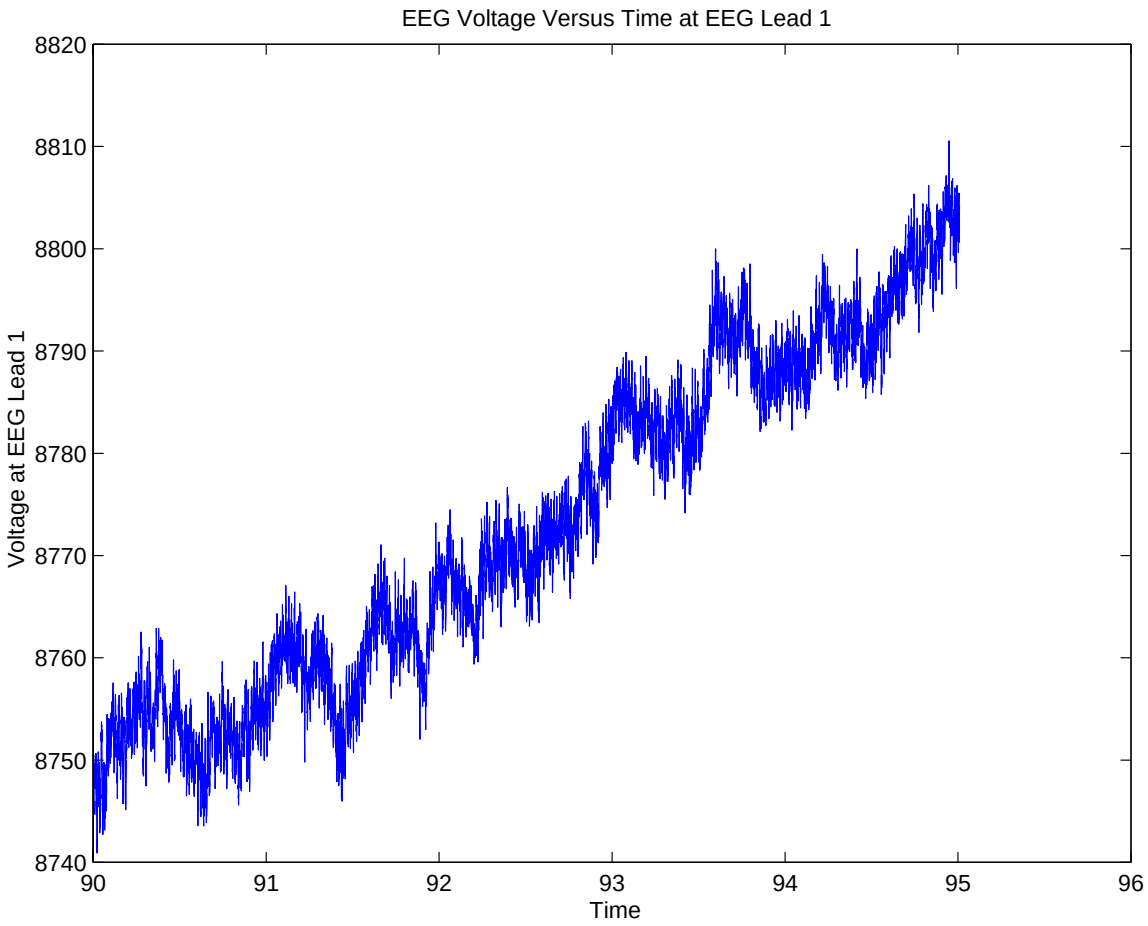

Figure 34: EEG Voltage Versus Time at EEG Lead 1

The voltage versus time at the first EEG lead location is shown in the graph.

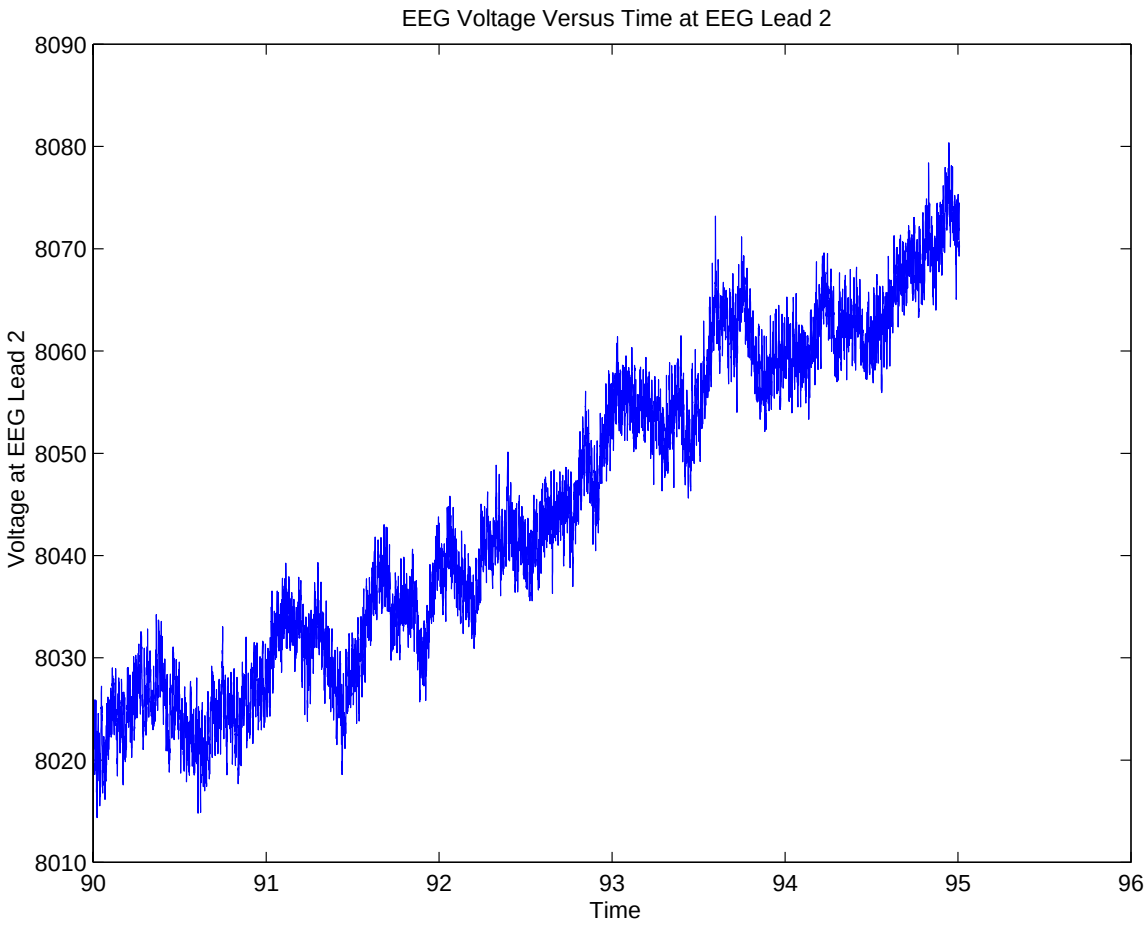

Figure 35: EEG Voltage Versus Time at EEG Lead 2

The voltage versus time at the second EEG lead location is shown in the graph. The local average of the voltage changes slowly but seems to be an increasing function of time.

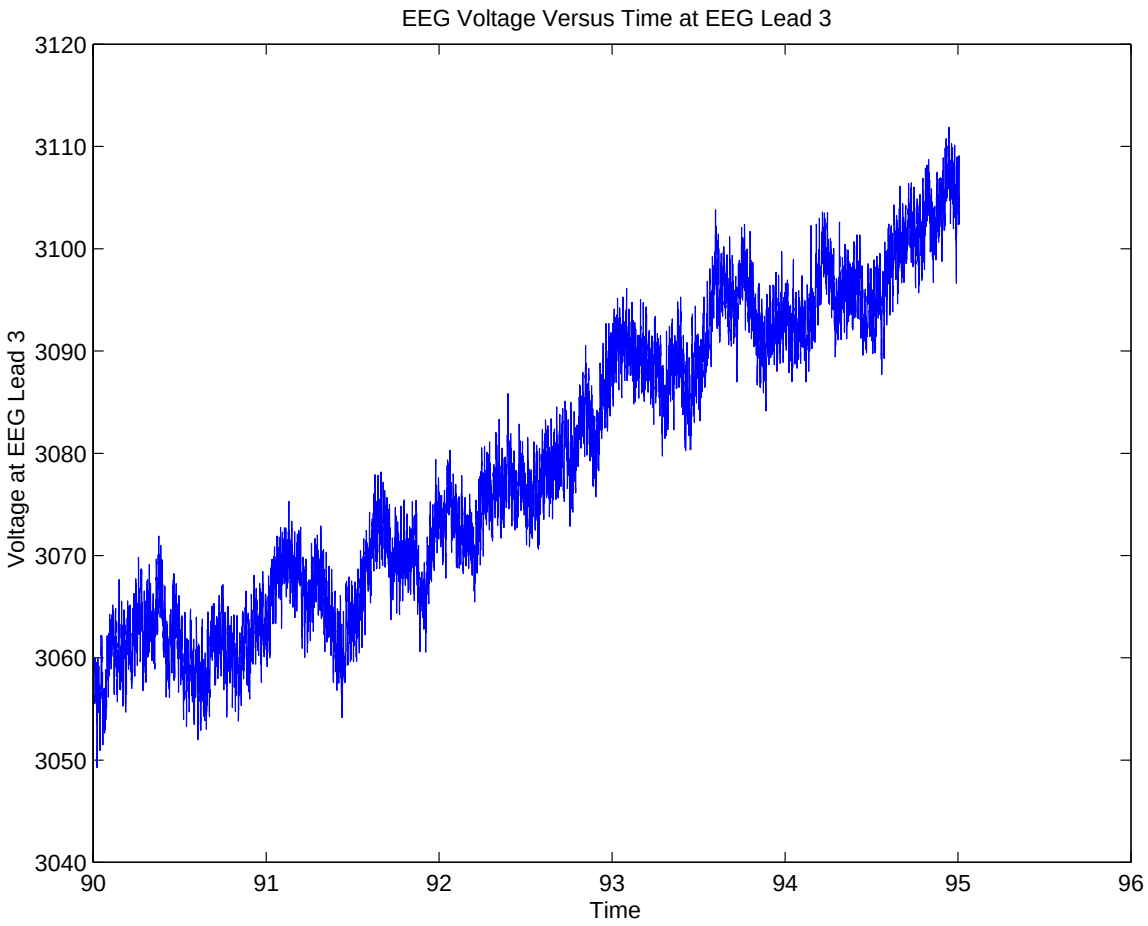

Figure 36: EEG Voltage Versus Time at EEG Lead 3

The voltage versus time at the third EEG lead location is shown in the graph. The local average of the voltage changes slowly but seems to be an increasing function of time.

We next describe the FORTRAN program and the COMMON BLOCK detrended the EEG data. There was a 33 Megabyte data file which had in the first row the 10240 times and rows 2 through 128+1, the EEG voltages at the 128 EEG leads. The data files EEG1.DAT through EEG128.DAT all had exactly 10240 lines. It appears that in the data the voltage is changing slowly and the local voltage average appears to be increasing linearly with time. To show the idea we give a shortened version of the program. The slope of the best fitting line is the covariance of the time and voltage data divided by the variance of the time data. The voltage axis intercept of this best fitting line is the difference between the average voltage and this slope multiplied by the average time.

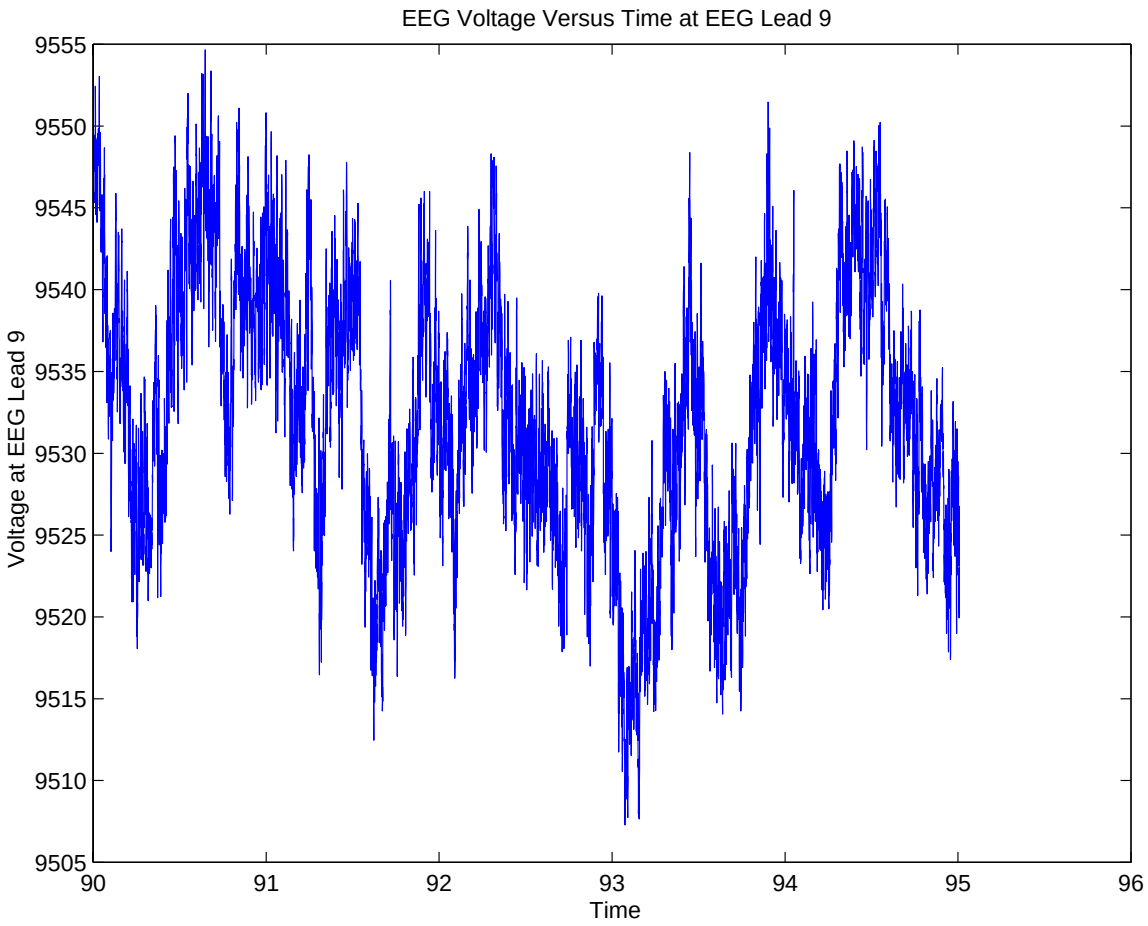

Figure 37: EEG Voltage Versus Time at EEG Lead 9

6.1.4 Sample Plot of the Undetrended and Detrended Voltage

We give a plot of the undetrended and detrended data for the 9th EEG lead recording site. The voltage versus time at the nineth EEG lead location is shown in the graph. The EEG recording appears to be comprised, in the Stone Weierstrass sense, of vertically displaced sinusoids and has a low frequency envelope.

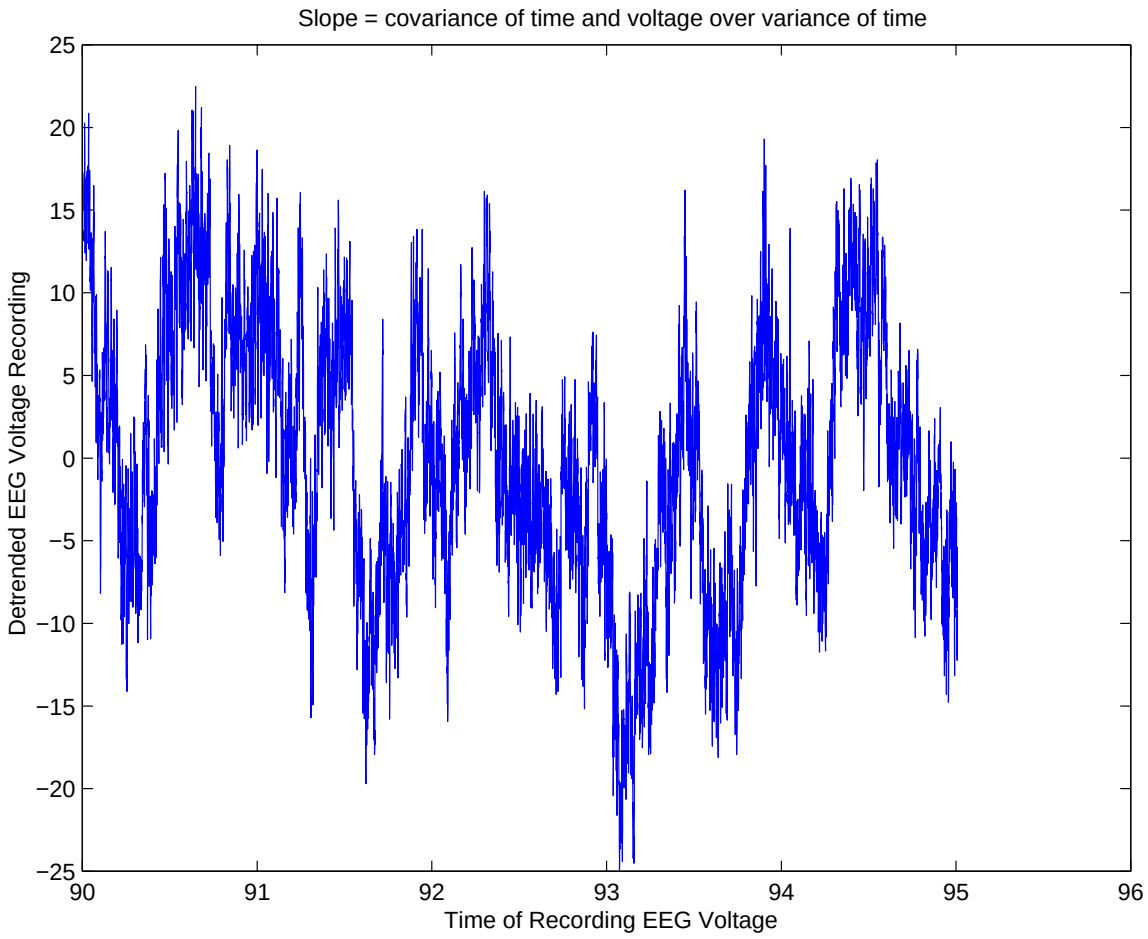

Figure 38: Detrended EEG Voltage Versus Time at EEG Lead 9

The detrended EEG recording is
This was recorded at the following location on the head surface.

r	θ	ϕ
0.1000000000E+00	-0.99.50000000	0.144.0000000

7 The Dynamic Head Surface Voltage Representation from $N \geq 128$ EEG Recording Sites

We use quadratic forms involving relationships between voltage recordings at given times t at different EEG recording sites.

7.1 The Concept of Using the Complete Time Profile of EEG Activity at a Finite Number of Sites to Recover Brain Activity

The key to the recovery of a head surface dynamic voltage representation from the complete time profile of activity, an infinite amount of information, at just a finite number of EEG recording sites is that the spherical Hankel functions used in representing the head surface brain activity have arguments that depend on frequency. We then interrogate the head surface representation with interrogating scalar functions which depend on physiology but which are independent of brain activity. Each interrogation gives us a new equation for recovery of the orientation of neurons and the activity on these neurons.

7.1.1 Quadratic Forms for Recovery of Head Surface Voltage Distributions from EEG Recordings

We want to create a dynamic head surface voltage distribution that can be interrogated to recover the brain activity. In the following we let

$$(p, \omega_j, \ell) \to k(p, (-1)^\ell \omega_j) \tag{7.1.1.1}$$

denote the propagation constant for the brain-activity vector potential component with a time dependence of the form

$$t \to \exp(i(-1)^\ell \omega_j t) \tag{7.1.1.2}$$

We let $p = 1$ denote the brain tissue region index and we let $p + 2$ be the index of the region just beyond the skull.

We create quadratic forms in the apriori unknown expansion coefficients

$$(n, m, \mathrm{j}, \ell) \to c(n, m, \mathrm{j}, \ell) \tag{7.1.1.3}$$

based on the difference between this a priori unknown series expansion

$$V_{(e,\text{series})}(t) = \sum_{j=1}^{J}\sum_{\ell=1}^{2}\left\{V_{(\ell,j)}(r_{\text{e}},\theta_{\text{e}},\phi_{\text{e}})\exp(i(-1)^{\ell}\text{j}\omega t)\right\}$$

$$= \sum_{j=1}^{J}\sum_{\ell=1}^{2}\sum_{n=0}^{n=N}\sum_{m=-n}^{m=+n}\Bigg\{ \quad \left[P_n^m(\cos(\theta_{\text{e}}))\exp(im\phi_{\text{e}})\exp(i(-1)^{\ell}\omega_j t)\right]$$

$$c(n,m,\text{j},\ell)\left\{h_n^{(\ell)}(k(p+2,(-1)^{\ell}j\omega)r_{\text{e}})j_n(k(p+2,(-1)^{\ell}\omega_j)r_2)\right\} \quad \Bigg\} \tag{7.1.1.4}$$

at an EEG, electroencephalogram, recording site indexed by e and given in head surface spherical coordinates by

$$e \to (r_e,\theta_e,\phi_e) \tag{7.1.1.5}$$

In equation (7.1.1.4) we mollified the Hankel function by multiplying it by a spherical Bessel function evaluated at the head boundary. The objective is of course to find the, a priori unknown coefficients

$$(n,m,\text{j},\ell) \to c(n,m,\text{j},\ell) \tag{7.1.1.6}$$

We want the series representation to match the recorded representation

$$e \to V_e(t) \tag{7.1.1.7}$$

at every EEG recording site. We have a fiber bundle of voltage vector spaces at each EEG recording site and we construct a vector consisting of all linear combinations of voltage fields $V_e(t)$ at the EEG recording sites. We consider multiple sets of multipliers $A_{(e,\text{i}_{set})}$ of the voltages $V_e(t)$ at time t at the EEG recording site with index e. Thus, for scalars $A_{(e,\text{i}_{\text{set}})}\in\mathbb{R}$ for e being one of $N(\mathcal{E})$ recording site indices we have a mapping

$$(A_{(1,\text{i}_{\text{set}})},\cdots,A_{(e,\text{i}_{\text{set}})},\cdots,A_{(N(\mathcal{E}),\text{i}_{\text{set}})}) \to \sum_{t\in\mathcal{T}}\sum_{e=1}^{e=N(\mathcal{E})}\left[\left\{A_{(e,\text{i}_{\text{set}})}V_{(e,\text{series})}(t) - A_{(e,\text{i}_{\text{set}})}V_e(t)\right\}\right] \tag{7.1.1.8}$$

If the $V_{(e,\text{series})}(t)$ given by (7.1.1.4) is a perfect representation of the dynamic voltage distribution over the surface of the head, then every one of the images (7.1.1.8) is the zero vector field. Thus, the simplest quadratic form, using just one of the potentially infinite number of interrelationships between the recording site measurements given by (7.1.1.8)

$$Q((A_{(1,\text{i}_{\text{set}})},\cdots,A_{(e,\text{i}_{\text{set}})},\cdots,A_{(N(\mathcal{E}),\text{i}_{\text{set}})}),(\cdots,c(n,m,\text{j},\ell)\cdots)) =$$

$$\sum_{e=1}^{e=N(\mathcal{E})}\left(\sum_{t\in\mathcal{T}}\left\{\left[A_{(e,\text{i}_{\text{set}})}V_{(e,\text{series})}(t) - A_{(e,\text{i}_{\text{set}})}V_e(t)\right]\left[A_{(e,\text{i}_{\text{set}})}\overline{V_{(e,\text{series})}(t)} - A_{(e,\text{i}_{\text{set}})}\overline{V_e(t)}\right]\right\} \quad\right) \tag{7.1.1.9}$$

where $V_e(t)$ is the recorded detrended voltage at time t and the EEG recording site with index e. Since the recorded voltages are real we could assume that each $A_{(e,\text{i}_{\text{set}})}$ is a real number, but to have more possibilities for equations we allow them to be complex numbers. In the

next section we show how to obtain more equations for the head surface voltage distribution representation by considering multiple sets of multipliers

$$(e, \mathrm{i}_{\mathrm{set}}) \to A_{(e,\mathrm{i}_{\mathrm{set}})} \tag{7.1.1.10}$$

that we can get independent equations with quadratic forms created by the difference between the linear combinations of series represenation of the head surface voltage representations at finite numbers of EEG recording sites and the same linear combinations of the recorded voltages. The linear equations are derived by computing partial derivatives of the quadratic forms with respect to the complex conjugates of the expansion coefficients.

7.1.2 Generalized Quadratic Forms for Recovery of Head Surface Dynamic Voltage Expansion Representations

We want to recover the expansion coefficients

$$(n, m, \mathrm{j}, \ell) \to c(n, m, \mathrm{j}, \ell) \tag{7.1.2.1}$$

in equation (7.1.1.4) which define the voltages

$$(r_e, \theta_e, \phi_e, t) \to V_{(e,\mathrm{series})}(t) \tag{7.1.2.2}$$

at the electroencephalogram recording sites

$$e \to (r_e, \theta_e, \phi_e) \tag{7.1.2.3}$$

We consider the electroencephalogram recording site locations

$$e \to (r_e, \theta_e, \phi_e) \tag{7.1.2.4}$$

on the head surface where

$$e \in \{1, \cdots, e, \cdots, N(\mathcal{E})\} \tag{7.1.2.5}$$

at which we have EEG voltage values $V_e(t)$ where $t \in \mathcal{T}$. Instead of considering just one set of multipliers A_e to define a single quadratic form (7.1.1.9) in the apriori unknown expansion coefficients we consider multiple sets $\mathcal{M}$ of multipliers

$$\mathcal{M} = \left\{(e, \mathrm{i}_{\mathrm{set}}) \to A_{(e,\mathrm{i}_{\mathrm{set}})} : e \in \{1, \cdots, N(\mathcal{E})\} \text{ and} \mathrm{i}_{\mathrm{set}} \in \{1, \cdots, N(\mathcal{Q})\}\right\} \tag{7.1.2.6}$$

and all defining the quadratic form

$$\mathcal{Q}((A_{(1,\mathrm{i}_{\mathrm{iset}})}, \cdots, A_{(e,\mathrm{i}_{\mathrm{iset}})}, \cdots, A_{(N(\mathcal{E}),\mathrm{i}_{\mathrm{iset}})}); (..., c(n, m, \mathrm{j}, \ell), ...) = \sum_{t \in \mathcal{T}} \Bigg\{$$

$$[\sum_{e=1}^{e=N(\mathcal{E})} \left\{A_{(e,i_{\mathrm{iset}})} V_{(e,\mathrm{series})}(t) - A_{(e,i_{\mathrm{iset}})} V_e(t)\right\}][\sum_{\tilde{e}=1}^{\tilde{e}=N(\mathcal{E})} \left\{\overline{A_{(\tilde{e},\mathrm{i}_{\mathrm{set}})}}\,\overline{V_{(\tilde{e},\mathrm{series})}(t)} - \overline{A_{(\tilde{e},\mathrm{i}_{\mathrm{set}})}} V_{\tilde{e}}(t)\right\} \Bigg\} \tag{7.1.2.7}$$

Now we compute the partial derivative of the quadratic form defined by (7.1.2.7) with respect to the complex conjugate

$$(n, m, \mathrm{j}, \ell) \to \overline{c(n, m, \mathrm{j}, \ell)} \tag{7.1.2.8}$$

of the expansion coefficients in the representation (7.1.1.4). We have

$$0 = (\partial/\partial\overline{c(n, m, \mathrm{j}, \ell)})\mathcal{Q}((A_{(1,\mathrm{i_{set}})}, \cdots, A_{(e,\mathrm{i_{set}})}, \cdots, A_{(N(\mathcal{E}),\mathrm{i_{set}})}); (..., c(n, m, \mathrm{j}, \ell), ...)) = \sum_{t\in\mathcal{T}} \Bigg\{$$

$$[\sum_{e=1}^{e=N(\mathcal{E})} \left\{A_{(e,i_{\mathrm{set}})}V_{(e,\mathrm{series})}(t) - A_{(e,i_{\mathrm{set}})}V_e(t)\right\}][\sum_{\tilde{e}=1}^{\tilde{e}=N(\mathcal{E})} \left\{\overline{A_{(\tilde{e},i_{\mathrm{set}})}}(\partial/\partial\overline{c(n, m, \mathrm{j}, \ell)})\overline{V_{(\tilde{e},\mathrm{series})}(t)}\right\}] \Bigg\} \tag{7.1.2.9}$$

The first set of equations derived from (7.1.2.9) correspond to $i_{\mathrm{set}} = 1$ and the last set of equations in the expansion coefficients

$$(n, m, \mathrm{j}, \ell) \to c(n, m, \mathrm{j}, \ell) \tag{7.1.2.10}$$

7.1.3 Linear Equations in the A Priori Unknown Coefficients Defining the Head Surface Voltage Distributions

From (7.1.2.9) we derive the equation

$$\sum_{t\in\mathcal{T}}\Bigg\{$$

$$\Bigg[\sum_{e=1}^{e=N(\mathcal{E})}\Bigg(A_{(e,\mathrm{i_{set}})}\quad\sum_{\tilde{j}=1}^{J}\sum_{\tilde{\ell}=1}^{2}\sum_{\tilde{n}=0}^{N}\sum_{\tilde{m}=-\tilde{n}}^{\tilde{m}=+\tilde{m}}c(\tilde{n},\tilde{m},\tilde{j},\tilde{\ell})\Bigg\{$$

$$\Big\{h_{\tilde{n}}^{(\tilde{\ell})}(k(p+2,(-1)^{\tilde{\ell}}\tilde{j}\omega)r_{\mathrm{e}})j_{\tilde{n}}(k(p+2,(-1)^{\tilde{\ell}}\tilde{j}\omega)R_{p+1})\Big\}$$

$$P_{\tilde{n}}^{\tilde{m}}(\cos(\theta_{\mathrm{e}}))\exp(i\tilde{m}\phi_{\mathrm{e}})\exp(+i(-1)^{\tilde{\ell}}\tilde{j}\omega t)\Big\}\quad\Bigg)\Big\}\Bigg]\cdot$$

$$\Bigg[\sum_{\tilde{\mathrm{e}}=1}^{\tilde{\mathrm{e}}=\mathcal{N}(\mathcal{E})}\overline{A_{(\tilde{\mathrm{e}},\mathrm{i_{set}})}}\Big\{\overline{h_n^{(\ell)}(k(p+2,(-1)^{\ell}j\omega)r_{\tilde{\mathrm{e}}})}\,\overline{j_n(k(p+2,(-1)^{\ell}j\omega)R_{p+1})}\Big\}$$

$$P_n^m(\cos(\theta_{\tilde{\mathrm{e}}}))\exp(-im\phi_{\tilde{\mathrm{e}}})\exp(-i(-1)^{\ell}j\omega t)\Big]\Big\}\Bigg]\quad\Bigg\}$$

$$=\sum_{t\in\mathcal{T}}\Bigg\{\quad\Bigg[\sum_{e=1}^{e=N(\mathcal{E})}A_{(\tilde{\mathrm{e}},\mathrm{i_{set}})}V_e(t)\Bigg]\cdot$$

$$\Bigg[\sum_{\tilde{\mathrm{e}}=1}^{\tilde{\mathrm{e}}=N(\mathcal{E})}\overline{A_{(\tilde{\mathrm{e}},i_{\mathrm{set}})}}\,\overline{h_n^{(\ell)}(k(p+2,(-1)^{\ell}j\omega)r_{\tilde{\mathrm{e}}})}\,\overline{j_n(k(p+2,(-1)^{\ell}j\omega)R_{p+2})}$$

$$P_n^m(\cos(\theta_{\tilde{\mathrm{e}}}))\exp(-im\phi_{\tilde{\mathrm{e}}})\exp(-i(-1)^{\ell}j\omega t)\quad\Bigg]\Bigg\}\tag{7.1.3.1}$$

Equations of the form (7.1.3.1) give a system of equations for the a priori unknown expansion coefficients

$$(\tilde{n},\tilde{m},\tilde{j},\tilde{\ell})\rightarrow c(\tilde{n},\tilde{m},\tilde{j},\tilde{\ell})\tag{7.1.3.2}$$

Since there are large numbers of time values in the EEG recordings, we reorder the summations in (7.1.3.1) and rewrite this equation as

$$
\begin{aligned}
&\Bigg\{ \\
&\left[\sum_{e=1}^{e=N(\mathcal{E})} \left(A_{(e,\mathrm{i_{set}})} \quad \sum_{\tilde{j}=1}^{J} \sum_{\tilde{\ell}=1}^{2} \sum_{\tilde{n}=0}^{N} \sum_{\tilde{m}=-\tilde{n}}^{\tilde{m}=+\tilde{n}} c(\tilde{n},\tilde{m},\tilde{j},\tilde{\ell}) \left\{ \right.\right.\right. \\
&\left\{ h_{\tilde{n}}^{(\tilde{\ell})}(k(p+2,(-1)^{\tilde{\ell}}\tilde{j}\omega)r_{\mathrm{e}}) j_{\tilde{n}}(k(p+2,(-1)^{\tilde{\ell}}\tilde{j}\omega)r_{p+1}) \right\} \left\{ P_{\tilde{n}}^{\tilde{m}}(\cos(\theta_{\mathrm{e}}))\exp(i\tilde{m}\phi_{\mathrm{e}}) \right\} \\
&\left.\left.\left. \left[\sum_{t\in\mathcal{T}} \exp(+i(-1)^{\tilde{\ell}}\tilde{j}\omega t)\exp(-i(-1)^{\ell}j\omega t) \right] \right\} \quad \right) \right\} \Bigg] \cdot \\
&\left[\quad \sum_{\tilde{\mathrm{e}}=1}^{\tilde{\mathrm{e}}=N(\mathcal{E})} \overline{A_{(\tilde{\mathrm{e}},\mathrm{i_{set}})}} \overline{h_n^{(\ell)}(k(p+2,(-1)^{\ell}j\omega)r_{\tilde{\mathrm{e}}}) j_{\tilde{n}}(k(p+2,(-1)^{\tilde{\ell}}\tilde{j}\omega)r_{p+1})} \right. \\
&\left. \left. P_n^m(\cos(\theta_{\tilde{\mathrm{e}}}))\exp(-im\phi_{\tilde{\mathrm{e}}}) \right] \right\} \right] \quad \Bigg\} \\
&= \Bigg\{ \quad \left[\sum_{e=1}^{e=N(\mathcal{E})} A_{(e,\mathrm{i_{set}})} \left\{ \sum_{t\in\mathcal{T}} V_e(t)\exp(-i(-1)^{\ell}j\omega t) \right\} \right] \cdot \\
&\left[\quad \sum_{\tilde{\mathrm{e}}=1}^{\tilde{\mathrm{e}}=N(\mathcal{E})} \overline{A_{(\tilde{\mathrm{e}},\mathrm{i_{set}})}} \overline{h_n^{(\ell)}(k(p+2,(-1)^{\ell}j\omega)r_{\tilde{\mathrm{e}}})} \overline{j_n(k(p+2,(-1)^{\ell}j\omega)R_{p+1})} \right. \\
&\left. P_n^m(\cos(\theta_{\tilde{\mathrm{e}}}))\exp(-im\phi_{\tilde{\mathrm{e}}}) \right] \quad \Bigg\} \\
&= \Bigg\{ \quad \left[\sum_{e=1}^{e=N(\mathcal{E})} A_{(e,\mathrm{i_{set}})} \left\{ \quad \sum_{t\in\mathcal{T}} V_e(t)\exp(-i(-1)^{\ell}j\omega t) \right\} \right] \Bigg\} \cdot \\
&\left[\sum_{\tilde{\mathrm{e}}=1}^{\tilde{\mathrm{e}}=N(\mathcal{E})} \left\{ \quad A_{(\tilde{\mathrm{e}},\mathrm{i_{set}})} \left[\overline{h_n^{(\ell)}(k(p+2,(-1)^{\ell}j\omega)r_{\tilde{\mathrm{e}}}) j_n^{(\ell)}(k(p+2,(-1)^{\ell}j\omega)r_{R_{p+1}})} \right] \cdot \right. \right. \\
&\left. \left. [P_n^m(\cos(\theta_{\tilde{\mathrm{e}}}))\exp(-im\phi_{\tilde{\mathrm{e}}})] \quad \right\} \right. \qquad (7.1.3.3)
\end{aligned}
$$

7.1.4 The Subroutines that Precompute Arrays Needed in Vector Space Homomorphism Representations and Vectors Derived from EEG Recordings to Determine Expansion Coefficients Defining the Head Surface Dynamic Voltage Representation

Our purpose here is to transform the relationships (7.1.1.4) and (7.1.3.3) into a matrix equation representation.

The subroutine

SUBROUTINE GHJNOL(NOFN,NOFJ,NOFEEG)

produces with $p = 1$ being the brain tissue region

HJNOL(NNDX,J,L,IEEG) =

$$h_n^{(\ell)}(k(p+2,(-1)^\ell\omega_j)r_{eeg})j_n(k(p+2.(-1)^\ell\omega_j)R_{p+1}) \tag{7.1.4.1}$$

The subroutine

| SUBROUTINE GPNMEXP(NOFN,NOFEEG) |

produces

PNMEXP(NNDX,MNDX,IEEG) =

$$P_n^{|m|}(\cos(\theta_{eeg}))\exp(im\phi_{eeg}) \tag{7.1.4.2}$$

The subroutine

SUBROUTINE GREPMTX(NOFN,NOFJ,NOFSET,NOFEEG)

produces the entries of the matrix multiplying the column of expansion coefficients that define the dynamic head surface voltage distribution stimulated by internal brain activity. In the FORTRAN program it produces the array

REPMTX(IROWCL,ICOLCL) =

$$\begin{aligned}
&\sum_{\mathrm{e}=1}^{\mathrm{e}=\mathcal{N}(\mathcal{E})} A_{(\mathrm{e},\mathrm{i_{set}})}\Bigg\{\quad\Big\{h_{\tilde{n}}^{(\tilde{\ell})}(k(p+2,(-1)^\ell\omega_{\tilde{j}})r_{\mathrm{e}})j_{\tilde{n}}(k(p+2,(-1)^\ell\omega_{\tilde{j}})r_{\mathrm{e}})\Big\}\cdot\\
&\qquad P_{\tilde{n}}^{|\tilde{m}|}(\cos(\theta_{\mathrm{e}}))\exp(i\tilde{m}\phi_{\mathrm{e}})\Big\}\cdot\\
&\qquad\Bigg[\sum_{t\in\mathcal{T}}\exp(+i(-1)^{\tilde{\ell}}\tilde{j}\omega t)\exp(-i(-1)^\ell j\omega t)\Bigg]\cdot\\
&\sum_{\tilde{\mathrm{e}}=1}^{\tilde{\mathrm{e}}=\mathcal{N}(\mathcal{E})}\Bigg\{\quad A_{(\tilde{\mathrm{e}},\mathrm{i_{set}})}\Big\{\overline{h_n^{(\ell)}(k(p+2,(-1)^\ell\omega_{\mathrm{j}}R_{\tilde{\mathrm{e}}})}\,\overline{j_n(k(p+2,(-1)^\ell\omega_{\mathrm{j}}R_{p+1})}\Big\}\\
&\qquad\big[P_n^{|m|}(\cos(\theta_{\tilde{\mathrm{e}}}))\exp(-im\phi_{\tilde{\mathrm{e}}})\big]\quad\Bigg\}
\end{aligned} \tag{7.1.4.3}$$

7.1.5 Row and Column Indices of the Matrices Defining the Representation of Dynamic Voltage from Local EEG Recordings

We use the indices appearing in equation (7.1.3.3) to find the row and column indices in the matrices $\overline{\overline{C}}$ that change (7.1.3.3) into the equivalent form

$$\overline{\overline{C}} \begin{bmatrix} \cdots \\ \cdots \\ \cdots \\ c(\tilde{n}, \tilde{m} = -\tilde{n}, \tilde{j}, \tilde{\ell}) \\ \cdots \\ \cdots \\ \cdots \\ c(\tilde{n}, \tilde{m} = 0, \tilde{j}, \tilde{\ell}) \\ \cdots \\ \cdots \\ \cdots \\ c(\tilde{n}, \tilde{m} = +\tilde{n}, \tilde{j}, \tilde{\ell}) \\ \cdots \\ \cdots \\ \cdots \end{bmatrix} = \begin{bmatrix} \cdots \\ \cdots \\ \cdots \\ \mathcal{VE}(\ell, j, \mathrm{i_{set}}) \mathcal{IF}(\mathrm{i_{set}}, n, \ell, m) \\ \cdots \\ \cdots \\ \cdots \end{bmatrix} \tag{7.1.5.1}$$

where

$$\mathcal{VE}(\ell, j, \mathrm{i_{set}}) = \left[\sum_{e=1}^{e=N(\mathcal{E})} A_{(e, \mathrm{i_{set}})} \left\{ \sum_{t \in \mathcal{T}} V_e(t) \exp(-i(-1)^{\ell} j \omega t) \right\} \right] \tag{7.1.5.2}$$

and

$$\mathcal{IF}(\mathrm{i_{set}}, n, \ell, m) = \left[\sum_{\tilde{\mathrm{e}}=1}^{\mathrm{e}=N(\mathcal{E})} \overline{A_{(\tilde{\mathrm{e}}, \mathrm{i_{set}})}} \overline{h_n^{(\ell)}(k((-1)^{\ell} j\omega) r_{\tilde{\mathrm{e}}})} P_n^m(\cos(\theta_{\tilde{\mathrm{e}}})) \exp(-im\phi_{\tilde{\mathrm{e}}}) \right] \tag{7.1.5.3}$$

The row index is

$$\begin{aligned} I_{row} = (\mathrm{i_{set}} - 1) LJN^2 + (\ell - 1) JN^2 \\ + (\mathrm{j} - 1) N^2 + n^2 + n + m + 1 \end{aligned} \tag{7.1.5.4}$$

and the column index is

$$I_{column} = (\tilde{\ell} - 1) JN^2 + (\tilde{j} - 1) N^2 + \tilde{n}^2 + \tilde{n} + \tilde{m} + 1 \tag{7.1.5.5}$$

We checked these equations comparing exact formulae above with results from augmenting a row and column variable in nested do loops. A snippet of computer data confirming equation (7.1.5.4) is

```
   1    1    2    6   -6 = IQ,L,J,N,M
 137 = IROW
 137 = predicted value of IROW
   1    1    2    6   -5 = IQ,L,J,N,M
 138 = IROW
 138 = predicted value of IROW
   1    1    2    6   -4 = IQ,L,J,N,M
 139 = IROW
 139 = predicted value of IROW
   1    1    2    6   -3 = IQ,L,J,N,M
 140 = IROW
 140 = predicted value of IROW
   1    1    2    6   -2 = IQ,L,J,N,M
 141 = IROW
 141 = predicted value of IROW
   1    1    2    6   -1 = IQ,L,J,N,M
 142 = IROW
 142 = predicted value of IROW
   1    1    2    6    0 = IQ,L,J,N,M
 143 = IROW
 143 = predicted value of IROW
   1    1    2    6    1 = IQ,L,J,N,M
 144 = IROW
 144 = predicted value of IROW
   1    1    2    6    2 = IQ,L,J,N,M
 145 = IROW
 145 = predicted value of IROW
   1    1    2    6    3 = IQ,L,J,N,M
 146 = IROW
 146 = predicted value of IROW
   1    1    2    6    4 = IQ,L,J,N,M
 147 = IROW
 147 = predicted value of IROW
   1    1    2    6    5 = IQ,L,J,N,M
 148 = IROW
 148 = predicted value of IROW
   1    1    2    6    6 = IQ,L,J,N,M
 149 = IROW
 149 = predicted value of IROW
```

A subset of the computer output confirming equation (7.1.5.5) is

```
1989 = predicted value of ICOL
1990 = ICOL
1990 = predicted value of ICOL
1991 = ICOL
```

```
1991 = predicted value of ICOL
1992 = ICOL
1992 = predicted value of ICOL
1993 = ICOL
1993 = predicted value of ICOL
1994 = ICOL
1994 = predicted value of ICOL
1995 = ICOL
1995 = predicted value of ICOL
1996 = ICOL
1996 = predicted value of ICOL
1997 = ICOL
1997 = predicted value of ICOL
1998 = ICOL
1998 = predicted value of ICOL
```

A program with a nested do loop was written to update the I_{column} variable in equation (7.1.5.5) and this was compared with the predicted value determined by equation (7.1.5.5).

7.2 Head Surface Anatomy and Coordinates Representing EEG Recording Sites

The head is assumed to be a ten centimeter radius sphere with the origin of the coordinate system at the center of the head. The x-y coordinate plane passes through the center of the head and intersects or is close to the nose and the left and right ears. The z-axis is the vertical coordinate and is oriented so that it goes through the electrode position just slightly forward of the crown of the head. The positive x-axis is in a direction toward the nose and the positive y-axis direction is toward the left ear giving us a right handed coordinate system.

Recording sites 1-32 are from the back of the head, recording sites 34-64 are from the right side of the head, recording sites 97-128 are on the left side of the head. The motor cortex region of the head controls the arm and hand movement.

BACK OF THE HEAD

IEEG	R	THETA	PHI
1	0.1000000000E+00	0.0000000000E+00	0.0000000000E+00
2	0.1000000000E+00	0.1150000000E+02	0.1800000000E+03
3	0.1000000000E+00	0.2300000000E+02	0.1800000000E+03
4	0.1000000000E+00	0.3450000000E+02	0.1800000000E+03
5	0.1000000000E+00	0.4600000000E+02	0.1575000000E+03
6	0.1000000000E+00	0.4600000000E+02	0.1350000000E+03
7	0.1000000000E+00	0.5750000000E+02	0.1350000000E+03
8	0.1000000000E+00	0.6900000000E+02	0.1440000000E+03
9	0.1000000000E+00	0.8050000000E+02	0.1440000000E+03
10	0.1000000000E+00	0.9200000000E+02	0.1440000000E+03
11	0.1000000000E+00	0.1035000000E+03	0.1440000000E+03

12	0.1000000000E+00	0.1150000000E+03	0.1440000000E+03
13	0.1000000000E+00	0.1150000000E+03	0.1620000000E+03
14	0.1000000000E+00	0.1035000000E+03	0.1620000000E+03
15	0.1000000000E+00	0.9200000000E+02	0.1620000000E+03
16	0.1000000000E+00	0.8050000000E+02	0.1620000000E+03
17	0.1000000000E+00	0.6900000000E+02	0.1620000000E+03
18	0.1000000000E+00	0.5750000000E+02	0.1575000000E+03
19	0.1000000000E+00	0.4600000000E+02	0.1800000000E+03
20	0.1000000000E+00	0.5750000000E+02	0.1800000000E+03
21	0.1000000000E+00	0.6900000000E+02	0.1800000000E+03
22	0.1000000000E+00	0.8050000000E+02	0.1800000000E+03
23	0.1000000000E+00	0.9200000000E+02	0.1800000000E+03
24	0.1000000000E+00	0.1035000000E+03	0.1800000000E+03
25	0.1000000000E+00	0.1150000000E+03	0.1800000000E+03
26	0.1000000000E+00	0.1150000000E+03	-0.1620000000E+03
27	0.1000000000E+00	0.1035000000E+03	-0.1620000000E+03
28	0.1000000000E+00	0.9200000000E+02	-0.1620000000E+03
29	0.1000000000E+00	0.8050000000E+02	-0.1620000000E+03
30	0.1000000000E+00	0.6900000000E+02	-0.1620000000E+03
31	0.1000000000E+00	0.5750000000E+02	-0.1575000000E+03
32	0.1000000000E+00	0.4600000000E+02	-0.1575000000E+03
		RIGHT SIDE OF THE HEAD (negative PHI)	
IEEG	R	THETA	PHI
33	0.1000000000E+00	0.1150000000E+02	-0.1080000000E+03
34	0.1000000000E+00	0.2300000000E+02	-0.1350000000E+03
35	0.1000000000E+00	0.4600000000E+02	-0.1350000000E+03
36	0.1000000000E+00	0.5750000000E+02	-0.1350000000E+03
37	0.1000000000E+00	0.6900000000E+02	-0.1440000000E+03
38	0.1000000000E+00	0.8050000000E+02	-0.1440000000E+03
39	0.1000000000E+00	0.9200000000E+02	-0.1440000000E+03
40	0.1000000000E+00	0.1035000000E+03	-0.1440000000E+03
41	0.1000000000E+00	0.1150000000E+03	-0.1440000000E+03
42	0.1000000000E+00	0.1035000000E+03	-0.1260000000E+03
43	0.1000000000E+00	0.9200000000E+02	-0.1260000000E+03
44	0.1000000000E+00	0.8050000000E+02	-0.1260000000E+03
45	0.1000000000E+00	0.6900000000E+02	-0.1260000000E+03
46	0.1000000000E+00	0.9200000000E+02	-0.1080000000E+03
47	0.1000000000E+00	0.8050000000E+02	-0.1080000000E+03
48	0.1000000000E+00	0.6900000000E+02	-0.1080000000E+03
49	0.1000000000E+00	0.5750000000E+02	-0.1125000000E+03
50	0.1000000000E+00	0.4600000000E+02	-0.1125000000E+03
51	0.1000000000E+00	0.3450000000E+02	-0.1200000000E+03
52	0.1000000000E+00	0.2300000000E+02	-0.9000000000E+02
53	0.1000000000E+00	0.3450000000E+02	-0.9000000000E+02
54	0.1000000000E+00	0.4600000000E+02	-0.9000000000E+02

55	0.1000000000E+00	0.5750000000E+02	-0.9000000000E+02
56	0.1000000000E+00	0.6900000000E+02	-0.9000000000E+02
57	0.1000000000E+00	0.8050000000E+02	-0.9000000000E+02
58	0.1000000000E+00	0.9200000000E+02	-0.9000000000E+02
59	0.1000000000E+00	0.9200000000E+02	-0.7200000000E+02
60	0.1000000000E+00	0.8050000000E+02	-0.7200000000E+02
61	0.1000000000E+00	0.6900000000E+02	-0.7200000000E+02
62	0.1000000000E+00	0.5750000000E+02	-0.6750000000E+02
63	0.1000000000E+00	0.4600000000E+02	-0.6750000000E+02
64	0.1000000000E+00	0.3450000000E+02	-0.6000000000E+02

FRONT OF THE HEAD (PHI has a small absolute value)

IEEG	R	THETA	PHI
65	0.1000000000E+00	0.1150000000E+02	-0.3600000000E+02
66	0.1000000000E+00	0.2300000000E+02	-0.4500000000E+02
67	0.1000000000E+00	0.4600000000E+02	-0.4500000000E+02
68	0.1000000000E+00	0.5750000000E+02	-0.4500000000E+02
69	0.1000000000E+00	0.6900000000E+02	-0.5400000000E+02
70	0.1000000000E+00	0.8050000000E+02	-0.5400000000E+02
71	0.1000000000E+00	0.9200000000E+02	-0.5400000000E+02
72	0.1000000000E+00	0.9200000000E+02	-0.3600000000E+02
73	0.1000000000E+00	0.8050000000E+02	-0.3600000000E+02
74	0.1000000000E+00	0.6900000000E+02	-0.3600000000E+02
75	0.1000000000E+00	0.3450000000E+02	-0.3000000000E+02
76	0.1000000000E+00	0.4600000000E+02	-0.2250000000E+02
77	0.1000000000E+00	0.5750000000E+02	-0.2250000000E+02
78	0.1000000000E+00	0.6900000000E+02	-0.1800000000E+02
79	0.1000000000E+00	0.8050000000E+02	-0.1800000000E+02
80	0.1000000000E+00	0.9200000000E+02	-0.1800000000E+02
81	0.1000000000E+00	0.9200000000E+02	0.0000000000E+00
82	0.1000000000E+00	0.8050000000E+02	0.0000000000E+00
83	0.1000000000E+00	0.6900000000E+02	0.0000000000E+00
84	0.1000000000E+00	0.5750000000E+02	0.0000000000E+00
85	0.1000000000E+00	0.4600000000E+02	0.0000000000E+00
86	0.1000000000E+00	0.3450000000E+02	0.0000000000E+00
87	0.1000000000E+00	0.2300000000E+02	0.0000000000E+00
88	0.1000000000E+00	0.3450000000E+02	0.3000000000E+02
89	0.1000000000E+00	0.4600000000E+02	0.2250000000E+02
90	0.1000000000E+00	0.5750000000E+02	0.2250000000E+02
91	0.1000000000E+00	0.6900000000E+02	0.1800000000E+02
92	0.1000000000E+00	0.8050000000E+02	0.1800000000E+02
93	0.1000000000E+00	0.9200000000E+02	0.1800000000E+02
94	0.1000000000E+00	0.9200000000E+02	0.3600000000E+02
95	0.1000000000E+00	0.8050000000E+02	0.3600000000E+02
96	0.1000000000E+00	0.6900000000E+02	0.3600000000E+02

LEFT SIDE OF THE HEAD (small positve PHI)

IEEG	R	THETA	PHI
97	0.1000000000E+00	0.1150000000E+02	0.3600000000E+02
98	0.1000000000E+00	0.2300000000E+02	0.4500000000E+02
99	0.1000000000E+00	0.4600000000E+02	0.4500000000E+02
100	0.1000000000E+00	0.5750000000E+02	0.4500000000E+02
101	0.1000000000E+00	0.6900000000E+02	0.5400000000E+02
102	0.1000000000E+00	0.8050000000E+02	0.5400000000E+02
103	0.1000000000E+00	0.9200000000E+02	0.5400000000E+02
104	0.1000000000E+00	0.9200000000E+02	0.7200000000E+02
105	0.1000000000E+00	0.8050000000E+02	0.7200000000E+02
106	0.1000000000E+00	0.6900000000E+02	0.7200000000E+02
107	0.1000000000E+00	0.5750000000E+02	0.6750000000E+02
108	0.1000000000E+00	0.4600000000E+02	0.6750000000E+02
109	0.1000000000E+00	0.3450000000E+02	0.6000000000E+02
110	0.1000000000E+00	0.2300000000E+02	0.9000000000E+02
111	0.1000000000E+00	0.1150000000E+02	0.1080000000E+03
112	0.1000000000E+00	0.2300000000E+02	0.1350000000E+03
113	0.1000000000E+00	0.3450000000E+02	0.1200000000E+03
114	0.1000000000E+00	0.3450000000E+02	0.9000000000E+02
115	0.1000000000E+00	0.4600000000E+02	0.9000000000E+02
116	0.1000000000E+00	0.5750000000E+02	0.9000000000E+02
117	0.1000000000E+00	0.6900000000E+02	0.9000000000E+02
118	0.1000000000E+00	0.8050000000E+02	0.9000000000E+02
119	0.1000000000E+00	0.9200000000E+02	0.9000000000E+02
120	0.1000000000E+00	0.9200000000E+02	0.1080000000E+03
121	0.1000000000E+00	0.8050000000E+02	0.1080000000E+03
122	0.1000000000E+00	0.6900000000E+02	0.1080000000E+03
123	0.1000000000E+00	0.5750000000E+02	0.1125000000E+03
124	0.1000000000E+00	0.4600000000E+02	0.1125000000E+03
125	0.1000000000E+00	0.6900000000E+02	0.1260000000E+03
126	0.1000000000E+00	0.8050000000E+02	0.1260000000E+03
127	0.1000000000E+00	0.9200000000E+02	0.1260000000E+03
128	0.1000000000E+00	0.1035000000E+03	0.1260000000E+03

8 Finding the Optimal Representation of Low Frequency Components of Brain Activity with A Comparison of Brain Activity Recovery Potential Using All the Interrelationships of the Full Time Profiles of Activity at Each Time on EEG Recording Sites Versus First Decomposing Each EEG Recording Individually into Frequency Components and Using these Components to Find the Dynamic Head Surface Voltage Representation

It is clear that first decomposing the EEG recordings into frequency components leads to smaller matrices and a faster determination of the dynamic head surface representation starting ab initio. However, if we carry out the singular value decomposition of the large brain activity independent matrix relation representation coefficients to EEG recordings ahead of time, it is hoped that the computation time which has the potential of recovering a greater amount of information could be tolerable to the person using their brain activity to control an artificial limb. We include a demonstration with a one dimensional model of brain activity to illustrate the potential of the two methods for recovering brain activity.

We can Fourier analyze the time profiles of activity at each EEG recording site to achieve faster spatial representation, or we can make use of all the relationships between voltages at the same time at all the EEG recording sites to recover the brain activity. With the first approach the matrices are smaller and, therefore, there is a more rapid determination of the matrices With the second approach the matrices are potentially very large and, to be practical for use with a person with physical needs the singular value decomposition of these brain-activity independent matrices would have to be carried out in advance.

In this section we include a "one dimensional brain activity recovery model" with wave source strengths at N fixed locations on the line and voltage wave measurement recordings a M locations on on the line. if you have measurements at times in a set $\mathcal{T}$, then if $M = 1$ is the number of measurement locations the number of equations relating source strengths to measurements is the number of time is $\mathcal{T}$. If you Fourier analyze first, then you have an unknown

$$t \to \cos(\omega_{\mathrm{j}} t)$$

and an unknown

$$t \to \sin(\omega_{\mathrm{j}} t)$$

multiplier at each source strength location x_{i} so that you would need to have $M \geq N$ in order to be able to find the source strength multipliers at each location.

There are at least two approaches to finding a spectral decomposition of an electroencephalogram signal. One approach would use the Stone Weierstrass theorem to find simultaneously the best N frequencies ω_j and the best multipliers A_j and B_j of sinusoidal terms with that frequency dependence which at each EEG site make for each EEG recording location

index $e \in \mathcal{E}$

$$\underset{\{\omega_j, A_j, B_j\} \subset \mathbb{R}}{\text{infimum}} \left[\underset{t \in \mathcal{T}}{\text{supremum}} \mid V_e(t) - \sum_{j=1}^{N} \{A_j \cos(\omega_j t) + B_j \sin(\omega_j t)\} \mid \right]$$

A second approach would be to assume a set of frequencies ω_j valid at each EEG recording site with index $e \in \mathcal{E}$ and find out which sets of multipliers

$$j \to (A_{(e,j)}, B_{(e,j)}$$

of the functions

$$t \to \cos(\omega_j t)$$

and

$$t \to \sin(\omega_j t)$$

best represents the signal by finding the minimum of the function

$$F(A_{(e,1)}, B_{(e,1)}, \cdots, A_{(e,j)}, B_{(e,j)}, \cdots, A_{(e,N)}, B_{(e,N)}) =$$

$$\sum_{t \in \mathcal{T}} \left[\left\{ \sum_{j=1}^{N} A_{(e,j)} \cos(\omega_j t) + B_{(e,j)} \sin(\omega_j t) \right\} - V_e(t) \right]^2$$

Both of these methods are described in this section.

8.1 Determination of the Expansion Coefficients Representing Low Frequency Components of Brain Activity

We determine the best representation of the EEG signal at each head surface EEG recording site location

$$e \to (x_e, y_e, z_e) = (r_e \sin(\theta_e) \cos(\phi_e), r_e \sin(\theta_e) \sin(\phi_e), r_e \cos(\theta_e)$$

that has the form of a trigonometric Fourier type series. The following section is presented as an alternative method of recovering brain activity which would be computationally faster. We didn't use this method in our inverse source programs, because the method we are using takes into account the interactions or relationships between recorded voltages at a given time at the different EEG recording locations.

8.1.1 A Trigonometric Series Representation of the Low Frequency Components of EEG Voltage Recordings at each EEG Recording Site

We suppose that $V_e(t)$ is the recorded EEG voltage at the head surface location with coordinates

$$(r_e, \theta_e, \phi_e) \to (r_e \sin(\theta_e) \cos(\phi_e), r_e \sin(\theta_e) \sin(\phi_e), r_e \cos(\theta_e)) \tag{8.1.1.1}$$

We minimize the function

$$F(A_{(e,1)}, B_{(e,1)}, \cdots, A_{(e,j)}, B_{(e,j)}, \cdots, A_{(e,N)}, B_{(e,N)}) =$$

$$\sum_{t\in\mathcal{T}}\left[\left\{\sum_{j=1}^{N}A_{(e,j)}\cos(\omega_j t)+B_{(e,j)}\sin(\omega_j t)\right\}-V_e(t)\right]^2 \tag{8.1.1.2}$$

We need to compute partial derivatives of the function defined by (8.1.1.2) with respect to $A_{(e,j)}$ and $B_{(e,j)}$. We have at the minimum of the F defined by (8.1.1.2) the relationship,

$$0=\frac{\partial F}{\partial A_{(e,j)}}=$$

$$\sum_{t\in\mathcal{T}}\left[\left\{\sum_{\tilde{j}=1}^{N}A_{(e,\tilde{j})}\cos(\omega_{\tilde{j}} t)+B_{(e,\tilde{j})}\sin(\omega_{\tilde{j}} t)\right\}-V_e(t)\right]\cos(\omega_j t) \tag{8.1.1.3}$$

Interchanging the order of summation in equation (8.1.1.3) we have

$$0=\frac{\partial F}{\partial A_{(e,j)}}=$$

$$\sum_{\tilde{j}=1}^{N}A_{(e,\tilde{j})}\left[\sum_{t\in\mathcal{T}}\left\{\cos(\omega_{\tilde{j}} t)\cos(\omega_j t)\right\}\right]$$

$$+B_{(e,\tilde{j})}\left[\sum_{t\in\mathcal{T}}\left\{\sin(\omega_{\tilde{j}} t)\cos(\omega_j t)\right\}\right]-V_e(t)\cos(\omega_j t) \tag{8.1.1.4}$$

Equation (8.1.1.4) in a form that is easy to transform into matrix language has the form

$$\sum_{\tilde{j}=1}^{N}A_{(e,\tilde{j})}\left[\sum_{t\in\mathcal{T}}\left\{\cos((\omega_{\tilde{j}}+\omega_j)t)+\cos((\omega_{\tilde{j}}-\omega_j)t)\right\}\right]$$

$$+\sum_{\tilde{j}=1}^{N}B_{(e,\tilde{j})}\left[\sum_{t\in\mathcal{T}}\left\{\sin((\omega_{\tilde{j}}+\omega_j)t)+\sin((\omega_{\tilde{j}}-\omega_j)t)\right\}\right]$$

$$=2\sum_{t\in\mathcal{T}}V_e(t)\cos(\omega_j t) \tag{8.1.1.5}$$

where to go from (8.1.1.4) to (8.1.1.5) we used the two trigonometric identities

$$(\cos(\alpha)\cos(\beta),\sin(\alpha)\cos(\beta))=\left(\frac{\cos(\alpha+\beta)+\cos(\alpha-\beta)}{2},\frac{\sin(\alpha+\beta)+\sin(\alpha-\beta)}{2}\right) \tag{8.1.1.6}$$

The partial derivatives with respect to $B_{(e,j)}$ of the function F defined by (8.1.1.2) is

$$0=\frac{\partial F}{\partial B_{(e,j)}}=$$

$$\sum_{t\in\mathcal{T}}\left[\left\{\sum_{\tilde{j}=1}^{N}A_{(e,\tilde{j})}\cos(\omega_{\tilde{j}} t)+B_{(e,\tilde{j})}\sin(\omega_{\tilde{j}} t)\right\}-V_e(t)\right]\sin(\omega_j t)$$

$$= \sum_{\tilde{j}=1}^{N} A_{(e,\tilde{j})} \left\{ 2 \sum_{t \in \mathcal{T}} \left[\cos(\omega_{\tilde{j}} t) \sin(\omega_j t) \right] \right\}$$
$$+ \sum_{\tilde{j}=1}^{N} B_{(e,\tilde{j})} \left\{ 2 \sum_{t \in \mathcal{T}} \left[\sin(\omega_{\tilde{j}} t) \sin(\omega_j t) \right] \right\}$$
$$-2 \sum_{t \in \mathcal{T}} \{ V_e(t) \sin(\omega_j t) \} \tag{8.1.1.7}$$

Using equation (8.1.1.7) and the trigonometric identities

$$(\cos(\alpha)\sin(\beta), \sin(\alpha)\sin(\beta)) = \left(\frac{\sin(\alpha+\beta) - \sin(\alpha-\beta)}{2}, \frac{\cos(\alpha-\beta) - \cos(\alpha+\beta)}{2} \right) \tag{8.1.1.8}$$

we have the relationship,

$$\sum_{\tilde{j}=1}^{N} A_{(e,\tilde{j})} \left\{ \sum_{t \in \mathcal{T}} \left[\sin((\omega_{\tilde{j}} + \omega_j)t) - \sin((\omega_{\tilde{j}} - \omega_j)t) \right] \right\}$$
$$+ \sum_{\tilde{j}=1}^{N} B_{(e,\tilde{j})} \left\{ \sum_{t \in \mathcal{T}} \left[\cos((\omega_{\tilde{j}} - \omega_j)t) - \cos((\omega_{\tilde{j}} + \omega_j)t) \right] \right\}$$
$$= 2 \sum_{t \in \mathcal{T}} V_e(t) \sin(\omega_j t) \tag{8.1.1.9}$$

We transform equations (8.1.1.5) and (8.1.1.9) into the matrix equation

$$\overline{\overline{C}} \begin{bmatrix} A_{(e,1)} \\ B_{(e,1)} \\ \cdots \\ \cdots \\ \cdots \\ A_{(e,\tilde{j})} \\ B_{(e,\tilde{j})} \\ \cdots \\ \cdots \\ \cdots \\ A_{(e,N)} \\ B_{(e,N)} \end{bmatrix} = \begin{bmatrix} R_{\mathcal{T}}(1) \\ R_{\mathcal{T}}(2) \\ \cdots \\ \cdots \\ \cdots \\ R_{\mathcal{T}}(2(j-1)+1) \\ R_{\mathcal{T}}(2(j-1)+2) \\ \cdots \\ \cdots \\ \cdots \\ R_{\mathcal{T}}(2(N-1)+1) \\ R_{\mathcal{T}}(2(N-1)+2) \end{bmatrix} \tag{8.1.1.10}$$

where equation (8.1.1.5) tells us that

$$R_{\mathcal{T}}(2(j-1)+1) = 2 \sum_{t \in \mathcal{T}} V_e(t) \cos(\omega_j t) \tag{8.1.1.11}$$

and that matrix element multiplier of $A_{(e,\tilde{j})}$ is

$$C(2(j-1)+1, 2(\tilde{j}-1)+1) = \left[\sum_{t\in\mathcal{T}} \left\{\cos((\omega_{\tilde{j}}+\omega_j)t) + \cos((\omega_{\tilde{j}}-\omega_j)t)\right\}\right] \tag{8.1.1.12}$$

Again for equation (8.1.1.5) the matrix element that is a multiplier of $B_{(e,\tilde{j})}$ is

$$C(2(j-1)+1, 2(\tilde{j}-1)+2) = \left[\sum_{t\in\mathcal{T}} \left\{\sin((\omega_{\tilde{j}}+\omega_j)t) + \sin((\omega_{\tilde{j}}-\omega_j)t)\right\}\right] \tag{8.1.1.13}$$

From the matrix equation (8.1.1.10) and (8.1.1.9) the right side of equation (8.1.1.9) is

$$R_{\mathcal{T}}(2(j-1)+2) = 2\sum_{t\in\mathcal{T}} V_e(t)\sin(\omega_j t) \tag{8.1.1.14}$$

The matrix element in equation (8.1.1.10) in the row corresponding to equation (8.1.1.9) that multiplies $A_{(e,\tilde{j})}$ is

$$C(2(j-1)+2, 2(\tilde{j}-1)+1) = \left\{\sum_{t\in\mathcal{T}} \left[\sin((\omega_{\tilde{j}}+\omega_j)t) - \sin((\omega_{\tilde{j}}-\omega_j)t)\right]\right\} \tag{8.1.1.15}$$

The matrix element in equation (8.1.1.10) in the row corresponding to equation (8.1.1.9) that multiplies $B_{(e,\tilde{j})}$ is

$$C(2(j-1)+2, 2(\tilde{j}-1)+2) = \left\{\sum_{t\in\mathcal{T}} \left[\cos((\omega_{\tilde{j}}-\omega_j)t) - \cos((\omega_{\tilde{j}}+\omega_j)t)\right]\right\} \tag{8.1.1.16}$$

The best fitting series representation is obtained by solving (8.1.1.9) using singular value decomposition.

8.1.2 A One Dimensional Model of Brain Activity Recovery to Demonstrate the Difference Between Time Domain and Frequency Domain Recovery of Brain Activity Representations

We suppose that we have M sources of a wave and that there are N frequency components representing the strength of the signal for each of the N frequency components at each site. We suppose that we know the site locations $\tilde{x}_i$ for i running from 1 through M and that we know frequencys ω_j and the wavelengths λ_j for each j running from 1 through N that the signal is

$$V(x,t) =$$

$$\sum_{i=1}^{M}\sum_{j=1}^{N} \left\{A_{(j,i)}\sin\left(\omega_j t - (x-\tilde{x}_i)/\lambda_j\right) + B_{(j,i)}\cos\left(\omega_j t - (x-\tilde{x}_i)/\lambda_j\right)\right\}$$

$$\left(\frac{B_{(j,i)} - iA_{(j,i)}}{2}\right)\exp(i\left(\omega_j t - (x-\tilde{x}_i)/\lambda_j\right))$$

$$\left(\frac{B_{(j,i)}+iA_{(j,i)}}{2}\right)\exp(-i\,(\omega_j t-(x-\tilde{x}_i)/\lambda_j))$$
$$=\sum_{j=1}^{N}\sum_{\ell=1}^{2}C_{(j,\ell,i)}\exp(i(-1)^{\ell}\omega_j t) \tag{8.1.2.1}$$

Suppose that at mesurement location x_p where p runs from 1 through P we have the measurements

$$V(x_p,t)=\sum_{j=1}^{N}\sum_{\ell=1}^{2}\left\{D_{(p,j,\ell)}\exp(i(-1)^{\ell}\omega_j t)\right\} \tag{8.1.2.2}$$

If we try to recover the strengths $C_{(j,\ell,i)}$ from the $D_{(p,j,\ell)}$ alone, the number of p must be at least as large as the number M of source locations. However, if this is carried out in the time domain knowing $V(x_p,t)$ for all time, we can sometimes do this with just one measurement location.

9 Description of the Interrogating Vector Field Inverse Source Solution

One brain activity recovery solution uses as a starting point the divergence free portion of the vector potential of Brain Activity.

Our program to recover brain activity from EEG recordings is based on the theory that brain activity produces a dynamic voltage wave ([74]) which propagates through the skull to the surface of the head which is picked up by electroencephalogram recordings.

9.1 A Cole-Cole Model of the Propagation of Different Frequency Components of a Brain-Wave Signal

Brain tissue is a dispersive material (Gabriel [46]) at brain activity frequencies. Our model determines and makes use of the propagation constant and permittivity of different tissue regions as a function of frequency to properly solve the boundary value problem and predict electric vectors $\boldsymbol{E}$ and $\boldsymbol{H}$ outside the head that are stimulated by internal brain waves.

9.1.1 Maxwell's Equations and the curl Operator

The electric vector $\boldsymbol{E}$ and the magnetic vector $\boldsymbol{H}$ stimulated by brain activity are related through Maxwell's equations by the curl operator. We take (Cohoon et al. [28])

$$\boldsymbol{E}=E_x\boldsymbol{e}_x+E_y\boldsymbol{e}_y+E_z\boldsymbol{e}_z \tag{9.1.1.1}$$

and

$$\nabla\times(\boldsymbol{E})=\left(\frac{\partial E_z}{\partial y}-\frac{\partial E_y}{\partial z}\right)\boldsymbol{e}_x+\left(\frac{\partial E_x}{\partial z}-\frac{\partial E_z}{\partial x}\right)\boldsymbol{e}_y+\left(\frac{\partial E_y}{\partial x}-\frac{\partial E_x}{\partial y}\right)\boldsymbol{e}_z \tag{9.1.1.2}$$

We consider $\boldsymbol{E}$ with a time dependence of the form

$$t \to \exp(i(-1)^{\ell}\omega t) \tag{9.1.1.3}$$

For this time dependence Maxwell's equations provide

$$\nabla \times (\boldsymbol{E}) = -i(-1)^{\ell}\omega\mu_0 \boldsymbol{H} \tag{9.1.1.4}$$

and

$$\nabla \times (\boldsymbol{H}) = i(-1)^{\ell}\omega\epsilon((-1)^{\ell}\omega)\boldsymbol{E} \tag{9.1.1.5}$$

where $\ell = 2$ represents a positive frequency and $\ell = 1$ a negative frequency. The permittivity ϵ of brain tissue is a function of frequency and the brain wave signal contains all frequency components. In the next section we shall describe Gabriel's ([46]) representation of the permittivity of skull bone, brain, and other human tissue at brain wave frequencies.

9.1.2 Brain Tissue Electromagnetic Properties as a Function of Frequency

We use the representation of Gabriel ([46]) to determine the complex permittivity of human tissue as a function of frequency. The fact that brain wave signals start and end at specific times means that they contain all frequencies. We denote frequency by

$$f = \frac{\omega}{2\pi} \tag{9.1.2.1}$$

The Cole-Cole relationship (Cole [32], Torres [116]) has the form

$$\epsilon_{relative} = \epsilon_{\infty} + \frac{\epsilon_{static} - \epsilon_{\infty}}{1 + (i\omega\tau)^{\alpha}} \tag{9.1.2.2}$$

Gabriel ([46]) fits experimental data using relationships of the form

$$\epsilon_{relative}(f) = \epsilon' - i\epsilon'' = \epsilon_{\infty} + \sum_{j=1}^{4}\left(\frac{\Delta\epsilon_j}{1 + (if/f_j)^{\alpha_j}}\right) - i\frac{\sigma}{\omega\epsilon_0} \tag{9.1.2.3}$$

The actual meter, kilogram, second permittivity as a function of ω is

$$\epsilon(\omega) = \epsilon_0\epsilon_{\infty} + \epsilon_0\sum_{j=1}^{4}\left(\frac{\Delta\epsilon_j}{1 + (i\omega/[2\pi f_j])^{\alpha_j}}\right) - i\frac{\sigma}{\omega} \tag{9.1.2.4}$$

For brain tissue we have for the four compartments from the data in Gabriel [46] and Hurt [64].

$$(\sigma, \epsilon_{\infty}) = (.02, 4) \tag{9.1.2.5}$$

and, as a further illustration of the use of the tissue tables which follow, we have

$$(\Delta\epsilon_1, f_1, \alpha_1) = (45, 2 \times 10^{10}, 9/10) \tag{9.1.2.6}$$

$$(\Delta\epsilon_2, f_2, \alpha_2) = (40, 1 \times 10^{7}, 85/100) \tag{9.1.2.7}$$

$$(\Delta\epsilon_3, f_3, \alpha_3) = (2 \times 10^{5}, 1.5 \times 10^{3}, 78/100) \tag{9.1.2.8}$$

$$(\Delta\epsilon_4, f_4, \alpha_4) = (4.5 \times 10^{7}, 30, 1) \tag{9.1.2.9}$$

From Gabriel ([46]) the first set of parameters describing the propagation of brain waves in tissue are in the following table.

Tissue	ϵ_∞	$\Delta\epsilon_1$	f_1	α_1	σ	$\Delta\epsilon_2$	f_2	α_2
bile	4	66	2.1×10^{10}	95/100	14/10	50	10^8	1
bladder	25/10	16	1.8×10^{10}	9/10	2/10	400	10^6	9/10
blood	4	56	1.9×10^{10}	9/10	7/10	520	1.2×10^6	9/10
blood vessel	4	40	1.8×10^{10}	9/10	25/10	50	5×10^7	9/10
body fluid	4	65	2.2×10^{10}	9/10	15/10	30	10^6	9/10
bone (cancellous)	25/10	18	1.2×10^{10}	78/100	7/100	300	2×10^6	75/100
bone (cortical)	25/10	10	1.2×10^{10}	8/10	2/100	180	2×10^6	8/10
brain	4	45	2×10^{10}	9/10	2/100	400	10^7	85/100
cerebral spinal fluid	4	65	2×10^{10}	9/10	2	40	10^8	1
fat	25/10	3	2×10^{10}	8/10	1/100	15	10^7	9/10
skin	4	32	2.2×10^{10}	1	2×10^{-4}	1100	4.9×10^6	8/10

For the same tissues the rest of the parameters needed to determine how brain waves propagate in these tissues are in the table below.

Tissue	$\Delta\epsilon_3$	f_3	α_3	$\Delta\epsilon_4$	f_4	α_4
bile	0	1000	8/10	0	10	8/10
bladder	10^5	1000	8/10	10^7	10	1
blood	0	1000	8/10	0	10	1
blood vessel	10^5	10^3	8/10	10^7	100	1
body fluid	0	1000	1	0	10	1
bone (cancellous)	5000	1000	8/10	2×10^7	10	1
bone (cortical)	5000	1000	8/10	10^5	10	1
brain	2×10^5	1500	78/100	4.5×10^7	300	1
cerebral spinal fluid	0	1000	1	0	10	1
fat	3.3×10^4	1000	95/100	10^7	20	99/100
skin	0	1000	8/10	0	10	8/10

9.2 Hodgkin Huxley Formulation of the Action Potential

We programmed the original 1952 Hodgkin and Huxley formulation description of (Hodgkin [61]) nerve axon activity where the dependent variables are transmembrane voltage and the potassium and sodium channel access probabilities and channel inhibition probabilities using the stiff differential equation subroutines of Morris ([85]). The neuronal currents that stimulate the electroencephalogram are then derived from the voltage differential equation as the product of the the transmembrane capacitance and the voltage derivative.

9.2.1 The Hodgkin Huxley System of Differential Equations

The transmembrane voltage is given by

$$\frac{dV}{dt} = \left(\frac{1}{C_M}\right)\Big\{ \quad I_{stimulus}(t)$$

$$- \left[G_K n(t)^4 (V(t) - V_K) + G_{Na}\left(m(t)^3 h(t)\left\{V(t) - V_{Na}\right\}\right) + G_L(V(t) - V_L)\right] \quad \Big\} \qquad (9.2.1.1)$$

The proportion, n, of K^+ ions inside the membrane and the proportion $1 - n$ of K^+ ions outside the membrane are related by

$$\frac{dn}{dt} = \alpha_n(V)(1 - n) - \beta_n(V)n \qquad (9.2.1.2)$$

where

$$\alpha_n(V) = \frac{1}{10}\alpha((V + 10)/10) \qquad (9.2.1.3)$$

where $\alpha(\xi)$ is defined by

$$\alpha(\xi) = \begin{cases} \xi/\left[\exp(\xi) - 1\right] & \text{if} \quad \xi \neq 0 \\ 1 & \text{if} \quad \xi = 0 \end{cases} \qquad (9.2.1.4)$$

and β_n is given by

$$\beta_n(V) = \frac{1}{8}\exp(V/8) \qquad (9.2.1.5)$$

The proportion, m of Na^+ ions outside the membrane is described by

$$\frac{dm}{dt} = \alpha_m(V)(1-m) - \beta_m(V)m \tag{9.2.1.6}$$

where

$$\alpha_m(V) = \alpha((V+25)/10) \tag{9.2.1.7}$$

and β_m is defined by

$$\beta_m(V) = 4\exp(V/18) \tag{9.2.1.8}$$

The probability, h, of finding an inactivation molecule for Na^+ conductance outside the membrane, and the probability, $1-h$, of finding a sodium conductance inactivating molecule inside the membrane are related by the differential equation

$$\frac{dh}{dt} = \alpha_h(V)(1-h) - \beta_h(V)h \tag{9.2.1.9}$$

where

$$\alpha_h(V) = \frac{7}{100}\exp(V/20) \tag{9.2.1.10}$$

and

$$\beta_h(V) = \frac{1}{\exp((V+30)/10)+1} \tag{9.2.1.11}$$

To achieve good accuracy and stability using the stiff differential equation package developed by Morris ([85]) we used analytical, closed-form Jacobians in this solver. Details are available on request.

Hodgkin and Huxley ([61], page 520) provided values of parameters for the above system of differential equations. The values are

Constant	Units	Value Chosen	Mean	Range
C_M	μFarads/cm^2	1.0	.91	.8 to 1.5
V_{Na}	millivolts	-115	-109	-95 to -119
V_K	millivolts	+12	+11	+9 to +14
G_{Na}	millimhos/cm^2	120	160	120 to 260
G_K	millimhos/cm^2	36	34	26 to 49
G_L	millimhos/cm^2	0.3	.26	.13 to .50

In addition to using the complete Hodgkin and Huxley model, we also used a Rinzel model as modified by Wilson ([131]) given by

$$C\frac{dV}{dt} = -\left\{17.81 + 47.58V + 33.8V^2\right\}(V - 0.48) - 26R(V + .95) + I \qquad (9.2.1.12)$$

and

$$\frac{dR}{dt} = \frac{1}{\lambda_R}\left\{-R + 1.29V + 0.79 + 3.3(V + 0.38)^2\right\} \qquad (9.2.1.13)$$

where λ_R is 5.6 milliseconds and the transmembrane capacitance C is given a value of 1 microfarad per square centimeter. The parameter values chosen were numerically fitted to produce good approximations to the human neocortical neuron action potential. The computer program reproduced the human neocortical neuron action potential with a constant input current I in the Rinzel voltage equation of 1.57 nano Amperes. This system was solved without using the stiff differential equation solver of Morris ([85]).

9.2.2 Transmembrane Current Representation

The transmembrane current, derived from the voltage differential equation, is

$$\mathcal{I}(t) = C_M\frac{dV}{dt} = \Bigg\{ \quad I_{stimulus}(t)$$

$$- \left[G_K n(t)^4(V(t) - V_K) + G_{Na}\left(m(t)^3 h(t)\left\{V(t) - V_{Na}\right\}\right) + G_L(V(t) - V_L)\right] \quad \Bigg\} \qquad (9.2.2.1)$$

We used our differential equations to find a Fourier series for the transmembrane current

$$t \to C\frac{dV}{dt} \qquad (9.2.2.2)$$

The differential equations were solved and a table of data points was created. Lagrange interpolation was used with the table to find two fixed time-interval end points, not necessarily in the table, so that the voltage value, $V(t)$, would be the same at each end of the time interval. Thus, our Fourier series, while accurately representing the transmembrane current over this time interval, will not have a constant term; the transmission of each component of the brain wave signal through the skull can then be easily computed.

9.3 Exact Analytical Brain Wave Source Solution

We can represent the electric and magnetic vectors of a general current source on an arbitrarily oriented dipole by an exact formula. To validate our vector spherical harmonic representation of the brain wave sources, these two representations of the brain wave source must agree.

9.3.1 Analysis of the Vector Potential for a Single Dipole Source

We let $\boldsymbol{e}_x$, $\boldsymbol{e}_y$, and $\boldsymbol{e}_z$ be the unit vectors in the direction of the positive x, y, and z coordinate axes in a Euclidean system so that

$$(\boldsymbol{e}_x, \boldsymbol{e}_y, \boldsymbol{e}_z) = (\nabla(x), \nabla(y), \nabla(z)) \tag{9.3.1.1}$$

We will be using spherical coordinates

$$(x, y, z) = (r\sin(\theta)\cos(\phi), r\sin(\theta)\sin(\phi), r\cos(\theta)) \tag{9.3.1.2}$$

$$r = \sqrt{x^2 + y^2 + z^2} \tag{9.3.1.3}$$

and

$$\boldsymbol{r} = r\sin(\theta)\cos(\phi)\boldsymbol{e}_x + r\sin(\theta)\sin(\phi)\boldsymbol{e}_y + r\cos(\theta)\boldsymbol{e}_z = x\boldsymbol{e}_x + y\boldsymbol{e}_y + z\boldsymbol{e}_z \tag{9.3.1.4}$$

We have

$$\boldsymbol{e}_r = \sin(\theta)\cos(\phi)\boldsymbol{e}_x + \sin(\theta)\sin(\phi)\boldsymbol{e}_y + \cos(\theta)\boldsymbol{e}_z \tag{9.3.1.5}$$

Now

$$\boldsymbol{e}_\theta = \frac{1}{r}\frac{\partial \boldsymbol{r}}{\partial \theta} = \cos(\theta)\cos(\phi)\boldsymbol{e}_x + \cos(\theta)\sin(\phi)\boldsymbol{e}_y - \sin(\theta)\boldsymbol{e}_z \tag{9.3.1.6}$$

and

$$\boldsymbol{e}_\phi = \left(\frac{1}{r\sin(\theta)}\right)\frac{\partial \boldsymbol{r}}{\partial \phi} = -\sin(\phi)\boldsymbol{e}_x + \cos(\phi)\boldsymbol{e}_y \tag{9.3.1.7}$$

and

$$\boldsymbol{e}_x = \nabla(r\sin(\theta)\cos(\phi)) = \sin(\theta)\cos(\phi)\boldsymbol{e}_r + \cos(\theta)\cos(\phi)\boldsymbol{e}_\theta - \sin(\phi)\boldsymbol{e}_\phi \tag{9.3.1.8}$$

$$\boldsymbol{e}_y = \nabla(r\sin(\theta)\sin(\phi)) = \sin(\theta)\sin(\phi)\boldsymbol{e}_r + \cos(\theta)\sin(\phi)\boldsymbol{e}_\theta + \cos(\phi)\boldsymbol{e}_\phi \tag{9.3.1.9}$$

and

$$\boldsymbol{e}_z = \nabla(z) = \nabla(r\cos(\theta)) = \cos(\theta)\boldsymbol{e}_r - \sin(\theta)\boldsymbol{e}_\theta \tag{9.3.1.10}$$

Using (9.3.1.4) the location of the brain activity source with index q is

$$\boldsymbol{r}_{\mathrm{q}} = r_{\mathrm{q}}\sin(\theta_{\mathrm{q}})\cos(\phi_{\mathrm{q}})\boldsymbol{e}_x + r_{\mathrm{q}}\sin(\theta_{\mathrm{q}})\sin(\phi_{\mathrm{q}})\boldsymbol{e}_y + r_{\mathrm{q}}\cos(\theta_{\mathrm{q}})\boldsymbol{e}_z = x_{\mathrm{q}}\boldsymbol{e}_x + y_{\mathrm{q}}\boldsymbol{e}_y + z_{\mathrm{q}}\boldsymbol{e}_z \quad (9.3.1.11)$$

We consider the real current on a dipole contributed by components whose frequencies are $+\omega$ and $-\omega$ of the form

$$I(t) = \mathrm{a}\cos(\omega t) + b\sin(\omega t) = \mathrm{a}\left(\frac{\exp(i\omega t) + \exp(-i\omega t)}{2}\right) + b\left(\frac{\exp(i\omega t) - \exp(-i\omega t)}{2i}\right) \quad (9.3.1.12)$$

which reduces to

$$I(t) = \left(\frac{\mathrm{a} - ib}{2}\right)\exp(+i\omega t) + \left(\frac{\mathrm{a} + ib}{2}\right)\exp(-i\omega t) \quad (9.3.1.13)$$

Components of the brain wave signal with different frequencies propagate at different speeds through tissues. The propagation constant, which has the units of frequency divided by speed, is in the tissue region with index p denoted by $k(p, (-1)^{\ell}\omega)$ where $\ell = 1$ denotes a negative frequency and $\ell = 2$ a positive frequency. The square of the propagation constant in the tissue region with index p is

$$k(p, (-1)^{\ell}\omega)^2 = \omega^2\mu_0\epsilon_p((-1)^{\ell}\omega) \quad (9.3.1.14)$$

where $\epsilon_p((-1)^{\ell}\omega)$ is the permittivity in tissue region p at frequency $(-1)^{\ell}\omega)$ defined by (9.1.2.4) using the work of Gabriel ([46]) and Hurt ([64]) and μ_0 is the permeability of a nonmagnetic material.

Considering a dipole current density given by (9.3.1.13) we assume, for the qth dipole at vector location $\boldsymbol{r}_q$ that the vector potential of the radiation, at the vector observation point $\boldsymbol{r}$ just outside the insulation has the form

$$\boldsymbol{A} = \frac{\mu}{4\pi}\left\{\left(\frac{\mathrm{a} + ib}{2}\right)\left(\frac{\exp(+ik(p, -\omega) \mid \boldsymbol{r} - \boldsymbol{r}_{\mathrm{q}} \mid)}{\mid \boldsymbol{r} - \boldsymbol{r}_{\mathrm{q}} \mid}\right)\exp(-i\omega t)\boldsymbol{e}_q + \right.$$

$$\left.\left(\frac{\mathrm{a} - ib}{2}\right)\left(\frac{\exp(-ik(p, +\omega) \mid \boldsymbol{r} - \boldsymbol{r}_{\mathrm{q}} \mid)}{\mid \boldsymbol{r} - \boldsymbol{r}_{\mathrm{q}} \mid}\right)\exp(+i\omega t)\boldsymbol{e}_q\right\} \quad (9.3.1.15)$$

where

$$\begin{aligned}\boldsymbol{r}_{\mathrm{q}} &= x_{\mathrm{q}}\boldsymbol{e}_x + y_{\mathrm{q}}\boldsymbol{e}_y + z_{\mathrm{q}}\boldsymbol{e}_z \\ &= r_{\mathrm{q}}\left\{\sin(\theta_{\mathrm{q}})\left[\cos(\phi_{\mathrm{q}})\boldsymbol{e}_x + \sin(\phi_{\mathrm{q}})\boldsymbol{e}_y\right] + \cos(\theta_{\mathrm{q}})\boldsymbol{e}_z\right\}\end{aligned} \quad (9.3.1.16)$$

and

$$\begin{aligned}\boldsymbol{r} &= x\boldsymbol{e}_x + y\boldsymbol{e}_y + z\boldsymbol{e}_z \\ &= r\left\{\sin(\theta)\left[\cos(\phi)\boldsymbol{e}_x + \sin(\phi)\boldsymbol{e}_y\right] + \cos(\theta)\boldsymbol{e}_z\right\}\end{aligned} \quad (9.3.1.17)$$

If $j_n(z)$ is the spherical Bessel function and $y_n(z)$ is the spherical Neumann function, then

$$h_n^{(1)}(z) = j_n(z) + iy_n(z) \tag{9.3.1.18}$$

which is given in (Abramowitz [1]) on page 437 and

$$h_n^{(2)}(z) = j_n(z) - iy_n(z) \tag{9.3.1.19}$$

The vector potential arising from the signal (9.3.1.13) on the dipole located $\boldsymbol{r}_{\mathrm{q}}$ is

$$\begin{aligned}
&\boldsymbol{A} = \\
&\frac{\mu}{4\pi}\left(\frac{\mathrm{a}-ib}{2}\right)\{-ik(p,+\omega)\}\left[\frac{\exp(-ik(p,+\omega)\mid \boldsymbol{r}-\boldsymbol{r}_{\mathrm{q}}\mid)}{-ik(p,+\omega)\mid \boldsymbol{r}-\boldsymbol{r}_{\mathrm{q}}\mid}\right]\exp(+i\omega t)\boldsymbol{e}_q \\
&+\frac{\mu}{4\pi}\left(\frac{\mathrm{a}+ib}{2}\right)\{ik(p,-\omega)\}\left[\frac{\exp(+ik(p,-\omega)\mid \boldsymbol{r}-\boldsymbol{r}_{\mathrm{q}}\mid)}{+ik(p,-\omega)\mid \boldsymbol{r}-\boldsymbol{r}_{\mathrm{q}}\mid}\right]\exp(-i\omega t)\boldsymbol{e}_q \\
&\quad = \frac{\mu}{4\pi}\frac{\mathrm{a}-ib}{2}\{-ik(p,+\omega)\}\,h_0^{(2)}(k(p,+\omega)\mid \boldsymbol{r}-\boldsymbol{r}_{\mathrm{q}}\mid)\exp(+i\omega t)\boldsymbol{e}_q \\
&+\frac{\mu}{4\pi}\frac{\mathrm{a}+ib}{2}\{+ik(p,-\omega)\}\,h_0^{(1)}(k(p,-\omega)\mid \boldsymbol{r}-\boldsymbol{r}_{\mathrm{q}}\mid)\exp(-i\omega t)\boldsymbol{e}_q
\end{aligned} \tag{9.3.1.20}$$

9.4 Fundamental Theory For Solving the Full Harmonic Prediction of External Fields Stimulated by Brain Activity

The theory in the next section simplifies the validation of the solution of the boundary value problem for predicting external fields.

9.4.1 A Proof that the Curl Operator is an Endomorphism of the Module of Vector Spherical over the Ring of Differentiable Functions of the Radial Variable

We used special functions in representing the vector spherical harmonics. The spherical Bessel functions $j_n(z)$, spherical Weber functions (also called spherical Neumann functions) $y_n(z)$, and spherical Hankel functions $h_n^{(\tilde{\ell})}$ for $\tilde{\ell}$ equal to 1 or 2 are all solutions of the differential equation

$$z^2\frac{d^2w}{dz^2} + 2z\frac{dw}{dz} + [z^2 - n(n+1)]w = 0 \tag{9.4.1.1}$$

The associated Legendre function $P_n^m(\cos(\theta))$ is a solution of the differential equation

$$-\frac{1}{\sin(\theta)}\frac{d}{d\theta}\left[\sin(\theta)\left(\frac{d}{d\theta}\right)P_n^m(\cos(\theta))\right]+\left(\frac{m^2}{\sin^2(\theta))}\right)P_n^m(\cos(\theta))=n(n+1)P_n^m(\cos(\theta)) \tag{9.4.1.2}$$

This function is used in representing the spatial variation of brain activity on the surface of the head. There are three vector fields that we use to describe the spatial variation of the brain wave signals on spherical measurement surfaces. These three vector fields are given by

$$\boldsymbol{C}_{(m,n)}(\theta,\phi)=P_n^{|m|}(\cos(\theta))\exp(im\phi)\boldsymbol{e}_r \tag{9.4.1.3}$$

$$\boldsymbol{A}_{(m,n)}(\theta,\phi)=\left[im\frac{P_n^{|m|}(\cos(\theta))}{\sin(\theta)}\boldsymbol{e}_\theta-\left(\frac{d}{d\theta}\right)P_n^{|m|}(\cos(\theta))\boldsymbol{e}_\phi\right]\exp(im\phi) \tag{9.4.1.4}$$

and

$$\boldsymbol{B}_{(m,n)}(\theta,\phi)=\left[\left(\frac{d}{d\theta}\right)P_n^{|m|}(\cos(\theta))\boldsymbol{e}_\theta+im\frac{P_n^{|m|}(\cos(\theta))}{\sin(\theta)}\boldsymbol{e}_\phi\right]\exp(im\phi) \tag{9.4.1.5}$$

The representation of the electric and magnetic fields stimulated by brain activity depends on the three curl operation identities (Cohoon [26]).

Theorem 9.1 *If $f(r)$ is any differentiable function of r, then*

$$\nabla\times(f(r)\boldsymbol{A}_{(m,n)}(\theta,\phi))=$$

$$n(n+1)\frac{f(r)}{r}\boldsymbol{C}_{(m,n)}(\theta,\phi)+\left[\frac{1}{r}\left(\frac{d}{dr}\right)(rf(r))\right]\boldsymbol{B}_{(m,n)}(\theta,\phi) \tag{9.4.1.6}$$

where the vector field $\boldsymbol{A}_{(m,n)}$ is defined by (9.4.1.4), the vector field $\boldsymbol{B}_{(m,n)}$ is defined by (9.4.1.5), and the vector field $\boldsymbol{C}_{(m,n)}$ is defined by (9.4.1.3) and the curl operator is given in spherical coordinates by

$$\nabla\times(E_r\boldsymbol{e}_r+E_\theta\boldsymbol{e}_\theta+E_\phi\boldsymbol{e}_\phi)=\frac{1}{r^2\sin(\theta)}\left\{\left[\left(\frac{\partial}{\partial\theta}\right)(r\sin(\theta)E_\phi)-\frac{\partial}{\partial\phi}(rE_\theta)\right]\boldsymbol{e}_r\right.$$

$$\left.+\quad r\left[\left(\frac{\partial}{\partial\phi}\right)E_r-\left(\frac{\partial}{\partial r}\right)(r\sin(\theta)E_\phi)\right]\boldsymbol{e}_\theta+r\sin(\theta)\left[\frac{\partial}{\partial r}(rE_\theta)-\left(\frac{\partial}{\partial\theta}\right)E_r\right]\boldsymbol{e}_\phi\right\} \tag{9.4.1.7}$$

Theorem 9.2 *If $g(r)$ is any differentiable function of r, then*

$$\nabla\times(g(r)\boldsymbol{B}_{(m,n)}(\theta,\phi))=\left[-\frac{1}{r}\left(\frac{d}{dr}\right)(rg(r))\right]\boldsymbol{A}_{(m,n)}(\theta,\phi) \tag{9.4.1.8}$$

where the vector field $\boldsymbol{A}_{(m,n)}$ is defined by (9.4.1.4), the vector field $\boldsymbol{B}_{(m,n)}$ is defined by (9.4.1.5), and the vector field $\boldsymbol{C}_{(m,n)}$ is defined by (9.4.1.3) and the curl operator is defined in spherical coordinates by (9.4.1.7).

Theorem 9.3 *For all differentiable functions $h(r)$*

$$\nabla \times (h(r)\boldsymbol{C}_{(m,n)}(\theta,\phi)) = \frac{h(r)}{r}\boldsymbol{A}_{(m,n)}(\theta,\phi) \tag{9.4.1.9}$$

where the curl is defined by (9.4.1.7), $\boldsymbol{C}_{(m,n)}$ is defined by (9.4.1.3), and $\boldsymbol{A}_{(m,n)}$ is defined by (9.4.1.4).

We define for all complex numbers z the relation

$$Z_n^{(\tilde{\ell})}(z) = \begin{cases} y_n(z) & \text{if} \quad \tilde{\ell} = -1 \\ j_n(z) & \text{if} \quad \tilde{\ell} = 0 \\ h_n^{(1)}(z) & \text{if} \quad \tilde{\ell} = 1 \\ h_n^{(2)}(z) & \text{if} \quad \tilde{\ell} = 2 \end{cases} \tag{9.4.1.10}$$

Related to $Z_n(z)$ we define the function $W_n(z)$ by

$$W_n^{(\tilde{\ell})}(z) = \frac{Z_n^{(\tilde{\ell})}(z)}{z} + \left(\frac{d}{dz}\right) Z_n^{(\tilde{\ell})}(z) \tag{9.4.1.11}$$

The functions $Z_n^{(\tilde{\ell})}(z)$ are used to define vector spherical harmonics needed to represent both brain wave signals and vector spherical harmonics needed to define interrogating vector fields.

A zero curl vector field used to represent the vector potential of brain activity (Hirvonen [59]) is

$$\boldsymbol{L}_{(n,p)}^{(m,\tilde{\ell},(-1)^{\ell}j\omega)} =$$

$$\left(\frac{d}{dz}\right) Z_n^{(\tilde{\ell})}(z) \mid_{z=k(p,(-1)^{\ell}j\omega)r} \boldsymbol{C}_{(m,n)}(\theta,\phi) + \left(\frac{Z_n^{(\tilde{\ell})}(k(p,(-1)^{\ell}j\omega)r)}{k(p,(-1)^{\ell}j\omega)r}\right) \boldsymbol{B}_{(m,n)}(\theta,\phi) \tag{9.4.1.12}$$

The following two vector fields are also needed (Hirvonen [59]) to describe the brain activity vector potential and are the only ones needed to represent the brain activity electric and magnetic fields.

The first vector field is a radial function multiplied by the vector field (9.4.1.4) and for us has the form

$$\boldsymbol{M}_{(n,p)}^{(m,\tilde{\ell},(-1)^{\ell}j\omega)} = Z_n^{(\tilde{\ell})}(k(p,(-1)^{\ell}j\omega)r)\boldsymbol{A}_{(m,n)}(\theta,\phi) \tag{9.4.1.13}$$

where $\boldsymbol{A}_{(m,n)}$ is given by (9.4.1.4), where $\ell = 1$ indicates a negative frequency, $\ell = 2$ a positive frequency, and $\tilde{\ell} = 0$ from equation (9.4.1.10) indicates that

$$Z_n^{(\tilde{\ell})}(k(p,(-1)^{\ell}j\omega)r) = Z_n^{(0)}(k(p,(-1)^{\ell}j\omega)r) = j_n(k(p,(-1)^{\ell}j\omega)r) \tag{9.4.1.14}$$

where in this relationship the function $Z_n^{(\tilde{\ell})}(k(p,(-1)^{\ell}j\omega)r)$ is defined by (9.4.1.10). The curl of this vector field is the propagation constant multiplied by the vector field

$$\boldsymbol{N}_{(n,p)}^{(m,\tilde{\ell},(-1)^{\ell}j\omega)} = n(n+1)\frac{Z_n^{(\tilde{\ell})}(k(p,(-1)^{\ell}j\omega)r)}{k(p,(-1)^{\ell}j\omega)r}\boldsymbol{C}_{(m,n)}(\theta,\phi) + W_n^{(\tilde{\ell})}(k(p,(-1)^{\ell}j\omega)r)\boldsymbol{B}_{(m,n)}(\theta,\phi) \tag{9.4.1.15}$$

where $W_n^{(\tilde{\ell})}(k(p,(-1)^{\ell}j\omega)r)$ is defined by (9.4.1.11). The curl of this vector field is the propagation constant times the previous vector field. Specifically

$$\nabla \times \left(\boldsymbol{N}_{(n,p)}^{(m,\tilde{\ell},(-1)^{\ell}j\omega)}\right) = k(p,(-1)^{\ell}j\omega)\boldsymbol{M}_{(n,p)}^{(m,\tilde{\ell},(-1)^{\ell}j\omega)} \tag{9.4.1.16}$$

and

$$\nabla \times \left(\boldsymbol{M}_{(n,p)}^{(m,\tilde{\ell},(-1)^{\ell}j\omega)}\right) = k(p,(-1)^{\ell}j\omega)\boldsymbol{N}_{(n,p)}^{(m,\tilde{\ell},(-1)^{\ell}j\omega)} \tag{9.4.1.17}$$

9.5 Full Maxwell Solver: Vector Spherical Harmonic Representation of Brain Wave Signals

Transmembrane currents inside the brain define a vector potential $\boldsymbol{A}$ that can, in turn, be used to define brain wave source magnetic and electric fields. Each brain wave stimulating transmembrane current is represented by a sum of sinusoids. We have used Hodgkin Huxley (Hogkin and Huxley [61]) and a modified Rinzel model (Wilson [131], Chapter 9) to represent the cortical neuron currents in our brain model.

Each site of brain activity defines a sum of vector potentials associated with each frequency component used to represent the transmembrane current at that site. Brain activity source electromagnetic fields are derived from this vector potential. These fields interact with tissue interfaces and some of the electromagnetic waves stimulated by brain activity are reflected back into the brain by the brain-skull interface. Of course, some of the electromagnetic fields generated by neuron activity propagate to the surface of the head and out into the air.

We begin with a dictionary of the meaning of symbols used to express the brain wave activity vector potentials.

q	an index defining a site of brain wave activity
$\boldsymbol{r}_q$	the vector location of the source of brain wave activity
r_q	the distance from the origin to $\boldsymbol{r}_q$
$\boldsymbol{r}$	the vector point where brain activity is observed
r	the distance from the origin to $\boldsymbol{r}$
ω	the smallest frequency component of a brain wave signal
j	a Fourier series index
$j\omega$	a Fourier series brain signal frequency component
μ_p	magnetic permeability of region p
$\mathrm{a}_{(q,j)}$	jth cosine Fourier coefficient at the qth location
$\mathrm{b}_{(q,j)}$	jth sine Fourier coefficient at the qth location
$\tilde{\alpha}_{(q,j)}$	complex Fourier coefficient multiple of $\exp(+ij\omega t)$ equal to $(\mathrm{a}_{(q,j)} - i\mathrm{b}_{(q,j)})/2$
$\tilde{\beta}_{(q,j)}$	complex Fourier coefficient multiple of $\exp(-ij\omega t)$ equal to $(\mathrm{a}_{(q,j)} + i\mathrm{b}_{(q,j)})/2$
p	a region index serving as a label for tissue electromagnetic properties
$\boldsymbol{A}_p$	total vector potential from sources in region p
t	the time at which the brain wave signal is observed
i	the square root of -1
$\exp(ij\omega t)$	the positive frequency time harmonic time variation of the jth component of the brain wave signal
$\exp(-ij\omega t)$	the conjugate time harmonic time variation of the jth component of the brain wave signal
ℓ	a frequency index with $\ell = 2$ indicating an $\exp(+j\omega t)$ frequency component, and $\ell = 1$ indicating an $\exp(-j\omega t)$ frequency component
$\boldsymbol{A}_{(p,q)}(\ell, (-1)^\ell j\omega, t)$	vector potential component from frequency component $\exp((-1)^\ell j\omega t)$ at location q in region p
C	neuronal transmembrane capacitance
V	neuronal transmembrane voltage
I(t)	neuronal transmembrane current

9.5.1 Transmembrane Current Orientation and Vector Field Notation

We need to describe in detail the transmembrane current orientation and expressions needed to define the vector potentials at the brain activity sites. This is found in the following table

$\boldsymbol{e}_x$	unit vector perpendicular to Cartesian coordinate plane x=0
$\boldsymbol{e}_y$	unit vector perpendicular to Cartesian coordinate plane y=0
$\boldsymbol{e}_z$	unit vector perpendicular to Cartesian coordinate plane z=0
$\boldsymbol{e}_q$	the transmembrane current orientation at the brain activity site at $\boldsymbol{r}_q$ with index q
d_q	the distance from the brain activity site $\boldsymbol{r}_q$ to the observation point at $\boldsymbol{r}$
(r_q, θ_q, ϕ_q)	the brain activity site in spherical coordinates
(r, θ, ϕ)	the observation point in spherical coordinates
$\boldsymbol{e}_r$	the unit vector perpendicular to the surface r = a constant
$\boldsymbol{e}_\theta$	the unit vector perpendicular to the surface θ = a constant
$\boldsymbol{e}_\phi$	the unit vector perpendicular to the surface ϕ = a constant
(U_q, V_q, W_q)	the Cartesian coordinates of transmembrane current orientation at the brain activity site with index q at location $\boldsymbol{r}_q$
$c(n, m, \tilde{\ell}, (-1)^\ell j\omega, p, q)$	addition theorem expansion coefficient of degree n and order m with frequency $j\omega$ in region p at the site with index q
$P_n^m(\cos(\theta_q))$	Associated Legendre function of degree n and order m at $\cos(\theta_q)$
$k(p, (-1)^\ell j\omega)$	the complex propagation constant in region p of the brain wave signal component with time harmonic time variation $\exp((-1)^\ell j\omega t)$
$\epsilon(p, (-1)^\ell j\omega)$	the electromagnetic permittivity in region p associated with the time harmonic time variation of the form $\exp((-1)^\ell j\omega t)$
$j_n(z)$	the spherical Bessel function of index n evaluated at the the complex number z equal to the product of the propagation constant $k(p, (-1)^\ell j\omega)$ and r_q
$h_n^{(\tilde{\ell})}(\zeta)$	the spherical Hankel function of type $\tilde{\ell}$ at the complex number ζ where $\tilde{\ell}$ is 1 or 2

The solution of our boundary value problem requires consideration of the transmission, absorption, and reflection of electromagnetic waves stimulated by brain activity. Our notation for the vector fields and expansion coefficients used in representing this solution is given in the following table.

$\boldsymbol{H}_{source}$	the vector magnetic field stimulated by all brain activity sources
$\boldsymbol{E}_{source}$	the vector electric field stimulated by all brain activity sources
$\boldsymbol{H}_{external}$	the vector magnetic field outside the head determined by solving the electromagnetic boundary value problem which includes reflection of source fields off of and transmission of source fields through all tissue interfaces
$\boldsymbol{E}_{external}$	the predicted vector electric field outside the head stimulated by brain activity
n	the order of the spherical Bessel or Hankel functions and the degree of the associated Legendre functions used to represent the spatial variation of the brain wave signals
m	the order of the associated Legendre functions used to represent the the variation of the brain wave signal over the head surface and outside the head
$\tilde{\ell}$	the type of the spherical Bessel or Hankel function used to describe the radial variation of the brain wave electromagnetic fields with $\tilde{\ell} = 0$ indicating the spherical Bessel function j_n and $\tilde{\ell} = 1$ for the spherical Hankel function $h_n^{(1)}$ and $\tilde{\ell} = 2$ for $h_n^{(2)}$
$\boldsymbol{M}_{(n,p)}^{(m,\tilde{\ell},(-1)^{\ell}j\omega)}$	the primary vector spherical harmonic in region p associated with the time dependence $\exp((-1)^{\ell}j\omega t)$
$\boldsymbol{N}_{(n,p)}^{(m,\tilde{\ell},(-1)^{\ell}j\omega)}$	the derived vector spherical harmonic in region p associated with the time dependence $\exp((-1)^{\ell}j\omega t)$

We next describe the expansion coefficients that are multipliers of the vector fields in the previous table.

$\tilde{\mathrm{a}}_{(m,n,q)}^{(p,\ell,(-1)^\ell j\omega))}$	the source expansion coefficient multiplier of $\boldsymbol{M}_{(n,p)}^{(m,\ell,(-1)^\ell j\omega)}$ in the representation of the brain wave source magnetic field
$\tilde{\mathrm{b}}_{(m,n,q)}^{(p,\ell,(-1)^\ell j\omega)}$	the source expansion coefficient multiplier of $\boldsymbol{N}_{(n,p)}^{(m,\ell,(-1)^\ell j\omega)}$ in the representation of the brain wave source magnetic field
$\alpha_{(m,n,q)}^{(p,0,(-1)^\ell j\omega))}$	the expansion coefficient multiplier of $\boldsymbol{M}_{(n,p)}^{(m,0,(-1)^\ell j\omega)}$ representing brain wave radiation reflected from tissue interfaces where the $\tilde{\ell}=0$ in the superscript signifies that we use the nonsingular spherical Bessel functions and their derivatives in the vector field instead of spherical Hankel functions
$\beta_{(m,n,q)}^{(p,0,(-1)^\ell j\omega)}$	the expansion coefficient multiplier of $\boldsymbol{N}_{(n,p)}^{(m,0,(-1)^\ell j\omega)}$ representing brain wave radiation reflected from tissue interfaces in the brain tissue reflected magnetic field expansion
$\mathrm{a}_{(m,n,q)}^{(p+2,\ell,(-1)^\ell j\omega))}$	the external $\boldsymbol{H}$ expansion coefficient multiplier of $\boldsymbol{M}_{(n,p+2)}^{(m,\ell,(-1)^\ell j\omega)}$
$\mathrm{b}_{(m,n,q)}^{(p+2,\ell,(-1)^\ell j\omega))}$	the external $\boldsymbol{H}$ expansion coefficient multiplier of $\boldsymbol{N}_{(n,p+2)}^{(m,\ell,(-1)^\ell j\omega)}$

9.5.2 The Permittivity $\epsilon(p,(-1)^{\ell}j\omega)$, Propagation Constants $k(p,(-1)^{\ell}j\omega)$, and Addition Theorem Expansion Coefficients $c(n,m,\tilde{\ell},(-1)^{\ell}j\omega,p,q)$ Associated with the Exact Analytical and Hirvonen ([59]) Expansion Representations of the Vector Potential, Electric and Magnetic Fields and Dynamic Voltage from Brain Activity

The complex brain tissue permittivity $\epsilon(p,(-1)^{\ell}j\omega)$ defines the brain wave propagation constant $k(p,(-1)^{\ell}j\omega)$ in terms of the frequency ω and the magnetic permeability μ_p by the relationship

$$k(p,(-1)^{\ell}j\omega)^2 = \omega^2\mu_p\epsilon(p,(-1)^{\ell}j\omega) \tag{9.5.2.1}$$

The addition theorem expansion coefficient at the qth site $\boldsymbol{r}_q$ of brain activity in region p with degree n and order m is given by for the vector potential $\boldsymbol{A}_{(p,q)}$ is given for $\tilde{\ell}$ equal to zero by

$$c(n,m,\tilde{\ell},(-1)^{\ell}j\omega,p,q) =$$

$$\left(\frac{(n-\mid m\mid)!}{(n+\mid m\mid)!}\right) Z_n^{(\tilde{\ell})}(k(p,(-1)^{\ell}j\omega)r_q)P_n^{|m|}(\cos(\theta_q))\exp(-im\phi_q) \tag{9.5.2.2}$$

where if $\tilde{\ell}$ is zero $Z_n^{(\tilde{\ell})}(z)$ is the spherical Bessel function $j_n(z)$. Definition (9.5.2.2) and the addition theorem tells us that

$$h_0^{(\tilde{\ell})}(k(p,(-1)^{\ell}j\omega)d_q) = \frac{\exp(-(-1)^{\tilde{\ell}}ik(p,(-1)^{\ell}j\omega)d_q)}{-(-1)^{\tilde{\ell}}ik(p,(-1)^{\ell}j\omega)d_q)}$$

$$= \sum_{n=0}^{\infty}(2n+1)\sum_{m=-n}^{m=+n} c(n,m,0,(-1)^{\ell}j\omega,p,q)P_n^{|m|}(\cos(\theta))\exp(im\phi)h_n^{(\ell)}(k(p,(-1)^{\ell}j\omega)r) \tag{9.5.2.3}$$

The vector potential to be expanded using this addition theorem is

$$\boldsymbol{A}_{(p,q)}(\tilde{\ell},(-1)^{\ell}j\omega,t) = \left(\frac{\mu_p\exp(i(-1)^{\ell}j\omega t)}{4\pi}\right)\frac{\exp(-i(-1)^{\tilde{\ell}}k(p,(-1)^{\ell}j\omega)\mid \boldsymbol{r}-\boldsymbol{r}_q\mid)}{\mid \boldsymbol{r}-\boldsymbol{r}_q\mid}\boldsymbol{e}_q \tag{9.5.2.4}$$

where d_q is $\mid \boldsymbol{r}-\boldsymbol{r}_q \mid$ or the distance from the brain activity site $\boldsymbol{r}_q$ to the observation point $\boldsymbol{r}$ and the brain activity current direction at the site q of potential activity is

$$\boldsymbol{e}_q = U_q\boldsymbol{e}_x + V_q\boldsymbol{e}_y + W_q\boldsymbol{e}_z \tag{9.5.2.5}$$

The transmembrane current direction $\boldsymbol{e}_q$ given by (9.5.2.5) and used in (9.5.2.4) also has the spherical coordinate representation

$$\begin{aligned}\boldsymbol{e}_q = U_q\left[\sin(\theta)\cos(\phi)\boldsymbol{e}_r + \cos(\theta)\cos(\phi)\boldsymbol{e}_\theta - \sin(\phi)\boldsymbol{e}_\phi\right]\\ +V_q\left[\sin(\theta)\sin(\phi)\boldsymbol{e}_r + \cos(\theta)\sin(\phi)\boldsymbol{e}_\theta + \cos(\phi)\boldsymbol{e}_\phi\right]\\ +W_q\left[\cos(\theta)\boldsymbol{e}_r - \sin(\theta)\boldsymbol{e}_\theta\right]\end{aligned} \tag{9.5.2.6}$$

Making the subsitutions

$$(\cos(\phi),\sin(\phi)) = \left(\frac{\exp(i\phi)+\exp(-i\phi)}{2},\frac{\exp(i\phi)-\exp(-i\phi)}{2i}\right) \tag{9.5.2.7}$$

into (9.5.2.6) we have

$$\begin{aligned}\boldsymbol{e}_q = \left(\frac{U_q - iV_q}{2}\right)\left[\sin(\theta)\exp(i\phi)\boldsymbol{e}_r + \cos(\theta)\exp(i\phi)\boldsymbol{e}_\theta + i\exp(i\phi)\boldsymbol{e}_\phi\right]\\ +\left(\frac{U_q + iV_q}{2}\right)\left[\sin(\theta)\exp(-i\phi)\boldsymbol{e}_r + \cos(\theta)\exp(-i\phi)\boldsymbol{e}_\theta - i\exp(-i\phi)\boldsymbol{e}_\phi\right]\\ +W_q\left[\cos(\theta)\boldsymbol{e}_r - \sin(\theta)\boldsymbol{e}_\theta\right]\end{aligned} \tag{9.5.2.8}$$

Using the definition of the spherical Hankel functions we have

$$\boldsymbol{A}_{(p,q)}(\tilde{\ell},(-1)^{\ell}j\omega,t) =$$

$$= \left(\mu_p\frac{\exp(i(-1)^{\ell}j\omega t)}{4\pi}\right)\left\{-(-1)^{\tilde{\ell}}ik(p,(-1)^{\ell}j\omega)\right\}\frac{\exp(-(-1)^{\tilde{\ell}}ik(p,(-1)^{\ell}j\omega)\mid \boldsymbol{r}-\boldsymbol{r}_q\mid)}{\left\{-(-1)^{\tilde{\ell}}ik(p,(-1)^{\ell}j\omega)\right\}\mid \boldsymbol{r}-\boldsymbol{r}_q\mid}$$

$$= \mu_p\left(\frac{\exp(i(-1)^{\ell}j\omega t)}{4\pi}\right)\left\{-(-1)^{\tilde{\ell}}ik(p,(-1)^{\ell}j\omega)\right\}h_0^{(\tilde{\ell})}(k(p,(-1)^{\ell}j\omega)\mid \boldsymbol{r}-\boldsymbol{r}_q\mid)\boldsymbol{e}_q \tag{9.5.2.9}$$

because if $\tilde{\ell}$ is 1 or 2, then $h_0^{(\tilde{\ell})}(z)$ is $\exp(-(-1)^{\tilde{\ell}}iz)$ divided by $-(-1)^{\tilde{\ell}}iz$.

9.5.3 Representing the Vector Potential from Brain Activity in terms of Vector Spherical Harmonics

In order to describe the transmission of electromagnetic waves from brain activity through the skull bone, we must solve the associated electromagnetic boundary value problem.

Using the definition (9.5.2.2) for $\tilde{\ell}$ equal to 0, we see that vector potential (9.5.2.4) arising from the frequency component

$$t \to \exp(i(-1)^{\ell} j\omega t) \tag{9.5.3.1}$$

at site q in region p has the vector spherical harmonic expansion

$$\boldsymbol{A}_{(p,q)}(\tilde{\ell}, (-1)^{\ell} j\omega, t)) =$$

$$\left(\frac{\mu_p(-(-1)^{\tilde{\ell}} ik(p,(-1)^{\ell} j\omega)\exp(i(-1)^{\ell} j\omega t)}{4\pi}\right) \sum_{n=0}^{\infty} \sum_{m=-n}^{m=+n} \left\{ c(n,m,0,(-1)^{\ell} j\omega, p, q) \left\{ \right.\right.$$

$$W_q \left\{ (n-m+1)\left(\boldsymbol{L}_{(n+1,p)}^{(m,\tilde{\ell},(-1)^{\ell} j\omega)} + \frac{1}{n+1}\boldsymbol{N}_{(n+1,p)}^{(m,\tilde{\ell},(-1)^{\ell} j\omega)}\right) \right.$$

$$-(n+m)\left(\boldsymbol{L}_{(n-1,p)}^{(m,\tilde{\ell},(-1)^{\ell} j\omega)} - \frac{1}{n}\boldsymbol{N}_{(n-1,p)}^{(m,\tilde{\ell},(-1)^{\ell} j\omega)}\right) + im\left(\frac{2n+1}{n(n+1)}\right)\boldsymbol{M}_{(n,p)}^{(m,\tilde{\ell},(-1)^{\ell} j\omega)} \Big\}$$

$$+\left(\frac{U_q - iV_q}{2}\right)\left\{\left(\boldsymbol{L}_{(n+1,p)}^{(m+1,\tilde{\ell},(-1)^{\ell} j\omega)} + \frac{1}{n+1}\boldsymbol{N}_{(n+1,p)}^{(m+1,\tilde{\ell},(-1)^{\ell} j\omega)}\right)\right.$$

$$\left. + \left(\boldsymbol{L}_{(n-1,p)}^{(m+1,\tilde{\ell},(-1)^{\ell} j\omega)} - \frac{1}{n}\boldsymbol{N}_{(n-1,p)}^{(m+1,\tilde{\ell},(-1)^{\ell} j\omega)}\right) - i\left(\frac{(2n+1)}{n(n+1)}\right)\boldsymbol{M}_{(n,p)}^{(m+1,\tilde{\ell},(-1)^{\ell} j\omega)}\right\}$$

$$-\left(\frac{U_q + iV_q}{2}\right)\left\{(n-m+1)(n-m+2)\left(\boldsymbol{L}_{(n+1,p)}^{(m-1,\tilde{\ell},(-1)^{\ell} j\omega)} + \frac{1}{n+1}\boldsymbol{N}_{(n+1,p)}^{(m-1,\tilde{\ell},(-1)^{\ell} j\omega)}\right)\right.$$

$$+(n+m)(n+m-1)\left(\boldsymbol{L}_{(n-1,p)}^{(m-1,\tilde{\ell},(-1)^{\ell} j\omega)} - \frac{1}{n}\boldsymbol{N}_{(n-1,p)}^{(m-1,\tilde{\ell},(-1)^{\ell} j\omega)}\right)$$

$$\left.\left.\left. +(n+m)(n-m+1)\left(\frac{i(2n+1)}{n(n+1)}\right)\boldsymbol{M}_{(n,p)}^{(m-1,\tilde{\ell},(-1)^{\ell} j\omega)}\right\}\right\}\right\} \tag{9.5.3.2}$$

where the three vector fields are defined by (9.4.1.12), (9.4.1.13), and (9.4.1.15). An equivalent expression is found in Hirvonen ([59]). We need this representation in order to solve the electromagnetic boundary value problem. Considering (9.5.2.5) the W_q term is the contribution from a vertical dipole. We used this term and the fact that a rotation of coordinates will make any dipole vertical in our analysis.

9.5.4 The Vector Potential from all Sources

The total vector potential from all sources has the form

$$\boldsymbol{A}_p = \sum_{q=1}^{Q} \left\{ \boldsymbol{A}_{(p,q)}(\tilde{\ell}, (-1)^{\ell} j\omega, t)) \right\} \tag{9.5.4.1}$$

where $\boldsymbol{A}_{(p,q)}(\tilde{\ell}, (-1)^{\ell} j\omega, t))$ is expressed in terms of the three vector spherical harmonics

$$(n, m, p, \tilde{\ell}, (-1)^{\ell}(j\omega)) \rightarrow (\boldsymbol{L}_{(n,p)}^{(m,\tilde{\ell},(-1)^{\ell} j\omega)}, \boldsymbol{M}_{(n,p)}^{(m,\tilde{\ell},(-1)^{\ell} j\omega)}, \boldsymbol{N}_{(n,p)}^{(m,\tilde{\ell},(-1)^{\ell} j\omega)}) \tag{9.5.4.2}$$

by (9.5.3.2). Note that these three vector fields used in the expansion defined by (9.5.3.2) and (9.5.4.1) are independent of the set of locations of the dipoles. Thus, we may collect coefficients in the sum of the expansions (9.5.3.2) represented by (9.5.4.1) depending on the dipoles in the sum. For the Hirvonen ([59]) expansion of the vector potential of brain activity there is a known relationship between multipliers of the zero curl vector fields (9.4.1.12)

$$n \rightarrow \boldsymbol{L}_{(n-1,p)}^{(m-1,\tilde{\ell},(-1)^{\ell} j\omega)} \tag{9.5.4.3}$$

and the multipliers of the non zero curl vector fields (9.4.1.12). If we can go backwards from $\boldsymbol{H}$ to the multipliers of the nonzero curl vector fields and recover the multipliers of the zero curl vector fields and consequently recover the vector potential of brain activity. For, this specific type of magnetic field, we can go back to the vector potential. We could always add any zero curl vector field (9.4.1.12) and have two different vector potentials that gave the same magnetic field.

9.6 The Full Wave Solution Boundary Value Problem

We rearrange terms in the expansion of the vector potential (9.5.3.2) describing brain activity so that the representations of the source electric and magnetic vector are identical to the representation used in (Cohoon [26]). While this works formally, considerable effort had to be taken to merge the expansion coefficients of the vector potential described in the following section with coefficients that represent the fields outside the head in order to accurately represent the electromagnetic fields outside the head arising from sources close to the skull bone. This was made possible by the special function program of Morris ([85]).

9.6.1 Expansion in Vector Spherical Harmonics

We derive a brain-activity source magnetic field by computing the curl of the vector potential from all sources for each frequency component. The source electric field is derived through Maxwell's equations from the curl of the magnetic vector. Through a change of indices in the sum, we put the source magnetic field in exactly the same form that is given in Cohoon ([26]). This solution is then used to solve the boundary value problem using the same transition matrices described in Cohoon ([26]) to relate representation in adjacent tissue layers by requiring that tangential components of $\boldsymbol{E}$ and $\boldsymbol{H}$ be continuous across tissue interfaces.

An addition theorem expansion factor that appears in the representation of the vector potential, the magnetic field, and the electric field is

$$c(n, m, \overline{\ell}, (-1)^{\ell} j\omega, p, q) =$$

$$\left(\frac{(n- \mid m \mid)!}{(n+ \mid m \mid)!}\right) Z_n^{(\overline{\ell})}(k(p, (-1)^{\ell} j\omega) r_q) P_n^{|m|}(\cos(\theta_q)) \exp(-im\phi_q) \tag{9.6.1.1}$$

where the parameters

$$q \rightarrow (r_q, \theta_q, \phi_q) \tag{9.6.1.2}$$

define the location of the qth brain activity site in spherical coordinates, $Z_n^{(\overline{\ell})}$ is defined by (9.4.1.10) and $P_n^{|m|}$ is the nonsingular associated Legendre function satisfying (9.4.1.2).

9.6.2 Solution of the Boundary Value Problem

We predict the brain wave electric and magnetic fields that are reflected back into the brain from tissue interfaces and which are transmitted outside the head one $j\omega$ frequency at a time where ω is the smallest positive frequency in the Fourier series used to represent the brain wave signal and $j\omega$ and $-j\omega$ are the positive and negative frequencies associated with the jth Fourier series index. We do this by requiring that tangential components of the electric and magnetic vectors are continuous across tissue interfaces.

The source field expansion coefficients are determined from just the representation of the brain wave source magnetic field in terms of vector spherical harmonics.

The brain activity source field expansion coefficients depend upon the tissue region index p, the index ℓ ranging from 1 to 2, the Fourier series index j (so that $\ell = 1$ means that the time dependence of the frequency component being considered has the form

$$t \to \exp(-ij\omega t) \tag{9.6.2.1}$$

and $\ell = 2$ means that the time dependence of the brain wave frequency component being considered has the form

$$t \to \exp(+ij\omega t), \tag{9.6.2.2}$$

the m is used to represent the spatial variation of the brain wave magnetic field with the equatorial angle ϕ and the index n used to represent the spatial variation of the brain wave magnetic field as a function of $\cos(\theta)$ where θ ranges from 0 at the North pole to 180 degrees at the South pole of the bench mark model. The source expansion coefficients representing the total source should have the form

$$(m, n, p, \ell, j) \to \left(\tilde{\mathrm{a}}_{(m,n)}^{(p,\ell,(-1)^\ell j\omega)}, \tilde{b}_{(m,n,q)}^{(p,\ell,(-1)^\ell j\omega)}\right) \tag{9.6.2.3}$$

To get these source coefficients we add up the contributions from source coefficients for each source location, q, so that the individual contributions are from source expansion coefficients

$$(m, n, q, p, \ell, j) \to \left(\tilde{\mathrm{a}}_{(m,n,q)}^{(p,\ell,(-1)^\ell j\omega)}, \tilde{b}_{(m,n,q)}^{(p,\ell,(-1)^\ell j\omega)}\right) \tag{9.6.2.4}$$

noting that the source expansion coefficients

$$(m, n, q, p, \ell, j) \to \tilde{\mathrm{a}}_{(m,n,q)}^{(p,\ell,(-1)^\ell j\omega)}, \tag{9.6.2.5}$$

using $\tilde{\ell} = \ell$, for each brain wave source location q are multipliers of the vector spherical harmonic

$$(n, p, m, \tilde{\ell}, (-1)^\ell j\omega) \to \boldsymbol{M}_{(n,p)}^{(m,\tilde{\ell},(-1)^\ell j\omega)} \tag{9.6.2.6}$$

Similarly, again for each brain wave source location index q, the source expansion coefficient

$$(m, n, q, p, \ell, (-1)^\ell j\omega) \to \tilde{b}_{(m,n,q)}^{(p,\ell,(-1)^\ell j\omega)}, \tag{9.6.2.7}$$

using $\tilde{\ell} = \ell$, are multipliers of the vector spherical harmonic

$$(n, p, m, \tilde{\ell}, (-1)^\ell j\omega) \to \boldsymbol{N}_{(n,p)}^{(m,\tilde{\ell},(-1)^\ell j\omega)} \tag{9.6.2.8}$$

By requiring that the correct boundary conditions are satisfied across tissue interfaces, the program predicts the total electric and magnetic vectors inside and outside the head arising from the brain activity.

The source electromagnetic fields have an alternative representation in terms of vector spherical harmonics. The source magnetic field is given by

$$\boldsymbol{H}_{source} = \sum_{j=1}^{\infty}\sum_{\ell=1}^{2}\sum_{n=0}^{\infty}\sum_{m=-n}^{m=+n}\Bigg\{$$

$$\tilde{\mathrm{a}}_{(m,n)}^{(p,\ell,(-1)^{\ell}j\omega)}\boldsymbol{M}_{(n,p)}^{(m,\ell,(-1)^{\ell}j\omega)} + \tilde{\mathrm{b}}_{(m,n)}^{(p,\ell,(-1)^{\ell}j\omega)}\boldsymbol{N}_{(n,p)}^{(m,\ell,(-1)^{\ell}j\omega)} \Bigg\} \tag{9.6.2.9}$$

The brain wave source field expansion coefficients

$$(m,n,p,\ell,j(-1)^{\ell}\omega) \rightarrow \left(\tilde{\mathrm{a}}_{(m,n)}^{(p,\ell,(-1)^{\ell}j\omega)}, \tilde{\mathrm{b}}_{(m,n)}^{(p,\ell,(-1)^{\ell}j\omega)}\right) \tag{9.6.2.10}$$

have all been determined by exact formulae from representation of the vector potentials of the sources in terms of the vector spherical harmonics

$$(n,p,m,\tilde{\ell},(-1)^{\ell}j\omega) \rightarrow \left(\boldsymbol{M}_{(n,p)}^{(m,\tilde{\ell},(-1)^{\ell}j\omega)}, \boldsymbol{N}_{(n,p)}^{(m,\tilde{\ell},(-1)^{\ell}j\omega)}\right) \tag{9.6.2.11}$$

The source electric and magnetic fields interact with tissue interfaces producing a signal that is regular everywhere in the interior of the brain. The magnetic field arising from this has the $\tilde{\ell} = 0$ representation

$$\boldsymbol{H}_{reflected} = \sum_{j=1}^{\infty}\sum_{\ell=1}^{2}\sum_{n=0}^{\infty}\sum_{m=-n}^{m=+n}\Bigg\{$$

$$\alpha_{(m,n)}^{(p,0,(-1)^{\ell}j\omega)}\boldsymbol{M}_{(n,p)}^{(m,0,(-1)^{\ell}j\omega)} + \beta_{(m,n)}^{(p,0,(-1)^{\ell}j\omega)}\boldsymbol{N}_{(n,p)}^{(m,0,(-1)^{\ell}j\omega)} \Bigg\} \tag{9.6.2.12}$$

where the 0 in the superscripts in the above equation indicate that the spherical Bessel functions

$$(n,(-1)^{\ell}j\omega,r) \rightarrow j_n(k(p,(-1)^{\ell}j\omega)r) \tag{9.6.2.13}$$

and their derivatives are used in the vector spherical harmonics rather than the spherical Hankel functions

$$(n,\tilde{\ell},(-1)^{\ell}j\omega,r) \rightarrow (h_n^{(\tilde{\ell})}(k(p,(-1)^{\ell}j\omega)r)), \tag{9.6.2.14}$$

using $\tilde{\ell} = \ell$ for ℓ equal to 1 or 2, and their derivatives. The back reflected radiation must be a smooth function at all interior points in the brain and use the $\tilde{\ell} = 0$ vector spherical harmonics. The expansion coefficients here are represented in terms of the known source expansion coefficients by requiring that the tangential components of electric and magnetic field vectors be continuous across tissue interfaces.

Similarly, instead of using vector potentials, we have an alternative representation of the source electric field as

$$\boldsymbol{E}_{source} = \sum_{j=1}^{\infty}\sum_{\ell=1}^{2}\sum_{n=0}^{\infty}\sum_{m=-n}^{m=+n}\Bigg\{$$

$$\left(\frac{k(p,(-1)^{\ell}j\omega)}{(i(-1)^{\ell}\epsilon(p,(-1)^{\ell}j\omega)}\right)\left\{\tilde{\mathrm{a}}_{(m,n)}^{(p,\ell,(-1)^{\ell}j\omega)}\boldsymbol{N}_{(n,p)}^{(m,\ell,(-1)^{\ell}j\omega)} + \tilde{\mathrm{b}}_{(m,n)}^{(p,\ell,(-1)^{\ell}j\omega)}\boldsymbol{M}_{(n,p)}^{(m,\ell,(-1)^{\ell}j\omega)}\right\}\Bigg\} \tag{9.6.2.15}$$

The magnetic vector and electric fields outside the head are given by

$$(x,y,z) \rightarrow (\boldsymbol{H}_{external}, \boldsymbol{E}_{external}) \tag{9.6.2.16}$$

measured at a point (x,y,z) outside the head for a two layer model with p=1 for a source of electrical activity in the brain itself is represented by expansion coefficients of the form

$$(m,n,p,\ell,j\omega) \rightarrow \left(\mathrm{a}_{(m,n)}^{(p+2,\ell,(-1)^{\ell}j\omega)}, b_{(m,n)}^{(p+2,\ell,(-1)^{\ell}j\omega)}\right) \tag{9.6.2.17}$$

The total magnetic field outside the head in terms of our vector spherical harmonics has the form

$$\boldsymbol{H}_{external} = \sum_{j=1}^{\infty}\sum_{\ell=1}^{2}\sum_{n=0}^{\infty}\sum_{m=-n}^{m=+n}\Bigg\{$$

$$\mathrm{a}_{(m,n)}^{(p+2,\ell,(-1)^{\ell}j\omega)}\boldsymbol{M}_{(n,p+2)}^{(m,\ell,(-1)^{\ell}j\omega)} + b_{(m,n)}^{(p+2,\ell,(-1)^{\ell}j\omega)}\boldsymbol{N}_{(n,p+2)}^{(m,\ell,(-1)^{\ell}j\omega)}\Bigg\} \tag{9.6.2.18}$$

The total electric field outside the head from all sources has the form

$$\boldsymbol{E}_{external} = \sum_{j=1}^{\infty}\sum_{\ell=1}^{2}\sum_{n=0}^{\infty}\sum_{m=-n}^{m=+n}\Bigg\{$$

$$\left(\frac{k(p+2,(-1)^{\ell}j\omega)}{(i(-1)^{\ell}\epsilon(p+2,(-1)^{\ell}j\omega)}\right)[\mathrm{a}_{(m,n)}^{(p+2,\ell,(-1)^{\ell}j\omega)}\boldsymbol{N}_{(n,p+2)}^{(m,\ell,(-1)^{\ell}j\omega)} + b_{(m,n)}^{(p+2,\ell,(-1)^{\ell}j\omega)}\boldsymbol{M}_{(n,p+2)}^{(m,\ell,(-1)^{\ell}j\omega)}]\Bigg\} \tag{9.6.2.19}$$

where $p+2$ is the index for the region outside the head, and where the vector spherical harmonics were selected so that the action of the curl operator, appearing the Maxwell equations, satisfies

$$\nabla \times (\boldsymbol{M}_{(n,p)}^{(m,\tilde{\ell},(-1)^{\ell}j\omega)}) = k(p,(-1)^{\ell}j\omega)\boldsymbol{N}_{(n,p)}^{(m,\tilde{\ell},(-1)^{\ell}j\omega)} \tag{9.6.2.20}$$

and

$$\nabla \times (\boldsymbol{N}_{(n,p)}^{(m,\tilde{\ell},(-1)^{\ell}j\omega)}) = k(p,(-1)^{\ell}j\omega)\boldsymbol{M}_{(n,p)}^{(m,\tilde{\ell},(-1)^{\ell}j\omega)} \tag{9.6.2.21}$$

When these conditions are satisfied, linear combinations of these vector fields as m and n vary automatically satisfy the Maxwell equations of electromagnetic theory for a time dependence of the form

$$t \to \exp(i(-1)^{\ell} j\omega t) \tag{9.6.2.22}$$

In solving the brain wave signal boundary value problem we require continuity of tangential components of electric and magnetic vectors across tissue interfaces. We derived in (Cohoon [26]) 2 by 2 transition matrices with low round off error exact formula inverses that depend only on the spherical Bessel function order, n, and not on the Legendre function order,m. One set of transition matrices gives two equations in the two unknowns

$$(p, n, m, (-1)^{\ell} j\omega) \to \left(\mathrm{a}_{(m,n)}^{(p+2,\ell,(-1)^{\ell} j\omega)}, \alpha_{(m,n)}^{(p,0,(-1)^{\ell} j\omega)} \right) \tag{9.6.2.23}$$

Again, just requiring continuity of tangential components of total $\boldsymbol{H}$ and $\boldsymbol{E}$ across tissue interfaces we obtain a set of two by two transition matrices just depending on the spherical Bessel function order n and completely independent of the associated Legendre function order m which give us two equations in the two unknowns

$$(p, n, m, (-1)^{\ell} j\omega) \to \left(\mathrm{b}_{(m,n)}^{(p+2,\ell,(-1)^{\ell} j\omega)}, \beta_{(m,n)}^{(p,0,(-1)^{\ell} j\omega)} \right) \tag{9.6.2.24}$$

This gives us complete knowledge of the electric vector $\boldsymbol{E}$ and the magnetic vector $\boldsymbol{H}$ inside and outside our model of the head. This will be use to test brain wave vector of activity recovery algorithms that are valid for physiologically realistic models of the human head.

9.7 Recovery of Brain Activity – Inverse Source Solution

We consider the problem of interrogating the electromagnetic waves from brain activity that are transmitted through the skull bone so that we may directly recovery both the orientation of the sources and the profile of activity on the sources.

9.7.1 Construction of the Interrogating Vector Fields

We construct an infinite family of interrogating vector fields $\boldsymbol{M}$ and which along with $\nabla \times (\boldsymbol{M})$ satisfy in each tissue region the vector Helmholtz equation

$$\Delta \boldsymbol{M} + k^2 \boldsymbol{M} = \boldsymbol{0} \tag{9.7.1.1}$$

where $\boldsymbol{0}$ is the zero vector field and the Laplace operator, Δ, satisfies

$$\Delta \boldsymbol{F} = \nabla \times (-\nabla \times (\boldsymbol{F})) + \nabla(+\nabla \cdot (\boldsymbol{F})) = \left(\frac{\partial^2}{\partial x^2} + \frac{\partial^2}{\partial y^2} + \frac{\partial^2}{\partial z^2} \right) \boldsymbol{F} \tag{9.7.1.2}$$

The interrogating vector fields $\boldsymbol{M}$, besides satisfying the vector Helmholtz equation (9.7.1.1) also satisfy the additional property that $\boldsymbol{M}$ and $\nabla \times (\boldsymbol{M})$ are continuous across tissue interfaces.

We consider two classes of interrogating vector fields. The $I_M = 1$ interrogating vector field within the brain has the form which is a spherical Bessel function multiplied by the vector field (9.4.1.4), the nonradial component of its curl is a multiple of the vector field (9.4.1.5). The vector field $\boldsymbol{N}_{(n,p)}^{(m,\tilde{\ell},(-1)^{\ell}j\omega)}$ is an $I_M = 2$ interrogating vector field in brain tissue when $\tilde{\ell} = 0$. If you apply the curl operator to either of these interrogating vector fields, the result will be the propagation constant multiplied by the other interrogating vector field.

For $I_M = 1$ the interrogating vector field in brain tissue, tissue region p, is smooth at all points in the brain and is given by

$$\boldsymbol{M}_{(p,1)} = \boldsymbol{M}_{(n,p)}^{(m,0,(-1)^{\ell}j\omega)} = j_n(k(p,(-1)^{\ell}j\omega)r)\boldsymbol{A}_{(m,n)}(\theta,\phi) \tag{9.7.1.3}$$

In the skull bone region the interrogating vector field has another form in order to assure that both the vector field and its curl are continuous across the tissue interface the interrogating vector field, in tissue region $p+1$ we avoid $r = 0$ so that the smooth $\boldsymbol{M}$ vector field in the bone region, the $I_M = 1$ vector field has the form

$$\boldsymbol{M}_{(p+1,1)} == \boldsymbol{M}(\tilde{\mathrm{a}} - \tilde{\alpha}, m, n, p+1, \ell, (-1)^{\ell}j\omega) =$$

$$\tilde{\mathrm{a}}_{(m,n)}^{(p+1,0,(-1)^{\ell}j\omega)}\boldsymbol{M}_{(n,p+1)}^{(m,0,(-1)^{\ell}j\omega)} + \tilde{\alpha}_{(m,n)}^{(p+1,\ell,(-1)^{\ell}j\omega)}\boldsymbol{M}_{(n,p+1)}^{(m,\ell,(-1)^{\ell}j\omega)} \tag{9.7.1.4}$$

and in the air region outside the head the $I_M = 1$ interrogating vector field has the form

$$\boldsymbol{M}_{(p+2,1)} == \boldsymbol{M}(\tilde{\mathrm{a}} - \tilde{\alpha}, m, n, p+2, \ell, (-1)^{\ell}j\omega) =$$

$$\tilde{\mathrm{a}}_{(m,n)}^{(p+2,0,(-1)^{\ell}j\omega)}\boldsymbol{M}_{(n,p+2)}^{(m,0,(-1)^{\ell}j\omega)} + \tilde{\alpha}_{(m,n)}^{(p+2,\ell,(-1)^{\ell}j\omega)}\boldsymbol{M}_{(n,p+2)}^{(m,\ell,(-1)^{\ell}j\omega)} \tag{9.7.1.5}$$

From our relationship between the two classes of vector fields the curl of the $I_M = 1$ vector field is

$$\nabla \times (\boldsymbol{M}_{(p+2,1)}) == \nabla \times (\boldsymbol{M}(\tilde{\mathrm{a}} - \tilde{\alpha}, m, n, p+2, \ell, (-1)^{\ell}j\omega)) =$$

$$k(p+2,(-1)^{\ell}j\omega)\tilde{\mathrm{a}}_{(m,n)}^{(p+2,0,(-1)^{\ell}j\omega)}\boldsymbol{N}_{(n,p+2)}^{(m,0,(-1)^{\ell}j\omega)} + k_{p+2}((-1)^{\ell}j\omega)\tilde{\alpha}_{(m,n)}^{(p+2,\ell,(-1)^{\ell}j\omega)}\boldsymbol{N}_{(n,p+2)}^{(m,\ell,(-1)^{\ell}j\omega)} \tag{9.7.1.6}$$

where we have used (9.4.1.17). To find the correct representation of this vector field in all regions we just have to find the coefficients

$$(p,n,m,\ell,(-1)^{\ell}(j\omega)) \rightarrow (\tilde{\mathrm{a}}_{(m,n)}^{(p+1,0,(-1)^{\ell}j\omega)}, \tilde{\alpha}_{(m,n)}^{(p+1,\ell,(-1)^{\ell}j\omega)}, \tilde{\mathrm{a}}_{(m,n)}^{(p+2,0,(-1)^{\ell}j\omega)}, \tilde{\alpha}_{(m,n)}^{(p+2,\ell,(-1)^{\ell}j\omega)}) \tag{9.7.1.7}$$

that cause the tangential components of these vector fields and their curls to be continuous across tissue interfaces. We develop transition matrices with exact formulae inverses to find these coefficients.

The $I_M = 2$ case is similar. For $I_M = 2$ the interrogating vector field $\boldsymbol{M}_{(p,2)}$, in brain tissue region p, is smooth at all points in the brain and is given by

$$\boldsymbol{N}_{(n,p)}^{(m,0,(-1)^\ell j\omega)} = n(n+1)\frac{Z_n^{(0)}(k(p,(-1)^\ell j\omega)r)}{k(p,(-1)^\ell j\omega)r}\boldsymbol{C}_{(m,n)}(\theta,\phi) + W_n^{(0)}(k(p,(-1)^\ell j\omega)r)\boldsymbol{B}_{(m,n)}(\theta,\phi) \tag{9.7.1.8}$$

where $\boldsymbol{C}_{(m,n)}$, $\boldsymbol{B}_{(m,n)}$ and $W_n^{(0)}(k(p,(-1)^\ell j\omega)r)$ are given by (9.4.1.3), (9.4.1.5) and (9.4.1.11), respectively. In the skull bone region the interrogating vector field has another form in order to assure that both the vector field and its curl are continuous across the tissue interface the interrogating vector field, in tissue region $p+1$ we avoid $r = 0$ so that the smooth $I_M = 2$ interrogating vector field has the form

$$\boldsymbol{M}_{(p+1,2)} == \boldsymbol{M}(\tilde{\mathrm{b}} - \tilde{\beta}, m, n, p+1, \ell, (-1)^\ell j\omega) =$$

$$\tilde{\mathrm{b}}_{(m,n)}^{(p+1,0,(-1)^\ell j\omega)}\boldsymbol{N}_{(n,p+1)}^{(m,0,(-1)^\ell j\omega)} + \tilde{\beta}_{(m,n)}^{(p+1,\ell,(-1)^\ell j\omega)}\boldsymbol{N}_{(n,p+1)}^{(m,\ell,(-1)^\ell j\omega)} \tag{9.7.1.9}$$

and in the air region outside the head the $I_M = 2$ interrogating vector field has the form

$$\boldsymbol{M}_{(p+2,2)} == \boldsymbol{M}(\tilde{\mathrm{b}} - \tilde{\beta}, m, n, p+2, \ell, (-1)^\ell j\omega) =$$

$$\tilde{\mathrm{b}}_{(m,n)}^{(p+2,0,(-1)^\ell j\omega)}\boldsymbol{N}_{(n,p+2)}^{(m,0,(-1)^\ell j\omega)} + \tilde{\beta}_{(m,n)}^{(p+2,\ell,(-1)^\ell j\omega)}\boldsymbol{N}_{(n,p+2)}^{(m,\ell,(-1)^\ell j\omega)} \tag{9.7.1.10}$$

9.8 Details of Matrix Formulation of the Orientation Inversion Algorithms

We are using interrogating vector fields to recover internal brain activity. Brain activity is modeled as a complex of possible sites of activity. We do not assume any knowledge of neuronal orientation at any of these sites. Both the orientation and time profile of neuronal activity are recovered by our inverse source solution. Our inverse source solution uses an identity relating the divergence of a cross product of vector fields and the scalar products of these vector fields with the curl of the other vector field.

In this section we give inversion algorithms for recovery of the time profile of activity on a set of generally oriented dipole sources and a second algorithm where we know just the location of the source, but we don't know the orientation.

9.8.1 Volume and Surface Integral Relationships for an Arbitrarily Oriented Dipole

We use the fact that if $\boldsymbol{U}$ and $\boldsymbol{V}$ are any differentiable vector fields, then

$$\nabla\cdot(\boldsymbol{U}\times\boldsymbol{V}) = V\cdot\nabla\times(\boldsymbol{U}) - \boldsymbol{U}\cdot\nabla\times(\boldsymbol{V}) \tag{9.8.1.1}$$

Our basic surface integral to volume integral relationship based upon the vector calculus identity (9.8.1.1) is

$$\int_{\partial\Omega} \{\boldsymbol{M} \times \nabla \times (\boldsymbol{E}) - (\boldsymbol{E} \times \nabla \times (\boldsymbol{M})\} \cdot \boldsymbol{n} d\text{area}$$

$$= \int_{\Omega} \{-\boldsymbol{M} \cdot \nabla \times (\nabla \times (\boldsymbol{E})) + \boldsymbol{E} \cdot \nabla \times (\nabla \times (\boldsymbol{M}))\} \, d\text{volume}$$

$$= \int_{\Omega} \left\{-\boldsymbol{M} \cdot \nabla \times (-i(-1)^{\ell}(j\omega)\mu_0 \boldsymbol{H}) + \boldsymbol{E} \cdot k^2 \boldsymbol{M}\right\} d\text{volume}$$

$$= \int_{\Omega} \left\{-\boldsymbol{M} \cdot (-i(-1)^{\ell}(j\omega)\mu_0 [\left\{i(-1)^{\ell}(j\omega)\epsilon\right\} \boldsymbol{E} + \boldsymbol{J}_{\text{brain wave}}] + \boldsymbol{E} \cdot (k^2 \boldsymbol{M}\right\} d\text{volume}$$

$$= \int_{\Omega} \left\{-\boldsymbol{M} \cdot k^2 \boldsymbol{E} - \boldsymbol{M} \cdot \left[-i(-1)^{\ell}(j\omega)\boldsymbol{J}_{\text{brain wave}}\right] + \boldsymbol{E} \cdot k^2 \boldsymbol{M}\right\} d\text{volume}$$

$$= \int_{\Omega} \boldsymbol{M} \cdot \left\{+i(-1)^{\ell}(j\omega)\mu_0 \boldsymbol{J}_{\text{brain wave}}\right\} d\text{volume} \tag{9.8.1.2}$$

To recover both the time profile of activity on and orientation of a generally oriented source of brain activity, we use the relationship

$$\int_{\partial\Omega} \{((\boldsymbol{M} \times \nabla \times (\boldsymbol{E}) - (\boldsymbol{E} \times \nabla \times (\boldsymbol{M})) \cdot \boldsymbol{n}\} \, d\text{area}$$

$$= \int_{\Omega} \left\{\boldsymbol{M} \cdot (+i(-1)^{\ell}(j\omega)\mu_0 \boldsymbol{J}_{\text{brain wave}})\right\} d\text{volume}$$

$$= -M_x(-i(-1)^{\ell} j\omega\mu_0 p_x((-1)^{\ell}(j\omega)))$$

$$-M_y(-i(-1)^{\ell} j\omega\mu_0 p_y((-1)^{\ell}(j\omega))) - M_z(-i(-1)^{\ell} j\omega\mu_0 p_z((-1)^{\ell}(j\omega))) \tag{9.8.1.3}$$

We can express the right side of (9.8.1.3) for a single source at

$$q \rightarrow (r_q \sin(\theta_q)\cos(\phi_q), r_q \sin(\theta_q \sin(\phi_q), r_q \cos(\theta_q)) \tag{9.8.1.4}$$

in terms of spherical coordinates if we make use of

$$M_x \boldsymbol{e}_x + M_y \boldsymbol{e}_y + M_z \boldsymbol{e}_z = M_r \boldsymbol{e}_r + M_\theta \boldsymbol{e}_\theta + M_\phi \boldsymbol{e}_\phi \tag{9.8.1.5}$$

which gives us

$$M_x \boldsymbol{e}_x + M_y \boldsymbol{e}_y + M_z \boldsymbol{e}_z = M_r \left\{\sin(\theta_q)\cos(\phi_q)\boldsymbol{e}_x + \sin(\theta_q)\sin(\phi_q)\boldsymbol{e}_y + \cos(\theta_q)\boldsymbol{e}_z\right\}$$

$$+M_\theta \left\{\cos(\theta_q)\cos(\phi_q)\boldsymbol{e}_x + \cos(\theta_q)\sin(\phi_q)\boldsymbol{e}_y - \sin(\theta_q)\boldsymbol{e}_z\right\} + M_\phi \left\{-\sin(\phi_q)\boldsymbol{e}_x + \cos(\phi_q)\boldsymbol{e}_y\right\} \tag{9.8.1.6}$$

Collecting terms in (9.8.1.6) we have

$$M_z = \cos(\theta_q)M_r - \sin(\theta_q)M_\theta \tag{9.8.1.7}$$

for a vertical dipole. For a dipole component parallel to the x-axis we have

$$M_x = M_r \left\{\sin(\theta_q)\cos(\phi_q)\right\}$$

$$+M_\theta \left\{\cos(\theta_q)\cos(\phi_q)\right\} + M_\phi \left\{-\sin(\phi_q)\right\} \tag{9.8.1.8}$$

and for a dipole parallel to the y-axis we have

$$M_y = M_r \left\{\sin(\theta_q)\sin(\phi_q)\right\}$$

$$+M_\theta \left\{\cos(\theta_q)\sin(\phi_q)\right\} + M_\phi \left\{\cos(\phi_q)\right\} \tag{9.8.1.9}$$

Thus, for a set of dipoles the volume and surface integral relationships are

$$\int_{\partial\Omega} \left\{\boldsymbol{M}\times\nabla\times(\boldsymbol{E}) - (\boldsymbol{E}\times\nabla\times(\boldsymbol{M})\right\}\cdot\boldsymbol{n}d\text{area}$$

$$= \int_\Omega \left\{-\boldsymbol{M}\cdot\nabla\times(\nabla\times(\boldsymbol{E})) + \boldsymbol{E}\cdot\nabla\times(\nabla\times(\boldsymbol{M}))\right\} d\text{volume}$$

$$= \int_\Omega \left\{-\boldsymbol{M}\cdot\nabla\times(-i(-1)^\ell(j\omega)\mu_0\boldsymbol{H}) + \boldsymbol{E}\cdot k^2\boldsymbol{M}\right\} d\text{volume}$$

$$= \int_\Omega \left\{-\boldsymbol{M}\cdot(-i(-1)^\ell(j\omega)\mu_0[\left\{i(-1)^\ell(j\omega)\epsilon\right\}\boldsymbol{E} + \boldsymbol{J}_{\text{brain wave}}] + \boldsymbol{E}\cdot(k^2\boldsymbol{M}\right\} d\text{volume}$$

$$= \int_\Omega \left\{-\boldsymbol{M}\cdot k^2\boldsymbol{E} - \boldsymbol{M}\cdot\left[-i(-1)^\ell(j\omega)\boldsymbol{J}_{\text{brain wave}}\right] + \boldsymbol{E}\cdot k^2\boldsymbol{M}\right\} d\text{volume}$$

$$= \int_\Omega \boldsymbol{M}\cdot\left\{+i(-1)^\ell(j\omega)\mu_0\boldsymbol{J}_{\text{brain wave}}\right\} d\text{volume}$$

$$= \sum_{q=1}^{Q}\left\{p_q((-1)^\ell(j\omega))i(-1)^\ell(j\omega)\mu_0\left[\quad M_x\sin(\alpha_q)\cos(\beta_q) + M_y\sin(\alpha_q)\sin(\beta_q) + M_z\cos(\alpha_q)\right]\right\}$$

$$= \sum_{q=1}^{Q}\left\{p_q((-1)^\ell(j\omega))\left\{i(-1)^\ell(j\omega)\mu_0\right\}\left[\right.\right.$$

$$\{M_r\sin(\theta_q)\cos(\phi_q) + M_\theta\cos(\theta_q)\cos(\phi_q) + M_\phi\left[-\sin(\phi_q)\right]\}\sin(\alpha_q)\cos(\beta_q)$$

$$+\{M_r[\sin(\theta_q)\sin(\phi_q)]M_\theta[\cos(\theta_q)\sin(\phi_q)] + M_\phi\}\sin(\alpha_q)\cos(\beta_q)$$

$$\left.\left.\{\cos(\theta_q)M_r - \sin(\theta_q)M_\theta\}\cos(\alpha_q\right]\right\} \tag{9.8.1.10}$$

9.8.2 Arbitrarily Many Arbitrarily Oriented Dipoles– A Simultaneous Recovery of the Individual Time Profiles of Activity and each Dipole's Orientation

We suppose that we have a set of interrogating vector fields

$$(n, m, I_M) \rightarrow \boldsymbol{M}(n, m, I_M) = M_x(n, m, I_M)\boldsymbol{e}_x + M_y(n, m, I_M)\boldsymbol{e}_z + M_z(n, m, I_M)\boldsymbol{e}_z \quad (9.8.2.1)$$

where these vector fields satisfy the property that they satisfy the vector Helmholtz equation in each tissue region and that their tangential components and the tangential components of their curl are continuous across tissue interfaces. Each interrogating vector field indexes a row of a matrix. The row indices are

$$\mathcal{I}(n, m, I_M) = 2n^2 + 2(n + m) + I_M \quad (9.8.2.2)$$

and the column index is

$$\mathcal{J}(q, j_C) = 3(q - 1) + j_C \quad (9.8.2.3)$$

If $j_C = 1$, the matrix entry is

$$C(\mathcal{I}(n, m, I_M), \mathcal{J}(q, j_C)) = i(-1)^{\ell}(j\omega)\mu_0)M_x(n, m, I_M) \quad (9.8.2.4)$$

If $j_C = 2$, the matrix entry is

$$C(\mathcal{I}(n, m, I_M), \mathcal{J}(q, j_C)) = i(-1)^{\ell}(j\omega)\mu_0)M_y(n, m, I_M) \quad (9.8.2.5)$$

If $j_C = 3$, the matrix entry is

$$C(\mathcal{I}(n, m, I_M), \mathcal{J}(q, j_C)) = i(-1)^{\ell}(j\omega)\mu_0)M_z(n, m, I_M) \quad (9.8.2.6)$$

For every row of the matrix there is a right side entry

$$\mathcal{Y}(n, m, I_M) =$$

$$\int_{\partial\Omega} \Big[\quad \{\boldsymbol{M}(n, m, I_M) \times \nabla \times (\boldsymbol{E}) - (\boldsymbol{E} \times \nabla \times (\boldsymbol{M}(n, m, I_M))\} \cdot \boldsymbol{n} \Big] d\text{area} \quad (9.8.2.7)$$

where $\boldsymbol{n}$ is the unit normal to the bounding surface. Thus, the equation that we solve is

$$\overline{\overline{C}} \begin{bmatrix} p_1((-1)^\ell(j\omega))\sin(\alpha_1)\cos(\beta_1) \\ p_1((-1)^\ell(j\omega))\sin(\alpha_1)\sin(\beta_1) \\ p_1((-1)^\ell(j\omega))\cos(\alpha_1) \\ \cdots \\ \cdots \\ \cdots \\ p_{\mathrm{q}}((-1)^\ell(j\omega))\sin(\alpha_{\mathrm{q}})\cos(\beta_{\mathrm{q}}) \\ p_{\mathrm{q}}((-1)^\ell(j\omega))\sin(\alpha_{\mathrm{q}})\sin(\beta_{\mathrm{q}}) \\ p_{\mathrm{q}}((-1)^\ell(j\omega))\cos(\alpha_q) \\ \cdots \\ \cdots \\ \cdots \\ p_Q((-1)^\ell(j\omega))\sin(\alpha_Q)\cos(\beta_Q) \\ p_Q((-1)^\ell(j\omega))\sin(\alpha_Q)\sin(\beta_Q) \\ p_Q((-1)^\ell(j\omega))\cos(\alpha_Q) \end{bmatrix} = \begin{bmatrix} \mathcal{Y}(n=0,m=0,I_M=1) \\ \mathcal{Y}(n=0,m=0,I_M=2) \\ \mathcal{Y}(n=1,m=-1,I_M=1) \\ \mathcal{Y}(n=1,m=-1,I_M=2) \\ \mathcal{Y}(n=1,m=0,I_M=1) \\ \mathcal{Y}(n=1,m=0,I_M=2) \\ \mathcal{Y}(n=1,m=+1,I_M=1) \\ \mathcal{Y}(n=1,m=+1,I_M=2) \\ \cdots \\ \cdots \\ \cdots \\ \mathcal{Y}(n=N_{max},m=-N_{max},I_M=1) \\ \mathcal{Y}(n=N_{max},m=-N_{max},I_M=2) \\ \cdots \\ \cdots \\ \cdots \\ \mathcal{Y}(n=N_{max},m=+N_{max},I_M=1) \\ \mathcal{Y}(n=N_{max},m=+N_{max},I_M=2) \end{bmatrix} \tag{9.8.2.8}$$

9.8.3 Computer Determination of Each Dipole's Orientation Angles α_q and β_q from the Recovered Complex Dipole Strength and Direction Vectors

What we recover from equation (9.8.2.8) the complex components of each of the individual dipole orientation vectors. The complex orientation vector from the qth dipole at frequency $j\omega$ appearing in the column vector on that the brain-activity-independent matrix on the left side of equation (9.8.2.8) is acting on is the right side of the function

$$(q,\ell,j\omega) \rightarrow \begin{bmatrix} p_{\mathrm{q}}((-1)^\ell(j\omega))\sin(\alpha_q)\cos(\beta_q) \\ p_{\mathrm{q}}((-1)^\ell(j\omega))\sin(\alpha_q)\sin(\beta_q) \\ p_{\mathrm{q}}((-1)^\ell(j\omega))\cos(\alpha_q) \end{bmatrix} \tag{9.8.3.1}$$

We create a real direction vector from the projection of the solution vector in equation (9.8.2.8) onto the complex three dimensional subspace generated by (9.8.3.1). We recover the angles from the equation for $\ell = 2$ or positive frequency or $\ell = 1$, negative frequency given by

$$\begin{bmatrix} R_q\sin(\alpha_q)\cos(\beta_q) \\ R_q\sin(\alpha_q)\sin(\beta_q) \\ R_q\cos(\alpha_q) \end{bmatrix} = \begin{bmatrix} Real\left\{p_{\mathrm{q}}((-1)^\ell(j\omega)\right\}\sin(\alpha_q)\cos(\beta_q) \\ Real\left\{p_{\mathrm{q}}((-1)^\ell(j\omega)\right\}\sin(\alpha_q)\sin(\beta_q) \\ Real\left\{p_{\mathrm{q}}((-1)^\ell(j\omega)\right\}\cos(\alpha_q) \end{bmatrix} \tag{9.8.3.2}$$

For the moment we suppose that equation (9.8.3.2) From equation (9.8.3.2) we recover R_q by the relationship

$$|R_q| = \sqrt{[R_q \sin(\alpha_q)\cos(\beta_q)]^2 + [R_q \sin(\alpha_q)\sin(\beta_q)]^2 + [R_q \cos(\alpha_q)]^2} \tag{9.8.3.3}$$

We then recover the pure direction vector up to a plus or minus sign by dividing the components of the real part of the complex direction vector by $|R_q|$. The actual sign of R_q will be exactly the same for the frequency $(-1)^\ell j\omega$ for both $\ell = 1$ and $\ell = 2$. Under the assumption now that we know which of

$$R_q = \begin{matrix} + \\ - \end{matrix} \mid R_q \mid \tag{9.8.3.4}$$

is correct we recover

$$\beta_q = DATAN2(R_q \sin(\alpha_q)\sin(\beta_q), R_q \sin(\alpha_q)\cos(\beta_q)) \tag{9.8.3.5}$$

which gives us

$$q \rightarrow R_q \sin(\alpha_q) \tag{9.8.3.6}$$

which in turn gives us, from the DATAN2 FORTRAN subroutine

$$\alpha_q = DATAN2(R_q \sin(\alpha_q), R_q \cos(\alpha_q)) \tag{9.8.3.7}$$

We could then determine an appropriate I_q, which is the imaginary part of the complex current on the neuron, as recovered by our inverse source solution, that would be consistent with saying that

$$\begin{bmatrix} I_q \sin(\alpha_q)\cos(\beta_q) \\ I_q \sin(\alpha_q)\sin(\beta_q) \\ I_q \cos(\alpha_q) \end{bmatrix} = \begin{bmatrix} Imag\left\{p((-1)^\ell(j\omega))\right\}\sin(\alpha_q)\cos(\beta_q) \\ Imag\left\{p((-1)^\ell(j\omega))\right\}\sin(\alpha_q)\sin(\beta_q) \\ Imag\left\{p((-1)^\ell(j\omega))\right\}\cos(\alpha_q) \end{bmatrix} \tag{9.8.3.8}$$

where for any complex current coefficient $A + iB$ we have

$$(Real(A+iB), Imag(A+iB)) = (A, B) \tag{9.8.3.9}$$

Thus, the orientation is determined up to a sign of the vector and we can determine the time profiles of activity that are consistent with this direction $\boldsymbol{e}_q$ or $-\boldsymbol{e}_q$ of the dipole.

We correctly find a line containing the dipole orientation. If we started at the dipole location on this line and selected the wrong direction, we would obtain an inverted brain wave signal for that dipole source when we put together all of the frequency components describing the activity at that source. Knowing the action potential shape, thus, our inversion algorithm yields the precise orientation of the neuron.

9.8.4 Computer Validation of the Angle Recovery Algorithm

We successfully recover the brain activity source current orientation angles α and β from the recovered complex amplitude vectors which have the form

$$p_{\rm x}\boldsymbol{e}_{\rm x}+p_{\rm y}\boldsymbol{e}_{\rm y}+p_{\rm z}\boldsymbol{e}_{\rm z}=(A+iB)\sin(\alpha)\cos(\beta)\boldsymbol{e}_{\rm x}+(A+iB)\sin(\alpha)\sin(\beta)\boldsymbol{e}_{\rm y}+(A+iB)\cos(\alpha)\boldsymbol{e}_{\rm z} \tag{9.8.4.1}$$

In the angle recovery code we make use of the fact that

$$\begin{aligned}&\sin(\pi-\alpha)\cos(\beta-\pi)\boldsymbol{e}_{\rm x}+\sin(\pi-\alpha)\sin(\beta-\pi)\boldsymbol{e}_{\rm y}+\cos(\pi-\alpha)\boldsymbol{e}_{\rm z}\\&\quad=-\left\{\sin(\alpha)\cos(\beta)\boldsymbol{e}_{\rm x}+\sin(\alpha)\sin(\beta)\boldsymbol{e}_{\rm y}+\cos(\alpha)\boldsymbol{e}_{\rm z}\right\}\end{aligned} \tag{9.8.4.2}$$

so that in the angle recovery code if β is calculated to be negative, we replace β by $\beta+\pi$ and replace α by $\pi-\alpha$ to get a vector pointing in the opposite direction.

The test dipole set for angle recovery is

r%	th	ph	a	b
10	70.0	38.0	22.0	36.0
18	165.0	218.0	44.0	72.0

where the columns are for the qth dipole

$$({\rm r}\%, th, ph, {\rm a}, {\rm b})=(100r_{\rm q}/R, \theta_{\rm q}, \phi_{\rm q}, \alpha_{\rm q}, \beta_{\rm q}) \tag{9.8.4.3}$$

In the following table we let i_{row} be the row of the matrix on the left side of (9.8.2.8), we let n and m be the indices of the interrogating vector field of type I_M and we let $\ell=1$ indicate an negative frequency and $\ell=2$ indicate a positive frequency component of the brain activity. The frequency is $(-1)^{\ell}\omega$. The first row of the volume and surface integral comparison table is the surface integral or the left side of equation (9.8.1.2) and the entry immediately following is the volume integral or the right side of (9.8.1.2).

$(i_{row}, n, m, I_M, \ell, \omega)$	volume and surface integral comparisons
(1, 0, 0, 2, 2, 1.0794306×10^3)	$0.000000000000000 \times 10^0 + 0.000000000000000 \times 10^0 i$ $0.000000000000000 \times 10^0 + 0.000000000000000 \times 10^0 i$
(2, 1, -1, 2, 2, 1.0794306×10^3)	$-1.320135022079054 \times 10^{-8} - 4.468247822403349 \times 10^{-9} i$ $-1.320135022079061 \times 10^{-8} - 4.468247822403294 \times 10^{-9} i$
(3 , 1, 0, 2, 2, 1.0794306×10^3)	$-4.089329856351770 \times 10^{-9} - 2.244830615710698 \times 10^{-8} i$ $-4.089329856351848 \times 10^{-9} - 2.244830615710694 \times 10^{-8} i$
(4 , 1, 1, 2, 2, 1.0794306×10^3)	$1.066360388068776 \times 10^{-8} - 9.655225939468862 \times 10^{-9} i$ $1.066360388068783 \times 10^{-8} - 9.655225939468971 \times 10^{-9} i$

The use of larger index interrogating vector fields enables us to discriminate between brain activity sources that might be quite close to one another. The following table of comparisons of the left and right sides of equations (9.8.1.2) or (9.8.1.10) when the interrogating vector fields have a more rapid spatial variation over the head surface.

$(i_{row}, n, m, I_M, \ell, \omega)$	volume and surface integral comparisons
(5, 2, -2, 2, 2, 1.0794306×10^3)	$-5.656663013791870 \times 10^{-13} - 3.330120308392874 \times 10^{-13} i$ $-5.656663013791797 \times 10^{-13} - 3.330120308392892 \times 10^{-13} i$
(6, 2, -1, 2, 2, 1.0794306×10^3)	$4.163604144291942 \times 10^{-13} - 1.075021093853240 \times 10^{-12} i$ $4.163604144292082 \times 10^{-13} - 1.075021093853259 \times 10^{-12} i$
(7 , 2, 0, 2, 2, 1.0794306×10^3)	$7.178816274648380 \times 10^{-13} + 4.974185383067127 \times 10^{-13} i$ $7.178816274648210 \times 10^{-13} + 4.974185383067257 \times 10^{-13} i$
(8 , 2, 1, 2, 2, 1.0794306×10^3)	$-6.069387102102143 \times 10^{-13} + 6.574869190019451 \times 10^{-13} i$ $-6.069387102102162 \times 10^{-13} + 6.574869190019583 \times 10^{-13} i$
(8 , 2, 1, 2, 2, 1.0794306×10^3)	$-6.069387102102143 \times 10^{-13} + 6.574869190019451 \times 10^{-13} i$ $-6.069387102102162 \times 10^{-13} + 6.574869190019583 \times 10^{-13} i$
(9 , 2, 2, 2, 2, 1.0794306×10^3)	$-3.056248668414576 \times 10^{-13} - 3.600373772113263 \times 10^{-13} i$ $-3.056248668414578 \times 10^{-13} - 3.600373772113235 \times 10^{-13} i$
(25 , 4, 4, 2, 2, $2.1588612 \times 10^{+3}$)	$1.122765566955568 \times 10^{-19} - 3.409032427668378 \times 10^{-20} i$ $1.122765566955462 \times 10^{-19} - 3.409032427667254 \times 10^{-20} i$

An abbridged comparison of actual directions and angles and those recovered by solving equation (9.8.2.8) along with the recovered complex current amplitudes and their actual values are shown below. The actual values appear in the second row of the tables. The recovered angles are frequency independent. In the following the Cartesian component of the neuronal current vector is x, y, or z. The dipole index is q. The value of ℓ is 1 for a negative frequency and 2 for a positive frequency. The frequency is $(-1)^\ell\omega$. The recovered complex amplitudes are from the solution column vector in the matrix equation (9.8.2.8).

(Cartesian component, q, ℓ, ω)	Calculated and actual complex amplitude
(x, 1, 2, 1.0794306×10^3)	$-0.460990849927645 \times 10^{-5} + 0.616939868458433 \times 10^{-6}i$
	$-0.460990849927383 \times 10^{-5} + 0.616939868457858 \times 10^{-6}i$
(y, 1, 2, 1.0794306×10^3)	$-0.334929457493588 \times 10^{-5} + 0.448233051656706 \times 10^{-6}i$
	$-0.334929457493581 \times 10^{-5} + 0.448233051656667 \times 10^{-6}i$
(z, 1, 2, 1.0794306×10^3)	$-0.141034415856990 \times 10^{-4} + 0.188745078086807 \times 10^{-5}i$
	$-0.141034415856988 \times 10^{-4} + 0.188745078086793 \times 10^{-5}i$

angle	dipole index q	Calculated Angle	Actual Angle
α	1	22.0	22.0
β	1	36.0	36.0

(Cartesian component, q, ℓ, ω)	Calculated and actual complex amplitude
(x, 2, 2, 1.0794306×10^3)	$-0.319914139971859 \times 10^{-5} + 0.786212668484572 \times 10^{-6}i$
	$-0.319914139972118 \times 10^{-5} + 0.786212668485148 \times 10^{-6}i$
(y, 2, 2, 1.0794306×10^3)	$-0.984594481901767 \times 10^{-5} + 0.241971378651542 \times 10^{-5}i$
	$-0.984594481901767 \times 10^{-5} + 0.241971378651537 \times 10^{-5}i$
(z, 2, 2, 1.0794306×10^3)	$-0.107204715527522 \times 10^{-4} + 0.263463520169600 \times 10^{-5}i$
	$-0.107204715527524 \times 10^{-4} + 0.263463520169605 \times 10^{-5}i$

angle	dipole index q	Calculated Angle	Actual Angle
α	2	44.0	44.0
β	2	72.0	72.0

The recovered dipole direction is

$$\boldsymbol{e}_q = \sin(\alpha_q)\cos(\beta_q)\boldsymbol{e}_x + \sin(\alpha_q)\sin(\beta_q)\boldsymbol{e}_y + \cos(\alpha_q)\boldsymbol{e}_z \tag{9.8.4.4}$$

Knowing the direction angles and the complex vector of component amplitudes in complex three dimensional space then gives us the complex amplitude of the dipole current.

9.9 Identity for Recovery of Brain Activity Through the Skull Bone

To recover brain activity through the skull bone we needed to interrogate, or derive information from, the electromagnetic fields outside the head that were stimulated by brain activity. For this purpose we used members of an infinite family of interrogating vector fields $\boldsymbol{M}$ which all satisfied the vector Helmholtz equation in each tissue region and had the property that the vector fields, along with their curls had tangential components that were continuous across tissue interfaces.

9.9.1 Properties of the N Layer Sphere Interrogating M Function

Our particular solution of the inverse source problem for brain activity uses a $\boldsymbol{M}$ function which in the pth layer satisfies the vector Helmholtz equation, for region p with propagation constant $k(p,(-1)^{\ell}\omega)$ defined by (9.3.1.14) at frequency $(-1)^{\ell}\omega$, which is

$$\Delta \boldsymbol{M} + k(p,(-1)^{\ell}\omega)^2 \boldsymbol{M} = 0 \tag{9.9.1.1}$$

We require that at every tissue interface with normal vector $\boldsymbol{n}$ we have

$$\boldsymbol{n} \times \boldsymbol{M}_{outside} = \boldsymbol{n} \times \boldsymbol{M}_{inside} \tag{9.9.1.2}$$

and

$$\boldsymbol{n} \times \nabla \times (\boldsymbol{M}_{outside}) = \boldsymbol{n} \times \nabla \times (\boldsymbol{M}_{inside}) \tag{9.9.1.3}$$

We can create such a vector field by letting $\boldsymbol{M}$ be the total electric vector solution of a scattering problem with an external source.

9.9.2 Recovery of Information Through the Skull

Let $\boldsymbol{M}$ be a vector field satisfying (9.9.1.2) and (9.9.1.3) We use these identities, the fact that tangential components of the electric and magnetic vector are continuous across tissue interfaces and the fact that in a triple scalar product for all vector fields $\boldsymbol{A}$, $\boldsymbol{B}$, and $\boldsymbol{C}$ that

$$\boldsymbol{A} \cdot (\boldsymbol{B} \times \boldsymbol{C}) = (\boldsymbol{A} \times \boldsymbol{B}) \cdot \boldsymbol{C} = \boldsymbol{B} \cdot (\boldsymbol{C} \times \boldsymbol{A}) \tag{9.9.2.1}$$

In equation (9.9.2.1) we are saying that the dot product is commutative and that we can interchange the dot product and the cross product in a triple scalar product. We have

$$\begin{aligned}
&\int_{\partial\Omega} \{(\boldsymbol{M}_{\text{outside}} \times \nabla \times (\boldsymbol{E}_{\text{outside}})) \cdot \boldsymbol{n}\}\, d\text{area} = \\
&\int_{\partial\Omega} \{(\boldsymbol{n} \times \boldsymbol{M}_{\text{outside}}) \cdot \nabla \times (\boldsymbol{E}_{\text{outside}})\}\, d\text{area} \\
&= \int_{\partial\Omega} \{(\boldsymbol{n} \times \boldsymbol{M}_{\text{inside}}) \cdot (-i\omega\mu_0 \boldsymbol{H}_{\text{outside}})\}\, d\text{area} \\
&= \int_{\partial\Omega} \{(-i\omega\mu_0 \boldsymbol{H}_{\text{outside}}) \cdot (\boldsymbol{n} \times \boldsymbol{M}_{\text{inside}})\}\, d\text{area}
\end{aligned}$$

$$= \int_{\partial\Omega} \{(-i\omega\mu_0 \boldsymbol{H}_{\text{outside}}) \times \boldsymbol{n}) \cdot \boldsymbol{M}_{\text{inside}})\}\, d\text{area}$$

$$= \int_{\partial\Omega} \{(-i\omega\mu_0 \boldsymbol{H}_{\text{inside}} \times \boldsymbol{n}) \cdot \boldsymbol{M}_{\text{inside}}\}\, d\text{area}$$

$$= \int_{\partial\Omega} \{\boldsymbol{M}_{\text{inside}} \cdot (-i\omega\mu_0 \boldsymbol{H}_{\text{inside}}) \times \boldsymbol{n})\}\, d\text{area}$$

$$= -i\omega\mu_0 \int_{\partial\Omega} \{(\boldsymbol{M}_{\text{inside}}) \times \boldsymbol{H}_{\text{inside}}) \cdot \boldsymbol{n}\}\, d\text{area}$$

$$= \int_{\partial\Omega} \{(\boldsymbol{M}_{\text{inside}} \times \nabla \times (\boldsymbol{E}_{\text{inside}}) \cdot \boldsymbol{n}\}\, d\text{area} \qquad (9.9.2.2)$$

This argument proves that the surface integrals are exactly the same on opposite sides of tissue interfaces.

We next use the continuity of tangential components of the curl of $\boldsymbol{M}$ across tissue interfaces. We simply interchange $\boldsymbol{E}$ and $\boldsymbol{M}$ in the above integral and use (9.9.2.1) repeatedly. We have

$$\int_{\partial\Omega} \{\boldsymbol{n} \cdot (\boldsymbol{E}_{\text{outside}} \times \nabla \times (\boldsymbol{M}_{\text{outside}}))\}\, d\text{area} =$$

$$\int_{\partial\Omega} \{(\boldsymbol{n} \times \boldsymbol{E}_{\text{outside}}) \cdot \nabla \times (\boldsymbol{M}_{\text{outside}})\}\, d\text{area}$$

$$= \int_{\partial\Omega} \{(\boldsymbol{n} \times \boldsymbol{E}_{\text{inside}}) \cdot \nabla \times (\boldsymbol{M}_{\text{outside}})\}\, d\text{area}$$

$$= \int_{\partial\Omega} \{\boldsymbol{n} \cdot (\boldsymbol{E}_{\text{inside}}) \times \nabla \times (\boldsymbol{M}_{\text{outside}}))\}\, d\text{area}$$

$$= \int_{\partial\Omega} \{(\boldsymbol{E}_{\text{inside}}) \times \nabla \times (\boldsymbol{M}_{\text{outside}}) \cdot \boldsymbol{n}\}\, d\text{area}$$

$$= \int_{\partial\Omega} \{\boldsymbol{E}_{\text{inside}} \cdot (\nabla \times (\boldsymbol{M}_{\text{outside}}) \times \boldsymbol{n}\}\, d\text{area}$$

$$= \int_{\partial\Omega} \{\boldsymbol{E}_{\text{inside}} \cdot (\nabla \times (\boldsymbol{M}_{\text{inside}}) \times \boldsymbol{n})\}\, d\text{area}$$

$$= \int_{\partial\Omega} \{(\boldsymbol{E}_{\text{inside}}) \times \nabla \times (\boldsymbol{M}_{\text{inside}}) \cdot \boldsymbol{n}\}\, d\text{area}$$

$$= \int_{\partial\Omega} \boldsymbol{n} \cdot \{(\boldsymbol{E}_{\text{inside}} \times \nabla \times (\boldsymbol{M}_{\text{inside}})\}\, d\text{area} \qquad (9.9.2.3)$$

Thus, all intermediate interior surface integrals vanish.

10 Proof of the Expansion Representation of the Exact Analytical Vector Potential of Brain Activity for Validation of the Algorithm for Dynamic Voltage Recovery of Brain Activity

The orthogonality of basis elements used in the expansion representation of dynamic voltage is the reason that we have a rapid recovery of brain activity.

We give in this section a proof of equation (9.5.3.2 where the three vector fields appearing in (9.5.3.2 are defined by (9.4.1.12), (9.4.1.13), and (9.4.1.15). The dynamic voltage expression involves only the terms arising the divergence of the $\boldsymbol{L}$ vector fields (9.4.1.12).

10.1 Recursion Relationships Needed for Rapid Recovery of Brain Activity

The recursion relationships are needed to establish the representation of the vector potential of brain activity which, in turn, gives us an expansion, in terms of orthogonal basis elements, of the dynamic head surface voltage distribution.

10.1.1 Spherical Bessel and Hankel Functions and Recursion Relationships

The spherical Bessel functions $j_n(z)$ and the spherical Neumann functions $y_n(z)$ have the representations

$$j_n(z) = z^n \left(-\frac{1}{z}\frac{d}{dz}\right)^n \frac{\sin(z)}{z} \tag{10.1.1.1}$$

and

$$y_n(z) = z^n \left(-\frac{1}{z}\frac{d}{dz}\right)^n \left(-\frac{\cos(z)}{z}\right) \tag{10.1.1.2}$$

Since brain waves have low frequency components we need small argument representations of the spherical Bessel and Neumann functions which are

$$j_n(z) = A_n(z)\exp(B_n(z)) \tag{10.1.1.3}$$

$$y_n(z) = C_n(z)\exp(D_n(z)) \tag{10.1.1.4}$$

where the complex valued functions A_n, B_n, C_n, and D_n have a modest size.

The spherical Bessel and Hankel functions are all solutions of the singular, self-adjoint, second order linear ordinary differential equation

$$\left(\frac{d}{dz}\left(z^2\frac{dw}{dz}\right)\right) + [z^2 - n(n+1)]w = 0 \tag{10.1.1.5}$$

We deduce immediately from (10.1.1.5) the following proposition.

Proposition 10.1 *If $f(z)$ and $g(z)$ are any two solutions of (10.1.1.5) then*

$$\frac{d}{dz}\left(z^2\left\{f(z)g'(z)-f'(z)g(z)\right\}\right)=0 \tag{10.1.1.6}$$

so that there is a constant K independent of z such that the Wronskian relationship

$$\left\{f(z)g'(z)-f'(z)g(z)\right\}=\frac{K}{z^2} \tag{10.1.1.7}$$

holds for all values of z.

Proof of Proposition. This is a simple consequence of the fact that if we replace w by $f_n(z)$ or $g_n(z)$, the differential equation (10.1.1.5) is satisfied.

In order to explain the vector spherical harmonics

$$(n,p,\tilde{\ell},(-1)^{\ell}j\omega)\rightarrow\left(\boldsymbol{M}_{(n,p)}^{p+2,\tilde{\ell},(-1)^{\ell}j\omega)},\boldsymbol{N}_{(n,p)}^{p+2,\tilde{\ell},(-1)^{\ell}j\omega)}\right) \tag{10.1.1.8}$$

used to describe brain activity we need the special function definitions.

Definition 10.1 *If $j_n(z)$ is the spherical Bessel function and $y_n(z)$ is the spherical Neumann function, then*

$$h_n^{(1)}(z)=j_n(z)+iy_n(z) \tag{10.1.1.9}$$

which is given in ([1]) on page 437 and

$$h_n^{(2)}(z)=j_n(z)-iy_n(z) \tag{10.1.1.10}$$

where

$$(j_n(z),y_n(z))=(z^n\left(\frac{(-1)}{z}\frac{d}{dz}\right)^n\frac{\sin(z)}{z},-z^n\left(\frac{(-1)}{z}\frac{d}{dz}\right)^n\frac{\cos(z)}{z}) \tag{10.1.1.11}$$

We have the following consequence of the definitions

Proposition 10.2 *If $h_n^{(\tilde{\ell})}$ is defined by (9.3.1.18) and (10.1.1.10) for $\tilde{\ell}$ equal to 1 and 2, then*

$$(h_0^{(1)}(z),h_0^{(2)}(z))=\left(\frac{\exp(iz)}{iz},\frac{\exp(-iz)}{-iz}\right) \tag{10.1.1.12}$$

Proof of Proposition. Observe that (10.1.1.11) for $n=0$ implies that

$$h_0^{(1)}(z)=j_0(z)+iy_0(z)=\frac{\sin(z)}{z}+i(-1)\frac{\cos(z)}{z}$$

$$=\frac{i}{i}\left\{\frac{(-i)\cos(z)+\sin(z)}{z}\right\}=\frac{\cos(z)+i\sin(z)}{iz}=\frac{\exp(iz)}{iz} \tag{10.1.1.13}$$

and

$$h_0^{(2)}(z)=j_0(z)-iy_0(z)=\frac{\sin(z)}{z}-i(-1)\frac{\cos(z)}{z}$$

$$= \frac{-i}{-i}\left\{\frac{(+i)\cos(z)+\sin(z)}{z}\right\} = \frac{\cos(z)-i\sin(z)}{-iz} = \frac{\exp(-iz)}{-iz} \tag{10.1.1.14}$$

Our complex arguments are the product z of the complex propagation constant and the distance r from the origin given by

$$z = k(p,(-1)^{\ell}j\omega)r \tag{10.1.1.15}$$

We define for all complex numbers z the relation

$$Z_n^{(\tilde{\ell})}(z) = \begin{cases} y_n(z) & \text{if } \tilde{\ell} = -1 \\ j_n(z) & \text{if } \tilde{\ell} = 0 \\ h_n^{(1)}(z) & \text{if } \tilde{\ell} = 1 \\ h_n^{(2)}(z) & \text{if } \tilde{\ell} = 2 \end{cases} \tag{10.1.1.16}$$

Related to $Z_n(z)$ we define the function $W_n(z)$ by

$$W_n^{(\tilde{\ell})}(z) = \frac{Z_n^{(\tilde{\ell})}(z)}{z} + \left(\frac{d}{dz}\right) Z_n^{(\tilde{\ell})}(z) \tag{10.1.1.17}$$

We first describe the Wronskian relationships needed for effective computation of the transition matrices

$$W_n^{(0)}(z)h_n^{(1)}(z) - W_n^{(1)}(z)j_n(z) = \frac{-i}{z^2} \tag{10.1.1.18}$$

the determinant is found to be

$$\det\begin{bmatrix} h_n^{(1)}(k_pR_p) & j_n(k_pR_p) \\ k_pW_n^{(1)}(k_pR_p)/(-i\omega\epsilon_p) & k_pW_n^{(0)}(k_pR_p)/(-i\omega\epsilon_p) \end{bmatrix}$$

$$= h_n^{(1)}(k_pR_p)k_pW_n^{(0)}(k_pR_p)/(-i\omega\epsilon_p) - j_n(k_pR_p)k_pW_n^{(1)}(k_pR_p)/(-i\omega\epsilon_p)$$

$$= \lim_{z\to k_pR_p}\left(\frac{k_p}{(-i\omega\epsilon_p)}\right)\left\{h_n^{(1)}(z)W_n^{(0)}(z) - j_n(z)W_n^{(1)}(z)\right\}$$

$$= \lim_{z\to k_pR_p}\left(\frac{k_p}{(-i\omega\epsilon_p)}\right)\left\{h_n^{(1)}(z)W_n^{(0)}(z) - j_n(z)W_n^{(1)}(z)\right\}$$

$$= \lim_{z\to k_pR_p}\left(\frac{k_p}{(-i\omega\epsilon_p)}\right)\left\{h_n^{(1)}(z)\left[\frac{j_n(z)}{z} + \left(\frac{d}{dz}\right)j_n(z)\right] - j_n(z)\left[\frac{h_n^{(1)}}{z} + \left(\frac{d}{dz}\right)h_n^{(1)}(z)\right]\right\}$$

$$= \lim_{z\to k_pR_p}\left(\frac{k_p}{(-i\omega\epsilon_p)}\right)\left\{h_n^{(1)}(z)\left[\left(\frac{d}{dz}\right)j_n(z)\right] - j_n(z)\left[\left(\frac{d}{dz}\right)h_n^{(1)}(z)\right]\right\}$$

$$= \lim_{z\to k_pR_p}\left(\frac{k_p}{(-i\omega\epsilon_p)}\right)\left\{\frac{1}{iz^2}\right\} = \frac{1}{\omega\epsilon_pk_pR_p^2} \tag{10.1.1.19}$$

We also use the definition that for all complex numbers z including the z value we use in our vector spherical harmonics which is

$$z = k(p,(-1)^{\ell}j\omega)r, \tag{10.1.1.20}$$

which is the product of the tissue propagation constant and the distance r from the origin to the brain wave signal observation point, by the rule (10.1.1.17)

We also need the relationships

Lemma 10.1 *If $f_n(z)$ represents a spherical Bessel or Hankel function that is a solution of the differential equation (10.1.1.5) then for all indices n or, in particular, for*

$$f_n(z) \in \left\{ j_n(z), y_n(z), h_n^{(1)}(z), h_n^{(2)}(z) \right\} \tag{10.1.1.21}$$

we have

$$(n+2)\frac{f_{n+1}(z)}{z} + \left(\frac{d}{dz}\right) f_{n+1}(z) = f_n(z) \tag{10.1.1.22}$$

and

$$-(n-1)\frac{f_{n-1}(z)}{z} + \left(\frac{d}{dz}\right) f_{n-1}(z) = -f_n(z) \tag{10.1.1.23}$$

A corollary of this lemma that we use is that for $\tilde{\ell}$ equal to 1 or 2 we have with $W_n^{(\tilde{\ell})}$ being defined by (10.1.1.17) and $Z_n^{(\tilde{\ell})}$ being defined by (10.1.1.16) that

$$\frac{Z_{n+1}^{(\tilde{\ell})}(z)}{z} + \frac{W_{n+1}^{(\tilde{\ell})}(z)}{n+1} = \frac{Z_{n+1}^{(\tilde{\ell})}(z)}{z} + \left(\frac{1}{n+1}\right)\left\{\frac{Z_{n+1}^{(\tilde{\ell})}(z)}{z} + \left(\frac{d}{dz}\right) Z_{n+1}^{(\tilde{\ell})}(z)\right\}$$

$$= \left(\frac{1}{n+1}\right)\left\{\frac{((n+1)+1)Z_{n+1}^{(\tilde{\ell})}(z)}{z} + \left(\frac{d}{dz}\right) Z_{n+1}^{(\tilde{\ell})}(z)\right\} = \left(\frac{1}{n+1}\right) Z_n^{(\tilde{\ell})}(z) \tag{10.1.1.24}$$

Now using equation (10.1.1.23) of the Lemma we have from the definition (10.1.1.17) of $W_n^{(\tilde{\ell})}$ that

$$\frac{Z_{n-1}^{(\tilde{\ell})}(z)}{z} - \frac{W_{n-1}^{(\tilde{\ell})}(z)}{n} = \frac{Z_{n-1}^{(\tilde{\ell})}(z)}{z} - \left(\frac{1}{n}\right)\left\{\frac{Z_{n-1}^{(\tilde{\ell})}(z)}{(}z) + \left(\frac{d}{dz}\right) Z_{n-1}^{(\tilde{\ell})}(z)\right\}$$

$$= \frac{1}{n}\left\{(n-1)\left(\frac{Z_{n-1}^{(\tilde{\ell})}(z)}{z}\right) - \left(\frac{d}{dz}\right) Z_{n-1}^{(\tilde{\ell})}\right\} = \frac{Z_n^{(\tilde{\ell})}}{n} \tag{10.1.1.25}$$

10.1.2 The Papperitz Differential Equation and Associated Legendre Functions

The associated Legendre function $P_n^{|m|}(\xi)$ can be computed from the Rodriques formula

$$P_n^{|m|}(\xi) = (1-\xi^2)^{|m|}/2\left(\frac{d}{d\xi}\right)^{n+|m|}(\xi^2-1)^n \tag{10.1.2.1}$$

These functions can be derived from the general Papperitz differential equation which has the form

$$\frac{d^2u}{dz^2} + \left\{\frac{1-\alpha-\tilde{\alpha}}{z-\mathrm{a}} + \frac{1-\beta-\tilde{\beta}}{z-\mathrm{b}} + \frac{1-\gamma-\tilde{\gamma}}{z-\mathrm{c}}\right\}\frac{du}{dz}$$
$$+ \left\{\alpha\tilde{\alpha}\left(\frac{(\mathrm{a}-\mathrm{b})(\mathrm{a}-\mathrm{c})}{z-\mathrm{a}}\right) + \beta\tilde{\beta}\left(\frac{(\mathrm{b}-\mathrm{c})(\mathrm{b}-\mathrm{a})}{z-\mathrm{b}}\right)\right.$$

$$+ \quad \gamma\tilde{\gamma}\left(\frac{(\mathrm{c}-\mathrm{a})(\mathrm{c}-\mathrm{b})}{z-\mathrm{c}}\right)\Bigg\}\frac{u}{(z-\mathrm{a})(z-\mathrm{b})(z-\mathrm{c})}=0 \tag{10.1.2.2}$$

The differential equation (10.1.2.2) was studied by Riemann ([133], page 206) who denoted it using the Riemann $\mathcal{P}$ function, or the Riemann $\mathcal{P}$ scheme in some literature, as

$$u(z)=\mathcal{P}\left\{\begin{array}{cccc}\mathrm{a} & \mathrm{b} & \mathrm{c} & \\ \alpha & \beta & \gamma & z \\ \tilde{\alpha} & \tilde{\beta} & \tilde{\gamma} & \end{array}\right\} \tag{10.1.2.3}$$

which represents a solution of the differential equation (10.1.2.2). We note that in equation (10.1.2.2) that every time there is an a, b, or an c in a numerator, there is also one in the denominator which means that we can take the limit of all terms in the differential equation (10.1.2.2) or (10.1.2.3) as one or more of these terms approach infinity. Thus, the Riemann $\mathcal{P}$ function defined by

$$w(z)=\mathcal{P}\left\{\begin{array}{ccccc} 0 & \infty & 1 & \\ m/2 & n+1 & m/2 & z \\ -m/2 & -n & -m/2 & \end{array}\right\} \tag{10.1.2.4}$$

is a solution of the differential equation

$$\frac{d^2w}{dz^2}+\left\{\frac{1}{z}+\frac{1}{z-1}\right\}\frac{dw}{dz}+\left[\frac{m^2/4}{z^2(z-1)}+\frac{(-n)(n+1)}{z(z-1)}+\frac{(-m^2/4}{(z(z-1))^2}\right]w=0 \tag{10.1.2.5}$$

Collecting terms in (10.1.2.5) gives

$$\frac{d^2w}{dz^2}+\frac{2z-1}{z(z-1)}\frac{dw}{dz}+\left[\frac{-m^2/4-n(n+1)z(z-1)}{(z(z-1))^2}\right]w=0 \tag{10.1.2.6}$$

If in equation (10.1.2.6) we set

$$z=\frac{1}{2}-\frac{\xi}{2} \tag{10.1.2.7}$$

and define

$$\psi(\xi)=w(z) \tag{10.1.2.8}$$

we see immediately that

$$4\frac{d^2\psi}{d\xi^2}-\left(\frac{8\xi}{1-\xi^2}\right)\frac{d\psi}{d\xi}+4\left[\frac{-m^2+n(n+1)(1-\xi^2}{(1-\xi^2)^2}\right]\psi(\xi)=0 \tag{10.1.2.9}$$

Multiplying all terms of (10.1.2.9) by

$$\xi\rightarrow\frac{(1-\xi^2)}{4} \tag{10.1.2.10}$$

we have

$$(1-\xi^2)\frac{d^2\psi}{d\xi^2}-2\xi\frac{d\psi}{d\xi}+\left[-\frac{m^2}{(1-\xi^2)}+n(n+1)\right]\psi(\xi)=0 \tag{10.1.2.11}$$

which is exactly the differential equation satisfied by the associated Legendre functions ([133], page 324). The Papperitz representation gives us access to powerful methods for verification of recursion relationships needed for validation of our brain activity measurement solutions.

10.1.3 Associated Legendre Function Recursion Relationships

We prove a series of theorems concerning associated Legendre function recursion relationships needed to validate our brain activity model.

When n is a nonnegative integer and m is a nonnegative integer not larger than n define negative order associated Legendre functions using the fact that for all nonnegative integers n and all nonnegative integers m not exceeding m that

$$P_n^m(x) = (1-x^2)^{m/2}\left(\frac{d}{dx}\right)^m\left(\frac{1}{2^n n!}\right)\left(\frac{d}{dx}\right)^n (x^2-1)^n \tag{10.1.3.1}$$

by

We can interpret the recursion relationships needed in this model for positive or negative orders through the following definition.

Notice that if you interchange m and $-m$ in equation (10.1.3.5), the new relationship is consistent.

The following theorem gives us the main identities for associated Legendre functions.

We need the following definition for negative degrees and negative orders

Definition 10.2 *For every nonnegative integer n and all integers m we have*

$$P_{-n-1}^m(x) = P_n^m(x) \tag{10.1.3.2}$$

which implies

$$P_{0-1}^0 = P_0(x) = 1 \tag{10.1.3.3}$$

and for all nonnegative integers n and all integers m ranging from $-n$ to $+n$ we have

$$P_n^{-m}(x) = (-1)^m \frac{(n-m)!}{(n+m)!} P_n^m(x) \tag{10.1.3.4}$$

which is equation (2.5.18) of Edmonds ([40]) and

$$\left(\frac{d}{d\theta}\right) P_n^{-m}(\cos(\theta)) = \left(\frac{(n-m)!}{(n+m)!}\right)\left(\frac{d}{d\theta}\right) P_n^m(\cos(\theta)) \tag{10.1.3.5}$$

The following theorem gives identities needed to establish representation of the vector potential.

Theorem 10.1 *If n is a nonnegative integer and m is a nonnegative integer not exceeding n, then*

$$P_n^m(x) = \left(1-x^2\right)^{m/2} \frac{d^m P_n(x)}{dx^m} = \left\{\frac{(1-x^2)^{m/2}}{2^n n!}\right\} \frac{d^{n+m}(x^2-1)^n}{dx^{n+m}} \tag{10.1.3.6}$$

We also have the relationship,

$$\sin(\theta) P_n^m(\cos(\theta)) = \left(\frac{1}{2n+1}\right)\left\{P_{n+1}^{m+1}(\cos(\theta)) - P_{n-1}^{m+1}(\cos(\theta))\right\} \tag{10.1.3.7}$$

$$\cos(\theta)P_n^m(\cos(\theta)) = \frac{(n-m+1)P_{n+1}^m(\cos(\theta)) + (n+m)P_{n-1}^m(\cos(\theta))}{2n+1} \qquad (10.1.3.8)$$

and

$$P_n^{m+1}(\cos(\theta)) = \frac{(n+m+1)\cos(\theta)P_n^m(\cos(\theta)) - (n-m+1)P_{n+1}^m(\cos(\theta))}{\sin(\theta)} \qquad (10.1.3.9)$$

A data table showing the correctness of (10.1.3.9) is shown below

```
3 1 = N,M
 37. = theta in degrees
   4.338762973472225E+00 = (P sub n sup m+1)
   4.338762973472225E+00 = [ (n+m+1) \cos(theta) (P sub n sup m) -
     (n-m+1) (P sub n+1 sup m )]/\sin(theta)
7 = NOFCAL =number of calculations
3 -3 = N,M
   3.615635811226854E-02 = (P sub n sup m+1)
   3.615635811226854E-02 = [ (n+m+1) \cos(theta) (P sub n sup m) -
     (n-m+1) (P sub n+1 sup m )]/\sin(theta)
 (n-m+1) \sin( theta) )
3 -2 = N,M
  -1.646786611136893E-01 = (P sub n sup m+1)
  -1.646786611136893E-01 = [ (n+m+1) \cos(theta) (P sub n sup m) -
     (n-m+1) (P sub n+1 sup m )]/\sin(theta)
 (n-m+1) \sin( theta) )
3 -1 = N,M
   7.550834780192207E-02 = (P sub n sup m+1)
   7.550834780192214E-02 = [ (n+m+1) \cos(theta) (P sub n sup m) -
     (n-m+1) (P sub n+1 sup m )]/\sin(theta)
 (n-m+1) \sin( theta) )
3 0 = N,M
   1.976143933364271E+00 = (P sub n sup m+1)
   1.976143933364271E+00 = [ (n+m+1) \cos(theta) (P sub n sup m) -
     (n-m+1) (P sub n+1 sup m )]/\sin(theta)
 (n-m+1) \sin( theta) )
3 1 = N,M
   4.338762973472225E+00 = (P sub n sup m+1)
   4.338762973472225E+00 = [ (n+m+1) \cos(theta) (P sub n sup m) -
     (n-m+1) (P sub n+1 sup m )]/\sin(theta)
 (n-m+1) \sin( theta) )
3 2 = N,M
   3.269492411096037E+00 = (P sub n sup m+1)
   3.269492411096035E+00 = [ (n+m+1) \cos(theta) (P sub n sup m) -
     (n-m+1) (P sub n+1 sup m )]/\sin(theta)
 (n-m+1) \sin( theta) )
3 3 = N,M
```

```
  0.000000000000000E+00 = (P sub n sup m+1)
  1.821731254024130E-15 = [ (n+m+1) \cos(theta) (P sub n sup m) -
    (n-m+1) (P sub n+1 sup m )]/\sin(theta)
(n-m+1) \sin( theta) )
```

We also have

$$-\sin(\theta)\frac{dP_n^m(\cos(\theta))}{d\theta} = (n+1)\cos(\theta)P_n^m(\cos(\theta)) - (n-m+1)P_{n+1}^m(\cos(\theta)) \quad (10.1.3.10)$$

and

$$-\sin(\theta)\frac{dP_n^m(\cos(\theta))}{d\theta} = (n+m)P_{n-1}^m(\cos(\theta)) - n\cos(\theta)P_n^m(\cos(\theta)) \quad (10.1.3.11)$$

which together tell us that

$$\frac{dP_n^m(\cos(\theta))}{d\theta} = \frac{n(n-m+1)P_{n+1}^m(\cos(\theta)) - (n+1)(n+m)P_{n-1}^m(\cos(\theta))}{(2n+1)\sin(\theta)} \quad (10.1.3.12)$$

Proof of Theorem. Some of these identities are found in Gradshteyn and Ryzhik ([51], pages 1004-1007) and in Magnus and Oberhettinger ([80]). Gradshteyn and Ryzhik ([51], page 1005, equation 4 of 8.7333) gives

$$P_{\nu-1}^{\mu}(x) - P_{\nu-1}^{\mu}(x) = (2\nu+1)\sqrt{1-x^2}P_{\nu}^{\mu-1}(x) \quad (10.1.3.13)$$

which is equivalent to equation (10.1.3.7) of the theorem.

Equation (10.1.3.8) of the theorem is equivalent to equation 2 of section 8.7333 of Gradshteyn and Ryzhik ([51], page 1005) which is given in the form

$$(2\nu+1)xP_{\nu}^{\mu}(x) = (\nu-\mu+1)P_{\nu+1}^{\mu}(x) + (\nu+\mu)P_{\nu-1}^{\mu}(x) \quad (10.1.3.14)$$

We prove the validity of equation (10.1.3.12) for all integer values of m and n. Dividing both sides of equation (10.1.3.10) by $n+1$ gives us

$$-\frac{\sin(\theta)}{n+1}\frac{dP_n^m(\cos(\theta))}{d\theta} = \cos(\theta)P_n^m(\cos(\theta)) - \frac{n-m+1}{n+1}P_{n+1}^m(\cos(\theta)) \quad (10.1.3.15)$$

Dividing both sides of equation (10.1.3.11) by n gives

$$-\frac{\sin(\theta)}{n}\frac{dP_n^m(\cos(\theta))}{d\theta} = -\cos(\theta)P_n^m(\cos(\theta)) + \frac{n+m}{n}P_{n-1}^m(\cos(\theta)) \quad (10.1.3.16)$$

Adding equations (10.1.3.15) and (10.1.3.16) gives us

$$\frac{(2n+1)}{n(n+1)}\frac{dP_n^m(\cos(\theta))}{d\theta} = \frac{1}{\sin(\theta)}\left[\frac{(n-m+1)}{(n+1)}P_{n+1}^m(\cos(\theta)) - \frac{(n+m)}{n}P_{n-1}^m(\cos(\theta)\right] \quad (10.1.3.17)$$

Multiplying both sides of equation (10.1.3.17) by the product of n and $n+1$ divided by $2n+1$ gives us equation (10.1.3.12). A computer check of this identity for negative as well as positive values of m is shown below.

```
          5           3   60.0000000000000      = N,M,THETAD
 0.500000000000000      = X = COSTH
 -1828.59910844391      = VLEFT=
 = (2n+1)\sin(theta)*(d/dtheta)P_{n}^{m}(x)
 -1828.59910844391      = VRIGHT=
 =(n(n-m+1))P_{n+1}^{m}(x)-(n+1)(n+m)P_{n-1}^{m}(x)
          5          -3 = N,M
-9.521484374999995E-003 = DPDTHR(N,M,THETA)
-2.114319833458096E-004 = ALF(N+1,M,COSTH)
 6.765823467065927E-003 =ALF(NM1,M,COSTH)
          5          -3   60.0000000000000
               = N,M,THETAD
 0.500000000000000      = X = COSTH
-9.070432085535253E-002 = VLEFT=
 = (2n+1)\sin(theta)*(d/dtheta)P_{n}^{m}(x)
-9.070432085535256E-002 = VRIGHT=
 =(n(n-m+1))P_{n+1}^{m}(x)-(n+1)(n+m)P_{n-1}^{m}(x)
```

Another major identity needed to verify that the θ components of the expansion of the vector potential $\boldsymbol{A}$ in terms of vector spherical harmonics and the expansion in terms of vector spherical harmonics are identical is the following.

Theorem 10.2 *For every nonnegative integer n and every integer m from $-n$ to $+n$ we have*

$$\left[\left(\frac{n-\mid m\mid+1}{n+1}\right)\frac{dP_{n+1}^{|m|}(\cos(\theta))}{d\theta}-\left(\frac{n+\mid m\mid}{n}\right)\frac{dP_{n-1}^{|m|}(\cos(\theta))}{d\theta}\right.$$
$$\left.-\left(\frac{m^2(2n+1)}{n(n+1)}\right)\frac{P_n^{|m|}(\cos(\theta))}{\sin(\theta)}\right]\exp(im\phi)$$
$$=-(2n+1)\sin(\theta)P_n^{|m|}(\cos(\theta))\exp(im\phi) \tag{10.1.3.18}$$

Using the definition in equation (10.1.3.4) we also have for all nonegative integers n and all integers m ranging from $-n$ to $+n$ the relationship

$$\left[\left(\frac{n-m+1}{n+1}\right)\frac{dP_{n+1}^{m}(\cos(\theta))}{d\theta}-\left(\frac{n+m}{n}\right)\frac{dP_{n-1}^{m}(\cos(\theta))}{d\theta}\right.$$
$$\left.-\left(\frac{m^2(2n+1)}{n(n+1)}\right)\frac{P_n^{m}(\cos(\theta))}{\sin(\theta)}\right]\exp(im\phi)$$
$$=-(2n+1)\sin(\theta)P_n^{m}(\cos(\theta))\exp(im\phi) \tag{10.1.3.19}$$

Proof of Theorem. This is obtained by the use of the ordinary differential equation satisfied by the associated Legendre function and equation (10.1.3.12) A data table showing the left and right sides of this equations as evaluated for several values of n and m by a computer program is shown below

```
This file is THETAID.DAT produced by ALFTSUM.FOR
  We next verify the complex theta identity
  We print out left and right sides of the identity
  CLEFT =
 [\frac{n-|m|+1}{n+1}(d/d \theta)
  P_{n+1}^{|m|}(\cos(\theta)) -
 \frac{n+|m|}{n}(d/d \theta)
  P_{n-1}^{|m|}(\cos( \theta)) -
  (mm(2n+1)/(n(n+1))
 P_{n}^{|m|}(\cos(\theta))/\sin(\theta)]\exp(im \phi)
  CRIGHT =
  -(2n+1)\sin(\theta)P_{n}^{|m|}(\cos(\theta))\exp(i m \phi)
       33.000000000000000 = THETAD
       37.000000000000000 = PHID
           1           -1           1 = N,M,MA
    (-7.107017754742906E-001,5.355522013238984E-001) = CLEFT
    (-7.107017754742910E-001,5.355522013238987E-001) = CRIGHT
           1            0           0 = N,M,MA
         (-1.370318186463901,0.000000000000000E+000) = CLEFT
         (-1.370318186463901,0.000000000000000E+000) = CRIGHT
           1            1           1 = N,M,MA
   (-7.107017754742906E-001,-5.355522013238984E-001) = CLEFT
   (-7.107017754742910E-001,-5.355522013238987E-001) = CRIGHT
           2           -2           2 = N,M,MA
         (-6.679679545720074E-001,2.329481092797287) = CLEFT
         (-6.679679545720080E-001,2.329481092797289) = CRIGHT
           2           -1           1 = N,M,MA
              (-2.980223308384224,2.245759344243680) = CLEFT
              (-2.980223308384225,2.245759344243681) = CRIGHT
           2            0           0 = N,M,MA
         (-1.511516241731492,0.000000000000000E+000) = CLEFT
         (-1.511516241731491,0.000000000000000E+000) = CRIGHT
           2            1           1 = N,M,MA
             (-2.980223308384224,-2.245759344243680) = CLEFT
             (-2.980223308384225,-2.245759344243681) = CRIGHT
           2            2           2 = N,M,MA
        (-6.679679545720074E-001,-2.329481092797287) = CLEFT
        (-6.679679545720080E-001,-2.329481092797289) = CRIGHT
           3           -3           3 = N,M,MA
               (3.310956837838389,8.625337451925956) = CLEFT
               (3.310956837838395,8.625337451925971) = CRIGHT
           3           -2           2 = N,M,MA
             (-3.921435446811742,13.675670617801000) = CLEFT
             (-3.921435446811744,13.675670617801000) = CRIGHT
           3           -1           1 = N,M,MA
```

```
          (-6.260533297103741,4.717650221835924) = CLEFT
          (-6.260533297103741,4.717650221835924) = CRIGHT
       3           0           0 = N,M,MA
(-8.262770302945248E-001,0.000000000000000E+000) = CLEFT
(-8.262770302945240E-001,0.000000000000000E+000) = CRIGHT
       3           1           1 = N,M,MA
         (-6.260533297103741,-4.717650221835924) = CLEFT
         (-6.260533297103741,-4.717650221835924) = CRIGHT
       3           2           2 = N,M,MA
        (-3.921435446811742,-13.675670617801000) = CLEFT
        (-3.921435446811744,-13.675670617801000) = CRIGHT
       3           3           3 = N,M,MA
          (3.310956837838389,-8.625337451925956) = CLEFT
          (3.310956837838395,-8.625337451925971) = CRIGHT
       4          -4           4 = N,M,MA
         (38.405738008763170,23.998568619135260) = CLEFT
         (38.405738008763190,23.998568619135280) = CRIGHT
       4          -3           3 = N,M,MA
         (24.991218464694390,65.104349935749170) = CLEFT
         (24.991218464694400,65.104349935749200) = CRIGHT
       4          -2           2 = N,M,MA
        (-11.793710424451120,41.129556080707920) = CLEFT
        (-11.793710424451120,41.129556080707920) = CRIGHT
       4          -1           1 = N,M,MA
          (-8.599039107647558,6.479840746560134) = CLEFT
          (-8.599039107647558,6.479840746560134) = CRIGHT
       4           0           0 = N,M,MA
 (4.813549172134375E-001,0.000000000000000E+000) = CLEFT
 (4.813549172134379E-001,0.000000000000000E+000) = CRIGHT
       4           1           1 = N,M,MA
         (-8.599039107647558,-6.479840746560134) = CLEFT
         (-8.599039107647558,-6.479840746560134) = CRIGHT
       4           2           2 = N,M,MA
       (-11.793710424451120,-41.129556080707920) = CLEFT
       (-11.793710424451120,-41.129556080707920) = CRIGHT
       4           3           3 = N,M,MA
        (24.991218464694390,-65.104349935749170) = CLEFT
        (24.991218464694400,-65.104349935749200) = CRIGHT
       4           4           4 = N,M,MA
        (38.405738008763170,-23.998568619135260) = CLEFT
        (38.405738008763190,-23.998568619135280) = CRIGHT
```

We prove the following theorem.

Theorem 10.3 *For all positive integers n and all nonnegative integers m satisfying*

$$m \in \{-n, -(n-1), \cdots, -1, 0, +1, \cdots, +n\} \tag{10.1.3.20}$$

we have for

$$\xi = \cos(\theta) \tag{10.1.3.21}$$

the relations

$$(2n+1)\cos(\theta)P_n^{|m|}(\cos(\theta)) = (n- \mid m \mid +1)P_{n+1}^{|m|}(\cos(\theta)) + (n+ \mid m \mid)P_{n-1}^{|m|}(\cos(\theta)) \tag{10.1.3.22}$$

and

$$(2n+1)\sin(\theta)P_n^{|m|}(\cos(\theta)) = P_{n+1}^{|m|+1}(\cos(\theta)) - P_{n-1}^{|m|+1}(\cos(\theta)$$
$$= (n+ \mid m \mid)(n+ \mid m \mid -1)P_{n-1}^{|m|-1}(\cos(\theta)) - (n- \mid m \mid +1)(n- \mid m \mid +2)P_{n+1}^{|m|-1}(\cos(\theta)) \tag{10.1.3.23}$$

A data snippet showing the calculation of the left and right sides of (10.1.3.23) from data file PMNRREL.DAT produced by program PMNAT.FOR is

```
33.0000000000000      = theta in degrees
          5            3 = N,M
   270.856905936849
  = (2n+1)\sin(theta)P_{n}^{m}(\cos(theta))
   270.856905936848
  = P_{n+1}^{m+1}(\cos(theta))-P_{n-1}^{m+1}(\cos(theta))
   270.856905936849      =
   (n+m)(n+m-1)P_{n-1}^{m-1}(\cos(theta))
  - (n-m+1)(n-m+2)P_{n+1}^{m-1}(\cos(theta))
```

We need the following identity for validation of the θ component of the $(U_q + iV_q)/2$ term of the expansion of the vector potential of brain activity in terms of vector spherical harmonics.

Theorem 10.4 *For all nonnegative integers n and all nonnegative integers m not exceeding n we have*

$$(-1)\left(\frac{(n-m+1)(n-m+2)}{n+1}\right)\left(\frac{d}{d\theta}\right)P_{n+1}^{m-1}(\cos(\theta))$$
$$+(-1)\left(\frac{(n+m)(n+m-1)}{n}\right)\left(\frac{d}{d\theta}\right)P_{n-1}^{m-1}(\cos(\theta))$$
$$+\left(\frac{(n+m)(n-m+1)(2n+1)(m-1)}{n(n+1)}\right)\left(\frac{P_n^{m-1}(\cos(\theta))}{\sin(\theta)}\right) = (2n+1)\cos(\theta)P_n(\cos(\theta)) \tag{10.1.3.24}$$

Equation (10.1.3.24) can be proven by expanding the Rodriques representations. A set of computer output showing the left and right sides of the above equation (10.1.3.24) is shown below.

```
The identity for the (U_{q}+iV_{q})/2
  theta component
          1           1 = N,M
```

```
 1.37031818646390
=-((n-m+1)(n-m+2)/(n+1))(d/d theta)P_{n+1}^{m-1}(\cos(theta))
-((n+m)(n+m-1)/n)(d/d theta)P_{n-1}^{m-1}(\cos(theta))
+ [(n+m)(n-m+1)(2n+1)(m-1)/(n(n+1))] *
P_{n}^{m}(\cos(theta))/\sin(\theta)
 1.37031818646390
= (2n+1)\cos(theta)P_{n}^{m}(\cos(theta))
         2           1 = N,M
 5.74622765853812
=-((n-m+1)(n-m+2)/(n+1))(d/d theta)P_{n+1}^{m-1}(\cos(theta))
-((n+m)(n+m-1)/n)(d/d theta)P_{n-1}^{m-1}(\cos(theta))
+ [(n+m)(n-m+1)(2n+1)(m-1)/(n(n+1))] *
P_{n}^{m}(\cos(theta))/\sin(\theta)
 5.74622765853812
= (2n+1)\cos(theta)P_{n}^{m}(\cos(theta))
         2           2 = N,M
 3.73164387369620
=-((n-m+1)(n-m+2)/(n+1))(d/d theta)P_{n+1}^{m-1}(\cos(theta))
-((n+m)(n+m-1)/n)(d/d theta)P_{n-1}^{m-1}(\cos(theta))
+ [(n+m)(n-m+1)(2n+1)(m-1)/(n(n+1))] *
P_{n}^{m}(\cos(theta))/\sin(\theta)
 3.73164387369620
= (2n+1)\cos(theta)P_{n}^{m}(\cos(theta))
         3           1 = N,M
 12.0710583961309
=-((n-m+1)(n-m+2)/(n+1))(d/d theta)P_{n+1}^{m-1}(\cos(theta))
-((n+m)(n+m-1)/n)(d/d theta)P_{n-1}^{m-1}(\cos(theta))
+ [(n+m)(n-m+1)(2n+1)(m-1)/(n(n+1))] *
P_{n}^{m}(\cos(theta))/\sin(\theta)
 12.0710583961309
= (2n+1)\cos(theta)P_{n}^{m}(\cos(theta))
         3           2 = N,M
 21.9073392084600
=-((n-m+1)(n-m+2)/(n+1))(d/d theta)P_{n+1}^{m-1}(\cos(theta))
-((n+m)(n+m-1)/n)(d/d theta)P_{n-1}^{m-1}(\cos(theta))
+ [(n+m)(n-m+1)(2n+1)(m-1)/(n(n+1))] *
P_{n}^{m}(\cos(theta))/\sin(\theta)
 21.9073392084600
= (2n+1)\cos(theta)P_{n}^{m}(\cos(theta))
         3           3 = N,M
 14.2267924287275
=-((n-m+1)(n-m+2)/(n+1))(d/d theta)P_{n+1}^{m-1}(\cos(theta))
-((n+m)(n+m-1)/n)(d/d theta)P_{n-1}^{m-1}(\cos(theta))
+ [(n+m)(n-m+1)(2n+1)(m-1)/(n(n+1))] *
P_{n}^{m}(\cos(theta))/\sin(\theta)
```

```
 14.2267924287275
= (2n+1)\cos(theta)P_{n}^{m}(\cos(theta))
         4           1 = N,M
 16.5799778218649
=-((n-m+1)(n-m+2)/(n+1))(d/d theta)P_{n+1}^{m-1}(\cos(theta))
-((n+m)(n+m-1)/n)(d/d theta)P_{n-1}^{m-1}(\cos(theta))
+ [(n+m)(n-m+1)(2n+1)(m-1)/(n(n+1))] *
P_{n}^{m}(\cos(theta))/\sin(\theta)
 16.5799778218649
= (2n+1)\cos(theta)P_{n}^{m}(\cos(theta))
         4           2 = N,M
 65.8862853409620
=-((n-m+1)(n-m+2)/(n+1))(d/d theta)P_{n+1}^{m-1}(\cos(theta))
-((n+m)(n+m-1)/n)(d/d theta)P_{n-1}^{m-1}(\cos(theta))
+ [(n+m)(n-m+1)(2n+1)(m-1)/(n(n+1))] *
P_{n}^{m}(\cos(theta))/\sin(\theta)
 65.8862853409620
= (2n+1)\cos(theta)P_{n}^{m}(\cos(theta))
         4           3 = N,M
 107.384328776183
=-((n-m+1)(n-m+2)/(n+1))(d/d theta)P_{n+1}^{m-1}(\cos(theta))
-((n+m)(n+m-1)/n)(d/d theta)P_{n-1}^{m-1}(\cos(theta))
+ [(n+m)(n-m+1)(2n+1)(m-1)/(n(n+1))] *
P_{n}^{m}(\cos(theta))/\sin(\theta)
 107.384328776183
= (2n+1)\cos(theta)P_{n}^{m}(\cos(theta))
         4           4 = N,M
 69.7361984976709
=-((n-m+1)(n-m+2)/(n+1))(d/d theta)P_{n+1}^{m-1}(\cos(theta))
-((n+m)(n+m-1)/n)(d/d theta)P_{n-1}^{m-1}(\cos(theta))
+ [(n+m)(n-m+1)(2n+1)(m-1)/(n(n+1))] *
P_{n}^{m}(\cos(theta))/\sin(\theta)
 69.7361984976710
= (2n+1)\cos(theta)P_{n}^{m}(\cos(theta))
         5           1 = N,M
 14.5281258312329
=-((n-m+1)(n-m+2)/(n+1))(d/d theta)P_{n+1}^{m-1}(\cos(theta))
-((n+m)(n+m-1)/n)(d/d theta)P_{n-1}^{m-1}(\cos(theta))
+ [(n+m)(n-m+1)(2n+1)(m-1)/(n(n+1))] *
P_{n}^{m}(\cos(theta))/\sin(\theta)
 14.5281258312329
= (2n+1)\cos(theta)P_{n}^{m}(\cos(theta))
         5           2 = N,M
 133.756953092333
=-((n-m+1)(n-m+2)/(n+1))(d/d theta)P_{n+1}^{m-1}(\cos(theta))
```

```
-((n+m)(n+m-1)/n)(d/d theta)P_{n-1}^{m-1}(\cos(theta))
+ [(n+m)(n-m+1)(2n+1)(m-1)/(n(n+1))] *
P_{n}^{m}(\cos(theta))/\sin(\theta)
 133.756953092333
= (2n+1)\cos(theta)P_{n}^{m}(\cos(theta))
         5           3 = N,M
 417.083059659375
=-((n-m+1)(n-m+2)/(n+1))(d/d theta)P_{n+1}^{m-1}(\cos(theta))
-((n+m)(n+m-1)/n)(d/d theta)P_{n-1}^{m-1}(\cos(theta))
+ [(n+m)(n-m+1)(2n+1)(m-1)/(n(n+1))] *
P_{n}^{m}(\cos(theta))/\sin(\theta)
 417.083059659375
= (2n+1)\cos(theta)P_{n}^{m}(\cos(theta))
         5           4 = N,M
 643.342669204362
=-((n-m+1)(n-m+2)/(n+1))(d/d theta)P_{n+1}^{m-1}(\cos(theta))
-((n+m)(n+m-1)/n)(d/d theta)P_{n-1}^{m-1}(\cos(theta))
+ [(n+m)(n-m+1)(2n+1)(m-1)/(n(n+1))] *
P_{n}^{m}(\cos(theta))/\sin(\theta)
 643.342669204362
= (2n+1)\cos(theta)P_{n}^{m}(\cos(theta))
         5           5 = N,M
 417.791614409267
=-((n-m+1)(n-m+2)/(n+1))(d/d theta)P_{n+1}^{m-1}(\cos(theta))
-((n+m)(n+m-1)/n)(d/d theta)P_{n-1}^{m-1}(\cos(theta))
+ [(n+m)(n-m+1)(2n+1)(m-1)/(n(n+1))] *
P_{n}^{m}(\cos(theta))/\sin(\theta)
 417.791614409267
= (2n+1)\cos(theta)P_{n}^{m}(\cos(theta))
```

The following identity is used with the ϕ component of the $(U_q+iV_q)/2$ term for describing an arbitrarily oriented dipole in the presence of a spherical interface.

Theorem 10.5 *For all nonnegative integers n and all integers m we have*

$$\begin{aligned}
&\left(\frac{(n-m+1)(n-m+2)(m-1)}{n+1}\right)\left(\frac{P_{n+1}^{m-1}(\cos(\theta))}{\sin(\theta)}\right)\\
&+\left(\frac{(n+m)(n+m-1)(m-1)}{n}\right)\left(\frac{P_{n-1}^{m-1}(\cos(\theta))}{\sin(\theta)}\right)\\
&-\left(\frac{(n+m)(n-m+1)(2n+1)}{n(n+1)}\right)\left\{\left(\frac{d}{d\theta}\right)P_n^{m-1}(\cos(\theta))\right\}\\
&=(2n+1)P_n^m(\cos(\theta)) \qquad (10.1.3.25)
\end{aligned}$$

This can be proven using the Rodrigues representation of the associated Legendre functions and their derivatives and collecting common powers of the independent variables.

We programmed the left and right sides of the identity (10.1.3.25) and obtained the following table.

```
(U_{q}+iV_{q})/2 phi component
  N,M =            1           1
   1.63391710504508
  = ((n-m+1)(n-m+2)(m-1)/(n+1))*
  P_{n+1}^{m-1}(\cos(theta))/\sin(theta)
  + ((n+m)(n-m+1)(2n+1)/(n(n+1))*
  P_{n-1}^{m-1}(\cos(theta))/\sin(theta)
  -(((n+m)(n-m+1)(2n+1))/(n*(n+1)))*
  (d/d theta)P_{n}^{m-1}(\cos(theta))
   1.63391710504508
  = (2n+1)P_{n}^{m-1}(\cos(theta))
  (U_{q}+iV_{q})/2 phi component
  N,M =            2           1
   6.85159093231951
  = ((n-m+1)(n-m+2)(m-1)/(n+1))*
  P_{n+1}^{m-1}(\cos(theta))/\sin(theta)
  + ((n+m)(n-m+1)(2n+1)/(n(n+1))*
  P_{n-1}^{m-1}(\cos(theta))/\sin(theta)
  -(((n+m)(n-m+1)(2n+1))/(n*(n+1)))*
  (d/d theta)P_{n}^{m-1}(\cos(theta))
   6.85159093231951
  = (2n+1)P_{n}^{m-1}(\cos(theta))
  (U_{q}+iV_{q})/2 phi component
  N,M =            2           2
   4.44947517693149
  = ((n-m+1)(n-m+2)(m-1)/(n+1))*
  P_{n+1}^{m-1}(\cos(theta))/\sin(theta)
  + ((n+m)(n-m+1)(2n+1)/(n(n+1))*
  P_{n-1}^{m-1}(\cos(theta))/\sin(theta)
  -(((n+m)(n-m+1)(2n+1))/(n*(n+1)))*
  (d/d theta)P_{n}^{m-1}(\cos(theta))
   4.44947517693150
  = (2n+1)P_{n}^{m-1}(\cos(theta))
  (U_{q}+iV_{q})/2 phi component
  N,M =            3           1
   14.3930869372256
  = ((n-m+1)(n-m+2)(m-1)/(n+1))*
  P_{n+1}^{m-1}(\cos(theta))/\sin(theta)
  + ((n+m)(n-m+1)(2n+1)/(n(n+1))*
  P_{n-1}^{m-1}(\cos(theta))/\sin(theta)
```

```
-(((n+m)(n-m+1)(2n+1))/(n*(n+1)))*
(d/d theta)P_{n}^{m-1}(\cos(theta))
 14.3930869372256
= (2n+1)P_{n}^{m-1}(\cos(theta))
(U_{q}+iV_{q})/2 phi component
N,M =            3           2
 26.1215071158734
= ((n-m+1)(n-m+2)(m-1)/(n+1))*
P_{n+1}^{m-1}(\cos(theta))/\sin(theta)
+ ((n+m)(n-m+1)(2n+1)/(n(n+1))*
P_{n-1}^{m-1}(\cos(theta))/\sin(theta)
-(((n+m)(n-m+1)(2n+1))/(n*(n+1)))*
(d/d theta)P_{n}^{m-1}(\cos(theta))
 26.1215071158734
= (2n+1)P_{n}^{m-1}(\cos(theta))
(U_{q}+iV_{q})/2 phi component
N,M =            3           3
 16.9635050668110
= ((n-m+1)(n-m+2)(m-1)/(n+1))*
P_{n+1}^{m-1}(\cos(theta))/\sin(theta)
+ ((n+m)(n-m+1)(2n+1)/(n(n+1))*
P_{n-1}^{m-1}(\cos(theta))/\sin(theta)
-(((n+m)(n-m+1)(2n+1))/(n*(n+1)))*
(d/d theta)P_{n}^{m-1}(\cos(theta))
 16.9635050668110
= (2n+1)P_{n}^{m-1}(\cos(theta))
(U_{q}+iV_{q})/2 phi component
N,M =            4           1
 19.7693569508258
= ((n-m+1)(n-m+2)(m-1)/(n+1))*
P_{n+1}^{m-1}(\cos(theta))/\sin(theta)
+ ((n+m)(n-m+1)(2n+1)/(n(n+1))*
P_{n-1}^{m-1}(\cos(theta))/\sin(theta)
-(((n+m)(n-m+1)(2n+1))/(n*(n+1)))*
(d/d theta)P_{n}^{m-1}(\cos(theta))
 19.7693569508258
= (2n+1)P_{n}^{m-1}(\cos(theta))
(U_{q}+iV_{q})/2 phi component
N,M =            4           2
 78.5603881418783
= ((n-m+1)(n-m+2)(m-1)/(n+1))*
P_{n+1}^{m-1}(\cos(theta))/\sin(theta)
+ ((n+m)(n-m+1)(2n+1)/(n(n+1))*
P_{n-1}^{m-1}(\cos(theta))/\sin(theta)
-(((n+m)(n-m+1)(2n+1))/(n*(n+1)))*
```

```
(d/d theta)P_{n}^{m-1}(\cos(theta))
 78.5603881418783
= (2n+1)P_{n}^{m-1}(\cos(theta))
(U_{q}+iV_{q})/2 phi component
N,M =            4           3
 128.041131858547
= ((n-m+1)(n-m+2)(m-1)/(n+1))*
P_{n+1}^{m-1}(\cos(theta))/\sin(theta)
+ ((n+m)(n-m+1)(2n+1)/(n(n+1))*
P_{n-1}^{m-1}(\cos(theta))/\sin(theta)
-(((n+m)(n-m+1)(2n+1))/(n*(n+1)))*
(d/d theta)P_{n}^{m-1}(\cos(theta))
 128.041131858547
= (2n+1)P_{n}^{m-1}(\cos(theta))
(U_{q}+iV_{q})/2 phi component
N,M =            4           4
 83.1508832705442
= ((n-m+1)(n-m+2)(m-1)/(n+1))*
P_{n+1}^{m-1}(\cos(theta))/\sin(theta)
+ ((n+m)(n-m+1)(2n+1)/(n(n+1))*
P_{n-1}^{m-1}(\cos(theta))/\sin(theta)
-(((n+m)(n-m+1)(2n+1))/(n*(n+1)))*
(d/d theta)P_{n}^{m-1}(\cos(theta))
 83.1508832705442
= (2n+1)P_{n}^{m-1}(\cos(theta))
(U_{q}+iV_{q})/2 phi component
N,M =            5           1
 17.3228039548639
= ((n-m+1)(n-m+2)(m-1)/(n+1))*
P_{n+1}^{m-1}(\cos(theta))/\sin(theta)
+ ((n+m)(n-m+1)(2n+1)/(n(n+1))*
P_{n-1}^{m-1}(\cos(theta))/\sin(theta)
-(((n+m)(n-m+1)(2n+1))/(n*(n+1)))*
(d/d theta)P_{n}^{m-1}(\cos(theta))
 17.3228039548639
= (2n+1)P_{n}^{m-1}(\cos(theta))
(U_{q}+iV_{q})/2 phi component
N,M =            5           2
 159.486881028878
= ((n-m+1)(n-m+2)(m-1)/(n+1))*
P_{n+1}^{m-1}(\cos(theta))/\sin(theta)
+ ((n+m)(n-m+1)(2n+1)/(n(n+1))*
P_{n-1}^{m-1}(\cos(theta))/\sin(theta)
-(((n+m)(n-m+1)(2n+1))/(n*(n+1)))*
(d/d theta)P_{n}^{m-1}(\cos(theta))
```

```
 159.486881028878
= (2n+1)P_{n}^{m-1}(\cos(theta))
(U_{q}+iV_{q})/2 phi component
N,M =            5           3
 497.314530401544
= ((n-m+1)(n-m+2)(m-1)/(n+1))*
P_{n+1}^{m-1}(\cos(theta))/\sin(theta)
+ ((n+m)(n-m+1)(2n+1)/(n(n+1))*
P_{n-1}^{m-1}(\cos(theta))/\sin(theta)
-(((n+m)(n-m+1)(2n+1))/(n*(n+1)))*
(d/d theta)P_{n}^{m-1}(\cos(theta))
 497.314530401544
= (2n+1)P_{n}^{m-1}(\cos(theta))
(U_{q}+iV_{q})/2 phi component
N,M =            5           4
 767.098183474380
= ((n-m+1)(n-m+2)(m-1)/(n+1))*
P_{n+1}^{m-1}(\cos(theta))/\sin(theta)
+ ((n+m)(n-m+1)(2n+1)/(n(n+1))*
P_{n-1}^{m-1}(\cos(theta))/\sin(theta)
-(((n+m)(n-m+1)(2n+1))/(n*(n+1)))*
(d/d theta)P_{n}^{m-1}(\cos(theta))
 767.098183474381
= (2n+1)P_{n}^{m-1}(\cos(theta))
(U_{q}+iV_{q})/2 phi component
N,M =            5           5
 498.159385076279
= ((n-m+1)(n-m+2)(m-1)/(n+1))*
P_{n+1}^{m-1}(\cos(theta))/\sin(theta)
+ ((n+m)(n-m+1)(2n+1)/(n(n+1))*
P_{n-1}^{m-1}(\cos(theta))/\sin(theta)
-(((n+m)(n-m+1)(2n+1))/(n*(n+1)))*
(d/d theta)P_{n}^{m-1}(\cos(theta))
 498.159385076280
= (2n+1)P_{n}^{m-1}(\cos(theta))
```

The following theorem enables us to prove the correctness of the θ component of the $(U_q - iV_q)/2$ term.

Theorem 10.6 *For all nonnegative integers n and all integers m ranging from $-n$ to $+n$ we have*

$$\frac{1}{n+1}\left(\frac{d}{d\theta}\right)P_{n+1}^{m+1}(\cos(\theta)) + \frac{1}{n}\left(\frac{d}{d\theta}\right)P_{n-1}^{m+1}(\cos(\theta))$$

$$+\frac{(m+1)(2n+1)}{n(n+1)}\frac{P_n^{m+1}(\cos(\theta))}{\sin(\theta)} = (2n+1)P_n^m(\cos(\theta))\cos(\theta) \qquad (10.1.3.26)$$

We show computer output which compares the left and right sides of the important identity (10.2.8.4).

```
 0.575958653158129      = THETHA0
  33.0000000000000      = THET0D
  1.00000000000000      = COSTH0**2+SINTH0**2
 0.287979326579064      = THET0D*PI/DFLOAT(180)
          0           1 = M,N
  1.22020992922740      =  DPDTH(N+1,M+1,THET0D)
          2           1  0.838670567945424      = N,M,X
  1.22020992922740     =-SINTH0*DALFF(N+1,M+1,COSTH0)
 0.000000000000000E+000 = DPDTH(N-1,M+1,THET0D)
          0           1  0.838670567945424      = N,M,X
 0.000000000000000E+000   =-SINTH0*DALFF(N-1,M+1,COSTH0)
  2.11010496461370
 = (1/(n+1))(d/d theta)P_{n+1}^{m+1}(\cos(theta))
 + (1/n)(d / d theta)P_{n-1}^{m+1}(\cos(theta))
 + [(m+1)(2n+1))/(n(n+1))]P_{n}^{m+1}(\cos(theta)) /
                                    \sin(theta)
  2.11010496461370
 = (2n+1)P_{n}^{m}(\cos(theta)) \cos(theta)
 0.575958653158129      = THETHA0
  33.0000000000000      = THET0D
  1.00000000000000      = COSTH0**2+SINTH0**2
 0.287979326579064      = THET0D*PI/DFLOAT(180)
          0           2 = M,N
-0.565442402871763      =  DPDTH(N+1,M+1,THET0D)
          3           1  0.838670567945424      = N,M,X
-0.565442402871763     =-SINTH0*DALFF(N+1,M+1,COSTH0)
 0.838670567945424      = DPDTH(N-1,M+1,THET0D)
          1           1  0.838670567945424      = N,M,X
 0.838670567945424        =-SINTH0*DALFF(N-1,M+1,COSTH0)
  2.32753090287902
 = (1/(n+1))(d/d theta)P_{n+1}^{m+1}(\cos(theta))
 + (1/n)(d / d theta)P_{n-1}^{m+1}(\cos(theta))
 + [(m+1)(2n+1))/(n(n+1))]P_{n}^{m+1}(\cos(theta)) /
                                    \sin(theta)
  2.32753090287902
 = (2n+1)P_{n}^{m}(\cos(theta)) \cos(theta)
 0.575958653158129      = THETHA0
  33.0000000000000      = THET0D
  1.00000000000000      = COSTH0**2+SINTH0**2
 0.287979326579064      = THET0D*PI/DFLOAT(180)
          1           2 = M,N
  9.06909745038895      =  DPDTH(N+1,M+1,THET0D)
```

```
         3           2  0.838670567945424      = N,M,X
 9.06909745038895     =-SINTH0*DALFF(N+1,M+1,COSTH0)
0.000000000000000E+000 = DPDTH(N-1,M+1,THET0D)
         1           2  0.838670567945424      = N,M,X
0.000000000000000E+000   =-SINTH0*DALFF(N-1,M+1,COSTH0)
 5.74622765853812
= (1/(n+1))(d/d theta)P_{n+1}^{m+1}(\cos(theta))
+ (1/n)(d / d theta)P_{n-1}^{m+1}(\cos(theta))
+ [(m+1)(2n+1))/(n(n+1))]P_{n}^{m+1}(\cos(theta)) /
                                  \sin(theta)
 5.74622765853812
= (2n+1)P_{n}^{m}(\cos(theta)) \cos(theta)
0.575958653158129      = THETHA0
 33.0000000000000      = THET0D
 1.00000000000000      = COSTH0**2+SINTH0**2
0.287979326579064      = THET0D*PI/DFLOAT(180)
         0           3 = M,N
-5.34647200179526      =  DPDTH(N+1,M+1,THET0D)
         4           1  0.838670567945424      = N,M,X
-5.34647200179526     =-SINTH0*DALFF(N+1,M+1,COSTH0)
 1.22020992922740      = DPDTH(N-1,M+1,THET0D)
         2           1  0.838670567945424      = N,M,X
 1.22020992922740        =-SINTH0*DALFF(N-1,M+1,COSTH0)
 1.27235504935530
= (1/(n+1))(d/d theta)P_{n+1}^{m+1}(\cos(theta))
+ (1/n)(d / d theta)P_{n-1}^{m+1}(\cos(theta))
+ [(m+1)(2n+1))/(n(n+1))]P_{n}^{m+1}(\cos(theta)) /
                                  \sin(theta)
 1.27235504935530
= (2n+1)P_{n}^{m}(\cos(theta)) \cos(theta)
0.575958653158129      = THETHA0
 33.0000000000000      = THET0D
 1.00000000000000      = COSTH0**2+SINTH0**2
0.287979326579064      = THET0D*PI/DFLOAT(180)
         1           3 = M,N
 12.6559607364621      =  DPDTH(N+1,M+1,THET0D)
         4           2  0.838670567945424      = N,M,X
 12.6559607364621     =-SINTH0*DALFF(N+1,M+1,COSTH0)
 2.74063637292780      = DPDTH(N-1,M+1,THET0D)
         2           2  0.838670567945424      = N,M,X
 2.74063637292780        =-SINTH0*DALFF(N-1,M+1,COSTH0)
 12.0710583961309
= (1/(n+1))(d/d theta)P_{n+1}^{m+1}(\cos(theta))
+ (1/n)(d / d theta)P_{n-1}^{m+1}(\cos(theta))
+ [(m+1)(2n+1))/(n(n+1))]P_{n}^{m+1}(\cos(theta)) /
```

```
                                    \sin(theta)
 12.0710583961309
= (2n+1)P_{n}^{m}(\cos(theta)) \cos(theta)
0.575958653158129      = THETHA0
 33.0000000000000      = THET0D
 1.00000000000000      = COSTH0**2+SINTH0**2
0.287979326579064      = THET0D*PI/DFLOAT(180)
         2           3 = M,N
 56.4830305953196      =  DPDTH(N+1,M+1,THET0D)
         4           3  0.838670567945424      = N,M,X
 56.4830305953196     =-SINTH0*DALFF(N+1,M+1,COSTH0)
0.000000000000000E+000 = DPDTH(N-1,M+1,THET0D)
         2           3  0.838670567945424      = N,M,X
0.000000000000000E+000   =-SINTH0*DALFF(N-1,M+1,COSTH0)
 21.9073392084600
= (1/(n+1))(d/d theta)P_{n+1}^{m+1}(\cos(theta))
+ (1/n)(d / d theta)P_{n-1}^{m+1}(\cos(theta))
+ [(m+1)(2n+1))/(n(n+1))]P_{n}^{m+1}(\cos(theta)) /
                                    \sin(theta)
 21.9073392084600
= (2n+1)P_{n}^{m}(\cos(theta)) \cos(theta)
```

10.2 Proof of the Vector Potential Expansion Representations of the Exact Analytical Vector Potential of Brain Activity

In this section we describe two representations of brain activity and prove that they are identical.

10.2.1 The Basic Addition Theorem

The complex brain tissue permittivity $\epsilon(p,(-1)^{\ell}j\omega)$ defines the brain wave propagation constant $k(p,(-1)^{\ell}j\omega)$ in terms of the frequency ω and the magnetic permeability μ_p by the relationship

$$k(p,(-1)^{\ell}j\omega)^2 = \omega^2\mu_p\epsilon(p,(-1)^{\ell}j\omega) \tag{10.2.1.1}$$

The addition theorem expansion coefficient at the qth site $\boldsymbol{r}_q$ of brain activity in region p with degree n and order m is given by for the vector potential $\boldsymbol{A}_{(p,q)}$ is given for $\overline{\ell}$ equal to zero by

$$c(n,m,\overline{\ell},(-1)^{\ell}j\omega,p,q) =$$
$$\left(\frac{(n-\mid m\mid)!}{(n+\mid m\mid)!}\right) Z_n^{(\overline{\ell})}(k(p,(-1)^{\ell}j\omega)r_q)P_n^{|m|}(\cos(\theta_q))\exp(-im\phi_q) \tag{10.2.1.2}$$

where if $\overline{\ell}$ is zero $Z_n^{(\overline{\ell})}(z)$ is the spherical Bessel function $j_n(z)$. Definition (10.2.1.2) and the addition theorem tell us that

$$h_0^{(\ell)}(k(p,(-1)^{\ell}j\omega)d_q) = \frac{\exp((-1)^{\ell}ik(p,(-1)^{\ell}j\omega)d_q)}{(-1)^{\ell}ik(p,(-1)^{\ell}j\omega)d_q)}$$

$$= \sum_{n=0}^{\infty}(2n+1)\sum_{m=-n}^{m=+n} c(n,m,0,(-1)^{\ell}j\omega,p,q)P_n^{|m|}(\cos(\theta))\exp(im\phi)h_n^{(\ell)}(k(p,(-1)^{\ell}j\omega)r) \tag{10.2.1.3}$$

Computer output illustrating the convergence of this infinite sum is shown in the following table using data from the file AOUT.DAT generated by the FORTRAN program PMNAT.FOR.

```
(1.485170053372780E-002,-1.329087450783936E-002) = CK=FK1 in CHECKA
(2.970340106745561E-004,-2.658174901567873E-004) = FK1*r_{0} in CHECKA
(8.911020320236682E-004,-7.974524704703618E-004) = FK1*r in CHECKA
(-556.662106688870,623.150743282911) = initial term of series
 = j_{0}(k_{1}R_{1})*h_{0}^{(2)}(k_{1}R)
(-1.418408530107035E-007,1.584980690603384E-007) = NTH TERM OF SERIES
         20 = N = term number
(-4.023235067037618E-008,4.495707511743944E-008) = NTH TERM OF SERIES
         21 = N = term number
(-9.386450512115296E-009,1.048875725734174E-008) = NTH TERM OF SERIES
         22 = N = term number
(-1.430991926411865E-009,1.599041822239793E-009) = NTH TERM OF SERIES
--> SUCCESSFUL CONVERGENCE
 7.078081354406533E-013 = ERROR
 1.000000000000000E-012 = requested accuracy
(-795.706934681846,890.268319923796) = CSUM
(-795.706934681283,890.268319923166) = EXACT ANSWER
         23 = NUMBER OF TERMS
```

10.2.2 Vector Potential Expansion for the $\exp((-1)^{\ell}j\omega t)$ Frequency Component at the qth Brain Activity Site

Using the definition (9.5.2.2) for $\overline{\ell}$ equal to 0, we see that vector potential (9.5.2.4) arising from the frequency component

$$t \to \exp(i(-1)^{\ell}j\omega t) \tag{10.2.2.1}$$

at site q in region p has a the vector spherical harmonic expansion

$$\boldsymbol{A}_{(p,q)}(\tilde{\ell},(-1)^{\ell}j\omega,t)) =$$

$$\left(\frac{\mu_p(-(-1)^{\tilde{\ell}}ik(p,(-1)^{\ell}j\omega)\exp(i(-1)^{\ell}j\omega t)}{4\pi}\right)\sum_{n=0}^{\infty}\sum_{m=-n}^{m=+n}\left\{c(n,m,0,(-1)^{\ell}j\omega,p,q)\left\{\right.\right.$$

$$W_q\left\{(n-m+1)\left(\boldsymbol{L}_{(n+1,p)}^{(m,\tilde{\ell},(-1)^{\ell}j\omega)}+\frac{1}{n+1}\boldsymbol{N}_{(n+1,p)}^{(m,\tilde{\ell},(-1)^{\ell}j\omega)}\right)\right.$$

$$-(n+m)\left(\boldsymbol{L}_{(n-1,p)}^{(m,\tilde{\ell},(-1)^{\ell}j\omega)}-\frac{1}{n}\boldsymbol{N}_{(n-1,p)}^{(m,\tilde{\ell},(-1)^{\ell}j\omega)}\right)+im\left(\frac{2n+1}{n(n+1)}\right)\boldsymbol{M}_{(n,p)}^{(m,\tilde{\ell},(-1)^{\ell}j\omega)}\Bigg\}$$

$$+\left(\frac{U_q-iV_q}{2}\right)\left\{\left(\boldsymbol{L}_{(n+1,p)}^{(m+1,\tilde{\ell},(-1)^{\ell}j\omega)}+\frac{1}{n+1}\boldsymbol{N}_{(n+1,p)}^{(m+1,\tilde{\ell},(-1)^{\ell}j\omega)}\right)\right.$$

$$+\left(\boldsymbol{L}_{(n-1,p)}^{(m+1,\tilde{\ell},(-1)^{\ell}j\omega)}-\frac{1}{n}\boldsymbol{N}_{(n-1,p)}^{(m+1,\tilde{\ell},(-1)^{\ell}j\omega)}\right)-i\left(\frac{(2n+1)}{n(n+1)}\right)\boldsymbol{M}_{(n,p)}^{(m+1,\tilde{\ell},(-1)^{\ell}j\omega)}$$

$$-\left(\frac{U_q+iV_q}{2}\right)\left\{(n-m+1)(n-m+2)\left(\boldsymbol{L}_{(n+1,p)}^{(m-1,\tilde{\ell},(-1)^{\ell}j\omega)}+\frac{1}{n+1}\boldsymbol{N}_{(n+1,p)}^{(m-1,\tilde{\ell},(-1)^{\ell}j\omega)}\right)\right.$$

$$+(n+m)(n+m-1)\left(\boldsymbol{L}_{(n-1,p)}^{(m-1,\tilde{\ell},(-1)^{\ell}j\omega)}-\frac{1}{n}\boldsymbol{N}_{(n-1,p)}^{(m-1,\tilde{\ell},(-1)^{\ell}j\omega)}\right)$$

$$\left.\left.+(n+m)(n-m+1)\left(\frac{i(2n+1)}{n(n+1)}\right)\boldsymbol{M}_{(n,p)}^{(m-1,\tilde{\ell},(-1)^{\ell}j\omega)}\right\}\right\}\right\} \tag{10.2.2.2}$$

We need this representation in order to solve the electromagnetic boundary value problem and predict measurable fields outside the head. We compare the $\boldsymbol{e}_r$, the $\boldsymbol{e}_\theta$, and the $\boldsymbol{e}_\phi$ components of the expansion given by (10.2.2.2) and the exact analytical addition theorem expansion for the same vector potential (9.5.2.4) is, using (9.5.2.2) given by

$$\tilde{\boldsymbol{A}}_{(p,q)}(\tilde{\ell},(-1)^{\ell}j\omega,t)) =$$

$$\left(\frac{\mu_p(-(-1)^{\tilde{\ell}}ik(p,(-1)^{\ell}j\omega)\exp(i(-1)^{\ell}j\omega t)}{4\pi}\right)\sum_{n=0}^{\infty}\sum_{m=-n}^{m=+n}\left\{c(n,m,0,(-1)^{\ell}j\omega,p,q)\left\{\right.\right.$$

$$(2n+1)P_n^{|m|}(\cos(\theta))\exp(im\phi)Z_n^{(\tilde{\ell})}(k(p,(-1)^{\ell}r)\left\{\right.$$

$$W_q\left[\cos(\theta)\boldsymbol{e}_r-\sin(\theta)\boldsymbol{e}_\theta\right]+\left(\frac{U_q-iV_q}{2}\right)\exp(i\phi)\left[\sin(\theta)\boldsymbol{e}_r+\cos(\theta)\boldsymbol{e}_\theta+i\boldsymbol{e}_\phi\right]$$

$$\left.\left.+\left(\frac{U_q+iV_q}{2}\right)\exp(-i\phi)\left[\sin(\theta)\boldsymbol{e}_r+\cos(\theta)\boldsymbol{e}_\theta-i\boldsymbol{e}_\phi\right]\right\}\right\} \tag{10.2.2.3}$$

We prove the following theorem.

Theorem 10.7 *The vector potentials defined by (10.2.2.2) and (10.2.2.3) are identical.*

Proof of Theorem. We define the common factor appearing in every summand of both (10.2.2.2) and (10.2.2.3) as

$$\mathcal{C}(p,\tilde{\ell},\ell,j,\omega,n,m,q) =$$
$$\left(\frac{\mu_p(-(1)^{\tilde{\ell}}ik(p,(-1)^{\ell}j\omega)\exp(i(-1)^{\ell}j\omega t)}{4\pi}\right)c(n,m,0,(-1)^{\ell}j\omega p,q) \tag{10.2.2.4}$$

where the propagation constant

$$(p,(-1)^{\ell}j\omega) \to k(p,(-1)^{\ell}j\omega)$$

is defined by (9.5.2.1) and the common factor

$$(n,m,\tilde{\ell},(-1)^{\ell}j\omega p,q) \to c(n,m,\tilde{\ell},(-1)^{\ell}j\omega p,q)$$

is defined by (9.5.2.2) and the transmembrane current direction at brain activity site q,

$$q \to (U_q,V_q,W_q)$$

is given by (9.5.2.5). The theorem's proof is divided into 9 parts showing that the dot products with respect to $\boldsymbol{e}_r$, $\boldsymbol{e}_\theta$, or $\boldsymbol{e}_\phi$ of the partial derivatives of the two representations of

$$(p,q,\tilde{\ell},(-1)^{\ell}j\omega,t) \to \tilde{\boldsymbol{A}}_{(p,q)}(\tilde{\ell},(-1)^{\ell}j\omega,t))$$

with respect to each component of

$$q \to (W_q,(U_q-iV_q)/2,(U_q+iV_q)/2) \tag{10.2.2.5}$$

followed by the partial derivative with respect to the $\mathcal{C}(p,\tilde{\ell},\ell,j,\omega,n,m,q)$ defined by (10.2.2.4) are identical.

This important theorem shows that we can represent the magnetic and electric vectors stimulated by brain activity in terms of vector spherical harmonics. This enables us to predict the external measurement assessment of brain activity.

For the first part of nine parts of the theorem we show that

$$\left(\frac{\partial}{\partial((U_q-iV_q)/2)}\right)\left(\frac{\partial}{\partial\mathcal{C}(p,\tilde{\ell},(-1)^{\ell}j\omega,n,m,q))}\right)\boldsymbol{A}_{(p,q)}(\tilde{\ell},(-1)^{\ell}j\omega)_{sphericalharmonics}\cdot\boldsymbol{e}_r =$$
$$\left(\frac{\partial}{\partial((U_q-iV_q)/2)}\right)\left(\frac{\partial}{\partial\mathcal{C}(p,\tilde{\ell},(-1)^{\ell}j\omega,n,m,q))}\right)\boldsymbol{A}_{(p,q)}(\tilde{\ell},(-1)^{\ell}j\omega)_{additiontheorem}\cdot\boldsymbol{e}_r \tag{10.2.2.6}$$

We carry out the proof in nine steps showing that the radial, θ, and ϕ components of the multiples of W, $(U-iV)/2$, and $(U+iV)/2$ in equations (10.2.2.2) and (10.2.2.3) are exactly the same. We make repeated use of the Lemma. If $f_n(z)$ represents a spherical Bessel or Hankel function that is a solution of the differential equation (9.4.1.1), then for all indices n or, in particular, for

$$f_n(z)\in\left\{j_n(z),y_n(z),h_n^{(1)}(z),h_n^{(2)}(z)\right\} \tag{10.2.2.7}$$

that f_n satisfies the recursion relationship (10.1.1.22) and (10.1.1.23)

To prove the theorem we need 9 separate formulae for the projections of the vector fields (9.4.1.12), (9.4.1.13), and (9.4.1.15) defining the vector spherical harmonics used in our expansion on the unit vectors $\boldsymbol{e}_r$, $\boldsymbol{e}_\theta$, and $\boldsymbol{e}_\phi$.

Lemma 10.2 *For the vector field*

$$\boldsymbol{L}_{(n,p)}^{(m,\tilde{\ell},(-1)^{\ell}j\omega)} = \left[\left(\frac{d}{dz}\right) Z_n^{(\tilde{\ell})}(z)\boldsymbol{C}_{(m,n)}(\theta,\phi) + \frac{Z_n^{(\tilde{\ell})}(z)}{z}\boldsymbol{B}_{(m,n)}(\theta,\phi)\right] |_{z=k(p,(-1)^{\ell}j\omega)r} \quad (10.2.2.8)$$

where the surface vector fields

$$(m,n,\theta,\phi) \to \big(\boldsymbol{B}_{(m,n)}(\theta,\phi), \boldsymbol{C}_{(m,n)}(\theta,\phi)\big) \quad (10.2.2.9)$$

are defined by (9.4.1.5), and (9.4.1.3), respectively and $Z_n^{(\tilde{\ell})}(z)$ is defined by (10.1.1.16) then for the associated Legendre function $P_n^{|m|}(\xi)$ defined by (10.1.2.1) which for ξ equal to $\cos(\theta)$ satisfies (9.4.1.2) we have

$$\boldsymbol{L}_{(n,p)}^{(m,\tilde{\ell},(-1)^{\ell}j\omega)} \cdot \boldsymbol{e}_r = \left[\left(\frac{d}{dz}\right) Z_n^{(\tilde{\ell})}(z) P_n^{|m|}(\cos(\theta))\exp(im\phi)\right] |_{z=k(p,(-1)^{\ell}j\omega)r} \quad (10.2.2.10)$$

where $\boldsymbol{e}_r$ is defined by (5.2.4.2)

$$\boldsymbol{L}_{(n,p)}^{(m,\tilde{\ell},(-1)^{\ell}j\omega)} \cdot \boldsymbol{e}_\theta = \left[\frac{Z_n^{(\tilde{\ell})}(z)}{z}\left(\frac{d}{d\theta}\right) P_n^{|m|}(\cos(\theta))\exp(im\phi)\right] |_{z=k(p,(-1)^{\ell}j\omega r} \quad (10.2.2.11)$$

where $\boldsymbol{e}_\theta$ is given by (5.2.4.3), and finally

$$\boldsymbol{L}_{(n,p)}^{(m,\tilde{\ell},(-1)^{\ell}j\omega)} \cdot \boldsymbol{e}_\phi = \left[\frac{Z_n^{(\tilde{\ell})}(z)}{z} im\left(\frac{P_n^{|m|}(\cos(\theta))}{\sin(\theta)}\right)\exp(im\phi)\right] |_{z=k(p,(-1)^{\ell}j\omega r} \quad (10.2.2.12)$$

where $\boldsymbol{e}_\phi$ is given by (5.2.4.4).

The next lemma gives us the projection of the vector field

$$\boldsymbol{M}_{(n,p)}^{(m,\tilde{\ell},(-1)^{\ell}j\omega)} = Z_n^{(\tilde{\ell})}(k(p,(-1)^{\ell}j\omega)r)\left[im\frac{P_n^{|m|}(\cos(\theta))}{\sin(\theta)}\boldsymbol{e}_\theta - \left(\frac{d}{d\theta}\right) P_n^{|m|}(\cos(\theta))\boldsymbol{e}_\phi\right]\exp(im\phi) \quad (10.2.2.13)$$

onto the unit vectors in spherical coordinates.

Lemma 10.3 *For the vector field defined by (10.2.2.13) and for the unit vector $\boldsymbol{e}_r$ is defined by (5.2.4.2) we have*

$$\boldsymbol{M}_{(n,p)}^{(m,\tilde{\ell},(-1)^{\ell}j\omega)} \cdot \boldsymbol{e}_r = \boldsymbol{0} \quad (10.2.2.14)$$

for the unit length vector $\boldsymbol{e}_\theta$ defined by (5.2.4.3) we have

$$\boldsymbol{M}_{(n,p)}^{(m,\tilde{\ell},(-1)^{\ell}j\omega)} \cdot \boldsymbol{e}_\theta = Z_n^{(\tilde{\ell})}(k(p,(-1)^{\ell}j\omega)r) im\left(\frac{P_n^{|m|}(\cos(\theta))}{\sin(\theta)}\right)\exp(im\phi) \quad (10.2.2.15)$$

and for the unit vector $\boldsymbol{e}_\phi$ defined by (5.2.4.4) we have

$$\boldsymbol{M}_{(n,p)}^{(m,\tilde{\ell},(-1)^{\ell}j\omega)} \cdot \boldsymbol{e}_\phi = Z_n^{(\tilde{\ell})}(k(p,(-1)^{\ell}j\omega)r)\left[\left(\frac{d}{d\theta}\right) P_n^{|m|}(\cos(\theta))\right]\exp(im\phi) \quad (10.2.2.16)$$

The last three projection equations that we use in the proof are given by the following lemma.

Lemma 10.4 *If $Z_n^{(\tilde{\ell})}$ is defined by (10.1.1.16) and $W_n^{(\tilde{\ell})}$ is defined by (10.1.1.17), then*

$$\boldsymbol{N}_{(n,p)}^{(m,\tilde{\ell},(-1)^\ell j\omega)} = n(n+1)\left(\frac{Z_n^{(\tilde{\ell})}(z)}{z}\right)|_{z=k(p,(-1)^\ell j\omega)r}\, P_n^{|m|}(\cos(\theta))\exp(im\phi)\boldsymbol{e}_r$$

$$+W_n^{(\tilde{\ell})}(z)\,|_{z=k(p,(-1)^\ell j\omega)r}\left[\left(\frac{d}{d\theta}\right)P_n^{|m|}(\cos(\theta))\boldsymbol{e}_\theta + im\left(\frac{P_n^{|m|}(\cos(\theta))}{\sin(\theta)}\right)\boldsymbol{e}_\phi\right]\exp(im\phi) \tag{10.2.2.17}$$

From (10.2.2.17) we have

$$\boldsymbol{N}_{(n,p)}^{(m,\tilde{\ell},(-1)^\ell j\omega)}\cdot\boldsymbol{e}_r = n(n+1)\left\{\left[\frac{Z_n^{(\tilde{\ell})}(z)}{z}\right]|_{z=k(p,(-1)^\ell j\omega)r}\right\}P_n^{|m|}(\cos(\theta))\exp(im\phi) \tag{10.2.2.18}$$

$$\boldsymbol{N}_{(n,p)}^{(m,\tilde{\ell},(-1)^\ell j\omega)}\cdot\boldsymbol{e}_\theta = W_n^{(\tilde{\ell})}(z)\,|_{z=k(p,(-1)^\ell j\omega)r}\left(\frac{d}{d\theta}\right)P_n^{|m|}(\cos(\theta))\exp(im\phi) \tag{10.2.2.19}$$

and

$$\boldsymbol{N}_{(n,p)}^{(m,\tilde{\ell},(-1)^\ell j\omega)}\cdot\boldsymbol{e}_\phi = W_n^{(\tilde{\ell})}(z)\,|_{z=k(p,(-1)^\ell j\omega)r}\left(\frac{P_n^{|m|}(\cos(\theta))}{\sin(\theta)}\right)\exp(im\phi) \tag{10.2.2.20}$$

We defined a common factor appearing in the vector spherical harmonic expansion (10.2.2.2) and the addition theorem expansion (10.2.2.3) of the vector potential by (10.2.2.4).

10.2.3 The r Component of the W_q Term

We consider the vector potentials defined by (10.2.2.2) using the three vector spherical harmonics

$$(n,p,m,\tilde{\ell},(-1)^\ell j\omega)\rightarrow\left(\boldsymbol{L}_{(n,p)}^{(m,\tilde{\ell},(-1)^{j\omega})},\boldsymbol{M}_{(n,p)}^{(m,\tilde{\ell},(-1)^{j\omega})},\boldsymbol{N}_{(n,p)}^{(m,\tilde{\ell},(-1)^{j\omega})},\right) \tag{10.2.3.1}$$

defined by (9.4.1.12), (9.4.1.13), and (9.4.1.15) and (10.2.2.3)

We prove the following theorem

Theorem 10.8 *For the spherical Harmonic representation vector potential defined by (10.2.2.2) and the addition theorem vector potential defined by (10.2.2.3) we have*

$$\left(\frac{\partial}{\partial(W_q/2)}\right)\left(\frac{\partial}{\partial\mathcal{C}(p,\tilde{\ell},(-1)^\ell j\omega,n,m,q))}\right)\boldsymbol{A}_{(p,q)}(\tilde{\ell},(-1)^\ell j\omega)_{sphericalharmonics}\cdot\boldsymbol{e}_r =$$

$$\left(\frac{\partial}{\partial(W_q)}\right)\left(\frac{\partial}{\partial\mathcal{C}(p,\tilde{\ell},(-1)^\ell j\omega,n,m,q))}\right)\boldsymbol{A}_{(p,q)}(\tilde{\ell},(-1)^\ell j\omega)_{additiontheorem}\cdot\boldsymbol{e}_r \tag{10.2.3.2}$$

Proof of Theorem. The left side of (10.2.3.2) is given by

$$\left(\frac{\partial}{\partial(W_q/2)}\right)\left(\frac{\partial}{\partial\mathcal{C}(p,\tilde{\ell},(-1)^{\ell}j\omega,n,m,q))}\right)\boldsymbol{A}_{(p,q)}(\tilde{\ell},(-1)^{\ell}j\omega)_{sphericalharmonics}\cdot\boldsymbol{e}_r$$

$$=(n-m+1)\left[\boldsymbol{L}_{(n+1,p)}^{(m,\tilde{\ell},(-1)^{\ell}j\omega)}+\frac{1}{n+1}\boldsymbol{N}_{(n+1,p)}^{(m,\tilde{\ell},(-1)^{\ell}j\omega)}\right]\cdot\boldsymbol{e}_r$$

$$+(-1)(n+\mid m\mid)\left[\boldsymbol{L}_{(n-1,p)}^{(m,\tilde{\ell},(-1)^{\ell}j\omega)}-\frac{1}{n}\boldsymbol{N}_{(n-1,p)}^{(m,\tilde{\ell},(-1)^{\ell}j\omega)}\right]\cdot\boldsymbol{e}_r+im\left(\frac{2n+1}{n(n+1)}\right)\boldsymbol{M}_{(n,p)}^{(m,\tilde{\ell},(-1)^{\ell}j\omega)}\cdot\boldsymbol{e}_r$$

$$=\left\{(n-m+1)\left[\left(\frac{d}{dz}\right)Z_{n+1}^{(\tilde{\ell})}(z)+\frac{(n+1)(n+2)}{n+1}\left(\frac{Z_{n+1}^{(\tilde{\ell})}(z)}{z}\right)\right]P_{n+1}^{m}(\cos(\theta))\right.$$

$$\left.+(-1)(n+m)\left[\left(\frac{d}{dz}\right)Z_{n-1}^{(\tilde{\ell})}(z)-\left(\frac{(n-1)n}{n}\right)\left(\frac{Z_{n-1}^{(\tilde{\ell})}(z)}{z}\right)\right]P_{n-1}^{m}(\cos(\theta))\right\}\exp(im\phi)\mid_{z=k(p,(-1)^{\ell}j\omega)r} \tag{10.2.3.3}$$

Substituting the recursion relationships (10.1.1.24), and (10.1.1.23) into (10.2.3.3) we have

$$\left(\frac{\partial}{\partial(W_q/2)}\right)\left(\frac{\partial}{\partial\mathcal{C}(p,\tilde{\ell},(-1)^{\ell}j\omega,n,m,q))}\right)\boldsymbol{A}_{(p,q)}(\tilde{\ell},(-1)^{\ell}j\omega)_{sphericalharmonics}\cdot\boldsymbol{e}_r$$

$$=\left[(n-m+1)P_{n+1}^{m}(\cos(\theta))+(n-m)P_{n-1}^{m}(\cos(\theta))\right]Z_{n}^{(\tilde{\ell})}(z)\exp(im\phi)\mid_{z=k(p,(-1)^{\ell}j\omega)r} \tag{10.2.3.4}$$

Now subsituting the associated Legendre function relationship (10.1.3.22) into (10.2.3.4) gives us

$$\left(\frac{\partial}{\partial(W_q/2)}\right)\left(\frac{\partial}{\partial\mathcal{C}(p,\tilde{\ell},(-1)^{\ell}j\omega,n,m,q))}\right)\boldsymbol{A}_{(p,q)}(\tilde{\ell},(-1)^{\ell}j\omega)_{sphericalharmonics}\cdot\boldsymbol{e}_r$$

$$=(2n+1)\cos(\theta)P_{n}^{m}(\cos(\theta))Z_{n}^{(\tilde{\ell})}(z)\exp(im\phi)\mid_{z=k(p,(-1)^{\ell}j\omega)r} \tag{10.2.3.5}$$

which is exactly the right side of equation (10.2.3.2) which is also exactly the $\boldsymbol{e}_r$ component of the W_q term of (10.2.2.3). This proves the theorem.

10.2.4 The θ Component of the W_q Term

We consider the vector potentials defined by (10.2.2.2) using the three vector spherical harmonics

$$(n,p,m,\tilde{\ell},(-1)^{\ell}j\omega)\rightarrow\left(\boldsymbol{L}_{(n,p)}^{(m,\tilde{\ell},(-1)^{j\omega})},\boldsymbol{M}_{(n,p)}^{(m,\tilde{\ell},(-1)^{j\omega})},\boldsymbol{N}_{(n,p)}^{(m,\tilde{\ell},(-1)^{j\omega})},\right) \tag{10.2.4.1}$$

defined by (9.4.1.12), (9.4.1.13), and (9.4.1.15) and (10.2.2.3)

We prove the following theorem

Theorem 10.9 *For the spherical Harmonic representation vector potential defined by (10.2.2.2) and the addition theorem vector potential defined by (10.2.2.3) we have*

$$\left(\frac{\partial}{\partial W_q}\right)\left(\frac{\partial}{\partial \mathcal{C}(p,\tilde{\ell},(-1)^{\ell}j\omega,n,m,q))}\right)\boldsymbol{A}_{(p,q)}(\tilde{\ell},(-1)^{\ell}j\omega)_{sphericalharmonics}\cdot\boldsymbol{e}_{\theta}=$$

$$\left(\frac{\partial}{\partial W_q}\right)\left(\frac{\partial}{\partial \mathcal{C}(p,\tilde{\ell},(-1)^{\ell}j\omega,n,m,q))}\right)\boldsymbol{A}_{(p,q)}(\tilde{\ell},(-1)^{\ell}j\omega)_{additiontheorem}\cdot\boldsymbol{e}_{\theta} \qquad (10.2.4.2)$$

Proof of Theorem. The left side of equation (10.2.4.2) after substituting equation (10.2.2.2) is

$$\begin{aligned}
&\left(\frac{\partial}{\partial W_q}\right)\left(\frac{\partial}{\partial \mathcal{C}(p,\tilde{\ell},(-1)^{\ell}j\omega,n,m,q))}\right)\boldsymbol{A}_{(p,q)}(\tilde{\ell},(-1)^{\ell}j\omega)_{sphericalharmonics}\cdot\boldsymbol{e}_{\theta}\\
&\quad=(n-m+1)\left[\boldsymbol{L}_{(n+1,p)}^{(m,\tilde{\ell},(-1)^{j\omega})}+\frac{1}{n+1}\boldsymbol{N}_{(n+1,p)}^{(m,\tilde{\ell},(-1)^{j\omega})}\right]\cdot\boldsymbol{e}_{\theta}\\
&\quad+(-1)(n+m)\left[\boldsymbol{L}_{(n-1,p)}^{(m,\tilde{\ell},(-1)^{j\omega})}+\frac{1}{n}\boldsymbol{N}_{(n-1,p)}^{(m,\tilde{\ell},(-1)^{j\omega})}\right]\\
&\quad+im\left(\frac{2n+1}{n(n+1)}\right)\boldsymbol{M}_{(n,p)}^{(m,\tilde{\ell},(-1)^{j\omega})}\cdot\boldsymbol{e}_{\theta} \qquad (10.2.4.3)
\end{aligned}$$

Substituting (9.4.1.12), (9.4.1.13), (9.4.1.15), (9.4.1.4), (9.4.1.5), and (9.4.1.3) into (10.2.4.3) gives us

$$\begin{aligned}
&\left(\frac{\partial}{\partial W_q}\right)\left(\frac{\partial}{\partial \mathcal{C}(p,\tilde{\ell},(-1)^{\ell}j\omega,n,m,q))}\right)\boldsymbol{A}_{(p,q)}(\tilde{\ell},(-1)^{\ell}j\omega)_{sphericalharmonics}\cdot\boldsymbol{e}_{\theta}\\
&\left\{\quad(n-m+1)\left[\frac{Z_{n+1}^{(\tilde{\ell})}(z)}{z}+\frac{W_{n+1}^{(\tilde{\ell})}(z)}{n+1}\right]\left(\frac{d}{d\theta}\right)P_{n+1}^{m}(\cos(\theta))\right.\\
&\quad+(-1)(n+m)\left[\frac{Z_{n-1}^{(\tilde{\ell})}(z)}{z}+\frac{W_{n-1}^{(\tilde{\ell})}(z)}{n}\right]\left(\frac{d}{d\theta}\right)P_{n+1}^{m}(\cos(\theta))\\
&+im\left(\frac{2n+1}{(n(n+1)}\right)\left.\left(\frac{imP_n^m(\cos(\theta))}{\sin(\theta)}\right)Z_n^{(\tilde{\ell})}(z)\right\}\exp(im\phi)\mid_{z=k(p,(-1)^{\ell}j\omega)} \qquad (10.2.4.4)
\end{aligned}$$

Substituting the spherical Bessel function recursions relationships (10.1.1.24) and (10.1.1.25) into (10.2.4.4) gives us

$$\begin{aligned}
&\left(\frac{\partial}{\partial W_q}\right)\left(\frac{\partial}{\partial \mathcal{C}(p,\tilde{\ell},(-1)^{\ell}j\omega,n,m,q))}\right)\boldsymbol{A}_{(p,q)}(\tilde{\ell},(-1)^{\ell}j\omega)_{sphericalharmonics}\cdot\boldsymbol{e}_{\theta}\\
&=\left\{\quad\left[\left(\frac{n-m+1}{n+1}\right)\left(\frac{d}{d\theta}\right)P_{n+1}^{m}(\cos(\theta))-\left(\frac{n+m}{n}\right)\left(\frac{d}{d\theta}\right)P_{n-1}^{m}(\cos(\theta))\right]\right.\\
&+\quad(-1)\left.\left(\frac{m^2(2n+1)}{n(n+1)}\right)\left(\frac{P_n^m(\cos(\theta))}{\sin(\theta)}\right)\right\}Z_n^{(\tilde{\ell})}(z)\exp(im\phi)\mid_{z=k(p,(-1)^{\ell}j\omega)r} \qquad (10.2.4.5)
\end{aligned}$$

Substituting the associated Legendre function recursion relationship (10.1.3.18) into (10.2.4.5) gives us

$$\left(\frac{\partial}{\partial W_q}\right)\left(\frac{\partial}{\partial \mathcal{C}(p,\tilde{\ell},(-1)^{\ell}j\omega,n,m,q))}\right)\boldsymbol{A}_{(p,q)}(\tilde{\ell},(-1)^{\ell}j\omega)_{sphericalharmonics}\cdot\boldsymbol{e}_{\theta}$$

$$=-(2n+1)Z_n^{(\tilde{\ell})}(z)\sin(\theta)P_n^m(\cos(\theta))\exp(im\phi)\mid_{z=k(p,(-1)^{\ell}j\omega)r} \tag{10.2.4.6}$$

which proves the theorem

10.2.5 The ϕ Component of the W_q Term

We consider the vector potentials defined by (10.2.2.2) using the three vector spherical harmonics

$$(n,p,m,\tilde{\ell},(-1)^{\ell}j\omega)\rightarrow\left(\boldsymbol{L}_{(n,p)}^{(m,\tilde{\ell},(-1)^{j\omega})},\boldsymbol{M}_{(n,p)}^{(m,\tilde{\ell},(-1)^{j\omega})},\boldsymbol{N}_{(n,p)}^{(m,\tilde{\ell},(-1)^{j\omega})},\right) \tag{10.2.5.1}$$

defined by (9.4.1.12), (9.4.1.13), and (9.4.1.15) and (10.2.2.3) for the exact analytical expression and show, in spite of the fact that there is a ϕ component in every term of (10.2.2.2) that they all cancel out exactly using the remarkable associated Legendre function identity (10.1.3.12).

$$\left(\frac{\partial}{\partial W_q}\right)\left(\frac{\partial}{\partial \mathcal{C}(p,\tilde{\ell},(-1)^{\ell}j\omega,n,m,q))}\right)\boldsymbol{A}_{(p,q)}(\tilde{\ell},(-1)^{\ell}j\omega)_{sphericalharmonics}\cdot\boldsymbol{e}_{\phi}=$$

$$\left(\frac{\partial}{\partial W_q}\right)\left(\frac{\partial}{\partial \mathcal{C}(p,\tilde{\ell},(-1)^{\ell}j\omega,n,m,q))}\right)\boldsymbol{A}_{(p,q)}(\tilde{\ell},(-1)^{\ell}j\omega)_{additiontheorem}\cdot\boldsymbol{e}_{\phi} \tag{10.2.5.2}$$

From (10.2.2.2) the left side of equation (10.2.5.2) is

$$(n-m+1)\left[\boldsymbol{L}_{(n+1,p)}^{(m,\tilde{\ell},(-1)^{\ell}j\omega)}+\frac{1}{n+1}\boldsymbol{L}_{(n+1,p)}^{(m,\tilde{\ell},(-1)^{\ell}j\omega)}\right]\cdot\boldsymbol{e}_{\phi}$$

$$+(-1)(n+m)\left[\boldsymbol{L}_{(n-1,p)}^{(m,\tilde{\ell},(-1)^{\ell}j\omega)}-\frac{1}{n}\boldsymbol{L}_{(n-1,p)}^{(m,\tilde{\ell},(-1)^{\ell}j\omega)}\right]\cdot\boldsymbol{e}_{\phi}$$

$$+im\left(\frac{2n+1}{n(n+1)}\right)\boldsymbol{M}_{(n,p)}^{(m,\tilde{\ell},(-1)^{\ell}j\omega)}\cdot\boldsymbol{e}_{\phi}$$

$$=\Bigg\{\quad(n-m+1)\left[\frac{Z_{n+1}^{(\tilde{\ell})}(z)}{z}+\frac{1}{n+1}W_{n+1}^{(\tilde{\ell})}(z)\right]im\left(\frac{P_{n+1}^m(\cos(\theta))}{\sin(\theta)}\right)\exp(im\phi)$$

$$+(-1)(n+m)\left[\frac{Z_{n-1}^{(\tilde{\ell})}(z)}{z}-\frac{1}{n}W_{n-1}^{(\tilde{\ell})}(z)\right]im\left(\frac{P_{n-1}^m(\cos(\theta))}{\sin(\theta)}\right)\exp(im\phi)$$

$$+\quad\left[\frac{2n+1}{n(n+1)}Z_n^{(\tilde{\ell})}(z)\right]\left(-\frac{d}{d\theta}\right)P_n^m(\cos(\theta))\exp(im\phi)\Bigg\}\mid_{z=k(p,(-1)^{\ell}j\omega)r} \tag{10.2.5.3}$$

Substituting (10.1.1.24) and (10.1.1.25) into (10.2.5.3) gives us

$$\left(\frac{\partial}{\partial W_q}\right)\left(\frac{\partial}{\partial \mathcal{C}(p,\tilde{\ell},(-1)^{\ell}j\omega,n,m,q))}\right)\boldsymbol{A}_{(p,q)}(\tilde{\ell},(-1)^{\ell}j\omega)_{sphericalharmonics}\cdot\boldsymbol{e}_{\phi}$$

$$=\left\{\quad\left(\frac{n-m+1}{n+1}\frac{P_{n+1}^{m+1}(\cos(\theta))}{\sin(\theta)}\right)+(-1)\left(\frac{n+m}{n}\frac{P_{n-1}^{m+1}(\cos(\theta))}{\sin(\theta)}\right)\right.$$

$$\left.-\quad\left(\frac{2n+1}{n(n+1)}\right)\left(\frac{d}{d\theta}\right)P_n^m(\cos(\theta))\right\}Z_n^{(\tilde{\ell})}(z)im\exp(im(\phi)\mid_{z=k(p,(-1)^{\ell}j\omega)r}\qquad(10.2.5.4)$$

Substituting the recursion relationship (10.1.3.12) or equivalently (10.1.3.17) into (10.2.5.4) shows that the ϕ component of the vector potential is exactly zero as it should be.

10.2.6 The Radial Component of the $(U_q - iV_q)/2$ Term

We begin by considering the radial component that multiplies $(U_q - iV_q)/2$ where q is the index of a potential site of brain activity. We use the explicit definitions (9.4.1.12), (9.4.1.13), and (9.4.1.15) for the vector spherical harmonics and observe that

$$\left(\frac{U_q-iV_q}{2}\right)\left\{\left(\boldsymbol{L}_{(n+1,p)}^{(m+1,\tilde{\ell},(-1)^{\ell}j\omega)}+\frac{1}{n+1}\boldsymbol{N}_{(n+1,p)}^{(m+1,\tilde{\ell},(-1)^{\ell}j\omega)}\right)\right.$$

$$\left.+\left(\boldsymbol{L}_{(n-1,p)}^{(m+1,\tilde{\ell},(-1)^{\ell}j\omega)}-\frac{1}{n}\boldsymbol{N}_{(n-1,p)}^{(m+1,\tilde{\ell},(-1)^{\ell}j\omega)}\right)-i\left(\frac{(2n+1)}{n(n+1)}\right)\boldsymbol{M}_{(n,p)}^{(m+1,\tilde{\ell},(-1)^{\ell}j\omega)}\right\}\cdot\boldsymbol{e}_r=$$

$$\left\{\left(\frac{U_q-iV_q}{2}\right)\left[\left(\frac{d}{dz}\right)Z_{n+1}^{(\tilde{\ell})}+\frac{(n+1)(n+2)}{n+1}\left(\frac{Z_{n+1}^{(\tilde{\ell})}(z)}{z}\right)\right]\mid_{z=k(p,(-1)^{\ell}j\omega)r}P_{n+1}^{m+1}(\cos(\theta))\right.$$

$$\left.+\left[\left(\frac{d}{dz}\right)Z_{n-1}^{(\tilde{\ell})}(z)-\left(\frac{(n-1)n}{n}\right)\frac{Z_{n-1}^{(\tilde{\ell})}(z)}{z}\right]\mid_{z=k(p,(-1)^{\ell}j\omega)r}P_{n-1}^{m+1}(\cos(\theta))\right\}\exp(i(m+1)\phi)$$

(10.2.6.1)

Substituting the spherical Hankel function relationships (10.1.1.24) and (10.1.1.25) into (10.2.6.1) gives us

$$\left(\frac{U_q-iV_q}{2}\right)\left\{\left(\boldsymbol{L}_{(n+1,p)}^{(m+1,\tilde{\ell},(-1)^{\ell}j\omega)}+\frac{1}{n+1}\boldsymbol{N}_{(n+1,p)}^{(m+1,\tilde{\ell},(-1)^{\ell}j\omega)}\right)\right.$$

$$\left.+\left(\boldsymbol{L}_{(n-1,p)}^{(m+1,\tilde{\ell},(-1)^{\ell}j\omega)}-\frac{1}{n}\boldsymbol{N}_{(n-1,p)}^{(m+1,\tilde{\ell},(-1)^{\ell}j\omega)}\right)-i\left(\frac{(2n+1)}{n(n+1)}\right)\boldsymbol{M}_{(n,p)}^{(m+1,\tilde{\ell},(-1)^{\ell}j\omega)}\right\}\cdot\boldsymbol{e}_r=$$

$$=\left(\frac{U_q-iV_q}{2}\right)Z_n^{(\tilde{\ell})}(z)\mid_{z=k(p,(-1)^{\ell}j\omega)}\left[P_{n+1}^{|m|+1}(\cos(\theta))-P_{n-1}^{|m|+1}\right]\exp(i(m+1)\phi)\qquad(10.2.6.2)$$

Substituting the associated Legendre function recursion relationship (10.1.3.23) into (10.2.6.2) gives us

$$\left(\frac{U_q-iV_q}{2}\right)\left\{\left(\boldsymbol{L}_{(n+1,p)}^{(m+1,\tilde{\ell},(-1)^{\ell}j\omega)}+\frac{1}{n+1}\boldsymbol{N}_{(n+1,p)}^{(m+1,\tilde{\ell},(-1)^{\ell}j\omega)}\right)\right.$$

$$+\left(\boldsymbol{L}_{(n-1,p)}^{(m+1,\tilde{\ell},(-1)^{\ell}j\omega)}-\frac{1}{n}\boldsymbol{N}_{(n-1,p)}^{(m+1,\tilde{\ell},(-1)^{\ell}j\omega)}\right)-i\left(\frac{(2n+1)}{n(n+1)}\right)\boldsymbol{M}_{(n,p)}^{(m+1,\tilde{\ell},(-1)^{\ell}j\omega)}\Bigg\}\cdot\boldsymbol{e}_r=$$

$$=\left(\frac{U_q-iV_q}{2}\right)Z_n^{(\tilde{\ell})}(z)\mid_{z=k(p,(-1)^{\ell}j\omega)}\left[(2n+1)P_n^{|m|}(\cos(\theta))\right]\exp(i(m+1)\phi)\qquad(10.2.6.3)$$

which exactly matches the corresponding term in (10.2.2.3)

10.2.7 The Radial Component of the $(U_q+iV_q)/2$ Term

We now verify that the radial component of the (m,n) term of the multiple of $(U_q+iV_q)/2$ for the spherical harmonic expansion exactly matches the radial component of the (m,n) term of the addition theorem expansion.

Theorem 10.10

$$\left(\frac{\partial}{\partial(U_q+iV_q)/2}\right)\left(\frac{\partial}{\partial\mathcal{C}(p,\tilde{\ell},(-1)^{\ell}j\omega,n,m,t)}\right)\boldsymbol{A}_{(p,q)}(\tilde{\ell},(-1)^{\ell}j\omega,t)_{sphericalharmonics}\cdot\boldsymbol{e}_r=$$

$$\left(\frac{\partial}{\partial(U_q+iV_q)/2}\right)\left(\frac{\partial}{\partial\mathcal{C}(p,\tilde{\ell},(-1)^{\ell}j\omega,n,m,t)}\right)\boldsymbol{A}_{(p,q)}(\tilde{\ell},(-1)^{\ell}j\omega,t)_{additiontheorem}\cdot\boldsymbol{e}_r\qquad(10.2.7.1)$$

Proof of Theorem For the spherical harmonics expansion we have

$$\left(\frac{\partial}{\partial(U_q+iV_q)/2}\right)\left(\frac{\partial}{\partial\mathcal{C}(p,\tilde{\ell},(-1)^{\ell}j\omega,n,m,t)}\right)\boldsymbol{A}_{(p,q)}(\tilde{\ell},(-1)^{\ell}j\omega,t)_{sphericalharmonics}\cdot\boldsymbol{e}_r=$$

$$-\Bigg\{(n-\mid m\mid+1)(n-\mid m\mid+2)\left(\boldsymbol{L}_{(n+1,p)}^{(m-1,\tilde{\ell},(-1)^{\ell}j\omega)}+\frac{1}{n+1}\boldsymbol{N}_{(n+1,p)}^{(m-1,\tilde{\ell},(-1)^{\ell}j\omega)}\right)$$

$$+(n+\mid m\mid)(n+\mid m\mid-1)\left(\boldsymbol{L}_{(n-1,p)}^{(m-1,\tilde{\ell},(-1)^{\ell}j\omega)}-\frac{1}{n}\boldsymbol{N}_{(n-1,p)}^{(m-1,\tilde{\ell},(-1)^{\ell}j\omega)}\right)$$

$$+(n+\mid m\mid)(n-\mid m\mid+1)\left(\frac{i(2n+1)}{n(n+1)}\right)\boldsymbol{M}_{(n,p)}^{(m-1,\tilde{\ell},(-1)^{\ell}j\omega)}\Bigg\}\cdot\boldsymbol{e}_r$$

$$=-\Bigg\{(n-\mid m\mid+1)(n-\mid m\mid+2)\left[\left(\frac{d}{dz}\right)Z_{n+1}^{(\tilde{\ell})}(z)\right.$$

$$\left.+\frac{1}{n+1}(n+1)(n+2)\left(\frac{Z_{n+1}^{(\tilde{\ell})}(z)}{z}\right)\right]\mid_{z=k(p,(-1)^{\ell}j\omega)r}P_{n+1}^{|m|-1}(\cos(\theta))\exp(im\phi)\exp(-i\phi)$$

$$(n+\mid m\mid)(n+\mid m\mid-1)\left[\left(\frac{d}{dz}\right)Z_{n-1}^{(\tilde{\ell})}(z)\right.$$

$$\left.-\frac{1}{n}n(n-1)\left(\frac{Z_{n-1}^{(\tilde{\ell})}(z)}{z}\right)\right]\mid_{z=k(p,(-1)^{\ell}j\omega)r}P_{n-1}^{|m|-1}(\cos(\theta))\exp(im\phi)\exp(-i\phi)\Bigg\}\qquad(10.2.7.2)$$

Substituting the spherical Bessel function recursion relationships (10.1.1.22) and (10.1.1.23) into (10.2.7.2) gives us

$$\left(\frac{\partial}{\partial(U_q+iV_q)/2}\right)\left(\frac{\partial}{\partial\mathcal{C}(p,\tilde{\ell},(-1)^\ell j\omega,n,m,t)}\right)\boldsymbol{A}_{(p,q)}(\tilde{\ell},(-1)^\ell j\omega,t)_{sphericalharmonics}\cdot\boldsymbol{e}_r$$

$$= Z_n^{(\tilde{\ell})}\mid_{z=k(p,(-1)^\ell j\omega)r}\Big[(n-\mid m\mid+1)(n-\mid m\mid+2)P_{n+1}^{|m|-1)}(\cos(\theta))$$

$$-(n+\mid m\mid)(n+\mid m\mid-1)P_{n-1}^{|m|-1}(\cos(\theta))\Big]\exp(i(m-1)\phi)) \tag{10.2.7.3}$$

Substituting the associated Legendre function recursion relationship (10.1.3.23) into (10.2.7.3) gives us

$$\left(\frac{\partial}{\partial(U_q+iV_q)/2}\right)\left(\frac{\partial}{\partial\mathcal{C}(p,\tilde{\ell},(-1)^\ell j\omega,n,m,t)}\right)\boldsymbol{A}_{(p,q)}(\tilde{\ell},(-1)^\ell j\omega,t)_{sphericalharmonics}\cdot\boldsymbol{e}_r$$

$$= Z_n^{(\tilde{\ell})}\mid_{z=k(p,(-1)^\ell j\omega)r}(2n+1)P_n^{|m|}(\cos(\theta))\exp(im\phi)\exp(-i\phi) \tag{10.2.7.4}$$

which corresponds to this term of the addition theorem expansion.

10.2.8 The θ component of the $(U_q - iV_q)/2$ Term

We now state a theorem concerning the θ component of the

$$q \to (U_q - iV_q)/2$$

term.

Theorem 10.11

$$\left(\frac{\partial}{\partial(U_q-iV_q)/2}\right)\left(\frac{\partial}{\partial\mathcal{C}(p,\tilde{\ell},(-1)^\ell j\omega,n,m,t)}\right)\boldsymbol{A}_{(p,q)}(\tilde{\ell},(-1)^\ell j\omega,t)_{sphericalharmonics}\cdot\boldsymbol{e}_\theta =$$

$$\left(\frac{\partial}{\partial(U_q-iV_q)/2}\right)\left(\frac{\partial}{\partial\mathcal{C}(p,\tilde{\ell},(-1)^\ell j\omega,n,m,t)}\right)\boldsymbol{A}_{(p,q)}(\tilde{\ell},(-1)^\ell j\omega,t)_{additiontheorem}\cdot\boldsymbol{e}_\theta \tag{10.2.8.1}$$

Proof of Theorem. Using (10.2.8.1) and (10.2.2.2) we have the left side of (10.2.8.1) is

$$\left\{\left(\boldsymbol{L}_{(n+1,p)}^{(m+1,\tilde{\ell},(-1)^\ell j\omega)}+\frac{1}{n+1}\boldsymbol{N}_{(n+1,p)}^{(m+1,\tilde{\ell},(-1)^\ell j\omega)}\right)\right.$$

$$\left.+\left(\boldsymbol{L}_{(n-1,p)}^{(m+1,\tilde{\ell},(-1)^\ell j\omega)}-\frac{1}{n}\boldsymbol{N}_{(n-1,p)}^{(m+1,\tilde{\ell},(-1)^\ell j\omega)}\right)-i\left(\frac{(2n+1)}{n(n+1)}\right)\boldsymbol{M}_{(n,p)}^{(m+1,\tilde{\ell},(-1)^\ell j\omega)}\right\}\cdot\boldsymbol{e}_\theta$$

$$=\left\{\left(\frac{d}{d\theta}\right)P_{n+1}^{m+1}(\cos(\theta))\left[\frac{Z_{n+1}^{(\tilde{\ell})}(z)}{z}+\frac{W_n^{(\tilde{\ell})}}{n+1}\right]\exp(i(m+1)\phi)\right.$$

$$\left(\frac{d}{d\theta}\right) P_{n-1}^{m+1}(\cos(\theta)) \left[\frac{Z_{n-1}^{(\tilde{\ell})}(z)}{z} - \frac{W_{n-1}^{(\tilde{\ell})}(z)}{z}\right] \exp(i(m+1)\phi)$$

$$-i\left(\frac{(2n+1)i(m+1)}{n(n+1)}\right) Z_n^{(\tilde{\ell})}(z) \left(\frac{P_n^{m+1}(\cos(\theta))}{\sin(\theta)} \exp(i(m+1)\phi)\right)\Bigg\} \tag{10.2.8.2}$$

Using the recursion relationships (10.1.1.24) and (10.1.1.25) in (10.2.8.2) we have that the left side of (10.2.8.1) is

$$\left(\frac{\partial}{\partial(U_q - iV_q)/2}\right)\left(\frac{\partial}{\partial \mathcal{C}(p,\tilde{\ell},(-1)^{\ell} j\omega, n, m, t)}\right) \boldsymbol{A}_{(p,q)}(\tilde{\ell},(-1)^{\ell} j\omega, t)_{spherical harmonics} \cdot \boldsymbol{e}_{\theta} =$$

$$\left(\frac{d}{d\theta}\right) P_{n+1}^{m+1}(\cos(\theta)) \left(\frac{Z_n^{(\tilde{\ell})}(z)}{n+1}\right) \exp(i(m+1)\phi)$$

$$+\left(\frac{d}{d\theta}\right) P_{n-1}^{m+1}(\cos(\theta)) \left(\frac{Z_n^{(\tilde{\ell})}(z)}{n}\right) \exp(i(m+1)\phi)$$

$$+\left(\frac{(m+1)(2n+1)}{n(n+1)}\right) \frac{P_n^{m+1}(\cos(\theta))}{\sin(\theta)} \exp(i(m+1)\phi) \tag{10.2.8.3}$$

We next use the following lemma.

Lemma 10.5 *For all nonnegative integers n and all integers m ranging from $-n$ to $+n$ we have*

$$\frac{1}{n+1}\left(\frac{d}{d\theta}\right) P_{n+1}^{m+1}(\cos(\theta)) + \frac{1}{n}\left(\frac{d}{d\theta}\right) P_{n-1}^{m+1}(\cos(\theta))$$

$$+\frac{(m+1)(2n+1)}{n(n+1)} \frac{P_n^{m+1}(\cos(\theta))}{\sin(\theta)} = (2n+1) P_n^m(\cos(\theta))\cos(\theta) \tag{10.2.8.4}$$

Proof of Lemma. Equation (10.2.8.4) or (10.1.3.26) relates derivatives of associated Legendre function to the product of the cosine function and the associated Legendre function.

We show computer output which compares the left and right sides of the important identity (10.2.8.4).

```
 0.575958653158129      = THETHA0
  33.0000000000000      = THET0D
  1.00000000000000      = COSTH0**2+SINTH0**2
 0.287979326579064      = THET0D*PI/DFLOAT(180)
         0           1 = M,N
  1.22020992922740      =  DPDTH(N+1,M+1,THET0D)
         2           1  0.838670567945424      = N,M,X
  1.22020992922740     =-SINTH0*DALFF(N+1,M+1,COSTH0)
 0.000000000000000E+000 = DPDTH(N-1,M+1,THET0D)
         0           1  0.838670567945424      = N,M,X
 0.000000000000000E+000   =-SINTH0*DALFF(N-1,M+1,COSTH0)
  2.11010496461370
```

```
 = (1/(n+1))(d/d theta)P_{n+1}^{m+1}(\cos(theta))
 + (1/n)(d / d theta)P_{n-1}^{m+1}(\cos(theta))
 + [(m+1)(2n+1))/(n(n+1))]P_{n}^{m+1}(\cos(theta)) /
                                    \sin(theta)
  2.11010496461370
 = (2n+1)P_{n}^{m}(\cos(theta)) \cos(theta)
 0.575958653158129      = THETHA0
  33.0000000000000      = THET0D
  1.00000000000000      = COSTH0**2+SINTH0**2
 0.287979326579064      = THET0D*PI/DFLOAT(180)
          0           2 = M,N
-0.565442402871763      =  DPDTH(N+1,M+1,THET0D)
          3           1  0.838670567945424      = N,M,X
-0.565442402871763     =-SINTH0*DALFF(N+1,M+1,COSTH0)
 0.838670567945424      = DPDTH(N-1,M+1,THET0D)
          1           1  0.838670567945424      = N,M,X
 0.838670567945424        =-SINTH0*DALFF(N-1,M+1,COSTH0)
  2.32753090287902
 = (1/(n+1))(d/d theta)P_{n+1}^{m+1}(\cos(theta))
 + (1/n)(d / d theta)P_{n-1}^{m+1}(\cos(theta))
 + [(m+1)(2n+1))/(n(n+1))]P_{n}^{m+1}(\cos(theta)) /
                                    \sin(theta)
  2.32753090287902
 = (2n+1)P_{n}^{m}(\cos(theta)) \cos(theta)
 0.575958653158129      = THETHA0
  33.0000000000000      = THET0D
  1.00000000000000      = COSTH0**2+SINTH0**2
 0.287979326579064      = THET0D*PI/DFLOAT(180)
          1           2 = M,N
  9.06909745038895      =  DPDTH(N+1,M+1,THET0D)
          3           2  0.838670567945424      = N,M,X
  9.06909745038895     =-SINTH0*DALFF(N+1,M+1,COSTH0)
 0.000000000000000E+000 = DPDTH(N-1,M+1,THET0D)
          1           2  0.838670567945424      = N,M,X
 0.000000000000000E+000   =-SINTH0*DALFF(N-1,M+1,COSTH0)
  5.74622765853812
 = (1/(n+1))(d/d theta)P_{n+1}^{m+1}(\cos(theta))
 + (1/n)(d / d theta)P_{n-1}^{m+1}(\cos(theta))
 + [(m+1)(2n+1))/(n(n+1))]P_{n}^{m+1}(\cos(theta)) /
                                    \sin(theta)
  5.74622765853812
 = (2n+1)P_{n}^{m}(\cos(theta)) \cos(theta)
 0.575958653158129      = THETHA0
  33.0000000000000      = THET0D
  1.00000000000000      = COSTH0**2+SINTH0**2
```

```
0.287979326579064      = THETOD*PI/DFLOAT(180)
         0           3 = M,N
-5.34647200179526      =  DPDTH(N+1,M+1,THETOD)
         4           1  0.838670567945424      = N,M,X
-5.34647200179526     =-SINTH0*DALFF(N+1,M+1,COSTH0)
 1.22020992922740      = DPDTH(N-1,M+1,THETOD)
         2           1  0.838670567945424      = N,M,X
 1.22020992922740        =-SINTH0*DALFF(N-1,M+1,COSTH0)
 1.27235504935530
= (1/(n+1))(d/d theta)P_{n+1}^{m+1}(\cos(theta))
+ (1/n)(d / d theta)P_{n-1}^{m+1}(\cos(theta))
+ [(m+1)(2n+1))/(n(n+1))]P_{n}^{m+1}(\cos(theta)) /
                                  \sin(theta)
 1.27235504935530
= (2n+1)P_{n}^{m}(\cos(theta)) \cos(theta)
0.575958653158129      = THETHA0
 33.0000000000000      = THETOD
 1.00000000000000      = COSTH0**2+SINTH0**2
0.287979326579064      = THETOD*PI/DFLOAT(180)
         1           3 = M,N
 12.6559607364621      =  DPDTH(N+1,M+1,THETOD)
         4           2  0.838670567945424      = N,M,X
 12.6559607364621     =-SINTH0*DALFF(N+1,M+1,COSTH0)
 2.74063637292780      = DPDTH(N-1,M+1,THETOD)
         2           2  0.838670567945424      = N,M,X
 2.74063637292780        =-SINTH0*DALFF(N-1,M+1,COSTH0)
 12.0710583961309
= (1/(n+1))(d/d theta)P_{n+1}^{m+1}(\cos(theta))
+ (1/n)(d / d theta)P_{n-1}^{m+1}(\cos(theta))
+ [(m+1)(2n+1))/(n(n+1))]P_{n}^{m+1}(\cos(theta)) /
                                  \sin(theta)
 12.0710583961309
= (2n+1)P_{n}^{m}(\cos(theta)) \cos(theta)
0.575958653158129      = THETHA0
 33.0000000000000      = THETOD
 1.00000000000000      = COSTH0**2+SINTH0**2
0.287979326579064      = THETOD*PI/DFLOAT(180)
         2           3 = M,N
 56.4830305953196      =  DPDTH(N+1,M+1,THETOD)
         4           3  0.838670567945424      = N,M,X
 56.4830305953196     =-SINTH0*DALFF(N+1,M+1,COSTH0)
0.000000000000000E+000 = DPDTH(N-1,M+1,THETOD)
         2           3  0.838670567945424      = N,M,X
0.000000000000000E+000   =-SINTH0*DALFF(N-1,M+1,COSTH0)
 21.9073392084600
```

```
= (1/(n+1))(d/d theta)P_{n+1}^{m+1}(\cos(theta))
+ (1/n)(d / d theta)P_{n-1}^{m+1}(\cos(theta))
+ [(m+1)(2n+1))/(n(n+1))]P_{n}^{m+1}(\cos(theta)) /
                                    \sin(theta)
 21.9073392084600
= (2n+1)P_{n}^{m}(\cos(theta)) \cos(theta)
```

Substituting (10.2.8.4) into (10.2.8.3) gives us the relationship

$$\left(\frac{\partial}{\partial(U_q - iV_q)/2}\right)\left(\frac{\partial}{\partial\mathcal{C}(p,\tilde{\ell},(-1)^{\ell}j\omega,n,m,t)}\right)\boldsymbol{A}_{(p,q)}(\tilde{\ell},(-1)^{\ell}j\omega,t)_{sphericalharmonics}\cdot\boldsymbol{e}_{\theta}$$

$$= \{(2n+1)P_n^m(\cos(\theta))\}\cos(\theta) \tag{10.2.8.5}$$

which is the right side of (10.2.8.1) which proves the theorem.

10.2.9 The ϕ Component of the $(U_q - iV_q)/2$ Term

We now state a theorem concerning the ϕ component of the

$$q \to (U_q - iV_q)/2$$

term.

Theorem 10.12

$$\left(\frac{\partial}{\partial(U_q - iV_q)/2}\right)\left(\frac{\partial}{\partial\mathcal{C}(p,\tilde{\ell},(-1)^{\ell}j\omega,n,m,t)}\right)\boldsymbol{A}_{(p,q)}(\tilde{\ell},(-1)^{\ell}j\omega,t)_{sphericalharmonics}\cdot\boldsymbol{e}_{\phi} =$$

$$\left(\frac{\partial}{\partial(U_q - iV_q)/2}\right)\left(\frac{\partial}{\partial\mathcal{C}(p,\tilde{\ell},(-1)^{\ell}j\omega,n,m,t)}\right)\boldsymbol{A}_{(p,q)}(\tilde{\ell},(-1)^{\ell}j\omega,t)_{additiontheorem}\cdot\boldsymbol{e}_{\phi} \tag{10.2.9.1}$$

Proof of the Theorem. We observe that the left side of equation (10.2.9.1) is

$$\left(\frac{\partial}{\partial(U_q - iV_q)/2}\right)\left(\frac{\partial}{\partial\mathcal{C}(p,\tilde{\ell},(-1)^{\ell}j\omega,n,m,t)}\right)\boldsymbol{A}_{(p,q)}(\tilde{\ell},(-1)^{\ell}j\omega,t)_{sphericalharmonics}\cdot\boldsymbol{e}_{\phi} =$$

$$\left\{\left(\boldsymbol{L}_{(n+1,p)}^{(m+1,\tilde{\ell},(-1)^{\ell}j\omega)} + \frac{1}{n+1}\boldsymbol{N}_{(n+1,p)}^{(m+1,\tilde{\ell},(-1)^{\ell}j\omega)}\right)\right.$$

$$\left. + + \left(\boldsymbol{L}_{(n-1,p)}^{(m+1,\tilde{\ell},(-1)^{\ell}j\omega)} - \frac{1}{n}\boldsymbol{N}_{(n-1,p)}^{(m+1,\tilde{\ell},(-1)^{\ell}j\omega)}\right) - i\left(\frac{(2n+1)}{n(n+1)}\right)\boldsymbol{M}_{(n,p)}^{(m+1,\tilde{\ell},(-1)^{\ell}j\omega)}\right\}\cdot\boldsymbol{e}_{\phi}$$

10.2.10 The θ Component of the $(U_q + iV_q)/2$ Term

Now we carry out the proof for the θ component of the $(U_q + iV_q)/2$ term.

Theorem 10.13 *If the vector potential at brain activity site q is (10.2.2.2) for the vector spherical harmonic expansion and by (10.2.2.3) for the addition theorem expansion and the dipole direction giving the transmembrane current direction at site q is given by (9.5.2.6), and the coefficient*

$$(p, q, \tilde{\ell}, (-1)^\ell j\omega, m, t) \to \mathcal{C}(p, q, \tilde{\ell}, (-1)^\ell j\omega, n, m, t) \tag{10.2.10.1}$$

is defined by (10.2.2.4) then

$$\left(\frac{\partial}{\partial(U_q + iV_q)/2}\right)\left(\frac{\partial}{\partial \mathcal{C}(p, q, \tilde{\ell}, (-1)^\ell j\omega, n, m, t)}\right) \boldsymbol{A}_{(p,q)}(\tilde{\ell}, (-1)^\ell j\omega, t)_{sphericalharmonics} \cdot \boldsymbol{e}_\theta =$$
$$\left(\frac{\partial}{\partial(U_q + iV_q)/2}\right)\left(\frac{\partial}{\partial \mathcal{C}(p, \tilde{\ell}, (-1)^\ell j\omega, n, m, t)}\right) \boldsymbol{A}_{(p,q)}(\tilde{\ell}, (-1)^\ell j\omega, t)_{additiontheorem} \cdot \boldsymbol{e}_\theta \tag{10.2.10.2}$$

Proof of Theorem. From equation (10.2.2.2) we see that the left side of (10.2.10.2) is

$$\left(\frac{\partial}{\partial(U_q + iV_q)/2}\right)\left(\frac{\partial}{\partial \mathcal{C}(p, q, \tilde{\ell}, (-1)^\ell j\omega, n, m, t)}\right) \boldsymbol{A}_{(p,q)}(\tilde{\ell}, (-1)^\ell j\omega, t)_{sphericalharmonics} \cdot \boldsymbol{e}_\theta =$$
$$-\Big\{ \quad (n-m+1)(n-m+2)\left[\boldsymbol{L}_{(n+1,p)}^{(m-1,\tilde{\ell},(-1)^\ell j\omega)} + \frac{1}{n+1}\boldsymbol{N}_{(n+1,p)}^{(m-1,\tilde{\ell},(-1)^\ell j\omega)}\right]$$
$$+(n+m)(n+m-1)\left[\boldsymbol{L}_{(n-1,p)}^{(m-1,\tilde{\ell},(-1)^\ell j\omega)} - \frac{1}{n1}\boldsymbol{N}_{(n-1,p)}^{(m-1,\tilde{\ell},(-1)^\ell j\omega)}\right]$$
$$+ \quad (n+m)(n-m+1)\left(\frac{i(2n+1)}{n(n+1)}\right)\boldsymbol{M}_{(n,p)}^{(m-1,\tilde{\ell},(-1)^\ell j\omega)}\Big\} \cdot \boldsymbol{e}_\theta \tag{10.2.10.3}$$

The exact value of the right side of (10.2.10.2) is

$$\left(\frac{\partial}{\partial(U_q + iV_q)/2}\right)\left(\frac{\partial}{\partial \mathcal{C}(p, \tilde{\ell}, (-1)^\ell j\omega, n, m, t)}\right) \boldsymbol{A}_{(p,q)}(\tilde{\ell}, (-1)^\ell j\omega, t)_{additiontheorem} \cdot \boldsymbol{e}_\theta$$
$$= (2n+1)\cos(\theta)P_n^m(\cos(\theta))Z_n^{(\tilde{\ell})}(z)\exp(i(m-1)\phi)\mid_{z=k(p,(-1)^\ell j\omega)r} \tag{10.2.10.4}$$

We need to compute

$$-\boldsymbol{e}_\theta \cdot \Big\{(n-m+1)(n-m+2)\left(\boldsymbol{L}_{(n+1,p)}^{(m-1,\tilde{\ell},(-1)^\ell j\omega)} + \frac{1}{n+1}\boldsymbol{N}_{(n+1,p)}^{(m-1,\tilde{\ell},(-1)^\ell j\omega)}\right)$$
$$+(n+m)(n+m-1)\left(\boldsymbol{L}_{(n-1,p)}^{(m-1,\tilde{\ell},(-1)^\ell j\omega)} - \frac{1}{n}\boldsymbol{N}_{(n-1,p)}^{(m-1,\tilde{\ell},(-1)^\ell j\omega)}\right)$$
$$+(n+m)(n-m+1)\left(\frac{i(2n+1)}{n(n+1)}\right)\boldsymbol{M}_{(n,p)}^{(m-1,\tilde{\ell},(-1)^\ell j\omega)}\Big\} \tag{10.2.10.5}$$

We begin with the following

Lemma 10.6 *For all nonnegative integers n and all integers m with $m-1$ not exceeding $n+1$ we have for*

$$(n,p,m,\tilde{\ell},(-1)^{\ell}j\omega) \to \left(\boldsymbol{L}_{(n+1,p)}^{(m-1,\tilde{\ell},(-1)^{\ell}j\omega)}, \boldsymbol{N}_{(n+1,p)}^{(m-1,\tilde{\ell},(-1)^{\ell}j\omega)}\right) \tag{10.2.10.6}$$

defined by (9.4.1.12) and (9.4.1.15) we have

$$\left[\boldsymbol{L}_{(n+1,p)}^{(m-1,\tilde{\ell},(-1)^{\ell}j\omega)} + \frac{1}{n+1}\boldsymbol{N}_{(n+1,p)}^{(m-1,\tilde{\ell},(-1)^{\ell}j\omega)}\right]\cdot \boldsymbol{e}_{\theta}$$

$$= \left(\frac{Z_n^{(\tilde{\ell})}(z)}{n+1}\right)\left(\frac{d}{d\theta}\right) P_{n+1}^{m-1}(\cos(\theta))\exp(i(m-1)\phi)\mid_{z=k(p,(-1)^{\ell}j\omega)r} \tag{10.2.10.7}$$

where

$$(n,z) \to Z_n^{(\tilde{\ell})}(z) \tag{10.2.10.8}$$

is defined by (10.1.1.16)

$$(n,z) \to W_n^{(\tilde{\ell})}(z) \tag{10.2.10.9}$$

is defined by (10.1.1.17) and

$$(n,m,\theta) \to P_{n+1}^{m-1}(\cos(\theta)) \tag{10.2.10.10}$$

is defined by (10.1.2.1)

Proof of Lemma. From the definitions (9.4.1.4), (9.4.1.5), and (9.4.1.3) of the standard vector fields

$$(m,n,\theta) \to \left(\boldsymbol{A}_{(m,n)}(\theta,\phi), \boldsymbol{B}_{(m,n)}(\theta,\phi), \boldsymbol{C}_{(m,n)}(\theta,\phi)\right) \tag{10.2.10.11}$$

(9.4.1.12) and (9.4.1.15) we have

$$\left[\boldsymbol{L}_{(n+1,p)}^{(m-1,\tilde{\ell},(-1)^{\ell}j\omega)} + \frac{1}{n+1}\boldsymbol{N}_{(n+1,p)}^{(m-1,\tilde{\ell},(-1)^{\ell}j\omega)}\right]\cdot \boldsymbol{e}_{\theta}$$

$$= \left[\frac{Z_{n+1}^{(\tilde{\ell})}(z)}{z}\left(\frac{d}{d\theta}\right) P_{n+1}^{m-1}(\cos(\theta))\exp(i(m-1)\phi)\right.$$

$$\left. + \quad \frac{W_{n+1}^{(\tilde{\ell})}(z)}{n+1}\left(\frac{d}{d\theta}\right) P_{n+1}^{m-1}(\cos(\theta))\exp(i(m-1)\phi)\right]\mid_{z=k(p,(-1)^{\ell}j\omega)r}$$

$$= \left[\frac{Z_{n+1}^{(\tilde{\ell})}(z)}{z} + \frac{W_{n+1}^{(\tilde{\ell})}(z)}{n+1}\right]\left(\frac{d}{d\theta}\right) P_{n+1}^{m-1}(\cos(\theta))\exp(i(m-1)\phi)\mid_{z=k(p,(-1)^{\ell}j\omega)r}$$

$$= \frac{Z_n^{(\tilde{\ell})}(z)}{n+1}\left(\frac{d}{d\theta}\right) P_{n+1}^{m-1}(\cos(\theta))\exp(i(m-1)\phi)\mid_{z=k(p,(-1)^{\ell}j\omega)r} \tag{10.2.10.12}$$

where in (10.2.10.12) we used the relation (10.1.1.24).

We also need the following.

Lemma 10.7 *From the definitions (9.4.1.4), (9.4.1.5), and (9.4.1.3) of the standard vector fields*

$$(m,n,\theta) \rightarrow \left(\boldsymbol{A}_{(m,n)}(\theta,\phi), \boldsymbol{B}_{(m,n)}(\theta,\phi), \boldsymbol{C}_{(m,n)}(\theta,\phi)\right) \tag{10.2.10.13}$$

(9.4.1.12) and (9.4.1.15) for

$$(n,p,m,\tilde{\ell},(-1)^{\ell}j\omega) \rightarrow \left(\boldsymbol{L}_{(n-1,p)}^{(m-1,\tilde{\ell},(-1)^{\ell}j\omega)}, \boldsymbol{N}_{(n-1,p)}^{(m-1,\tilde{\ell},(-1)^{\ell}j\omega)}\right) \tag{10.2.10.14}$$

we have

$$\left[\boldsymbol{L}_{(n-1,p)}^{(m-1,\tilde{\ell},(-1)^{\ell}j\omega)} - \frac{1}{n}\boldsymbol{N}_{(n-1,p)}^{(m-1,\tilde{\ell},(-1)^{\ell}j\omega)}\right] \cdot \boldsymbol{e}_{\theta}$$

$$= \left(\frac{Z_n^{(\tilde{\ell})}(z)}{n}\right)\left\{\left(\frac{d}{d\theta}\right)P_{n-1}^{m-1}(\cos(\theta))\right\}\exp(i(m-1)\phi)\mid_{z=k(p,(-1)^{\ell}j\omega)r} \tag{10.2.10.15}$$

where $Z_n^{(\tilde{\ell})}$ is defined by (10.1.1.16) and $P_{n-1}^{m-1}(x)$ is defined by (10.1.2.1).

Proof of Lemma. From the definitions (9.4.1.4), (9.4.1.5), (9.4.1.3), (9.4.1.12) and (9.4.1.15) we have

$$\left[\boldsymbol{L}_{(n-1,p)}^{(m-1,\tilde{\ell},(-1)^{\ell}j\omega)} - \frac{1}{n}\boldsymbol{N}_{(n-1,p)}^{(m-1,\tilde{\ell},(-1)^{\ell}j\omega)}\right] \cdot \boldsymbol{e}_{\theta}$$

$$= \left[\frac{Z_{n-1}^{(\tilde{\ell})}(z)}{z}\left\{\left(\frac{d}{d\theta}\right)P_{n-1}^{m-1}(\cos(\theta))\right\}\exp(i(m-1)\phi)\right.$$

$$\left. - \quad \frac{W_{n-1}^{(\tilde{\ell})}(z)}{n}\left\{\left(\frac{d}{d\theta}\right)P_{n-1}^{m-1}(\cos(\theta))\right\}\exp(i(m-1)\phi)\right]\mid_{z=k(p,(-1)^{\ell}j\omega)r}$$

$$= \left[\frac{Z_{n-1}^{(\tilde{\ell})}(z)}{z} - \frac{W_{n-1}^{(\tilde{\ell})}(z)}{n}\right]\left\{\left(\frac{d}{d\theta}\right)P_{n-1}^{m-1}(\cos(\theta))\right\}\exp(i(m-1)\phi)\mid_{z=k(p,(-1)^{\ell}j\omega)r}$$

$$= \frac{Z_n^{(\tilde{\ell})}(z)}{n}\left\{\left(\frac{d}{d\theta}\right)P_{n-1}^{m-1}(\cos(\theta))\right\}\exp(i(m-1)\phi)\mid_{z=k(p,(-1)^{\ell}j\omega)r} \tag{10.2.10.16}$$

where we have made use of the spherical Bessel function recursion relationship (10.1.1.25). This completes the proof of (10.2.10.15) and the lemma.

We need another lemma to complete the proof of the theorem of these section.

Lemma 10.8 *For all nonnegative integers n and all nonnegative integers m not exceeding $n+1$ we have*

$$\boldsymbol{M}_{(n,p)}^{(m-1,\tilde{\ell},(-1)^{\ell}j\omega)} \cdot \boldsymbol{e}_{\theta}$$

$$= Z_n^{(\tilde{\ell})}(z)\left\{i(m-1)\right\}\left(\frac{P_n^{m-1}(\cos(\theta))}{\sin(\theta)}\right)\exp(i(m-1)\phi)\mid_{z=k(p,(-1)^{\ell}j\omega)r} \tag{10.2.10.17}$$

Proof of Lemma. This follows from the definition (9.4.1.13) of

$$(n,m,p,\tilde{\ell},(-1)^{\ell}j\omega) \rightarrow \boldsymbol{M}_{(n,p)}^{(m-1,\tilde{\ell},(-1)^{\ell}j\omega)} \tag{10.2.10.18}$$

and the definition (9.4.1.4) of $\boldsymbol{A}_{(m,n)}$.

We combine the previous lemmas to prove the following.

Lemma 10.9 *For all brain activity site indices q, all tissue layers p, all frquency indices j and ℓ, and spherical Bessel function types $\tilde{\ell}$ we have*

$$\left(\frac{\partial}{\partial(U_q+iV_q)/2}\right)\left(\frac{\partial}{\partial\mathcal{C}(p,q,\tilde{\ell},(-1)^\ell j\omega,n,m,t)}\right)\boldsymbol{A}_{(p,q)}(\tilde{\ell},(-1)^\ell j\omega,t)_{sphericalharmonics}\cdot\boldsymbol{e}_\theta$$

$$= Z_n^{(\tilde{\ell})}(z)\exp(i(m-1)\phi)\left[(-1)\left(\frac{(n-m+1)(n-m+2)}{n+1}\right)\left(\frac{d}{\theta}\right)P_{n+1}^{m-1}(\cos(\theta))\right.$$

$$+(-1)\left(\frac{(n+m)(n+m-1)}{n}\right)\left(\frac{d}{d\theta}\right)P_{n-1}^{m-1}(\cos(\theta))$$

$$\left.+\quad\left(\frac{(n+m)(n-m+1)(m-1)(2n+1)}{n(n+1)}\right)\left(\frac{P_n^{m-1}(\cos(\theta))}{\sin(\theta)}\right)\right]|_{z=k(p,(-1)^\ell j\omega)r} \quad (10.2.10.19)$$

Proof of Lemma. We simply combine equations (10.2.10.7), (10.2.10.15), and (10.2.10.17) from the previous lemmas we derive (10.2.10.19).

Proof of Theorem. From equation (10.2.10.19) and the associated Legendre function identity (10.1.3.24) we immediately deduce that the left side of (10.2.10.2) is equal to (10.2.10.19) which is, in turn, equal to (10.2.10.4) which is the right side of (10.2.10.2). which proves the theorem.

10.2.11 The ϕ Component of the $(U_q+iV_q)/2$ Term

We have the following theorem.

Theorem 10.14

$$\left(\frac{\partial}{\partial(U_q+iV_q)/2}\right)\left(\frac{\partial}{\partial\mathcal{C}(p,q,\tilde{\ell},(-1)^\ell j\omega,n,m,t)}\right)\boldsymbol{A}_{(p,q)}(\tilde{\ell},(-1)^\ell j\omega,t)_{sphericalharmonics}\cdot\boldsymbol{e}_\phi =$$

$$\left(\frac{\partial}{\partial(U_q+iV_q)/2}\right)\left(\frac{\partial}{\partial\mathcal{C}(p,\tilde{\ell},(-1)^\ell j\omega,n,m,t)}\right)\boldsymbol{A}_{(p,q)}(\tilde{\ell},(-1)^\ell j\omega,t)_{additiontheorem}\cdot\boldsymbol{e}_\phi \quad (10.2.11.1)$$

where the vector potential

$$(p,q,\tilde{\ell},(-1)^\ell j\omega,t)\rightarrow\boldsymbol{A}_{(p,q)}(\tilde{\ell},(-1)^\ell j\omega,t) \quad (10.2.11.2)$$

is defined by (9.5.2.4) and (10.2.2.2) and the coefficient

$$(p,\tilde{\ell},(-1)^\ell j\omega,n,m,t)\rightarrow\mathcal{C}(p,\tilde{\ell},(-1)^\ell j\omega,n,m,t) \quad (10.2.11.3)$$

is defined by (10.2.2.4).

Proof of Theorem. We begin with the following Lemma which uses (10.2.2.2).

Lemma 10.10 *For all indices n, p, m, $\tilde{\ell}$, and frequencies $(-1)^{\ell} j\omega$ we have*

$$\left(\frac{\partial}{\partial(U_q + iV_q)/2}\right)\left(\frac{\partial}{\partial \mathcal{C}(p,q,\tilde{\ell},(-1)^{\ell} j\omega,n,m,t)}\right) \boldsymbol{A}_{(p,q)}(\tilde{\ell},(-1)^{\ell} j\omega,t)_{sphericalharmonics} \cdot \boldsymbol{e}_{\phi} =$$

$$(-1)(n- \mid m \mid +1)(n- \mid m \mid +2)\left[\boldsymbol{L}_{(n+1,p)}^{(m-1,\tilde{\ell},(-1)^{\ell} j\omega)} + \frac{1}{n+1}\boldsymbol{N}_{(n+1,p)}^{(m-1,\tilde{\ell},(-1)^{\ell} j\omega)}\right] \cdot \boldsymbol{e}_{\phi}$$

$$+(-1)(n+ \mid m \mid)(n+ \mid m \mid -1)\left[\boldsymbol{L}_{(n-1,p)}^{(m-1,\tilde{\ell},(-1)^{\ell} j\omega)} - \frac{1}{n}\boldsymbol{N}_{(n-1,p)}^{(m-1,\tilde{\ell},(-1)^{\ell} j\omega)}\right] \cdot \boldsymbol{e}_{\phi}$$

$$+(-1)(n+ \mid m \mid)(n- \mid m \mid +1)\left[\left(\frac{i(2n+1)}{n(n+1)}\right)\boldsymbol{M}_{(n,p)}^{(m-1,\tilde{\ell},(-1)^{\ell} j\omega)}\right] \cdot \boldsymbol{e}_{\phi}$$

$$= (-i)(2n+1)Z_n^{(}\tilde{\ell})(z)P_n^m(\cos(\theta))\exp(i(m-1)\phi) \mid_{z=k(p,(-1)^{\ell} j\omega)r} \qquad (10.2.11.4)$$

Proof of Lemma. This lemma gives the theorem since the right side of equation (10.2.11.4) is the right side of (10.2.11.1) in view of equation (5.2.5.6) and (10.2.2.3).

We break down the proof of this lemma into three easier lemmas and an associated Legendre function identity.

Lemma 10.11 *For all nonnegative integers n and all integers m we have*

$$\left[\boldsymbol{L}_{(n+1,p)}^{(m-1,\tilde{\ell},(-1)^{\ell} j\omega)} + \frac{1}{n+1}\boldsymbol{N}_{(n+1,p)}^{(m-1,\tilde{\ell},(-1)^{\ell} j\omega)}\right] \cdot \boldsymbol{e}_{\phi} =$$

$$\left[\left(\frac{Z_{n+1}^{(\tilde{\ell})}(z)}{z}\right) i(m-1)\left(\frac{P_{n+1}^{m-1}(\cos(\theta))}{\sin(\theta)}\right)\right.$$

$$\left. + \quad \left(\frac{W_{n+1}^{(\tilde{\ell})}(z)}{n+1}\right) i(m-1)\left(\frac{P_{n+1}^{(m-1)}(\cos(\theta))}{\sin(\theta)}\right)\right]$$

$$= \left[\frac{Z_{n+1}^{(\tilde{\ell})}(z)}{z} + \frac{W_{n+1}^{(\tilde{\ell})}(z)}{n+1}\right]\left(\frac{P_{n+1}^{m-1}(\cos(\theta))}{\sin(\theta)}\right) i(m-1)\exp(i(m-1)\phi)$$

$$\left(\frac{Z_n^{(\tilde{\ell})}(z)}{n+1}\right)\left(\frac{P_{n+1}^{m-1}(\cos(\theta))}{\sin(\theta)}\right) i(m-1)\exp(i(m-1)\phi) \mid_{z=k(p,(-1)^{\ell} j\omega)r} \qquad (10.2.11.5)$$

Proof of Lemma. This is just a consequence of the spherical Bessel function recursion relationship (10.1.1.24).

The second lemma helps us with the second term of the left side of equation (10.2.11.4).

Lemma 10.12 *For all nonnegative integers n and all integers m and all spherical Bessel function types $\tilde{\ell}$ and all frequencies $(-1)^{\ell} j\omega$ we have*

$$\left[\boldsymbol{L}_{(n-1,p)}^{(m-1,\tilde{\ell},(-1)^{\ell} j\omega)} - \frac{1}{n}\boldsymbol{N}_{(n-1,p)}^{(m-1,\tilde{\ell},(-1)^{\ell} j\omega)}\right] \cdot \boldsymbol{e}_{\phi}$$

$$= \left(\frac{Z_n^{\tilde{\ell})}(z)}{n+1}\right)\left(\frac{P_{n-1}^{m-1}(\cos(\theta))}{\sin(\theta)}\right) i(m-1)\exp(i(m-1)\phi) \mid_{z=k(p,(-1)^{\ell} j\omega)r} \qquad (10.2.11.6)$$

Proof of Lemma. The left side of equation (10.2.11.6) is

$$\left[\boldsymbol{L}_{(n-1,p)}^{(m-1,\tilde{\ell},(-1)^{\ell}j\omega)} - \frac{1}{n}\boldsymbol{N}_{(n-1,p)}^{(m-1,\tilde{\ell},(-1)^{\ell}j\omega)}\right]\cdot \boldsymbol{e}_{\phi}$$

$$= \left[\left(\frac{Z_{n-1}^{(\tilde{\ell})}(z)}{z}\right) i(m-1)\frac{P_{n-1}^{m-1}(\cos(\theta))}{\sin(\theta)}\right.$$

$$\left. - \left(\frac{W_{n-1}^{(\tilde{\ell})}(z)}{n}\right) i(m-1)\frac{P_{n-1}^{m-1}(\cos(\theta))}{\sin(\theta)}\right] \exp(i(m-1)\phi)\mid_{z=k(p,(-1)^{\ell}j\omega)r}$$

$$= \left[\frac{Z_{n-1}^{(\tilde{\ell})}(z)}{z} - \frac{W_{n-1}^{(\tilde{\ell})}(z)}{n}\right] i(m-1)\frac{P_{n-1}^{m-1}(\cos(\theta))}{\sin(\theta)}\exp(i(m-1)\phi)\mid_{z=k(p,(-1)^{\ell}j\omega)r}$$

$$= \frac{Z_{n}^{(\tilde{\ell})}(z)}{n} i(m-1)\left(\frac{P_{n-1}^{m-1}(\cos(\theta))}{\sin(\theta)}\right)\exp(i(m-1)\phi) \tag{10.2.11.7}$$

which is a consequence of the spherical Bessel function recursion relationship (10.1.1.25).

The next lemma enables us to evaluate the third term of the left side of equation (10.2.11.4).

Lemma 10.13 *For all all nonnegative integers n and all integers m all spherical Bessel functin types $\tilde{\ell}$ and all frequencies $(-1)^{\ell}j\omega$ we have*

$$\boldsymbol{M}_{(n,p)}^{(m-1,\tilde{\ell},(-1)^{\ell}j\omega)}\cdot \boldsymbol{e}_{\phi} =$$

$$Z_{n}^{(\tilde{\ell})}(z)\mid_{z=k(p,(-1)^{\ell}j\omega)r}\left(-\frac{d}{d\theta}\right) P_{n}^{m-1}(\cos(\theta))\exp(i(m-1)\phi) \tag{10.2.11.8}$$

Proof of Lemma. This is a consequence of the definitions (9.4.1.13) and (9.4.1.4). Putting together equations (10.2.11.5), (10.2.11.6), and (10.2.11.8) we have the following lemma

Lemma 10.14

$$\left(\frac{\partial}{\partial(U_q + iV_q)/2}\right)\left(\frac{\partial}{\partial\mathcal{C}(p,q,\tilde{\ell},(-1)^{\ell}j\omega,n,m,t)}\right)\boldsymbol{A}_{(p,q)}(\tilde{\ell},(-1)^{\ell}j\omega,t)_{spherical harmonics}\cdot\boldsymbol{e}_{\phi}$$

$$= (-i)\left[\left(\frac{(n-m+1)(n-m+2)(m-1)}{n+1}\right)\left(\frac{P_{n+1}^{m-1}(\cos(\theta))}{\sin(\theta)}\right)\right.$$

$$+\left(\frac{(n+m)(n+m-1)(m-1)}{n}\right)\left(\frac{P_{n-1}^{m-1}(\cos(\theta))}{\sin(\theta)}\right)$$

$$\left. - \left(\frac{(n+m)(n-m+1)(2n+1)}{n(n+1)}\right)\left\{\left(\frac{d}{d\theta}\right)P_{n}^{m-1}(\cos(\theta))\right\}\right]\exp(i(m-1)\phi)Z_{n}^{(\tilde{\ell})}(z)\mid_{z=k(p,(-1)^{\ell}j\omega)r}$$

$$= (-i)(2n+1)P_{n}^{m}(\cos(\theta))\exp(i(m-1)\phi)Z_{n}^{(\tilde{\ell})}(z) \tag{10.2.11.9}$$

Proof of Lemma We just use the associated Legendre function identity

$$\left(\frac{(n-m+1)(n-m+2)(m-1)}{n+1}\right)\left(\frac{P_{n+1}^{m-1}(\cos(\theta))}{\sin(\theta)}\right)$$
$$+\left(\frac{(n+m)(n+m-1)(m-1)}{n}\right)\left(\frac{P_{n-1}^{m-1}(\cos(\theta))}{\sin(\theta)}\right)$$
$$-\left(\frac{(n+m)(n-m+1)(2n+1)}{n(n+1)}\right)\left\{\left(\frac{d}{d\theta}\right)P_n^{m-1}(\cos(\theta))\right\}$$
$$=(2n+1)P_n^m(\cos(\theta)) \qquad (10.2.11.10)$$

Substituting (10.2.11.10) or equivalently (10.1.3.25) into (10.2.11.9) gives the lemma and the theorem proving (10.2.11.4). Following (10.1.3.25) there is table of computed values of the left and right sides of this equation showing agreement to machine precision.

10.3 The Expansion of the Source Dynamic Voltage Representation of Brain Activity

We use the relationship (10.2.2.2) to compute the expansion of the divergence of the vector potential of brain activity and consequently that of the dynamic voltage associated with brain activity.

10.3.1 Expansion of the Divergence of the Vector Potential of Brain Activity

We apply the divergence operation to each side of (10.2.2.2) remembering that the divergence of the $\boldsymbol{M}$ and $\boldsymbol{N}$ vector fields are zero since they are each separately multiples of the application of the curl operation to the other and the divergence of any curl of a vector field is zero.

$$\nabla\cdot(\boldsymbol{A}_{(p,q)}(\tilde{\ell},(-1)^{\ell}j\omega,t))) =$$
$$\left(\frac{\mu_p(-(-1)^{\tilde{\ell}}ik(p,(-1)^{\ell}j\omega)\exp(i(-1)^{\ell}j\omega t)}{4\pi}\right)\sum_{n=0}^{\infty}\sum_{m=-n}^{m=+n}\left\{c(n,m,0,(-1)^{\ell}j\omega,p,q)\left\{\right.\right.$$
$$W_q\left\{(n-m+1)\left(\nabla\cdot(\boldsymbol{L}_{(n+1,p)}^{(m,\tilde{\ell},(-1)^{\ell}j\omega)})+\frac{1}{n+1}\nabla\cdot(\boldsymbol{N}_{(n+1,p)}^{(m,\tilde{\ell},(-1)^{\ell}j\omega)})\right)\right.$$
$$-(n+m)\left(\nabla\cdot(\boldsymbol{L}_{(n-1,p)}^{(m,\tilde{\ell},(-1)^{\ell}j\omega)})-\frac{1}{n}\nabla\cdot(\boldsymbol{N}_{(n-1,p)}^{(m,\tilde{\ell},(-1)^{\ell}j\omega)})\right)$$
$$\left.+im\left(\frac{2n+1}{n(n+1)}\right)\nabla\cdot(\boldsymbol{M}_{(n,p)}^{(m,\tilde{\ell},(-1)^{\ell}j\omega)})\right\}$$
$$+\left(\frac{U_q-iV_q}{2}\right)\left\{\left(\nabla\cdot(\boldsymbol{L}_{(n+1,p)}^{(m+1,\tilde{\ell},(-1)^{\ell}j\omega)})+\frac{1}{n+1}\nabla\cdot(\boldsymbol{N}_{(n+1,p)}^{(m+1,\tilde{\ell},(-1)^{\ell}j\omega)})\right)\right.$$
$$+\left(\nabla\cdot(\boldsymbol{L}_{(n-1,p)}^{(m+1,\tilde{\ell},(-1)^{\ell}j\omega)})-\frac{1}{n}\nabla\cdot(\boldsymbol{N}_{(n-1,p)}^{(m+1,\tilde{\ell},(-1)^{\ell}j\omega)})\right)$$
$$-i\left(\frac{(2n+1)}{n(n+1)}\right)\nabla\cdot(\boldsymbol{M}_{(n,p)}^{(m+1,\tilde{\ell},(-1)^{\ell}j\omega)})$$
$$-\left(\frac{U_q+iV_q}{2}\right)\left\{(n-m+1)(n-m+2)\left(\nabla\cdot(\boldsymbol{L}_{(n+1,p)}^{(m-1,\tilde{\ell},(-1)^{\ell}j\omega)})\right.\right.$$
$$\left.+\frac{1}{n+1}\nabla\cdot(\boldsymbol{N}_{(n+1,p)}^{(m-1,\tilde{\ell},(-1)^{\ell}j\omega)})\right)$$
$$+(n+m)(n+m-1)\left(\nabla\cdot(\boldsymbol{L}_{(n-1,p)}^{(m-1,\tilde{\ell},(-1)^{\ell}j\omega)})-\frac{1}{n}\nabla\cdot(\boldsymbol{N}_{(n-1,p)}^{(m-1,\tilde{\ell},(-1)^{\ell}j\omega)})\right)$$
$$\left.\left.+(n+m)(n-m+1)\left(\frac{i(2n+1)}{n(n+1)}\right)\nabla\cdot(\boldsymbol{M}_{(n,p)}^{(m-1,\tilde{\ell},(-1)^{\ell}j\omega)})\right\}\right\}\right\} \tag{10.3.1.1}$$

10.3.2 The Dynamic Voltage Expansion

We want to move from measurements of external voltages outside the skull bone to brain activity and use this to help handicapped naturally operate an artificial limb.

The dynamic voltage satisfies the scalar Helmholtz equation. The relationship between the electric vector and the gradient of the voltage is

$$\boldsymbol{E}=-\frac{\partial\boldsymbol{A}}{\partial t}-\nabla(V) \tag{10.3.2.1}$$

Applying the divergence operator to each side of (10.3.2.1) and assuming that there are no net charge accumulations in the brain which is interpreted as

$$\nabla\cdot(\boldsymbol{E})=0 \tag{10.3.2.2}$$

we have

$$0 = \nabla\cdot(\boldsymbol{E}) = -i(-1)^{\ell}\omega\,\nabla\cdot(\boldsymbol{A}) - \nabla\cdot(\nabla(V)) \tag{10.3.2.3}$$

Substituting

$$\nabla\cdot(\nabla(V)) + k(p,(-1)^{\ell}\omega)^2 V = 0 \tag{10.3.2.4}$$

into (10.3.2.3) gives

$$V = \left(\frac{i(-1)^{\ell}\omega}{k(p,(-1)^{\ell}\omega)^2}\right)\nabla\cdot(\boldsymbol{A}) \tag{10.3.2.5}$$

so that

$$\nabla(V) = \left(\frac{i(-1)^{\ell}\omega}{k(p,(-1)^{\ell}\omega)^2}\right)\nabla(\nabla\cdot(\boldsymbol{A})) \tag{10.3.2.6}$$

Now using the fact that the divergence of the $\boldsymbol{N}$ and $\boldsymbol{M}$ vector fields are zero in equation (10.3.1.1) we have using (10.3.2.5) the dynamic voltage expansion from the neuronal source with index q is.

$$V_{(source,p,q)} = \left(\frac{i(-1)^\ell j\omega}{k(p,(-1)^\ell j\omega)^2}\right)\nabla\cdot(\boldsymbol{A}_{(p,q)}(\tilde{\ell},(-1)^\ell j\omega,t))) =$$

$$\left(\frac{i(-1)^\ell \omega}{k(p,(-1)^\ell \omega)^2}\right)\Bigg[\quad\left(\frac{\mu_p(-(-1)^{\tilde{\ell}} ik(p,(-1)^\ell j\omega)\exp(i(-1)^\ell j\omega t)}{4\pi}\right)\sum_{n=0}^{\infty}\sum_{m=-n}^{m=+n}\Bigg\{$$

$$c(n,m,0,(-1)^\ell j\omega,p,q)\Bigg\{$$

$$W_q\Bigg\{(n-m+1)\left(\nabla\cdot(\boldsymbol{L}_{(n+1,p)}^{(m,\tilde{\ell},(-1)^\ell j\omega)})\right)\quad-(n+m)\left(\nabla\cdot(\boldsymbol{L}_{(n-1,p)}^{(m,\tilde{\ell},(-1)^\ell j\omega)})\right)\Bigg\}$$

$$+\left(\frac{U_q-iV_q}{2}\right)\Bigg\{\left(\nabla\cdot(\boldsymbol{L}_{(n+1,p)}^{(m+1,\tilde{\ell},(-1)^\ell j\omega)})\right)+\left(\nabla\cdot(\boldsymbol{L}_{(n-1,p)}^{(m+1,\tilde{\ell},(-1)^\ell j\omega)})\right)\Bigg\}$$

$$-\left(\frac{U_q+iV_q}{2}\right)\Bigg\{(n-m+1)(n-m+2)\left(\nabla\cdot(\boldsymbol{L}_{(n+1,p)}^{(m-1,\tilde{\ell},(-1)^\ell j\omega)})\right)$$

$$+(n+m)(n+m-1)\left(\nabla\cdot(\boldsymbol{L}_{(n-1,p)}^{(m-1,\tilde{\ell},(-1)^\ell j\omega)})\right)\Bigg\}\quad\Bigg\}\quad\Bigg\}\quad\Bigg] \tag{10.3.2.7}$$

To evaluate the divergence of the $\boldsymbol{L}$ vector fields in (10.3.2.7) we use following notation for a general form of spherical Bessel and Hankel functions We define for all complex numbers z the relation

$$Z_n^{(\tilde{\ell})}(z) = \begin{cases} y_n(z) & \text{if} \quad \tilde{\ell}=-1 \\ j_n(z) & \text{if} \quad \tilde{\ell}=0 \\ h_n^{(1)}(z) & \text{if} \quad \tilde{\ell}=1 \\ h_n^{(2)}(z) & \text{if} \quad \tilde{\ell}=2 \end{cases} \tag{10.3.2.8}$$

so that using (10.3.2.7), (9.4.1.3), (9.4.1.5), (9.4.1.12), (10.1.1.5), (9.4.1.2), (4.1.1.66), (9.4.1.2), and (10.3.2.8)

$$\nabla\cdot(\boldsymbol{L}_{(n,p)}^{(m,\tilde{\ell},(-1)^\ell j\omega)})$$

$$= k(p,(-1)^\ell j\omega)Z_n^{(\tilde{\ell})}(k(p,(-1)^\ell j\omega)r)P_n^m(\cos(\theta))\exp(im\phi) \tag{10.3.2.9}$$

This relationship is also given in Stratton ([110]). We define

$$\Phi_{(n,p)}^{(m,\tilde{\ell},(-1)^\ell j\omega)} =$$

$$\Phi_{(n,p)}^{(m,\tilde{\ell},(-1)^\ell j\omega)}(r,\theta,\phi) = Z_n^{(\tilde{\ell})}(k(p,(-1)^\ell j\omega)r)P_n^m(\cos(\theta))\exp(im\phi) \tag{10.3.2.10}$$

Substituting (10.3.2.10) into (10.3.2.7) gives

$$V_{(source,p,q)} = \left(\frac{i(-1)^\ell j\omega}{k(p,(-1)^\ell j\omega)^2}\right)\nabla\cdot(\boldsymbol{A}_{(p,q)}(\tilde{\ell},(-1)^\ell j\omega,t)))$$

$$= i(-1)^\ell\omega\Bigg[\quad\left(\frac{\mu_p(-(-1)^{\tilde{\ell}} i\exp(i(-1)^\ell j\omega t)}{4\pi}\right)\sum_{n=0}^{\infty}\sum_{m=-n}^{m=+n}\Bigg\{$$

$$c(n,m,0,(-1)^{\ell}j\omega,p,q)\left\{\right.$$

$$W_q\left\{(n-m+1)\left(\Phi_{(n+1,p)}^{(m,\tilde{\ell},(-1)^{\ell}j\omega)}(r,\theta,\phi)\right) \quad -(n+m)\left(\Phi_{(n-1,p)}^{(m,\tilde{\ell},(-1)^{\ell}j\omega)}(r,\theta,\phi)\right)\right\}$$

$$+\left(\frac{U_q-iV_q}{2}\right)\left\{\left(\Phi_{(n+1,p)}^{(m+1,\tilde{\ell},(-1)^{\ell}j\omega)})(r,\theta,\phi)\right)+\left(\Phi_{(n-1,p)}^{(m+1,\tilde{\ell},(-1)^{\ell}j\omega)}(r,\theta,\phi)\right)\right\}$$

$$-\left(\frac{U_q+iV_q}{2}\right)\left\{(n-m+1)(n-m+2)\left(\Phi_{(n+1,p)}^{(m-1,\tilde{\ell},(-1)^{\ell}j\omega)}(r,\theta,\phi)\right)\right.$$

$$\left.+(n+m)(n+m-1)\left(\Phi_{(n-1,p)}^{(m-1,\tilde{\ell},(-1)^{\ell}j\omega)}(r,\theta,\phi)\right)\right\} \quad \left.\right\} \quad \left.\right\} \quad \left.\right] \qquad (10.3.2.11)$$

11 Limb Control and Behavior Prediction

Considerable effort has been expended in development of methods of controlling artificial limbs. Dr. Hanson at Boston Digital Arm has had success with myoelectrodes inmplanted in the chest Marks ([81], June 19, 2006). Kamitani ([123]) has had success with a system where he asks subjects to make shapes with their hands and then simultanously records the functional magnetic resonance imaging scans of the brain and then having them think about the shape of the robot hand and using their thoughts and the MRI scan to control the shape of the robot hand. Suggestions of methods of design of neuroprosthetic devices are described in ([111], 2003).

We are concerned with the control of artificial limbs with brain activity. We consider the shoulder direction, the elbow direction, the wrist direction, the thumb and the thumb joint directions and the directions of each of the fingers and the primary joint of each of the four fingers; the second joints could be added. We assume that we know the direction vectors at a time $t - T$ and that we recover brain activity from time $t - T$ to the present time t and assume a model with a convolution control at each brain activity site that would be carried out by digital signal processing ([122], 1993).

$\boldsymbol{s}$	=	direction vector of the shoulder
$\boldsymbol{e}$	=	direction vector of the elbow
$\boldsymbol{w}$	=	direction vector of the wrist
$\boldsymbol{t}$	=	direction vector of the thumb
$\boldsymbol{t}_j$	=	direction vector of the thumb joint
$\boldsymbol{f}_1$	=	direction vector of first finger
$\boldsymbol{f}_{(1,j)}$	=	direction vector of first finger joint
$\boldsymbol{f}_2$	=	direction vector of second finger
$\boldsymbol{f}_{(2,j)}$	=	direction vector of middle finger joint
$\boldsymbol{f}_3$	=	direction vector of third finger
$\boldsymbol{f}_{(3,j)}$	=	direction vector of ring finger joint
$\boldsymbol{f}_4$	=	direction vector of fourth finger
$\boldsymbol{f}_{(4,j)}$	=	direction vector of little finger joint

We want to be able to derive influence functions that will be able to put the artificial arm in the desired position in a natural way. Help will be sought from others who have successfully controlled limbs by transplanting nerves from the arm to the chest in the case of Jessie Sullivan, a shoulder level amputee. Letting X_{n} represent the recovered brain activity at location n, we have the following functional relationships to be constructed where we are supposing that if we recovered the brain activity $X_n(\tau)$ for times τ from $t-T$ to T and that X_n is taken to be zero otherwise for convolution operation representation purposes, we would hypothesize relationships

$\boldsymbol{s}(t)$	$=$	$F(\boldsymbol{s}(t-T), \beta_{(s,1)} * X_1(t), \cdots, \beta_{(s,n)} * X_n(t))$
	$=$	shoulder direction vector
$\boldsymbol{e}(t)$	$=$	$F(\boldsymbol{e}(t-T), \beta_{(e,1)} * X_1(t), \cdots, \beta_{(e,n)} * X_n(t))$
	$=$	elbow direction vector
$\boldsymbol{w}$	$=$	$F(\boldsymbol{w}(t-T), \beta_{(w,1)} * X_1(t), \cdots, \beta_{(w,n)} * X_n(t))$
	$=$	wrist direction vector
$\boldsymbol{t}$	$=$	$F(\boldsymbol{t}(t-T), \beta_{(\boldsymbol{t},1)} * X_1(t), \cdots, \beta_{(\boldsymbol{t},n)} * X_n(t))$
	$=$	direction vector of the thumb
$\boldsymbol{t}_j$	$=$	$F(\boldsymbol{t}_j(t-T), \beta_{(\boldsymbol{t}_j,1)} * X_1(t), \cdots, \beta_{(\boldsymbol{t}_j,n)} * X_n(t))$
	$=$	direction vector of the thumb joint
$\boldsymbol{f}_1$	$=$	$F(\boldsymbol{f}_1(t-T), \beta_{(\boldsymbol{f}_1,1)} * X_1(t), \cdots, \beta_{(\boldsymbol{f}_1,n)} * X_n(t))$
	$=$	direction vector of first finger
$\boldsymbol{f}_{(1,j)}$	$=$	$F(\boldsymbol{f}_{(1,j)}(t-T), \beta_{(\boldsymbol{f}_{(1,j)},1)} * X_1(t), \cdots, \beta_{(\boldsymbol{f}_{(1,j)},n)} * X_n(t))$
	$=$	direction vector of first finger joint
$\boldsymbol{f}_2$	$=$	$F(\boldsymbol{f}_2(t-T), \beta_{(\boldsymbol{f}_2,1)} * X_1(t), \cdots, \beta_{(\boldsymbol{f}_2,n)} * X_n(t))$
	$=$	direction vector of second finger
$\boldsymbol{f}_{(2,j)}$	$=$	$F(\boldsymbol{f}_{(2,j)}(t-T), \beta_{(\boldsymbol{f}_{(2,j)},1)} * X_1(t), \cdots, \beta_{(\boldsymbol{f}_{(2,j)},n)} * X_n(t))$
	$=$	direction vector of second finger joint
$\boldsymbol{f}_3$	$=$	$F(\boldsymbol{f}_3(t-T), \beta_{(\boldsymbol{f}_3,1)} * X_1(t), \cdots, \beta_{(\boldsymbol{f}_3,n)} * X_n(t))$
	$=$	direction vector of third finger
$\boldsymbol{f}_{(3,j)}$	$=$	$F(\boldsymbol{f}_{(3,j)}(t-T), \beta_{(\boldsymbol{f}_{(3,j)},1)} * X_1(t), \cdots, \beta_{(\boldsymbol{f}_{(3,j)},n)} * X_n(t))$
	$=$	direction vector of ring finger joint
$\boldsymbol{f}_4$	$=$	$F(\boldsymbol{f}_4(t-T), \beta_{(\boldsymbol{f}_4,1)} * X_1(t), \cdots, \beta_{(\boldsymbol{f}_4,n)} * X_n(t))$
	$=$	direction vector of fourth finger
$\boldsymbol{f}_{(4,j)}$	$=$	$F(\boldsymbol{f}_{(4,j)}(t-T), \beta_{(\boldsymbol{f}_{(4,j)},1)} * X_1(t), \cdots, \beta_{(\boldsymbol{f}_{(4,j)},n)} * X_n(t))$
	$=$	direction vector of little finger joint

11.1 Homotopy Recovery of Brain Activity

Homotopy ([27]) could be used to identify the convolution operators

$$t-\tau \rightarrow \left(\beta_{\boldsymbol{s}}, \cdots, \beta_{(\boldsymbol{f}_{(4,j)},n)}\right)(t-\tau)$$

particularly if they are defined by digital signal processing filter transform operators ([122], 1993) and (Wu, [138], 2004).

11.1.1 Homotopy Methods in Using Recovered Brain Activity to Control Limbs

The article ([27]) uses concepts such as judicious selection of complex thickensses to determine a starting problem at the beginning of the homotopy path that has an obvious known solution.

Statistical modeling has been used in an attempt to develop brain computer interfaces (Shoham [102], 2005), (Wu [137], 2006). We applied the homotopy method of ([27]) to find maximum likelihood estimate parameters without any a priori knowledge of the correct values. We propose the use a homotopy path connecting a problem that is easy to solve exactly and the brain activity control problem of interest. The sought after likelihood estimator parameters were the terminal point of the orbit of a dynamical system defined by a system of differential equations; this orbit is the homotopy path connecting the simple problem to the problem of interest. This was the classic problem of maximum likelihood estimator determination and the Hessian of the equations defining the nonlinear problem to be solved had an everywhere negative definite quadratic form which meant that there was only one global maximum and no local maximums other than the unique absolute maximum. The key idea is to find a critical point of a function representing the difference between the left and right sides of the homotopy relationship giving a system of differential equations involving the parameters being sought and a homotopy path parameter $\lambda(s)$ where when $\lambda(s)$ is 1 and the left and right sides of the homotopy relationships are satisfied from $\lambda(0) = 0$ to $\lambda(s) = 1$, we are guaranteed to have identified the coordinates of the critical point.

We found that Newton methods for locating these parameter values are successful if we start very close to the correct answer. However, our globally convergent homotopy method is robust and stable permitting us to quickly find the best parameter values to high precision without any a priori knowledge about the proper values of the estimator parameters.

We generally have a matrix function differential equation system of the form

$$\overline{\overline{M}} \begin{bmatrix} (d/ds)\lambda(s) \\ (d/ds)\beta_0(s) \\ \cdots \\ \cdots \\ \cdots \\ (d/ds)\beta_\ell(s) \\ \cdots \\ \cdots \\ \cdots \\ (d/ds)\beta_L(s) \end{bmatrix} = \begin{bmatrix} 0 \\ 0 \\ \cdots \\ \cdots \\ \cdots \\ 0 \\ \cdots \\ \cdots \\ \cdots \\ 0 \end{bmatrix} \tag{11.1.1.1}$$

which represents $L+1$ equations, one for each maximum likelihood estimator parameter, in $L+2$ unknowns which are the derivative of the homotopy parameter $\lambda(s)$ and the derivatives of each of the $L+1$ maximum likelihood estimator functions $\beta_\ell(s)$, where the first row of $\overline{\overline{M}}$ is given by

$$M_{(1,1)} = -\frac{n}{2} + \sum_{i=1}^{n} Y_i \tag{11.1.1.2}$$

$$M_{(1,2)} = -\sum_{i=1}^{n} (P_i - P_i^2) \tag{11.1.1.3}$$

and for ℓ going from 1 through L

$$M_{(1,\ell+2)} = -\sum_{i=1}^{n} (P_i - P_i^2) X_{(\ell,i)} \tag{11.1.1.4}$$

The last L rows have the form for ℓ running from 1 through L

$$M_{(\ell+1,1)} = -\frac{1}{2} \sum_{i=1}^{n} X_{(\ell,i)} + \sum_{i=1}^{n} X_{(\ell,i)} Y_i \tag{11.1.1.5}$$

$$M_{(\ell+1,2)} = -\sum_{i=1}^{n} (P_i - P_i^2) X_{(\ell,i)} \tag{11.1.1.6}$$

and for $\tilde{\ell}$ running from 1 through L

$$M_{(\ell+1,\tilde{\ell}+2)} = -\sum_{i=1}^{n} (P_i - P_i^2) X_{(\ell,i)} X_{(\tilde{\ell},i)} \tag{11.1.1.7}$$

We have all entries of the coefficient matrix.

The homotopy differential equation is given by the Lagrange expansion of the determinant where $\boldsymbol{e}_{\mathrm{j}}$ is the unit vector along the jth coordinate of $L+2$ dimensional space given by

$$\frac{d\lambda(s)}{ds}\boldsymbol{e}_1+\frac{d\beta_0(s)}{ds}\boldsymbol{e}_2+\cdots+\frac{d\beta_\ell(s)}{ds}\boldsymbol{e}_{\ell+2}+\cdots+\frac{d\beta_L(s)}{ds}\boldsymbol{e}_{L+2}$$

$$=\det\begin{bmatrix}\boldsymbol{e}_1 & \boldsymbol{e}_2 & \cdots & \boldsymbol{e}_{\ell+2} & \cdots & \boldsymbol{e}_{L+2}\\ M_{(1,1)} & M_{(1,2)} & \cdots & M_{(1,\ell+2)} & \cdots & M_{(1,L+2)}\\ \cdots & \cdots & \cdots & \cdots & \cdots & \cdots\\ M_{(\ell+1,1)} & M_{(\ell+2,2)} & \cdots & M_{(\ell+1,\ell+2)} & \cdots & M_{(\ell+1,L+2)}\\ \cdots & \cdots & \cdots & \cdots & \cdots & \cdots\\ \cdots & \cdots & \cdots & & & \\ M_{(L+1,1)} & M_{(L+1,2)} & \cdots & M_{(L+1,\ell+2)} & \cdots & M_{(L+1,L+2)}\end{bmatrix} \tag{11.1.1.8}$$

Thus, the right sides of the derivatives of the homotopy differential equation dependent variables are the components of the $L+2$ dimensional cross product of the vectors formed from each of the $L+1$ differential equations resulting modifying the left sides of the equations resulting from setting the derivatives of the logarithm of the Maximum likelihood estimator probability $g(Y)$ with respect to β_0 through β_L equal to zero and then differentiating both sides of each of these equations with respect to the homotopy parameter s giving us $L+1$ ordinary differential equations with $L+2$ dependent variables. The components of the vectors whose $L+2$ dimensional cross product of the rows of $\overline{\overline{M}}$ are equal to the derivatives of the $L+2$ dependent variables. Save the $\lambda(s)$ data around $\lambda(s)=1$ and use Lagrange interpolation as before to find the maximum likelihood estimator parameters β_ℓ for ℓ running from 0 through L.

$$\frac{d\lambda(s)}{ds}\boldsymbol{e}_1+\frac{d\beta_0(s)}{ds}\boldsymbol{e}_2+\cdots+\frac{d\beta_\ell(s)}{ds}\boldsymbol{e}_{\ell+2}+\cdots+\frac{d\beta_L(s)}{ds}\boldsymbol{e}_{L+2}$$

$$=\sum_{j=1}^{L+2}\left\{(-1)^{1+j}\det\begin{bmatrix}N^{(j)}_{(1,1)} & \cdots & N^{(j)}_{(1,\ell+1)} & \cdots & N^{(j)}_{(1,L+1)}\\ \cdots & \cdots & \cdots & \cdots & \cdots\\ N^{(j)}_{(L+1,1)} & \cdots & N^{(j)}_{(L+1,\ell+1)} & \cdots & N^{(j)}_{(L+1,L+1)}\end{bmatrix}\boldsymbol{e}_j\right\} \tag{11.1.1.9}$$

11.1.2 Uniqueness of Control Parameter Determination

We want to avoid error in sending signals to control an artificial limb. We need conditions under which the problem of determination of control parameters has a unique solution.

We prove the following theorem concerning conditions under which a function,G of N variables cannot have more than one local maximum where we use the notation

$$D_{U_{\mathrm{j}}}G(U_1,U_2,\cdots,U_N)=\left(\frac{\partial}{\partial U_{\mathrm{j}}}\right)G(U_1,U_2,\cdots,U_N) \tag{11.1.2.1}$$

Theorem 11.1 *A real analytic function*

$$(U_1,U_2,\cdots,U_N)\rightarrow G(U_1,U_2,\cdots,U_N)=G \tag{11.1.2.2}$$

of N variables in $\mathbb{R}^N$ cannot have more than one local maximum if the quadratic form

$$(U_1, U_2, \cdots, U_N) \rightarrow$$

$$(U_1, U_2, \cdots, U_N) \begin{pmatrix} D^2_{U_1} G & \cdots & D_{U_1} D_{U_j} G & \cdots & D_{U_1} D_{U_N} G \\ \cdots & \cdots & \cdots & \cdots & \cdots \\ D_{U_i} D_{U_1} G & \cdots & D_{U_i} D_{U_j} G & \cdots & D_{U_i} D_{U_N} G \\ \cdots & \cdots & \cdots & \cdots & \cdots \\ D_{U_N} D_{U_1} G & \cdots & D_{U_N} D_{U_j} G & \cdots & D^2_{U_N} G \end{pmatrix} \begin{pmatrix} U_1 \\ \cdots \\ U_j \\ \cdots \\ U_N \end{pmatrix} \tag{11.1.2.3}$$

is strictly negative for all vectors satisfying

$$(U_1, U_2, \cdots, U_N) \neq (0, 0, \cdots, 0) \tag{11.1.2.4}$$

Proof of Theorem. This theorem is based on the obvious generalization of the following lemma to functions of N variables.

Lemma 11.1 *If the everywhere real analytic function $G(V, W)$ had an isolated local maximum at two distinct points (V_1, W_1) and (V_2, W_2) in $\mathbb{R}^2$, then there would be a local minimum of the function*

$$h(\lambda) = G((1-\lambda)V_1 + \lambda V_2, (1-\lambda)W_1 + \lambda W_2) \tag{11.1.2.5}$$

at a value λ with $0 < \lambda < 1$ and the quadratic form associated with the Hessian is not negative definite at this point.

Proof. We can assume that

$$G(V_1, W_1) \leq G(V_2, W_2) \tag{11.1.2.6}$$

so that the fact that with a strict local maximum we would have $h'(\lambda) < 0$ for λ close to 0 which means that means that we have a minimum

$$h(\lambda_*) = G((1-\lambda)V_1 + \lambda V_2, (1-\lambda)W_1 + \lambda W_2) < minimum\,\{G(V_1, W_1), G(V_2, W_2)\} \tag{11.1.2.7}$$

where necessarily the first derivative $h^{(1)}(\lambda_*)$ is zero and a locally convergent Taylor series expansion

$$h(\lambda) = h(\lambda_*) + h^{(2)}(\lambda_*) \left(\frac{(\lambda - \lambda_*)^2}{2!} \right) + \text{higher order terms} \tag{11.1.2.8}$$

which means that it would be impossible to have

$$h^{(2)}(\lambda_*) < 0 \tag{11.1.2.9}$$

since if $h(\lambda_*)$ is a local minimum, then $h(\lambda)$ would have to be larger than $h(\lambda_*)$ for all $\lambda \neq \lambda_*$ that are near λ_*. Observe that using the notation

$$(D_v, D_w) = \left(\frac{\partial}{\partial v}, \frac{\partial}{\partial w} \right) \tag{11.1.2.10}$$

we have

$$h^{(1)}(\lambda) = D_v G(1-\lambda)V_1 + \lambda V_2, (1-\lambda)W_1 + \lambda W_2)\{V_2 - V_1\} +$$
$$D_w G((1-\lambda)V_1 + \lambda V_2, (1-\lambda)W_1 + \lambda W_2)\{W_2 - W_1\} \quad (11.1.2.11)$$

and suppressing the argument

$$\lambda \to (1-\lambda)V_1 + \lambda V_2, (1-\lambda)W_1 + \lambda W_2) \quad (11.1.2.12)$$

we have that at the minimum that

$$h^{(2)}(\lambda) = D_v^2 G\left\{(V_2 - V_1)^2\right\} + 2D_v D_w\left\{(V_2 - V_1)(W_2 - W_1)\right\} + D_w\left\{(W_2 - W_1)^2\right\}$$

$$(V_2 - V_1, W_2 - W_1)\begin{pmatrix} D_v^2 G & D_v D_w G \\ D_w D_v G & D_w^2 G \end{pmatrix}\begin{pmatrix} V_2 - V_1 \\ W_2 - W_1 \end{pmatrix} \geq 0 \quad (11.1.2.13)$$

Thus, at the local minimum on a line between two isolated strict local maximum, the quadratic form associated with the Hessian of G is not negative.

Even in a probabilistic model relating limb control to brain activity we need a unique solution of the influence parameters.

Corollary 11.1 *The maximum log likelihood function*

$$\ell n(f(\beta_0, \beta_1)) = \ell n(g(Y_1, \cdots, Y_i, \cdots, Y_n)) = \ell n(\prod_{i=1}^{n} P_i^{Y_i}(1-P_i)^{1-Y_i})$$

$$= \sum_{i=1}^{n}\{Y_i \ell n(P_i) + (1-Y_i)\ell n(1-P_i)\} \quad (11.1.2.14)$$

has only one local maximum which is the global maximum when P_i is given by

$$P_i = \frac{\exp(\beta_0 + \beta_1 X_i)}{1 + \exp(\beta_0 + \beta_1 X_i)} \quad (11.1.2.15)$$

so that

$$\frac{\partial P_i}{\partial \beta_0} = P_i - P_i^2 \quad (11.1.2.16)$$

and

$$\frac{\partial P_i}{\partial \beta_1} = X_i\left\{P_i - P_i^2\right\} \quad (11.1.2.17)$$

Proof of Corollary. The definition (11.1.2.15) of P_i and the basic partial derivative relationships (11.1.2.16) and (11.1.2.17) give us the following.

Using (11.1.2.16) we see that

$$\frac{\partial \ell n(P_i)}{\partial \beta_0} = 1 - P_i \quad (11.1.2.18)$$

and

$$\left(\frac{\partial}{\partial \beta_0}\right)\ell n(1-P_i) = -P_i \quad (11.1.2.19)$$

so that

$$\left(\frac{\partial}{\partial\beta_0}\right)\ell n(f(\beta_0,\beta_1) == \sum_{i=1}^{n}\{Y_i - P_i\} \tag{11.1.2.20}$$

Using (11.1.2.17) we see that

$$\left(\frac{\partial}{\partial\beta_1}\right)\ell n(f(\beta_0,\beta_1) = \sum_{i=1}^{n}\{X_i[Y_i - P_i]\} \tag{11.1.2.21}$$

The associated Hessian, which we must prove to be negative definite, is

$$(\beta_0,\beta_1) \to \begin{pmatrix} A & B \\ C & D \end{pmatrix} \tag{11.1.2.22}$$

where

$$A = \left(\frac{\partial^2}{\partial\beta_0^2}\right)\ell n(f(\beta_0,\beta_1) = -\sum_{i=1}^{n}(P_i - P_i^2) \tag{11.1.2.23}$$

$$B = C = \left(\frac{\partial^2}{\partial\beta_0\partial\beta_1}\right)\ell n(f(\beta_0,\beta_1) = -\sum_{i=1}^{n}X_i(P_i - P_i^2) \tag{11.1.2.24}$$

and

$$D = \left(\frac{\partial^2}{\partial\beta_1^2}\right)\ell n(f(\beta_0,\beta_1) = -\sum_{i=1}^{n}X_i^2(P_i - P_i^2) \tag{11.1.2.25}$$

The Laplacian

$$\Delta = \frac{\partial^2}{\partial\beta_0^2} + \frac{\partial^2}{\partial\beta_1^2} \tag{11.1.2.26}$$

of the function

$$\ell n(f(\beta_0,\beta_1)) = \sum_{i=1}^{n}\{Y_i\ell n(P_i) + (1-Y_i)\ell n(1-P_i)\} \tag{11.1.2.27}$$

is everywhere negative and using (11.1.2.23), (11.1.2.24), and (11.1.2.25) we have

$$AD - BC = \left(\sum_{i=1}^{N}X_i(P_i - P_i^2)\right)\left(\sum_{j=1}^{N}X_j(P_j - P_j^2)\right)$$

$$-\sum_{i=1}^{n}\sum_{j=1}^{n}X_iX_j(P_i - P_i^2)(P_j - P_j^2)$$

$$= \sum_{\{i,j\}\subset\{1,\cdots,n\}}\Big\{$$

$$\left[-2X_iX_j + X_i^2 + X_j^2\right](P_i - P_i^2)(P_j - P_j^2) \quad \Big\} > 0 \tag{11.1.2.28}$$

provided that there is just one pair with $X_i \neq X_j$. Thus, since $A < 0$ the Hessian of the function

$$(\beta_0, \beta_1) \rightarrow \ell n f(\beta_0, \beta_1) \tag{11.1.2.29}$$

which has the form

$$\mathcal{Q}(\beta_0, \beta_1) =$$
$$A \left\{ \left[\beta_0 + \left(\frac{B}{A} \right) \beta_1 \right]^2 + \left[\frac{DA - B^2}{A^2} \right] \beta_1^2 \right\} < 0 \tag{11.1.2.30}$$

since equation (11.1.2.28) proves that

$$DA - B^2 \geq 0 \tag{11.1.2.31}$$

is everywhere negative definite and cannot have more than one local maximum and consequently has only one pair β_0 and β_1 which gives the maximum value.

12 References

References

[1] Abramowitz, Milton and Irene A. Stegun. *Handbookof Mathematical Functions with Formulas, Graphs, and Mathematical Tables. National Bureau of Standards. Applied Mathematics Series 55* Washington, D. C.: United States Department of Commerce, Luther H. Hodges, Secretary and A. V. Astin, Director (December, 1965)

[2] Agranovich, Y. Ya. "The theory of operators with dominant main diagonal. I." *Positivity, Volume 2* (1998) pages 153-164

[3] Amir, A. "Uniqueness of the Generators of Brain Evoked Potential Maps." *IEEE Transactions on Biomedical Engineering. Volume 41* (1994) pages 1-11.

[4] Ammari, Habib, Gang Bao, and John Fleming. "An Inverse Source Problem for Maxwell's Equations in Magnetoencephalography" *SIAM Journal of Applied Mathematics. Volume 62, Number 4* (2002) pages 1369-1382.

[5] Ammari, Habib, J. C. Nedelec. "Propagation d'Ondes Electromagnetique a Basse Frequencies" *Journal Math. Pures Appl., Volume 9, Number 77* (1998) pages 839-849.

[6] Amos, Donald E., S. L. Daniel, and M. K. Weston. *CDC 6600 Subroutines for Bessel Functions $J_\nu(x)$, $x \geq 0$, $\nu \geq 0$ and Airy Functions $A_i(x)$, $A_i'(x)$, $-\infty < x < \infty$. Report SAND 75-0147* Albuquerque, New Mexico: Sandia Laboratories: Albuquerque, New Mexico (1975)

[7] Arfken, George and Hans J. Weber. *Mathematical Methods for Physicists. Fourth Edition.* New York: Academic Press (1995)

[8] Baev, Konstantin Vailevich. *Biological Neural Networks: Hierarchical Concept of Brain Function.* Boston: Birkhauser (1997).

[9] Barichello, L. B. and R. D. M. Garcia and C. E. Siewert. "A Spherical Harmonics Solution for Radiative Transfer Problems with Reflecting Boundaries and Internal Sources" *Journal of Quantitative Spectroscopy and Radiative Transfer. Volume 60, Number 2* (1998) pages 247-260.

[10] Bateman, Harry. *Partial Differential Equations of Mathematical Physics* Cambridge: At the University Press and New York: The MacMillan Company (1932)

[11] Bateman, Harry. *Higher Transcendental Functions Volume I* New York: McGraw Hill Book Company, Inc. and Washington DC: Office of Naval Research Project NR 043-045 (1953)

[12] Bateman, Harry. *Higher Transcendental Functions Volume II.* New York: McGraw Hill Book Company, Inc. and Washington DC: Office of Naval Research Project NR 043-045 (1953)

[13] Bateman, Harry. *Higher Transcendental Functions Volume III.* New York: McGraw Hill Book Company, Inc. and Washington DC: Office of Naval Research Project NR 043-045 (1953).

[14] Bell, Earl L., David K. Cohoon, John W. Penn. *Electromagnetic Energy Deposition in a Concentric Spherical Model of the Human or Animal Head. SAM TR-79-6* Brooks AFB, Texas 78235: USAF School of Aerospace Medicine (December, 1979) 96 pages

[15] Bell, E. L., D. K. Cohoon, and J. W. Penn. *Mie: A Fortran Program for Computing Power Deposition in Spherical Dielectrics Through Application of Mie Theory. SAM TR-77-11* San Antonio, Texas: USAF School of Aerospace Medicine (1977) 77 pages

[16] Bellman, Richard, Robert E. Kalaba, and Jo Ann Lockett *Numerical Inversion of the Laplace Transform: Application to Biology, Economics, Engineering and Physics* New York: Elsevier (1966)

[17] Betz, Randal R., M.D., J. J. Mulcahey, James McCarthy, M.D., Therese Johnston, and Brian T. Smith. "Philadelphia Hospital Functional Electrical Stimulation for Upright Mobility in Young Children and Asolescents with Spinal Cord Injuries." *http://www.shrinershq.org/research/bluebook2001/philfunctional.html* (June 4, 2005) pages 1-5.

[18] Boyd, W. G. C. and T. M. Dunster. "Uniform Asymptotic Solutions of a Class of Second Order Linear Differential Equations Having a Turning Point and Regular Singularity, with an Application to Legendre Functions" *SIAM Journal of Mathematical Analysis. Volume 17* (1986) pages 422-450

[19] Brent, Richard P. *Algorithms for Minimization without Derivatives* Englewood Cliffs, New Jersey: Prentice Hall (1973)

[20] Bresadola, Marco. "History of Neuroscience. Medicine and Science in the Life of Luigi Galvani (1737-1798)" *Brain Research Bulletin, Volume 46, Number 5* (1998) pages 367-380.

[21] Brock, Samuel and Howeard P. Krieger. *The Basis of Clinical Neurology. The Anatomy and Physiology of the Nervous System in Their Application to Clinical Neurology.* Baltimore: The Williams and Wilkins Company (1963).

[22] Brown, David. "For First Woman with Bionic Arm, a New Life is Within Reach" Washington, D.C.: *Washington Post* (September 14, 2006) page A01.

[23] Burr, John G., David K. Cohoon, Earl L Bell, and John W. Penn. "Thermal Response of a Simulated Cranial Structure Exposed to Radiofrequency Radiation," *IEEE Transactions on Biomedical Engineering. Volume BME-27, Number 8* (August, 1980) pp 452-460

[24] Chalupa, Leo M. "The Nature and Nurture of the Retinal Ganglion Cell Development" *IN* Gazzaniga, Michael S. (Editor in Chief) (et al.) *The Cognitive Neurosciences* Cambridge: MIT Press (1995) pages 37-50

[25] Cohoon, David K., John W. Penn, Earl L. Bell, David R. Lyons, and Arthur G. Cryer. *A Computer Model Predicting the Thermal Response to Microwave Radiation SAM TR 82 22* San Antonio, Texas: USAF School of Aerospace Medicine (December, 1982) 152 pages

[26] Cohoon, D. K. "An Exact Solution of Mie Type for Scattering by a Multilayer Anisotropic Sphere" *Journal of Electromagnetic Waves and Applications, Volume 3, Number 5* (1989) pp 421 - 448

[27] Cohoon, D. K. and R. M. Purcell. "Homotopy as an Electromagnetic Design Method Applied to a Perfect Conductor Coated with Bianisotropic Coatings Having Nontrivially Dispersive Magnetic Properties" *Journal of Wave Material Interaction, Volume 4, Numbers 1-3* (January, 1989) pages 123-142.

[28] Cohoon, D. K. and O. I. Sindoni "Recovery of Properties of Layered Magnetic Materials Using Obliquely Incident Radiation" *Journal of the Optical Society of America. Volume 13. Number 6* (June, 1966) pages 1258 - 1276.

[29] Cohoon, D. K., R. James Swanson, and Ronald J. Young "Using Invariants of Swimming Motion in Biotoxicity Testing via Computerized Microscopy" *IN* Salem, Harry and Sidney A. Katz. *Advances in Animal Alternatives for Safety and Efficacy Testing* New York: M. Dekker (1998)

[30] Cole, K. S. and H. J. Curtis. "Electric Impedance of the Squid Giant Axon During Activity." *Journal of General Physiology. Volume 22.* (1939) pages 649-670.

[31] Cole, Kenneth S. *Membranes, Ions and Impulses. A Chapter of Classical Biophysics* Berkeley: University of California Press(1972)

[32] Cole, Kenneth S. and Robert H. Cole. "Dispersion and Absorption in Dielectrics I. Alternating Current Characteristics" *Journal of Chemical Physics. Volume 9* (April, 1941) pages 341-351

[33] Colton, David and Rainer Kress. *Inverse Acoustic and Electromagnetic Scattering Theory* New York: Springer (1998)

[34] Davis, R. and Patrick J. Barriskill. "A development of functional electrical stimulators utilizing cochlear implant technology" *Medical Engineering Physics. Volume 23* (2001) pages 61-68.

[35] Deutsch, Sid. *Models of the Nervous System* New York: John Wiley and Sons (1967)

[36] Deans, Stanley R. *The Radon Transform and Some of Its Applications* New York: Wiley (1983)

[37] Didonato, Armido and A. H. Morris. "Algorithm 708 Significant Digit Computation of the Incomplete Beta Function Ratios," *Association of Computing Machinery Transactions. Mathematical Software 18* (1992) pages 360-373.

[38] Dunster, T. M. "Canonical Functions with One or Both Parameters Large." *Proceedings of the Royal Society of Edinburgh. Volume 119A* (1991) pages 311-327.

[39] du Bois-Reymond, Emile. *Untersuchungen uber thierische elektricitat, 2 voll.* Berlin: Reimer, 1848-1884.

[40] Edmonds, A. R. *Angular Momentum in Quantum Mechanics* Princeton, New Jersey: Princeton University Press (1957)

[41] Erdelyi, A. et al. *Higher Transcendental Functions. Volumes I, II, and III* New York: McGraw Hill (1954).

[42] Feller, William. *An Introduction to Probability Theory and its Applications* New York: Wiley (1950)

[43] Ferree, Thomas C. *Spline Interpolation of the Scalp EEG. Technical Note.* Electrical Geodesics Incorporated (August 22, 2000)

[44] Flack, F. C., E.D. James, and D. M. Schlapp. "Mutual Inductance of Air-Cored Coils: Effect on Design of Radio Frequency Coupled Implants." *Medical and Biological Engineering. Volume 9* (1971) pages 79-84

[45] Fokas, A. S., Y. Kurylev, and V. Marinakis. "The Unique Determination of Neuronal Currents in the Brain via Magnetoencephalography" *Inverse Problems, Volume 20*(2004) pages 1067- 1082.

[46] Gabriel, Camelia. *Compilation of the Dielectric Properties of Body Tissues at RF and Microwave Frequencies. AL/OE-TR-1996-0037* Brooks AFB, Texas 78235-5102: Occupational and Environmental Health Directorate. RadioFrequency Radiation Division (June, 1996)

[47] Galvani, L. "De Viribus electricitatis in motu musculari commentarius." *Bon. Sci. Art. Inst. Acad. Comm. Vol. 7* (1791) pages 363-418.

[48] Garnder, Ernest, M.D. *Fundamentals of Neurobiology. A Psychophysiological Approach.* Philadelpha: W. B. Saunders (1968)

[49] Gazzaniga, Michael S. (Editor in Chief) et al. *The Cognitive Neurosciences.* Cambridge: The MIT Press (1995)

[50] Gershgorin, S. "Uber die abgrenzung der eigenwerte einer matrix" Izv. Akad. Nauk. S. S. S. R. Volume 7 (1931) pages 749-754.

[51] Gradshteyn, I. S. and I. M. Ryzhik. *Table of Integrals, Series, and Products. Fourth Edition Prepared by Yu. V. Geronimus, and M. Yu. Tseytlin and edited by Alan Jeffrey with contributions by J. E. Bowcok, T. J. Boyer, D. J Buch, F. Calogero, Herman, W. Chew, R. W. Cleary, D. K. Cohoon, J. W. Criss, A. Degasperis, K. Evans, G. R. Gamertsfelder, I. J. Good, J. Good, T. Hagfors, D. O. Harris, R. E. Hise, Y. IKsbe, B. Jancovici, D. Monowalow, L. P. Kok, S. L. Levie, I. Manning, J. Marmur, C. Muhlhausen, P. Noerdlinger, A. H. Nutall, J. R. Roth, and G. K. Tannahill.* New York: Academic Press (1965)

[52] Graglia, R. D. and R. Tascone "Propagation in Waveguides of Arbitrary Cross Section with Anisotropic Boundary" *IN* Uslenghi, P. L. E. (Editor) *Electromagnetics, Volume 4* Washington, D. C.: Hemisphere Publishing Corporation (1984) pages 377-391.

[53] Granit, Ragnar. *Muscular Afferents and Motor Control. Nobel Symposium I* New York: John Wiley and Sons (1965)

[54] Halmos, P. R. *A Hilbert Space Problem Book* New York Springer Verlag (1982).

[55] Hamalainen, M., R. Hari, and R. J. Ilmoniemi, J. Knuutila, and O. V. Lounasmaa. "Magnetoencephalography Theorey Instrumentation and Application to Noninvasive Studies of the Working Human Brain" *Reviews of Modern Physics, Volume 65* (1993) pages 59-70.

[56] He, S. "Frequency Series Expansion of an Explicit Solution for a Dipole Inside a Conducting Sphere at Low Frequency" *IEEE Transactions of Biomedical Engineering, Volume 45* (1998) pages 1-10

[57] He, S. and V. G. Romanov. "Identification of Dipole Sources in a Bounded Domain for Maxwell's Equations" *Wave Motion. Volume 28* (1998) pages 25-40

[58] Hershey, A. V. *Computation of Special Functions, Report TR-3788* Dahlgren, Virgina (1978)

[59] Hirvonen, M. T. "Electromagnetic Field of an Oscillating Point Dipole in the Presence of Spherical Interfaces" *Acta Polytechnica Scandinavica Ma39* (1983) pages 1-37

[60] Hirvonen, M. T. "Solutions of the Electromagnetic Wave Equations for Point Dipole Sources and Spherical Boundaries" *Quarterly of Applied Mathematics* (July, 1981) pages 275-286.

[61] Hodgkin, A. L. and A. F. Huxley. "A Quantitative Description of Membrane Current and its Application to Conduction and Excitation in Nerve" *Journal of Physiology* (1952) pages 500-544

[62] Hoke, M., K. Lehnertz, C. Pantev, B. Lutkenhoner. "Spatiotemporal aspects of Synergetic Processes in the Auditory Cortex as Revealed by the Magnetoencephalogram" *In* Baser, E. and T. H. Bullock (Editors) *Brain Dynamics* New York: Springer Verlag (1991) pages 84-108.

[63] Hovhannessian, S. S. and V. A. Baregamian. "The diffraction of a plane electromagnetic wave by an anisotropic sphere," *Izdatelstva Akad. Nauk of Armenia S. S. R. Physics, Volume 16* (1981) pages 37-43

[64] Hurt, William D. *Radiofrequency Radiation Dosimetry Workship: Present Status and Recommendations for Future Research. AL/OE-SR-1996-0003.* Brooks AFB, Texas 78235-5324: Occupational and Environmental Health Directorate Radio Frequency Radiation Division. 8305 Hawks Road. Brooks AFB, Texas 78235-5324 (June, 1996)

[65] Isakov, F. "Inverse Source Problems" *Math. Surveys Monograph. Volume 34* Providence, Rhode Island: American Mathematical Society (1990)

[66] Jackson, John David. *Classical Electrodynamics. Second Edition* New York: John Wiley and Sons

[67] Johnston, Therese E., Brian T. Smith, Randal R. Betz, Brian J. Benda, M. J. Mulcahey, Ross Davis, and Andrew Barriskill. "Initial Experiences with Upright Mobility Using the praxis Multi-Functional Implanted FES." (June 4, 2005) pages 1-3

[68] Johnston, T. E., R. R. Betz, B. T. Smith, and M. J. Mulcahey. "Implanted Functional Electrical Stimulation: An Alternative for Standing and Walking in Pediatric Spinal Cord Injury." *Spinal Cord. Volume 4* (2003) pages 144-152.

[69] Kamitani, Yukiyasu, Vidya M. Bhalodia, Yoshihisa Kubota, and Shinsuke Shimojo. "A Model of Magnetic Stimulation of Neocortical Neurons." *NeuroComputing, Volumes 38-40* (2001) pages 697-703.

[70] Karmon, Thodore V. and Maurice A. Biot. *Mathematical Methods in Engineering* New York: McGraw Hill (1940).

[71] Kaas, Jon H. "The Reorganization of Sensory and Motor Maps in Adult Mammals" *IN* Gazzaniga, Michael S. (Editor in Chief) (et al.) *The Cognitive Neurosciences* Cambridge: MIT Press (1995) pages 51-71

[72] King, Chris C. "Fractal and Chaotic Dynamics in Nervous Systems" *Nervous Systems. Progress in Neurobiology. Volume 36* (1991) pages 279-308

[73] Kirkwood, John G. and Raymond M. Fuoss. "Anomalous Dispersion and Dielectric Loss in Polar Molecules" *Journal of Chemical Physics. Volume 9* (April, 1941) pages 329-340

[74] Kovetz, Attay. *Electromagnetic Theory* New York: Oxford University Press, Inc. (2000)

[75] Lakes, Roderic. "Fundamental Limits on the Photon Mass and Cosmic Magnetic Vector Potential" *Physical Review Letters, Volume 80, Number 9* (March 2, 1998) pages 1826-1829.

[76] Law, S. K., P. L. Nunez and R. S. Wijesinghe. "High Resolution EEG using spline gnerated surface Laplacians on spherical and ellipsoidal surfaces." *IEEE Transactions on Biomedical Engineering. Volume 40, Number 2* (1993) pages 145-153

[77] Linz, Deborah. "Spinal Cord Patients Walk Again"

`http://www.wchstv.com/newsroom/healthyforlife/2068.shtml`

(June 4, 2005) pages 1-5

[78] Lock, J. A. "Semiclassical scattering of an electric dipole source inside a spherical particle" *Journal of the Optical Society of America. Optical Image Science of Vision. Volume 18, Number 12* (2001) pages 3085-3097.

[79] MacRobert, T. M. and I. N. Sneddon. *Spherical Harmonics. An Elementary Treatise on Harmonic Functions with Applications* New York: Pergamon Press (1967)

[80] Magnus, W. and F. Oberhettinger. *Foreln und Satze fur die speziellen Funktionen der mathematischen Physik* Berlin: Springer Verlag (1950).

[81] Marks, Aaron. "Liberating Technologies Introduces Advanced Prosthetic Arms" Los Angeles, California: Axistive United States (June 19, 2006).

[82] Matteucci, C. "Deuxieme memoire sur le courant electrique proper de la grenouille et sur celui des animaux a sang chaud" *Ann. Chim. Phys. V. 6, Ser. 3* (1842) pages 301-339.

[83] McKivergan, Daniel M. "The Shriners Childrens Hospitals Helping Children Free of Charge for Nearly Eight Decades" *The Philanthropy Roundtable*

`http://www.philanthropyroundtable.org/magazines/1999/`
`mckivergan.html`

[84] Melrose, D. B. and R. C. McPhedran. *Electromagnetic Processes in Dispersive Media* Cambridge: Cambridge University Press (1991)

[85] Morris, Jr., Alfred H. *NSWC Library of Mathematics Subroutines. NSWCDD/TR 92/425* (January, 1993) 608 pages

[86] Morse, Philip M. and Herman Feshbach. *Methods of Theoretical Physics* New York: McGraw Hill (1953).

[87] Mosher, John C., Richard M. Leahy, and Paul S. Lewis. "EEG and MEG Forward Solutions for Inverse Methods." *IEEE Transactions on Biomedical Engineering, Volume 46, Number 3* (March, 1999), pages 245-259

[88] Muller, Claus. *Foundations of the Mathematical Theory of Electromagnetic Waves* New York: Springer Verlag (1969)

[89] Ola, P. and L. Paivarinta and E. Somersalo. "An Inverse Boundary Value Problem in Electrodynamics" *Duke Mathematics Journal, Volume 70*(1993) pages 617-653

[90] Olver, F. W. J. *Asymptotics and Special Functions* New York: Academic Press (1974)

[91] Olver, F. W. J. "Legendre Functions with Both Parameters Large." *Philos. Trans. Royal Society London Series A. Volume 278* (1975) pages 175-185.

[92] Olver, F. W. J. "Unsolved Problems in the Asymptotic Estimation of Special Functions" *In* Richard Askey (editor). *Theory and Application of Special Functions* New York: Academic Press (1975) pages 585-596.

[93] Penn, John W. and David K. Cohoon. *Analysis of a Fortran Program for Computing Electric Field Distributions in Heterogeneous Penetrable Nonmagnetic Bodies of Arbitrary Shape Through Application of Tensor Green's Functions. SAM TR-78-40* San Antonio, Texas: USAF School of Aerospace Medicine (December, 1978) 83 pages

[94] Perrin, F., J. Perner "Scalp Current Density Mapping: Value and Estimation from Potential Datas. *IEEE Transactions on Biomedical Engineering. Volume 34, Number 4* (1987) pages 283-288.

[95] Petrowsky, I.G. "Sur l'analyticite des solutions d'equations differentielles. *Rec. Math. Volume 47* (1939).

[96] Piccolino, Marco. "History of Neurosciene. Animal Electricity and the Birth of Electrophysiology: The Legacy of Luigi Galvani" *Brain Research Bulletin, Volume 46, Number 5* (1998) pages 381-407

[97] Press, William H., Brian Flannery, Saul Teukolsky, and William T. Vetterling. *Numerical Recipies. The Art of Scientific Computing* Cambridge: Cambridge University Press (1986)

[98] Rinzel, J. and B. Ermentrout. "Analysis of Neural Excitability and Oscillations" *In* Koch, C. and I. Segev, Editors. *Methods in Neuronal Modeling from Ions to Networks* Cambridge, Massachusetts: MIT Press (1998) pages 251-291

[99] Sadiku, Matthew N. O. *Numerical Techniques in Electromagnetics. Second Edition* Boca Raton, Florida: CRC Press (2001)

[100] Sansone, G., Ainsley H. Diamond, and Einar Hille. *Orthogonal Functions* New York: Interscience (1959).

[101] Sarvas. J. "Basic Mathematical and Electromagnetic Concepts of the Bioelectromagnetic Inverse Problem." *Physics in Medicine and Biology, Volume 32* (1987) pages 11-22

[102] Shoham, S., L. M. Paninski, M. R. Fellows, N. G. Hatsopoulos, J. P. Donoghue, and R. A. Normann. "Statistical Encoding Model for a Pimary Motor Cortical Brain-Machine Interface" *IEEE Transactions on Biomedical Engineering, Volume 52, Number 7* (2005) pages 1312-1322.

[103] Sneddon, G. E. and W. W. Read. "The method of Particular Solutions for the Helmholtz Equation" ANZIAM J. Australian Mathematical Society Volume 46 E. (June 29, 2005) pages 544-557.

[104] Snow, C. "Mutual Inductance of any Two Circles" *Bureau Standards Journal of Research, Volume 1* (1928) pages 531-542.

[105] Spain, Barry and M. G. Smith. *Functions of Mathematical Physics* London: Van Nostrand Reinhold Company (1970)

[106] Srinivasan, R., P. L. Nunez, D. M. Tucker, R. B. Silberstein, and P. J. Caducsh "Spatial Sampling and Filter of EEG with Spline Laplacians to Estimate Cortical Potentials." *Brain Topography. Volume 8, Number 4* (1996) pages 355-366

[107] Stakgold, I. *Green's Functions and Boundary Value Problems* New York: Wiley-Interscience Publications (1979)

[108] Stone, Alexander P. "A Differential Geometric Approach to Electromagnetic Lens Design" *IN* Uslenghi, P. L. E. (Editor) *Electromagnetics, Volume 4* Washington, D. C.: Hemisphere Publishing Corporation (1984) pages 63-88.

[109] Stratton, Donald B. *Neurophysiology* New York: McGraw Hill (1981)

[110] Stratton, Julius. *Electromagnetic Theory* New York: McGraw Hill (1941)

[111] Serruya, M. D. and J. P. Donoghue. "Chapter III: Desing Principles of a Neuromotor Prosthetic Device" *IN* Horch, Kenneth W, and Gurpreet S. Dhillon (Editors) *Neuroprosthetics: Theory and Practice* (2003) pages 1158-1156.

[112] Tai, C. T. *Dyadic Green Functions in Electromagnetic Theory* Pscataway, New Jersey: IEEE Press (1994)

[113] Tai, C. T. and Robert E. Collin. "Radiation of a Hertzian Dipole Immersed in a Dissipative Medium" *IEEE Transaction on Antennas and Propagation. Volume 48, Number 10*

[114] Talman, James D. *Special Functions: A Group Theoretic Approach* New York: W. A. Benjamin, Inc. (1968)

[115] Temme, N. M. *An Introduction to the Classical Functions of Mathematical Physics.* New York: John Wiley and Sons (1996).

[116] Torres, Francois, Patrick Vaudon and Bernard Jecko. "Application of Fractional Derivatives to the FDTD Modeling of Pulse Propagating in a Cole-Cole Dispersive Medium" *Microwave and Optical Technology Letters. Volume 13, Number 5* (December 5, 1996) pages 300-304

[117] Tortora, Gerard J. and Nicholas P. Anagnostakos *Principles of Anatomy and Physiology, Fifth Edition* New York: Harper and Row (1987)

[118] Treves, Francois. *Locally Convex Spaces and Linear Partial Differential Equations* New York: Springer Verlag (1967)

[119] Treves, Francios. Lectures on Partial Differential Equations with Constant Coefficients. *Notas de Matematica, No. 7* Rio de Janeiro (1961).

[120] Ursell, F. "Integrals with a Large Parameter: Legendre Functions of Large Degree and Fixed Order." *Math. Proc. Cambridge Philosophical Society. Volume 95* (1984) pages 367-380.

[121] Uslenghi, P. L. E. (Editor) *Electromagnetics, Volume 4* Washington, D. C.: Hemisphere Publishing Corporation (1984)

[122] Vaidyanathan, P. P. *Multirate Systems and Filter Banks. Prentice Hall Signal Processing Series*. Englewood Cliffs, New Jersey: Prentice Hall (1993).

[123] van der Heijden, Dennis. "Robot Hand Controlled by Thought" Los Angeles, California: Axistive (July 28, 2006).

[124] Van Gemert, M. J. C. "A Note on the Cole - Cole Dielectric Permittivity Equation in Connection with Causality" *Chemical Physics Letters. Volume 14, Number 5* (July 1, 1975) pages 606 - 608

[125] Van Tuyl, Andrew. *Axially Symmetric Flows Around an New Family of Half Bodies. Naval Ordinance Laboratory Maryland 9539*. White Oak, Maryland: Naval Ordinance Laboratory Maryland (1949)

[126] Von Wahl, W. "Estimating $\bigtriangledown \boldsymbol{u}$ by $div(\boldsymbol{u})$ and $\nabla \times (\boldsymbol{u})$" *Methods of Applied Science, Volume 15* (1992) pages 123-143.

[127] Walker, James S. *Fast Fourier Transforms, Second Edition* Boca Raton: CRC Press (1996).

[128] Wang, Jun Wang and Jacques Beumont. "Parameter Estimation of the Hodgkin Huxley Gating Model: An Inversion Procedure" *SIAM Journal of Applied Mathematics. Volume 64, Number 4* (2004) pages 1249-1267

[129] Weinstein, David, Leonid Zhukov, and Chris Johnson. "Lead Field Bases for Electroencephalogram Source Imaging" *Annals of Biomedical Engineering, Volume 28, Number 9* (September, 2000) pages 1059-1164.

[130] Wilson, Hugh R. "Simplified Dynamics of Human and Mammalian Neocortical Neurons" *Journal of Theoretical Biology. Volume 200* (1999) pages 375-388.

[131] Wilson, H. R. *Spikes, Decisions, and Actions. The Dynamical Foundations of Neuroscience*. New York: Oxford University Press (1999)

[132] Weinberger, H. F. *A First Course in Partial Differential Equations with Complex Variables and Transform Methods* Waltham, Massachusetts: Blaisdell Publishing Company (1965)

[133] Whittaker, E. T. and G. N. Watson. *A Course of Modern Analysis* London: Cambridge at the University Press (1962)

[134] Wiener, Norbert. *Cybernetics; or Control and Communication in the Animal and Machine* New York: MIT Press (1961).

[135] Wolters, C. H., L. Grasedyck, and W. Hackbusch. "Efficient Computation of Lead Field Bases and Influence Matrix for the FEM Based EEG and MEG Inverse Problem" *Inverse Problems. Volume 20* (2004) pages 1099-1116.

[136] Wolpaw, Jonathan R. and Dennis J. McFarland. "Control of a Two-Dimensional Movement Signal by a Noninvasive Brain-Computer Interface in Humans" *Proceedings of the National Academy of Science. Volume 101, Number 51.* (December 21, 2004) pages 17849-17854.

[137] Wu, W., Y. Gao, E. Bienenstock, J. P. Donoghue, and E. N. Brown. "Bayesian Population Decoding of Motor Cortical Activity Using a Kalman Filter" *Neural Computation, Volume 18, Number 1* (2006) pages 80-118.

[138] Wu, W., M.J. Black, D. Mumford, Y. Gao, E. Bienenstock, and J. P. Donoghue. "Modeling and Decoding Motor Cortical Activity Using a Switching Kalman Filter" *IEEE Transactions on Biomedical Engineering, Volume 51, Number 6* (June, 2004) pages 933-942.

[139] Yosida, Kosaku. *Functional Analysis* New York: Academic Press (1965).

[140] Zhou, Pei-bai. "Numerical Analysis of Electromagnetic Fields" New York: Springer Verlag (1993).

[141] Zhukov, Leonid, David Weinstein,and Chris Johnson. "Independent Component Analysis for EEG Source Localization" IEEE Engineering in Medicine and Biology (May, June 2000) pages 87-95

[142] Zhukov, Loenid, David Weinstein, and Chris Johnson. *Independent Component Analysis for EEG Source Localization In Realistic Head Models* Salt Lake City, Utah: University of Utah Center for Scientific Computing and Imaging (2004) pages 1-10 Zhukov, L. E. and D. W. Weinstein *Lead Field Basis for FEM Source Localization* University of Utah Technical Report UUCS-99-014 Salt Lake City: University of Utah Center for Scientific Computing and Imaging (1999)